

Bifurcation Phenomena in Non-Isothermal Reactive Gas Absorption

by

Usamah Ahmed Al-Mubaiyedh

A Thesis Presented to the

FACULTY OF THE COLLEGE OF GRADUATE STUDIES

KING FAHD UNIVERSITY OF PETROLEUM & MINERALS

DHAHRAN, SAUDI ARABIA

In Partial Fulfillment of the
Requirements for the Degree of

MASTER OF SCIENCE

In

CHEMICAL ENGINEERING

December, 1996

INFORMATION TO USERS

This manuscript has been reproduced from the microfilm master. UMI films the text directly from the original or copy submitted. Thus, some thesis and dissertation copies are in typewriter face, while others may be from any type of computer printer.

The quality of this reproduction is dependent upon the quality of the copy submitted. Broken or indistinct print, colored or poor quality illustrations and photographs, print bleedthrough, substandard margins, and improper alignment can adversely affect reproduction.

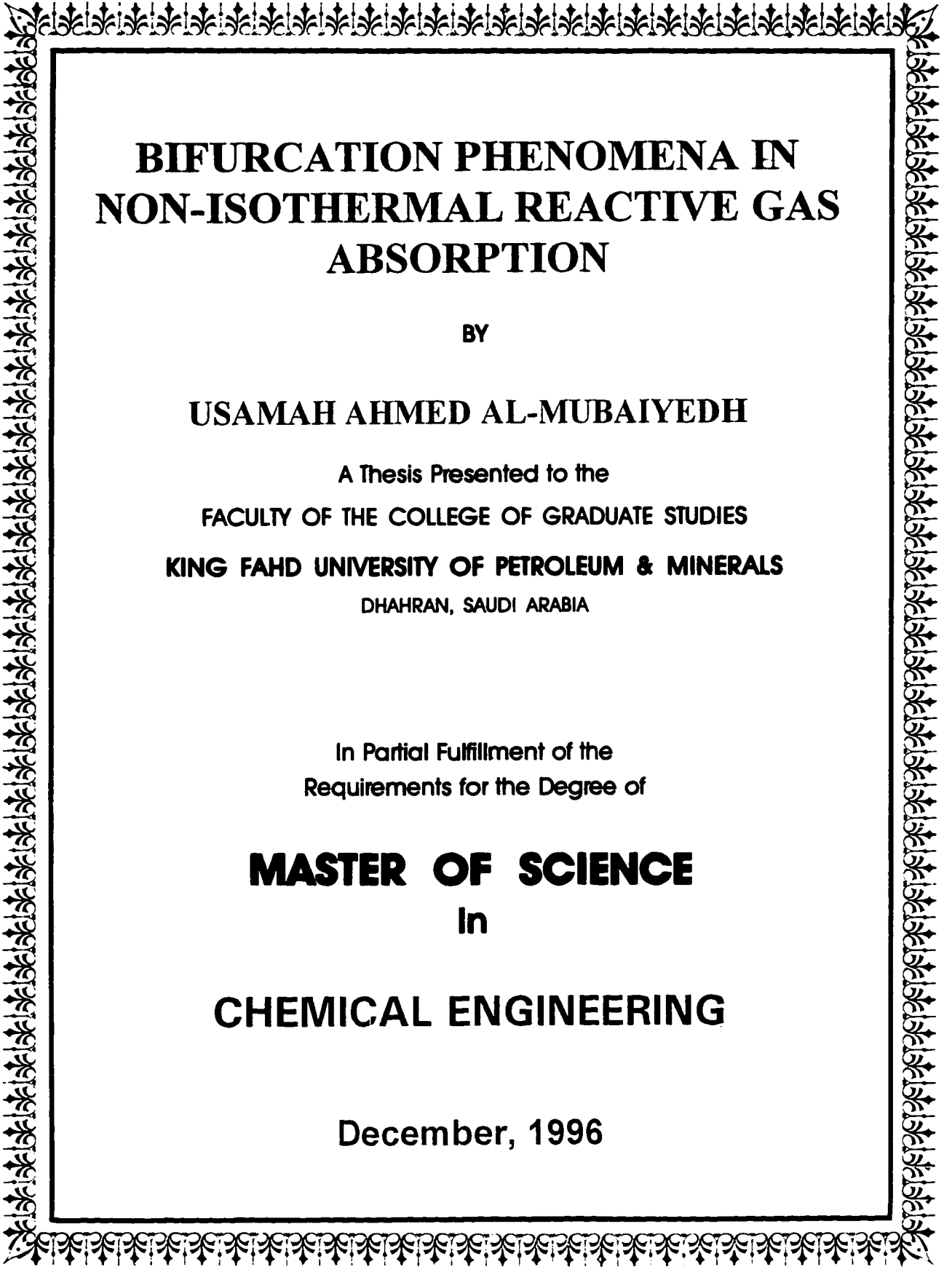
In the unlikely event that the author did not send UMI a complete manuscript and there are missing pages, these will be noted. Also, if unauthorized copyright material had to be removed, a note will indicate the deletion.

Oversize materials (e.g., maps, drawings, charts) are reproduced by sectioning the original, beginning at the upper left-hand corner and continuing from left to right in equal sections with small overlaps. Each original is also photographed in one exposure and is included in reduced form at the back of the book.

Photographs included in the original manuscript have been reproduced xerographically in this copy. Higher quality 6" x 9" black and white photographic prints are available for any photographs or illustrations appearing in this copy for an additional charge. Contact UMI directly to order.

UMI

**A Bell & Howell Information Company
300 North Zeeb Road, Ann Arbor MI 48106-1346 USA
313/761-4700 800/521-0600**



BIFURCATION PHENOMENA IN NON-ISOTHERMAL REACTIVE GAS ABSORPTION

BY

USAMAH AHMED AL-MUBAIYEDH

A Thesis Presented to the
FACULTY OF THE COLLEGE OF GRADUATE STUDIES
KING FAHD UNIVERSITY OF PETROLEUM & MINERALS
DHAHRAN, SAUDI ARABIA

In Partial Fulfillment of the
Requirements for the Degree of

MASTER OF SCIENCE
In
CHEMICAL ENGINEERING

December, 1996

UMI Number: 1384108

UMI Microform 1384108
Copyright 1997, by UMI Company. All rights reserved.

**This microform edition is protected against unauthorized
copying under Title 17, United States Code.**

UMI
300 North Zeeb Road
Ann Arbor, MI 48103

KING FAHD UNIVERSITY OF PETROLEUM AND MINERALS
Dhahran 31261, SAUDI ARABIA

COLLEGE OF GRADUATE STUDIES

This thesis, written by

USAMAH AHMAD AL-MUBAIYEDH

under the direction of his Thesis Advisor and approved by his Thesis Committee, has been presented to and accepted by the Dean of the College of Graduate Studies, in partial fulfillment of the requirements for the degree of

MASTER OF SCIENCE IN CHEMICAL ENGINEERING.


Thesis Committee



Dr. Abdullah A. Shaikh
(Chairman)



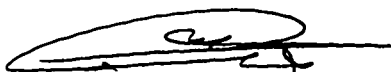
Dr. Shareefdeen M. Zarook
(Member)



Dr. Mohammad B. Elgendi
(Member)



Dr. Abdullah A. Shaikh
(Department Chairman)



Dr. Abdulla M. Al-Shehri
(Dean, College of Graduate Studies)



Date : 19-1-97

ACKNOWLEDGMENTS

I am most grateful to Almighty ALLAH for giving me the opportunity to pursue my MS degree and the capability to complete this work successfully.

My deep appreciation to my thesis advisor Dr. Abdullah A. Shaikh for his guidance and encouragement. The training and experience I got from him was wonderful.

I am thankful to my thesis committee members Dr. S. M. Zarook and Dr. M. B. Elgendi for their comments and suggestions.

Also, I would like to thank the chemical engineering faculty members and staff for their cooperation and help.

TABLE OF CONTENTS

<i>Chapter</i>	<i>Page</i>
LIST OF TABLES.....	v
LIST OF FIGURES	vi
ABSTRACT (Arabic).....	ix
ABSTRACT (English).....	x
 1. INTRODUCTION	 1
1.1 OBJECTIVES.....	5
 2. LITERATURE REVIEW	 6
2.1 NONISOTHERMAL PHYSICAL GAS ABSORPTION	7
2.2 NONISOTHERMAL CHEMICAL GAS ABSORPTION	12
2.2.a Experimental Studies.....	12
2.2.b Pseudo-First-Order Reaction.....	15
2.2.c Instantaneous Reaction.....	18
2.2.d Second Order Reaction.....	19
2.2.e Steady State Multiplicity in Gas-Liquid “Reactions”	23
2.2.f Steady State Multiplicity in Gas-Liquid “Reactors”.....	24
 3. GENERALIZED FILM MODEL.....	 31
3.1 FILM THEORY AND PHYSICAL PICTURE.....	31
3.2 MODEL ASSUMPTIONS	33
3.3 MODEL EQUATIONS	37
3.4 DIMENSIONLESS FORM OF FILM-MODEL EQUATIONS	41
3.5 THE ASYMPTOTIC BEHAVIOR OF THE NEW MODEL	47
 4. RESULTS AND DISCUSSION :	
SOLUTION AND INVESTIGATION OF THE FILM THEORY MODEL.....	50
4.1 SOLUTION METHOD	50
4.2 MODEL SOLUTION FOR SOME TYPICAL MODEL PARAMETERS.....	51
4.3 PARAMETRIC STUDY	62
4.3.a The Effect of Reaction Orders and the Stoichiometry Parameter	62
4.3.b The Effect of Lewis Number.....	64
4.3.c The Effect of Dimensionless Activation Energies	67
4.3.d The Effect of Dimensionless Heats of Reaction, Solution and Evaporation.....	70
4.3.e The Effect of Biot Numbers and Parameter ω	76

4.3.f The Effect of Bulk Liquid Reaction Parameters	81
4.3g The Effect of Reactor Inlet Temperatures and Inlet Liquid Concentration..	86
4.4 LUMPING OF THE HEATS OF REACTION AND SOLUTION PARAMETERS	86
4.5 MODEL APPLICATION TO SOME INDUSTRIAL GAS-LIQUID REACTIONS	96
5. RESULTS AND DISCUSSION :	
LOCAL MODEL APPLICATION TO A GLOBAL REACTOR DESIGN	
PROBLEM	118
5.1 GLOBAL MODEL ASSUMPTIONS	118
5.2 DERIVATION OF THE GLOBAL MODEL EQUATIONS	119
5.3 THE GLOBAL MODEL EQUATIONS IN DIMENSIONLESS FORM	122
5.4 METHOD OF SOLUTION	125
5.5 GLOBAL MODEL SIMULATION RESULTS AND DISCUSSION	126
6. CONCLUSIONS AND RECOMMENDATIONS	141
NOMENCLATURE	144
REFERENCES	148
APPENDIX A : DERIVATION OF GAS FILM MODEL EQUATIONS	155
APPENDIX B1 : SAMPLE OF INPUT SUBROUTINES TO AUTO	161
APPENDIX B2 : SAMPLE OF MAINE PROGRAM AND INPUT SUBROUTINES TO COLNEW	168
APPENDIX B3 : PROGRAM XPOLY TO FIT OUTPUT OF COLNEW AND USE IT AS A GUESS FOR AUTO	175
APPENDIX B4 : SAMPLE OF PROGRAM AND SUBROUTINES USED TO SOLVE THE REACTOR PROBLEM	179

LIST OF TABLES

Table 2.1	Summary of Literature	8
Table 2.2	Experimental Studies for Nonisothermal Gas-Liquid Systems.....	14
Table 2.3	Summary of MSS Studies for the Local Gas Absorption Problem.....	25
Table 3.1	Definition of Dimensionless Variables and Groups.....	44
Table 4.1	Typical Film Theory Model Parameters Used for Parametric Study	52
Table 4.2	Values of ϵ_R , ϵ_S , β_R and β_S Used to Test the Validity of Equations 4.1 and 4.2	93
Table 4.3	Physiochemical Data for the Chlorination of n-Decane System	102
Table 4.4	Physiochemical Data for the Sulfonation of Dodecylbenzene System	103
Table 4.5	Physiochemical Data for the Chlorination of Toluene System	104
Table 5.1	Definition of Dimensionless Variables and Groups.....	123
Table 5.2	Parameters Used for the CSTR Simulation	132

LIST OF FIGURES

Figure 1.1	Different Reaction Regimes in Film Model.....	4
Figure 2.1	Bahattacharya et al. (1987) Film Model	22
Figure 3.1	A Conceptual Model Describing Mass Transfer, Heat Transfer and Chemical Reaction Phenomena in Chemical Gas Absorption.....	34
Figure 3.2	Proposed Film Model.....	35
Figure 3.3	The Asymptotic Behavior of the New Model.....	49
Figure 4.1	The Nonisothermal Enhancement Factor Versus the Hatta Number for the Basic Model Parameters	53
Figure 4.2	The Surface Temperature Rise Versus the Hatta Number for the Basic Model Parameters	54
Figure 4.3	Model Prediction for the Concentration and Temperature Profiles for the Basic Model Parameters, $\sqrt{M} = 0.0$	56
Figure 4.4	Model Prediction for the Concentration and Temperature Profiles for the Basic Model Parameters, $\sqrt{M} = 0.355$	57
Figure 4.5	Model Prediction for the Concentration and Temperature Profiles for the Basic Model Parameters, $\sqrt{M} = 2.569$	58
Figure 4.6	Model Prediction for the Concentration and Temperature Profiles for the Basic Model Parameters, $\sqrt{M} = 0.991$	59
Figure 4.7	Model Prediction for the Concentration and Temperature Profiles for the Basic Model Parameters, $\sqrt{M} = 0.652$	60
Figure 4.8	Model Prediction for the Concentration and Temperature Profiles for the Basic Model Parameters, $\sqrt{M} = 50.170$	61
Figure 4.9	The Effect of the Reaction Orders	63
Figure 4.10	The Effect of Parameter S	65

Figure 4.11 The Effect of Parameter Le	66
Figure 4.12 The Effect of Parameter ε_{DA}	68
Figure 4.13 The Effect of Parameter ε_R	69
Figure 4.14 The Effect of Parameter ε_S	71
Figure 4.15 The Effect of Parameter ε_V	72
Figure 4.16 The Effect of Parameter β_R	73
Figure 4.17 The Effect of Parameter β_S	74
Figure 4.18 The Effect of Parameter β_V	75
Figure 4.19 The Effect of Parameter Bi_H	77
Figure 4.20 The Effect of Parameter Bi_M	78
Figure 4.21.a The Effect of Parameter ω on the Enhancement Factor	79
Figure 4.21.b The Effect of Parameter ω on the Surface Temperature Rise.....	80
Figure 4.22.a The Effect of Parameter α' on the Enhancement Factor.....	82
Figure 4.22.b The Effect of Parameter α' on the Surface Temperature Rise.....	83
Figure 4.23.a The Effect of Parameter β' on the Enhancement Factor	84
Figure 4.23.b The Effect of Parameter β' on the Surface Temperature Rise	85
Figure 4.24.a The Effect of Parameter γ' on the Enhancement Factor.....	87
Figure 4.24.b The Effect of Parameter γ' on the Surface Temperature Rise.....	88
Figure 4.25 The Effect of Parameter θ_0	89
Figure 4.26 The Effect of Parameter θ_G	90
Figure 4.27 The Effect of Parameter A_0	91
Figure 4.28 The Enhancement Factor for Constant ε_{eff} with different Values of ε_R and ε_S as Shown in Table 4.2	94
Figure 4.29 The Dimensionless Surface Temperature Rise for Constant ε_{eff} and Different Values of ε_R and ε_S as Shown in Table 4.2.....	95
Figure 4.30 The Enhancement Factor for Constant β_{eff} and Different Values of β_R and β_S	97

Figure 4.31	The Dimensionless Surface Temperature Rise for Constant β_{eff} and Different Values of β_R and β_S as Shown in Table 4.2	98
Figure 4.32	Two Parameter Continuation for ϵ_{eff}	99
Figure 4.33	Two Parameter Continuation for β_{eff}	100
Figure 4.34	The Enhancement Factor for Cl_2 -Decane System ($Bi_H = 0.1$)	106
Figure 4.35	The Surface Temperature Rise for Cl_2 -Decane System ($Bi_H = 0.1$)	107
Figure 4.36	The Enhancement Factor for Cl_2 -Decane System ($Bi_H = 10.0$)	108
Figure 4.37	The Surface Temperature Rise for Cl_2 -Decane System ($Bi_H = 10.0$)	109
Figure 4.38	The Enhancement Factor for DDB System ($Bi_H = 0.1$)	110
Figure 4.39	The Surface Temperature Rise for DDB System ($Bi_H = 0.1$)	111
Figure 4.40	The Enhancement Factor for DDB System ($Bi_H = 10.0$)	112
Figure 4.41	The Surface Temperature Rise for DDB System ($Bi_H = 10.0$)	113
Figure 4.42	The Enhancement Factor for Cl_2 -Toluene System ($Bi_H = 0.1$)	114
Figure 4.43	The Surface Temperature Rise for Cl_2 -Toluene System ($Bi_H = 0.1$)	115
Figure 4.44	The Enhancement Factor for Cl_2 -Toluene System ($Bi_H = 10.0$)	116
Figure 4.45	The Surface Temperature Rise for Cl_2 -Toluene System ($Bi_H = 10.0$)	117
Figure 5.1	Link Between Local and Global Problems	135
Figure 5.2	Algorithm for Main Program to Find Multiple Solutions of Equation (5.22) ($F(\theta_b)$)	136
Figure 5.3	Algorithm for Subroutine EFACTOR.....	137
Figure 5.4	Algorithm for Subroutine NISO	138
Figure 5.5	Change of Reactor Temperature with the Liquid Residence Time	139
Figure 5.6	Change of the Gas Conversion with the Liquid Residence Time	140
Figure 5.7	Change of the Liquid Conversion with the Liquid Residence Time.....	141
Figure 5.8	Change of the Hatta Number with the Liquid Residence Time	142
Figure 5.9	Change of the Enhancement Factor with the Liquid Residence Time.....	142
Figure 5.10	Change of the Gaseous Reactant Concentration in the Bulk Liquid with the Liquid Residence Time.....	143

ملخص الرسالة

أسم الطالب : أ. سامه أحمد إبراهيم المبيض
موضوع الدراسة : ظاهره التفرع في امتصاص الغاز المتفاعل غير ثابت الحرارة
حقل التخصص : هندسه كيميائية
تاريخ الحرجه : شعبان، ١٤١٧

لقد طور نموذج الطبقة الرقيقة لتفاعلات الغاز مع السائل غير ثابتة الحرارة مع أخذ تبخر السائل بعين الاعتبار. لقد درسة حركة التفاعل الـ (m,n) الغير عكسيه بدون سابق أي افتراضات على منطقة التفاعل لتشمل التفاعلات البطيئة والسريعة واللحظية. يشمل النموذج الجوانب المهمه لتفاعلات الغاز مع السائل غير ثابتة الحرارة التي طالما أهملت في الأبحاث العلميه السابقه. لأول مره نأخذ هنا في الاعتبار ثلاث طبقات رقيقه : طبقة الغاز و طبقة السائل لانتقال الماده و طبقة السائل لانتقال الحرارة. حلت معادلات النموذج باستخدام الطرق العدديه : التمكين العمودي المصاحب في العناصر المحدوده وباستخدام برامج COLNEW و AUTO.

لقد أظهر حل النموذج وجود التفرع الثابت أو تعدد حلول الحاله المستقره في حدود اجتماع معين من عناصر النموذج. كما عملت دراسه شامله لعناصر النموذج واختبرت حساسية تلك العناصر على معامل الزيادة وعلى زيادة حرارة السطح. لقد ظهر أن عناصر النموذج تؤثر على امكانية حدوث تعددية الحلول وعلى أماكن تلك التعدديه. لقد تم الحصول على عنصر فعال لطاقه التنشيط يشمل عناصر تنشيط التفاعل و النوبان وتم الحصول كذلك على عنصر فعال لحرارتي التفاعل و النوبان يشمل عناصر حرارتي التفاعل و النوبان. تم شمل تلك العناصر بالفهم الفيزيائي للنموذج وكذلك بطريقة التجربه. لقد طبق النموذج لثلاث تفاعلات صناعيه للغاز مع السائل، تلك التفاعلات تشمل تفاعل الكلور مع الديكان وتفاعل الكبريت للوديسايلينزين وتفاعل الكلور مع التولوين. وهنا كذلك لأول مره وصل نموذج الطبقة الرقيقه بنموذج المفاعل بدون أي تقريبات على معامل الزيادة وعلى تركيز السائل. كما تم وصل نموذج الطبقة الرقيقه لحالة ثبات الحرارة وعدم التبخر لتفاعل الكلور مع الديكان في مفاعل CSTR. ومن هنا الحل أثبت حدوث التعدديه في نموذج المفاعل.

درجة الماجستير في العلوم
جامعة الملك فهد للبترول والمعادن
الطهران، المملكة العربية السعودية
شعبان، ١٤١٧

THESIS ABSTRACT

NAME OF STUDENT : *Usamah Ahmed Al-Mubaiyedh*
TITLE OF STUDY : *Bifurcation Phenomena in Nonisothermal Reactive Gas Absorption*
MAJOR FIELD : *Chemical Engineering*
DATE OF DEGREE : *December, 1996*

A generalized film theory model for nonisothermal gas-liquid reactions has been developed including the possibility of liquid evaporation. Irreversible (m,n)th reaction kinetics were considered without a priori restrictions on the reaction regime, thus including the slow, fast and instantaneous reactions. The model considers the important aspects of nonisothermal gas-liquid reactions that were mostly ignored in the literature. For the first time, three films were analyzed, a gas film, a liquid mass transfer film and a liquid heat transfer film. The model equations were solved using the method of orthogonal collocations on finite elements with the application of the software codes, COLNEW and AUTO.

Solution of the model indicated the existence of static bifurcation, or steady state multiplicity under certain model parameters combinations. A comprehensive parametric study was carried out and the sensitivity of model parameters on the enhancement factor and surface temperature rise was tested. The model parameters were shown to affect the possibility of steady state multiplicity as well as the regions of multiple steady states. An effective activation energy parameter was obtained by lumping the dimensionless activation energies of reaction and solubility parameters, also, an effective heat of reaction and solution parameter was obtained by lumping the dimensionless heats of reaction and solution. No matter how the individual parameters are changed, the model predictions will be the same as long as the lumped parameter is kept constant. Parameter lumping was obtained through the physical understanding of the model as well as some trial and error computations. The model was applied to three industrial gas-liquid reaction systems, namely, the chlorination of n-decane, the sulfonation of dodecylbenzene, and the chlorination of toluene. For the first time, the local film model was linked with a global reactor design problem in the differential form without using any approximation for the enhancement factor and the bulk liquid concentration for the gas reactant. For demonstration purposes, an isothermal nonvolatile gas-liquid reaction case was considered using the chlorination of n-decane system in a non-nonadiabatic CSTR. The solution showed the existence of steady state multiplicity for the global behavior of the reactor.

MASTER OF SCIENCE DEGREE
KING FAHD UNIVERSITY OF PETROLEUM AND MINERALS
Dhahran, Saudi Arabia
December, 1996

CHAPTER 1

INTRODUCTION

Gas-liquid reactions are very important in industrial and biological operations. Reactive gas absorption is a common engineering operation in the chemical, petrochemical, petroleum and pollution treatment processes. Doraiswamy and Sharma (1984) listed more than fifty industrial examples of gas-liquid reactions including the type of gas-liquid contactor usually used. Design and operation of gas-liquid reactors needs a fundamental understanding of the interaction between the transfer phenomena and the accompanying chemical reaction. For a gas to react with a liquid it has to be absorbed first, then it will react consequently in the liquid phase. After reaction, the concentration gradient of gas component between the gas and the liquid will be increased due to its consumption in the liquid phase. The concentration gradient increase will lead to an enhanced rate of absorption.

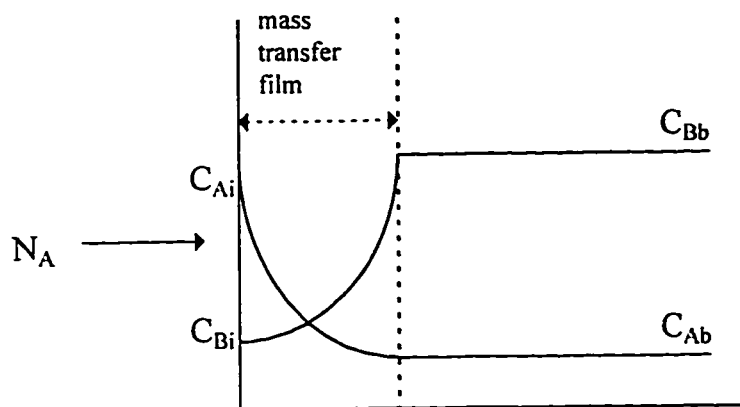
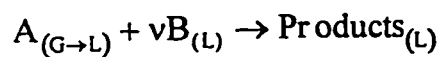
Heat effects can be a very important consideration when modeling reactive gas absorption. The dissolution of the gas at the gas-liquid interface will release heat of solution and the reaction in the liquid phase will also release (or absorb) heat of reaction. There are a number of industrially important gas-liquid reactions which are highly exothermic such as sulfonations, nitrations, halogenations, alkylations, oxidations and hydrogenation reactions.

Basically, there are three classic theories describing the mass transfer at a gas-liquid interface, namely the film theory by Whitman (1923), the penetration theory by Higbie (1935) and the surface renewal theory by Danckwerts (1951). The film theory assumes that a stagnant liquid film will be established when the gas meets the liquid surface and an instantaneous equilibrium will be established. The liquid film does not move from the gas-liquid interface as long as the gas bubble is inside the absorption equipment. The penetration theory has a better physical explanation for the absorption process, that a liquid element comes from the bulk liquid phase to the gas-liquid interface and stays for a certain time then it leaves and gets replaced by another fresh element. The time that the element spends at the interface is called the "*contact time*" and the rate of absorption is averaged with respect to this time. The surface renewal theory, on the other hand, assumes more realistically that different liquid elements stay for different contact times and the rate of absorption for each element is weighted with respect to a certain time distribution function. The film theory is a steady state model while the penetration and the surface renewal theories are time dependent models.

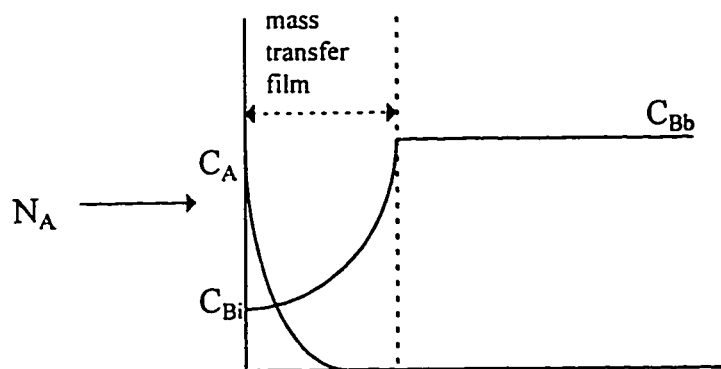
The film and penetration theories were applied widely in the literature to describe the coupled mass and heat transfer phenomena in reactive and unreactive absorption problems. However, very little attention, by comparison, was paid to the surface renewal theory due to its mathematical complexity. Among the three theories, the film theory is easier in visualizing the process of gas dissolution, diffusion, film reaction, then the process of material transfer to the bulk liquid phase and the subsequent reaction in the

bulk liquid phase. Also, the mathematical representation of the combined mass and heat transfer processes is relatively easier for the film theory.

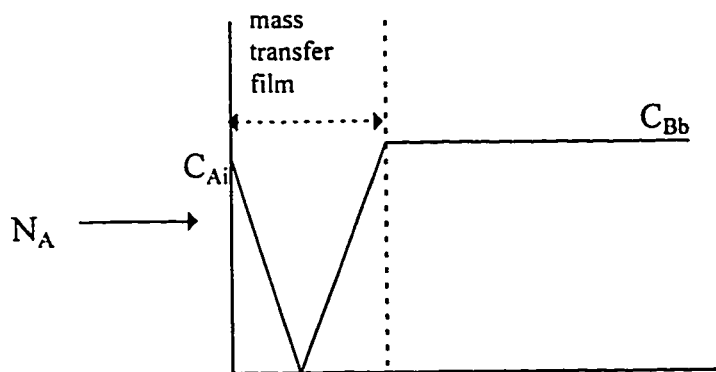
The temperature rise due to heats of solution and reaction (in the exothermic case) can lead to two opposing effects, first, the solubility of the gas in the liquid will be reduced, second, the rate of reaction will be increased. Depending on the relative effect of temperature rise on both parameters, the rate of gas absorption can be enhanced or inhibited. Consequently, when modeling the process of gas absorption, heat effects are an important factor to be considered. Beside changing the rate of gas absorption, the temperature rise can also change the reaction *regime* from slow to fast to instantaneous reaction. The famous Hatta number, \sqrt{M} , is the main parameter which might be used to describe the regime in which the reaction is happening. The reaction regime can be fast, instantaneous or general (slow or moderately slow) as shown in Figure 1.1. If the Hatta number is small, then the reaction is slow such that it will happen in the liquid film and it will continue in the bulk liquid phase, Figure 1.1(a). However, if it is high, then the reaction will be completed within the liquid film and the concentration of the gas component 'A' will be zero at the edge of the mass transfer film, Figure 1.1(b). For the case of an instantaneous reaction (a very high Hatta number), the gas and liquid reactants will react instantaneously as soon as they meet at a reaction plane inside the liquid film as shown in Figure 1.1(c).



(a) Slow Reaction



(b) Fast Reaction



(c) Instantaneous Reaction

Figure 1.1 Different Reaction Regimes in Film Model

1.1 OBJECTIVES

Following are the objectives of the present thesis work :

1. A literature survey will be carried out to cover most of the previous work conducted for the gas-liquid reactions and reactors.
2. A film theory model will be developed to include the heat effects and it will be general in form without any a priori assumption for the reaction regime, also it will consider general irreversible reaction kinetics.
3. The solution of the model will be presented and a comprehensive parametric study will be investigated. Bifurcation phenomena will be analyzed and an application of some industrial gas-liquid reactions will be demonstrated for the local film model.
4. The model will be applied to a reactor design problem, in which the steady state multiplicity will be investigated for the global reactor performance.

CHAPTER 2

LITERATURE REVIEW

The problem of heat effects in gas-liquid reactions was first studied by Danckwerts (1953) for first-order reactions. Using the penetration theory, he assumed the temperature rise to be too small to affect the solubility, diffusivity and the reaction rate constant. Using that assumption, Danckwerts studied the absorption of CO₂ in a buffer solution and he concluded that for periods of contact times less than 0.5 seconds, the rise in temperature would be too small to affect the rate of absorption. Carberry (1966) studied the CO₂-buffer solution system and found that the heat effects are too small to affect the rate of gas absorption process. He made a general conclusion: the heat effects are negligible and need not be considered in gas-liquid reactions, mainly because of the small activation energies associated with those reactions.

Danckwerts' and Carberry's analyses were limited to systems with low gas solubilities and low reaction activation energies like the CO₂-buffer solution system. However, there are a lot of gas-liquid reaction systems which are highly exothermic and in which the gas solubility is very high. Chiang and Toor (1964) reported an interfacial temperature rise of 17 °C for the absorption of ammonia in water. Clegg and Kilgannon (1971) reported an interfacial temperature rise of 20.4 °C for the absorption of hydrogen chloride in ethylene glycol system. Large interfacial temperature rises were also reported

in the literature for reactive and unreactive gas absorption systems. Thus, for gas-liquid systems involving highly soluble gases and high reaction activation energies, the heat effects can be a very important consideration when modeling those reactions, and when designing reactors in which such reactions are carried out.

In this chapter a review of the available literature for the reactive and unreactive nonisothermal gas absorption will be presented in brief. Table 2.1 contains a summary of most of the papers in the area, including the theory used, reaction order, reaction regime and heat effects.

2.1 Nonisothermal Physical Gas Absorption.

Chiang and Toor (1964) developed a penetration theory model for the problem of nonisothermal physical absorption system. In their model, the liquid phase was assumed to be nonvolatile, the physical properties and transport coefficients were constant, and the interfacial gas concentration was linearly related to the interfacial temperature. Further, the volume change of the liquid phase was included in their model. Chiang and Toor obtained an approximate solution for the problem and they compared their theoretical predictions with the experimental data of ammonia absorption in water using a laminar jet apparatus. Actually, ammonia reacts with water to produce ammonium hydroxide, but this reaction is very rapid to the point that once ammonia contacts the water surface, they react exothermically. Due to this reason, this process is assumed to be physical absorption, and the heat of reaction and solution are lumped together as a sort of heat of solution. The experimental rate of absorption was compared with that obtained from the

Table 2.1 Summary of the Literature

AUTHORS	MASS TRANSFER * THEORY			REACTION ORDER		REACTION REGIME			HEAT EFFECTS
	F	P	SR	First	Second	General	Fast	Instan- taneous	
Danckwerts (1950)		✓		✓			✓		isothermal
Danckwerts (1953)		✓		✓			✓		nonisothermal
Chiang et al. (1964)		✓		physical					isothermal
Chiang et al. (1964)		✓		physical					nonisothermal
Hikita et al. (1964)	✓	✓		(m,n) th			✓		isothermal
Carberry (1966)	✓			✓			✓		nonisothermal
Danckwerts (1967)		✓		✓			✓		nonisothermal
Clegg et al. (1969)	✓			✓			✓		nonisothermal
Hiroaka et al. (1969)	✓			✓			✓		nonisothermal
Cook et al. (1972)		✓		✓			✓		nonisothermal
Shah (1972)		✓		✓			✓		nonisothermal
Tripathi et al. (1974)		✓		✓			✓		nonisothermal
Verma et al. (1975)		✓		physical					nonisothermal
Mann et al. (1977)	✓			✓			✓		nonisothermal
Ikemizuk et al. (1979)		✓			✓			✓	nonisothermal
Allan et al. (1982)	✓			✓			✓		nonisothermal
Mann et al. (1982)	✓				✓	✓			nonisothermal
Suresh et al. (1983)		✓		physical					nonisothermal
Datta et al. (1984)		✓		✓			✓		isothermal
Asai et al. (1985)		✓		✓			✓	✓	nonisothermal
White et al. (1985)	✓			✓			✓		nonisothermal

Table 2.1 Summary of the Literature (continued)

AUTHORS	MASS TRANSFER * THEORY			REACTION ORDER		REACTION REGIME			HEAT EFFECTS
	F	P	SR	First	Second	General	Fast	Instantaneous	
White et al. (1986)		✓		✓			✓	✓	nonisothermal
White et al. (1986)		✓			✓		✓	✓	nonisothermal
Bahattacharya et al. (1987)	✓				✓	✓			nonisothermal
Chatterjee et al. (1987)	✓	✓		✓			✓		nonisothermal
Bahattacharya et al. (1988)	✓				✓		✓		nonisothermal
Bahattacharya et al. (1988)	✓				✓		✓		nonisothermal
Starzak et al. (1988)	✓				✓	✓			isothermal
Chang et al. (1988)	✓			✓			✓		nonisothermal
Al-Ubaidi et al. (1990)	✓				✓		✓		nonisothermal
Evans et al. (1990)		✓			✓		✓		nonisothermal
Landau (1990)	✓			zeroth		✓	✓		nonisothermal
Al-Ubaidi et al. (1992)	✓				✓		✓		nonisothermal
Frank et al. (1995a)	✓			✓	✓		✓	✓	
Frank et al. (1995b)	✓			✓	✓		✓	✓	
Shaikh et al. (1995)	✓				✓	✓			isothermal

* F = film theory, P = penetration theory, SR = surface renewal theory

theoretical predictions for three different cases. Namely, they analyzed the cases of isothermal absorption, nonisothermal absorption, and nonisothermal absorption with volume change in the liquid phase. Predictions from the isothermal absorption and the nonisothermal absorption with volume change in the liquid phase correlated very well with experimental data. However, the case of nonisothermal absorption deviates 12% below the experimental data. A surface temperature rise of 17 °C was reported for this system. They concluded that the heat effects and volume change in the liquid phase are two opposing effects which canceled each other.

Clegg and Kilgannon (1971) studied the system of hydrogen chloride absorption in ethylene glycol in a laminar jet apparatus at initial gas and liquid conditions of 25 °C and 1 atm. They used the Chiang and Toor (1964) model to compare their experimental rate of absorption. The gas diffusivity was considered to be variant with temperature and the Wilke-Chang correlation was used for that purpose. Clegg and Kilgannon investigated the three cases considered by Chiang and Toor (1964). Their predictions showed that the case of nonisothermal absorption with volume change in the liquid phase was very well correlated with experimental findings. The nonisothermal absorption case underestimated the experiments. Finally, the isothermal absorption case was the worst case to fit the experimental data. This study showed that the volume change in the liquid phase and heat effects did not cancel each other. They explained the difference between their findings and those of Chiang and Toor (1964), because for the system of hydrogen chloride absorption in ethylene glycol, the solubility is less sensitive to temperature than

that of ammonia absorption in water. Also, the diffusion coefficient varied considerably with temperature which was assumed to be constant in the previous study.

Green and Chiang (1971) used a constant pressure batch absorption system for the absorption of butane in decane and propane in decane as well. They developed their apparatus carefully to measure the surface temperature rise associated with absorption using fine wire thermocouples. They reported a surface temperature rise from 1.3 to 1.5 °C for the propane-decane system and from 7.2 to 8.0 °C for the butane-decane system. Also, the volume change in the liquid phase was measured experimentally.

Verma and Delancey (1975) developed a penetration theory model for the nonisothermal physical absorption problem. They used a linear solubility temperature relationship. In the model, the liquid density was variant and the volume change in the liquid phase was included. A pseudo-Dufour effect which accounts for the energy flux due to concentration gradient in the liquid phase was included as well. Further, they did absorption experiments using a Pyrex cylindrical vessel. They experimented with the propane-decane system at 1 atm, in addition to the ammonia-water system at 1.0, 0.737, 0.467 and 0.2 atm. They measured the interfacial temperature rise and the net interfacial mass transfer rate. A surface temperature rise of 18.2 °C for the ammonia-water system at 1 atm was reported. Their theoretical predictions agreed very well with the experimental findings.

Suresh and coworkers (1983) developed a penetration theory model and used Arrhenius temperature relationships for the diffusivity, solubility and thermal

conductivity. No volume change in the liquid phase was considered and the bulk flow, Dufour and Soret effects were assumed negligible. They developed a rigorous model to evaluate the surface temperature rise and the enhancement factor. Their finding is that the absorption behavior is dependent on a combination of activation energies rather than individual energies.

2.2 *Nonisothermal Chemical Gas Absorption.*

2.2.a Experimental Studies

Some experimental studies were reported in the literature for some gas-liquid reaction systems. Ponter and coworkers (1974) studied the sulfur trioxide absorption in sulfuric acid using a wetted-wall column. They determined the liquid surface temperature by measuring the amount of infra-red radiation emitted from the liquid surface. They reported the surface temperature rise versus the axial column length for different liquid flow rates. The experimental data was compared with the theoretical predictions of the energy equation applied for the liquid film. The energy equation did not trace the experimental findings very well.

Mann and Clegg (1975) measured the rate of absorption of pure chlorine in toluene using a laminar jet apparatus at initial gas and liquid conditions of 25 °C and 1 atm. They calculated the surface temperature rise by carrying out an integral heat balance at the jet surface after measuring the bulk liquid temperature rise. They further carried out a kinetic

study for this complex branching chain reaction, from which they found a fifth order dependency for the chlorine concentration to simulate this reaction.

Mann and Moyes (1977) studied the sulfonation of dodecylbenzene using a laminar jet technique. The sulfur trioxide was diluted with nitrogen. The liquid surface temperature rise was calculated by measuring the bulk temperature rise. A surface temperature increase of 100 °C for 30 % SO₃ in the gas phase was reported. Discoloring was observed at high SO₃ concentration in the gas phase.

Ikemizu and coworkers (1979) studied the instantaneous reaction of ammonia absorption in water and in aqueous solutions of HCl, HNO₃ and H₂SO₄ in laminar jet. They measured the rate of ammonia absorption at different bulk liquid temperatures and at different bulk liquid reactant concentrations and they compared the experimental measurements with the theoretical predictions. The theoretical rate of absorption which was calculated on the basis that the heat of solution was released at the liquid interface and the heat of reaction was released in the reaction plane, agreed very well with the experimental rate of absorption. Mann, Knysh and Allan (1982) studied again the sulfonation of dodecylbenzen in a laminar jet apparatus and in a stirred cell. In the laminar jet experiments, the surface temperature rise was estimated to be 89 °C at the base of the jet for 30 % SO₃ (in N₂) in the gas phase. They studied the discoloring effects in the liquid using the stirred cell contactor. The previous experimental studies are summarized in Table 2.2 .

Table 2.2 Experimental Studies for Nonisothermal Gas-Liquid Systems

AUTHOR	GAS-LIQUID SYSTEM	LABORATORY REACTOR	OBSERVATIONS
Ponter et al. (1974)	SO ₃ /H ₂ SO ₄	wetted wall column	- measured interfacial temperature (infra-red technique). - reported $\Delta T_i = 20$ °C
Mann and Clegg (1975)	Cl ₂ /Toluene	laminar jet	-measure the rate of absorption. - carried kinetic study.
Mann and Moyes (1977)	SO ₃ /DDB	laminar jet	- calculated the surface temperature rise -reported $\Delta T_i = 100$ °C for gas composition 30 % SO ₃ in Nitrogen
Ikemizu et al. (1979)	NH ₃ /H ₂ O and aqueous HCl, HNO ₃ , H ₂ SO ₄	laminar jet	- measured rate of gas absorption at different liquid compositions
Mann et al. (1982)	SO ₃ /DDB	laminar jet stirred cell	- measured $\Delta T_i = 89$ °C for gas composition 30 % SO ₃ in Nitrogen

Many different theoretical studies were reported in the literature for different reaction orders using the penetration and film theories. The following part of this section will contain some of them.

2.2.b Pseudo-First-Order Reaction

Danckwerts (1953) obtained an analytical solution for the liquid surface temperature rise using the penetration theory analysis for first-order reactions. The liquid surface temperature rise was calculated with the assumption that it will be too small to affect the gas diffusivity and solubility and the reaction rate constant. If that temperature rise becomes high, the analysis of isothermal absorption rate will be rejected. He applied his analysis to the carbon dioxide absorption in carbonate-bicarbonate buffer solution. For the system under study, the analysis showed that for periods of contact times less than 0.5 sec, the surface temperature rise will be too small. Using the same assumption, Danckwerts (1967) derived expressions for the reactant interfacial concentration, the product interfacial concentration and the interfacial temperature rise as functions of time.

For fast first-order reactions, Hiroaka and Tanaka (1969) used the film theory to model chemical gas absorption. They used a linear solubility temperature relationship and they used a linear approximation for the reaction rate expression with respect to temperature and concentration. They obtained an analytical solution for the resulting linear boundary value problem. They applied their results for the example of liquid cyclohexane oxidation at 10 atm, in which they studied the effect of reaction rate on the concentration and temperature profiles and interfacial mass transfer rates.

Clegg and Mann (1969) used the penetration theory for first-order gas-liquid reactions with the assumption of constant reaction rate constant. They used a linear solubility temperature relationship and obtained an analytical solution. They illustrated their model with the example of chlorine absorption in toluene, in which the enhancement factor was decreasing with the parameter kt (a product of the reaction rate constant with contact time) to reach a minimum value at $kt = 1.6$. The results showed that the gas absorption can be reduced due to heat effects.

Using an Arrhenius temperature dependence for the gas diffusivity, solubility and reaction rate constant, Shah (1972) numerically solved the penetration theory equations for first-order kinetics. The results showed that even when heat effects are very high, one can use Danckwerts analysis (1953) as long as the following combination of variables is satisfied : $\epsilon_{\text{eff}} = \epsilon_S - (\epsilon_R + \epsilon_D)/2 = 0$. His analysis showed that the interfacial temperature increases with decreasing $\epsilon_{\text{eff}} < 0$ and it decreases with increasing $\epsilon_{\text{eff}} > 0$. Cooke and Moor (1972) obtained a semi-analytical solution for the problem using a constant gas diffusivity and a linear solubility temperature relationship. The reaction rate constant was also varying linearly with temperature. Their results were compared with those of Danckwerts and Kennedy (1954) and Sullivan (1965)¹.

Tripathi et al. (1974) solved the penetration theory equations using the perturbation technique for a first-order gas-liquid reaction with a linear reaction rate constant with respect to temperature. The average absorption rate calculated with their

¹ Work cited in Cooke and Moor (1972)

model varied from that with constant reaction rate constant. Mann and Moyes (1977) used the film theory approach for first-order reactive gas absorption with a constant gas diffusivity and a linear temperature dependent gas solubility. Because the heat transfer film is orders of magnitude greater than the mass transfer film, the interface temperature was assumed constant in the mass transfer film and the temperature profile is linear in the heat transfer film. That decoupled the mass and heat balance differential equations and an analytical solution was feasible. The model was applied to the experimental absorption of sulfur trioxide (diluted with nitrogen) in dodecylbenzene (DDB). The surface temperature rise and the enhancement factor were plotted for different gas concentrations and different reaction activation energies.

Allan and Mann (1979) extended the work of Mann and Moyes (1977) by using a hyperbolic solubility temperature relation. Results of the surface temperature rise and the enhancement factor for the SO_3 -DDB system varied from the previous study at high values of Hatta numbers. Asai et al. (1985) used a linearized Arrhenius expressions for the temperature dependent diffusivity, solubility and reaction rate constant. They obtained an approximate solution for first-order kinetics using the penetration theory. The surface temperature rise and the enhancement factor results were compared with those of Danckwerts (1953) and Shah (1972).

Chatterjee and Altwickler (1987) used the van't Hoff expression for the temperature solubility relation and Arrhenius expression for the reaction rate constant. The gas diffusivity was assumed constant on the other hand. For fast first-order reactions,

a semi-analytical solution was obtained using the film theory. The results were compared with penetration theory results of Asai et al. (1985). It was found that the film model underestimates the surface temperature rise and overestimates the enhancement factor. Chang and Hwang (1988) developed a film theory model with a constant interfacial temperature through the mass transfer film and a linear temperature profile in the heat transfer film. The gas solubility was linear in temperature and the interfacial gas-liquid resistance was included in the model. The analytical solution results showed that the interfacial resistance affects the gas absorption rate significantly. The coupling of surface resistance with the exothermic effects decreases the gas absorption and thus reduces the absorption enhancement factor.

2.2.c Instantaneous Reaction

Danckwerts (1970) used the penetration theory to derive two expressions for the surface temperature rise due to heat of solution and heat of reaction, respectively. In his analysis, the gas solubility and diffusivity were assumed to be temperature independent. Danckwerts surface temperature expressions were independent of contact time. Ikemizu et al. (1979) used a penetration theory model with a constant solubility and diffusivity and obtained analytical expressions for the surface temperature rise and the mean absorption rate. They applied their results for the ammonia absorption in water and ammonia absorption in acidic solutions. The theoretical absorption rate agreed very well with the experimental predictions when using the assumption that the heat of solution is released at the gas-liquid interface and the heat of reaction is released at the reaction plane.

Asai et al. (1985) also used a penetration theory model with a linearly temperature dependent gas diffusivity and solubility. They obtained an approximate solution for their rigorous model by evaluating the gas diffusivity and solubility at the gas-liquid interfacial temperature and the reaction rate constant at the reaction plane temperature. Results for the surface temperature rise and the enhancement factor for the approximate model and the rigorous model agreed very well.

2.2.d Second-Order Reaction

White and Johns (1986a) used the penetration theory to model a bimolecular gas-liquid reaction. In their model it was assumed that the thermal diffusivity far exceeds the mass diffusivity, as a result the reaction is considered to take place at a certain temperature T_i (the interfacial temperature). They used the approximations introduced by van Krevelen and Hoftijzer (1948), Sherwood et al. (1975) and De Coursey (1974) to derive expressions for the enhancement factor and the surface temperature rise.

Bhattacharya et al. (1987) developed a film theory model for a bimolecular gas-liquid reaction for a nonvolatile liquid without assuming the concentration of the gas component in the bulk liquid phase to be zero. The gas diffusivity was constant in their model, however, the gas solubility and the reaction rate constant were related to temperature by Arrhenius expressions. To solve the problem analytically, they assumed the interfacial temperature to be constant throughout the mass transfer film. Further, they neglected the contribution of the reactant concentration profile and the temperature gradient between the mass transfer film and the heat transfer film. Accordingly, the

reaction rate equation is evaluated at the bulk liquid conditions after the mass transfer film. They derived analytical expressions for the gas reactant concentration at the bulk liquid and the interfacial temperature rise. Figure 2.1. shows a schematic diagram of Bhattacharya's et al. (1987) film model.

Al-Ubaidi et al. (1990) developed another film model for fast bimolecular reactions. They used Arrhenius temperature relations for the gas diffusivities, gas solubility and the reaction rate constant and the liquid reactant was assumed nonvolatile in their model. The nonlinear model was solved numerically using B-spline collocation. Also, they obtained an approximate solution for the problem using the approach of Bhattacharya et al. (1987). Their approximate solution gave a maximum difference of 12 % for the surface temperature rise when compared with the numerical solution and a maximum difference of 7 % for the enhancement factor. Al-Ubaidi and Selim (1992) used the same model of Al-Ubaidi et al. (1990) with the inclusion of the liquid volatility. The liquid volatility was detrimental to the enhancement factor at moderate values of Hatta numbers. Further, they applied their model to two reaction cases, namely, the chlorination of toluene and the sulfonation of dodecylbenzene. The volatility effects were more important for the chlorination of toluene system than the sulfonation of dodecylbenzene system. Evans and Selim (1990) developed a penetration model for a bimolecular gas-liquid reaction with a nonvolatile liquid assumption. Their temperature dependence for the physiochemical properties was the same as that of Al-Ubaidi et al.

(1990). The nonlinear parabolic partial differential equations were solved using the Suul'yev (1964) explicit numerical technique.

Recently, Frank and coworkers (1995a) studied the chemical gas absorption using the film theory approach. They used the Maxwell-Stafan theory to describe the mass transfer process. The theory is considered to have a better representation for the mass fluxes of a multicomponent system since the interaction phenomena due to simultaneous diffusion of several components play an important role. The flux of any diffusing component is implicit and it depends on the fluxes of other diffusing components. The driving force for the mass transfer is the chemical potential and the Soret and Dufor effects were neglected in Frank's et al. model. They developed a nonisothermal model for the chemical gas absorption and they solved the isothermal chemical absorption for several limiting cases, including physical absorption, instantaneous reactions, first-order reactions, second-order reactions and second-order reversible reactions.

Frank and coworkers (1995b) solved the nonisothermal model assuming a nonvolatile liquid and constant heats of solution and reaction. The Arrhenius temperature dependence was used for the solubility, reaction rate constants, and binary diffusion coefficients. They derived an approximate solution for the problem by decoupling the mass and heat balance equations. The heat transfer film was assumed to be orders of magnitude greater than the mass transfer film and the interfacial temperature was assumed constant in the mass transfer film region. Simulations were carried to study the importance of heat effects in the problem. They concluded that the thermal effects can affect the mass transfer rates by a factor of 30. Heat withdrawal rate and heat production

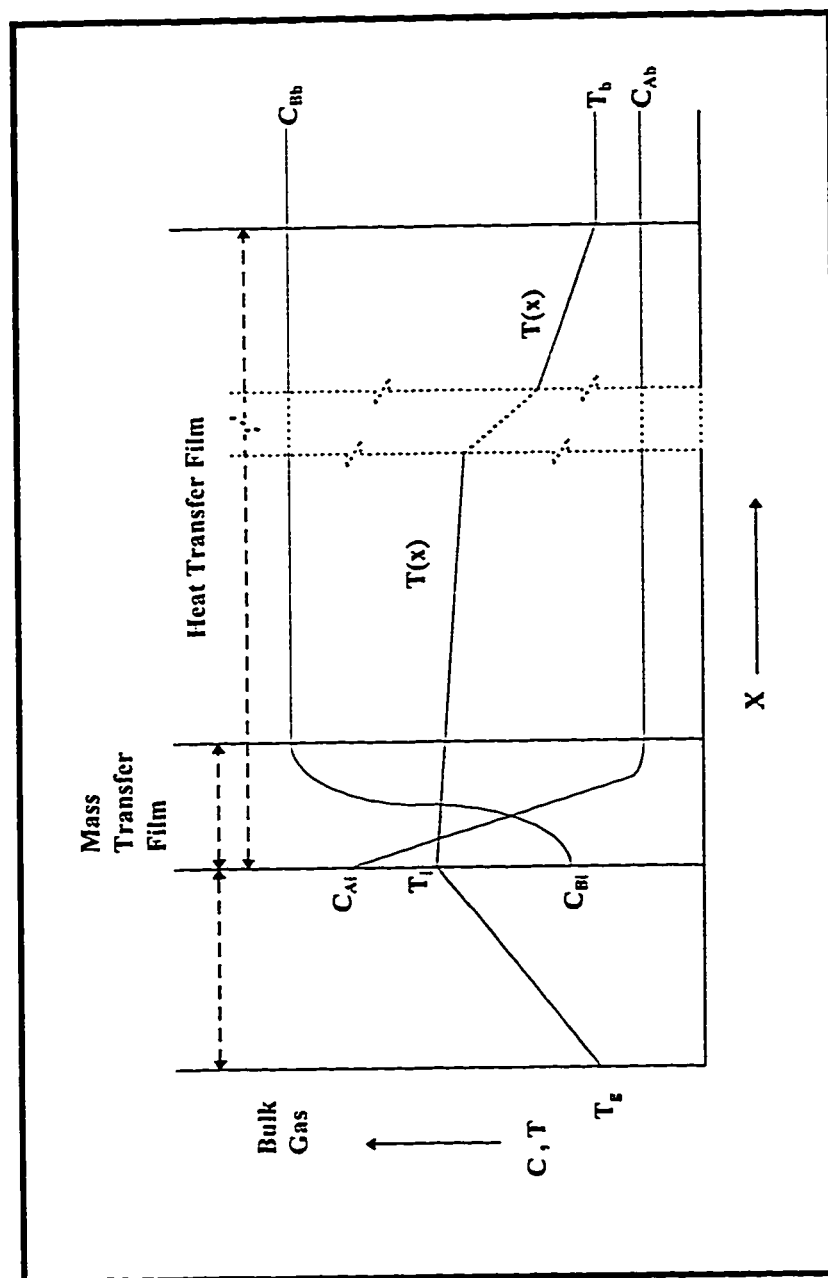


Fig 2.1 Bhattacharya et al. (1987) film model

rate were drawn as functions of the interfacial temperature rise and they showed the possibility of multiple steady state solutions for some cases.

2.2.e Steady State Multiplicity in Gas-Liquid “Reactions”

Allan and Mann (1982) studied the surface temperature rise and the enhancement factor multiplicities at the local mass transfer film, they used the film theory model developed by Mann and Moyes (1977). The model was for a first-order reaction with a constant gas diffusivity and a linear solubility temperature relationship. An analytical solution was obtained for the problem by decoupling the heat and mass transfer balance equations. Multiple solutions were obtained for the enhancement factor and the surface temperature rise when plotted versus the Hatta number. They reported that the multiplicity will be noticed at high values of the reaction activation energy. White and Johns (1985) used the same model equations of Allan and Mann (1982) and derived an expression for the surface temperature rise. Further, they derived conditions under which the surface temperature rise equation exhibits two or four turning points (limit points) . They reported a 1-3-5-3-1 multiplicity behavior for the surface temperature rise as a function of the Hatta number.

Bhattacharya et al. (1988) used the film theory to model second-order reactions. The earlier assumptions of Bhattacharya et al. (1987) were implemented and the approximation of Hikita and Asai (1964) for the reaction rate equation was included to obtain an analytical solution for the problem. An iterative computer algorithm was used to solve a set of implicit algebraic equations and to predict the surface temperature rise

and the enhancement factor as functions of the Hatta number. Multiple solutions were obtained and they reported five steady state solutions for certain model parameters combinations. Table 2.3 contains a summary of the literature for the multiple steady state (MSS) solutions for nonisothermal gas-liquid reactions (i.e. the local problem).

2.2.f Steady State Multiplicity in Gas-Liquid “Reactors”

A number of studies has been carried out to investigate the possible occurrence of multiple steady states in two phase gas-liquid reactors. Most of the studies were confined to gas-liquid CSTRs. A relevant experimental study was carried by Ding et al. (1974) who studied the chlorination of n-decane in a CSTR. They used three different lots of n-decane with different purities, 99.9 %, 97.0 % and 99.3 %. A fourth lot was specially prepared by purifying the first lot to an almost 100 % pure n-decane. Semibatch experiments were conducted first by bubbling the chlorine through a fixed amount of n-decane for the four different lots. It was observed that small amounts of impurities will change the qualitative behavior of the system. Steady state experiments were conducted for the most active lot (100 % n-decane) and one steady state solution was obtained. However, two stable steady state solutions were observed, high and low temperature branches, when using n-decane lots 2 and 3. The reactor startup procedure determined which steady state branch was attained. A branch of unstable steady states was obtained by preferentially heating the reactor to the initial temperature at which transition from one stable steady state to another would happen.

Table 2.3 Summary of MSS Studies for the Local Gas Absorption Problem

AUTHORS	THEORY	ASSUMPTIONS	OBSERVATIONS
Allan and Mann (1982)	Film	<ul style="list-style-type: none"> - First order reaction. - Fast reaction. - Constant gas diffusivity. - Gas solubility is linear in temperature. - Liquid is nonvolatile 	<ul style="list-style-type: none"> - Analytical solution. - Multiplicity noticed at high reaction activation energies.
White and Johns (1985)	Film	<ul style="list-style-type: none"> - First order reaction. - Fast reaction. - Constant gas diffusivity. - Gas solubility is linear in temperature. - Liquid is nonvolatile 	<ul style="list-style-type: none"> - Analytical solution. - Derived expressions for the turning points for the surface temperature rise equation. - 1-3-5-3-1 multiplicity behavior was reported.
Bhattacharya et al. (1988)	Film	<ul style="list-style-type: none"> - Second order reaction. - Mass and energy fluxes equal zero at edge of mass transfer film. - Constant gas diffusivity. - Gas solubility is linear in temperature. - Liquid is nonvolatile 	<ul style="list-style-type: none"> - Analytical solution. - Multiple solutions were reported.

A lot of theoretical studies of gas-liquid CSTRs are available in literature and the film theory was used to model the local reactive gas absorption problem. Hoffman et al. (1975) studied a second-order reaction in a two phase CSTR assuming a nonvolatile liquid. The chlorination of n-decane system was studied and five steady state solutions were reported. The same assumptions were implemented by Sharma et al. (1976) who studied two consecutive second-order gas-liquid reactions in a two phase CSTR. The experimental data of Ding et al. (1974) was used to test the model validity. The model agreed very well with the experiments and predicted one steady state solution for the most active n-decane lot. Like the experiments, the model showed two stable multiple steady states for the less active lots. The model agreed well with the experiments, however, there was some deviation at the high temperature branch because it did not account for the heat loss due to evaporation. It was reported that the deviation will increase further at high liquid residence times because the formation of the tri- and higher chlorides was not accounted for. An extensive parametric study was conducted using the same gas and liquid flow rates and up to seven steady state solutions were reported.

Raghuram and Shah (1977) studied three different gas-liquid reactions, slow pseudo-first-order, fast (1,n)th order reaction (first order with respect to the gas reactant and n-th order with respect to the liquid reactant) and instantaneous reaction in an adiabatic CSTR. Analytical conditions for uniqueness and possible multiplicity for the steady state were derived. It was shown that up to five steady state solutions are possible for the slow pseudo-first-order reaction and three for the fast (1,n)th order reaction. On

the other hand, uniqueness was shown for the instantaneous reaction. A conclusion was drawn that the possibility of five steady state solutions in gas-liquid CSTR is a direct consequence with liquid phase concentration of the gaseous reactant being non-zero (i.e. general reaction). Raghuram et al. (1979) considered a pseudo-first-order reaction in non-adiabatic gas liquid CSTR. Two cases were studied, a single CSTR and a cascade of n CSTRs with backflow. For a single CSTR, they observed a very narrow region of heat transfer coefficients within which five steady state solutions are possible. For the n CSTRs in series without backflow, when increasing the number of CSTRs, multiplicity was found to be destroyed. Finally, they analyzed two CSTRs in series with backflow and it was reported that when increasing the backflow up to five steady states were possible.

Huang and Varma (1981a) used the analytical solution of Hoffman et al. (1975) for a single second order gas-liquid reaction in a two phase CSTR. The experimental data of Ding et al. (1974) was used to test the model validity. The model agreement with the experimental data was quite good, however, the complex reaction model of Sharma et al. (1976) agreed better. They carried out reactor simulations and reported five steady state solutions for an adiabatic reactor case. It was found that a small heat loss from the reactor will reduce the number of steady state solutions to three. In another study, Huang and Varma (1981b) compared the steady state gas-liquid CSTR performance with a general second-order reaction versus, fast second-order reaction, general pseudo-first-order reaction and fast pseudo-first-order reaction. The fast second-order reaction model predicted the same reactor multiplicity patterns as those for the general second-order

reaction. However, the former predicted reactor steady state uniqueness when the value of the reaction activation energy dropped from 29000 to 20000 cal/mol unlike the general second-order case. The general pseudo-first-order reaction model predicted multiplicity regions agreeing well with those for the general second-order reaction, however, the multiplicity patterns differed significantly for the two cases. Finally, the fast pseudo-first-order reaction model was shown to be better than the fast second-order reaction model in the prediction of the multiplicity regions.

Huang and Varma (1981c) developed a mathematical model to predict the steady state and dynamic behavior of a non-adiabatic gas-liquid CSTR for the case of fast-pseudo-first order reactions. Necessary and sufficient criteria for the steady state uniqueness and multiplicity were derived. Analysis was carried out to provide necessary and sufficient conditions for the local reactor steady state stability. It was found that the occurrence of limit cycles (periodic oscillations) is usually not possible at least for the reaction model they considered. Singh et al. (1982) studied the effect of gas feed temperature on the regions of multiple steady states for a fast pseudo-first-order reaction in an adiabatic CSTR. For certain reactor parameters, an increase in gas feed temperature shrinks the multiplicity region until a point is reached above which a unique steady state is attained.

Shaikh and Varma (1984a) analyzed the steady state behavior of a non-adiabatic gas-liquid CSTR with a fast pseudo-first-order reaction. The effect of gas feed composition and the effect of gas-liquid interfacial area variation with temperature and

onversion was studied. It was shown that the size of multiplicity region increases as the reactant mole fraction increases in the gas feed. Large differences were discovered in the predictions of uniqueness and multiplicity if the effect of interfacial area variation is not taken into consideration, especially for solute-rich gas feeds. Shaikh and Varma (1984b) studied the liquid volatility effects for a general second-order reaction in a gas liquid CSTR. Their reactor model solution for volatile and non-volatile liquid cases were compared with the experimental data of Ding et al. (1974). The volatile liquid model predicted the experimental data better. They concluded that failing to account for the liquid reactant volatility in modeling gas-liquid CSTRs can lead to different predictions of the number and regions of multiple steady states.

Shaikh (1987) studied the effect of gas-side resistance on the steady state uniqueness and multiplicity for a pseudo-first-order reaction in a gas-liquid CSTR. It was proved that the likelihood of multiplicity decrease in the presence of this resistance. An upper bound of gas-side resistance was shown to exist beyond which multiplicity cannot arise. Shaikh et al. (1991) developed an approximate closed-form enhancement factor equation for a general second-order gas-liquid reaction with a volatile liquid. The earlier enhancement factor of Shaikh and Varma (1984b) involved repetitive tedious calculations. They demonstrated that errors in predicting the number and regions of uniqueness and multiplicity of steady states can arise when neglecting the volatility of the liquid reactant.

In all of the previous studies the *isothermal* film-theory model was used to model the local gas absorption problem in reactor design. In contrast, White and Johns (1986)

used the penetration theory to model a second-order nonvolatile gas-liquid reaction in a CSTR. They introduced the effect of surface temperature rise into gas-liquid reactor modeling and they established conditions under which it is important. By plotting the relative rate of absorption versus the chemical reactivity, they found that the steady state solutions of the reactor model can lie in five operating regions. In each of the five regions only one solution can be possible, hence at most five multiple steady state solutions for the reactor model are possible.

CHAPTER 3

GENERALIZED FILM MODEL

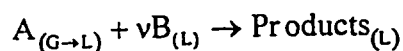
In the literature review presented earlier, the film and the penetration theories were extensively used to model nonisothermal reactive gas absorption. The film theory presented by Whitman (1923) assumes steady state profiles for concentrations of the gas and liquid reactants. These profiles are established instantaneously once the gas hits the surface of the liquid. Although the steady state assumption is physically unrealistic, the film theory explains the essential features for the gas dissolution, diffusion, reaction and transfer to the bulk liquid. Therefore, it is not unreasonable, at least for illustrative if not predictive purposes, to use the film theory to show the importance of heat effects in chemical gas absorption. Finally, no judgment can be made about which theory gives better predictions of the absorption behavior until solutions of both theories are compared carefully with each other and with experimental data.

3.1 *Film Theory and Physical Picture*

It is well known that for many systems in which physical absorption occurs, the temperature profile extends approximately ten times further into the liquid than the concentration profile. This is due to the fact that the thermal diffusivity is much greater in magnitude than the molecular diffusivity, i.e. $\alpha \gg D$. The effect of chemical reaction on

gas absorption is to increase the absorption rate and reduce the penetration depth of the absorbing gas. When the gas is dissolved in the liquid, heat of solution will be released in the gas liquid interface, and if the reaction is exothermic, an additional heat of reaction will also be released in the liquid phase. This results in an increase of the ratio of heat to mass transfer penetration depths. Therefore, for nonisothermal gas absorption with chemical reaction the thickness of the heat transfer film is greater than the thickness of the mass transfer film.

The following problem will be considered here, that a gas component A is absorbed into a liquid and reacts in the liquid phase with component B which is already present in the liquid phase. The following reaction stoichiometry will be considered :



The reaction is assumed to be m-th-order with respect to species A and n-th-order with respect to species B. Several subcases can be derived from this kinetics. A schematic diagram for the film model, general reaction regime case, is given in Figure 3.1. The figure shows the absorption of gas across the gas film through the gas-liquid interface, consequently, diffusion and reaction in the liquid films. Material and energy will be lost from the liquid films by means of convection to the gas phase and diffusion to the liquid phase. The bulk liquid phase is well mixed and there will be material and energy carry out by the flowing liquid. The bulk liquid reaction is introduced as there might be some

of the gas reactant in the bulk liquid phase. A schematic diagram for the concentration and temperature profiles is given in Figure 3.2.

3.2 *Model Assumptions*

The mathematical model for the film theory equations, given in the following subsection, was developed using the following assumptions:

1. The physical properties of the liquid phase such as density, heat capacity, and thermal conductivity are independent of temperature and conversion.
2. The interfacial resistance to mass transfer is negligible, and consequently Henry's law is applicable. In most gas-liquid systems this assumption is reasonable unless some type of emulsion is formed at the surface.
3. Bulk flow, Dufour effect (the heat transfer flux generated due to an established concentration gradient), and Soret effect (the mass transfer flux generated due to an established temperature gradient) are negligible. For highly soluble gases, the bulk flow effect becomes appreciable only for very small values of $(C_{Bb} D_{Bb} / \nu C_{Ai} D_{Ab})$; in other words, near the physical absorption regime (Ikemizu et al., 1978, 1979).
4. The temperature dependence of the diffusivities, solubility, chemical reaction rate constant, and Henry's law constant may be reasonably expressed over a wide range of temperatures as:

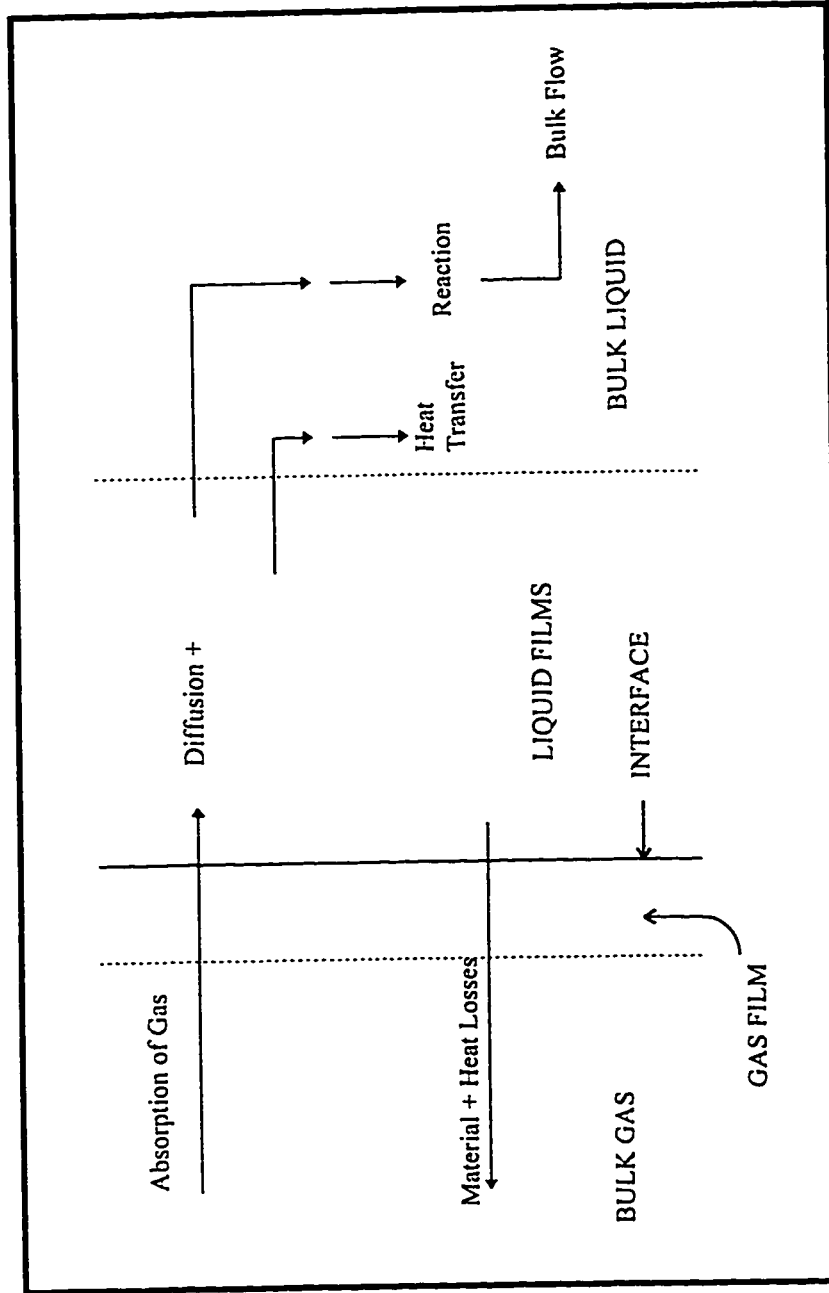


Figure 3.1 A Conceptual Model Describing Mass Transfer ,HeatTransfer and Chemical Reaction Phenomena in Chemical Gas Absorption .

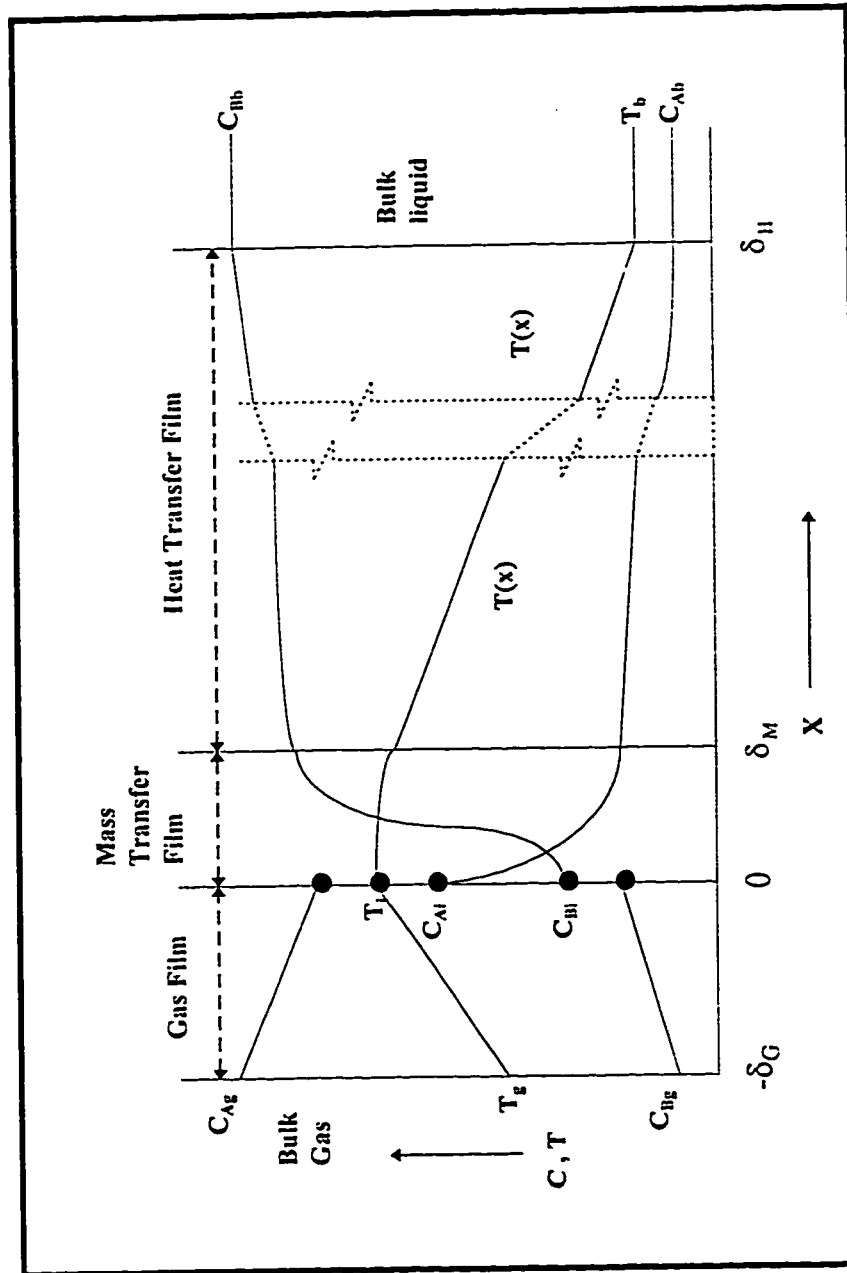


Figure 3.2 Proposed film model

$$D_A(T) = D_{Ab} \exp \left[-\frac{E_{DA}}{R} \left(\frac{1}{T} - \frac{1}{T_b} \right) \right] \quad (3.1)$$

$$D_B(T) = D_{Bb} \exp \left[-\frac{E_{DB}}{R} \left(\frac{1}{T} - \frac{1}{T_b} \right) \right] \quad (3.2)$$

$$C_{Ai}(T) = C_{Aib} \exp \left[+\frac{(-\Delta H_s)}{R} \left(\frac{1}{T} - \frac{1}{T_b} \right) \right] \quad (3.3)$$

$$k_{(m,n)}(T) = k_{(m,n)b} \exp \left[-\frac{E_R}{R} \left(\frac{1}{T} - \frac{1}{T_b} \right) \right] \quad (3.4)$$

$$H_B(T) = H_{Bb} \exp \left[-\frac{(\Delta H_v)}{R} \left(\frac{1}{T} - \frac{1}{T_b} \right) \right] \quad (3.5)$$

Where the heat of solution (ΔH_s), the heat of reaction (ΔH_R), and the activation energies E_{DA} , E_{DB} , and E_R are assumed independent of temperature and composition.

5. No chemical reaction occurs in the gas film.
6. The gas diffusivity of the liquid component in the gas film is independent of temperature and it is evaluated as follows :

$$D_{Bg}(T) = D_{Bg} \exp \left[-\frac{E_{DB}}{R} \left(\frac{1}{T_g} - \frac{1}{T_b} \right) \right] \quad (3.6)$$

7. The volumetric flow rates of the gas and liquid streams are constant throughout the reactor.

3.3 Model Equations

The differential equations which describe the simultaneous reaction, diffusion, and conduction in the liquid side are given by:

$$\frac{d}{dx} \left[D_A(T) \frac{dC_A}{dx} \right] - k_{(m,n)}(T) C_A^m C_B^n = 0 \quad (3.7)$$

$$\frac{d}{dx} \left[D_B(T) \frac{dC_B}{dx} \right] - \nu k_{(m,n)}(T) C_A^m C_B^n = 0 \quad (3.8)$$

$$\frac{d^2 T}{dx^2} + \frac{(-\Delta H_R)}{K_L} k_{(m,n)}(T) C_A^m C_B^n = 0 \quad (3.9)$$

Two sets of concentration and temperature boundary conditions are necessary to complete the description of the problem. The first set as usual represents what happens at the gas-liquid interface, i.e. at $x = 0$:

$$C_A = C_{Ai}(T) = C_{Aib} \exp \left[+ \frac{(-\Delta H_S)}{R} \left(\frac{1}{T} - \frac{1}{T_b} \right) \right] \quad (3.10)$$

$$D_B(T) \frac{dC_B}{dx} = k_{GB} H_B(T) (C_B - C_{BG}) \quad (3.11)$$

$$\begin{aligned}
 (-\Delta H_s) \left[-D_A(T) \frac{dC_A}{dx} \right] = & -K_L \frac{dT}{dx} + h_G (T - T_G) \\
 & + (+\Delta H_v) \left[D_B(T) \frac{dC_B}{dx} \right]
 \end{aligned}
 \quad (3.12)$$

The gas solubility is inversely related to temperature as described by Equation (3.10). Equation (3.11) indicates that the liquid reactant is volatile so that material loss will take place from the liquid-side interfacial region to the gas-side interfacial region. Equation (3.12) is a heat balance around the gas-liquid interface: the heat of solution which results from dissolution of component A is partly conducted to the liquid side, partly convected towards the gas side, and the last part contributes to the vaporization of component B.

The other set of boundary conditions is more appropriately written for a general reaction case at the outer edge of the heat transfer film, i.e. at $x = \delta_H$:

$$C_B = C_{Bb} \quad (3.13)$$

$$-a D_A(T) \frac{dC_A}{dx} = k_{(m,n)}(T) C_A^m C_B^n (V_L - a \delta_H) + F_L (C_A - C_{A0}) \quad (3.14)$$

$$-a K_L \frac{dT}{dx} = (-\Delta H_R) k_{(m,n)} C_A^m C_B^n (V_L - a \delta_H) + F_L \rho_L c_{pL} (T - T_0) \quad (3.15)$$

Equations (3.14) and (3.15) are material and heat balances around the bulk liquid, respectively. Equation (3.14) states that the amount of species A leaving the heat transfer film can react in the bulk liquid and in a continuous-flow system can leave with the exit liquid stream. Equation (3.15) on the other hand indicates that the thermal state of the bulk liquid is due to three sources: the heat conducted from the film side, the heat released due to reaction in the bulk liquid, and the heat carried by the incoming liquid feed. Note that the term $(V_L - a\delta_H)$ is the volume of the bulk liquid beyond the heat transfer film. Note also that in deriving conditions (3.14) and (3.15), the bulk liquid is assumed to be perfectly-mixed. This assumption is consistent with the film theory and it has been used to model the liquid phase in agitated and nonagitated gas-liquid reactors.

In order to quantify the importance of heat effects in gas-liquid reactions, we introduce at this stage the nonisothermal enhancement factor, E_{non}^* , which is defined as the ratio of the actual rate of nonisothermal gas absorption to the isothermal rate of physical gas absorption (i.e. in the absence of heat and volatility effects):

$$E_{\text{non}}^* = \frac{-D_A(T_i) \left[\frac{dC_A}{dx} \right]_{x=0}}{k_l^0 C_{Aib}} \quad (3.16)$$

The term in the denominator is based on the results of the classic isothermal film theory, therefore the mass-transfer coefficient is $k_l^0 = D_{Ab} / \delta_M$.

Equations from (3.7) through (3.15) are written for the liquid films domain (i.e. from $x = 0$ to $x = \delta_H$), however, C_{BG} was introduced. To make the problem complete, other material and energy balances need to be written for the gas film domain (i.e. from $x_g = -\delta_g$ to $x_g = 0$) to obtain C_{BG} . *This is done here for the first time, as unfortunately, in recent previous studies C_{BG} was chosen arbitrarily.* Detailed derivation of the gas film equations is given in Appendix A. Using the simplifying assumptions 5, 6 and 7, the following simplified material balance can be written for component B in the gas film:

$$\frac{d^2 C_{Bg}}{dx_g^2} = 0 \quad (3.17)$$

where the subscript g indicates the gas film domain. Two boundary conditions are needed for equation (3.17) :

at $x_g = -\delta_g$:

$$aD_{Bg} \frac{dC_{Bg}}{dx_g} = F_g (C_{Bg} - C_{Bg0}) \quad (3.18)$$

and at $x_g = 0$

$$C_{Bg} = C_{Bgi} \quad (3.19)$$

where C_{Bg0} is the concentration of the liquid reactant in the fresh (feed) gas stream and C_{Bgi} is the interfacial concentration of the liquid reactant in the gas domain. Equation (3.17) with boundary conditions (3.18) and (3.19) constitute a linear boundary value problem which can be solved analytically. Detailed analytical solution of equations

(3.17), (3.18) and (3.19) is given in Appendix A. From the analytical solution, the bulk gas composition of the liquid reactant can be obtained as follows :

$$C_{Bg}(-\delta_g) = \frac{C_{Bgi} + \frac{F_g \delta_g}{aD_{Bg}} C_{Bgo}}{1 + \frac{F_g \delta_g}{aD_{Bg}}} \quad (3.20)$$

where $C_{Bg}(-\delta_g) = C_{BG}$ (in equation (3.11)). If the fresh gas stream carries no liquid reactant equation (3.20) simplifies to :

$$C_{Bg}(-\delta_g) = \frac{C_{Bgi}}{1 + \frac{F_g \delta_g}{aD_{Bg}}} \quad (3.21)$$

Equation (3.21) can be substituted in equation (3.11) to replace C_{BG} , and as a result equation (3.11) can be rewritten as follows:

$$D_B(T) \frac{dC_B}{dx} = k_{GB} H_B(T) \left(C_B - \frac{C_{Bgi}}{1 + \frac{F_g \delta_g}{aD_{Bg}}} \right) \quad (3.22)$$

3.4 Dimensionless Form of Film-Model Equations

In order to cast the preceding set of equations in dimensionless form, a number of dimensionless variables and groups must be introduced. The basic variables and groups introduced are given in Table 3.1. Consequently, the governing differential equations become:

$$\frac{d}{dX} \left[\exp \left[\varepsilon_{DA} \left(\frac{\theta}{1+\theta} \right) \right] \frac{dA}{dX} \right] - Le M \exp \left[\varepsilon_R \left(\frac{\theta}{1+\theta} \right) \right] A^m B^n = 0 \quad (3.24)$$

$$\frac{d}{dX} \left[\exp \left[\varepsilon_{DB} \left(\frac{\theta}{1+\theta} \right) \right] \frac{dB}{dX} \right] - Le S M \exp \left[\varepsilon_R \left(\frac{\theta}{1+\theta} \right) \right] A^m B^n = 0 \quad (3.25)$$

$$\frac{d^2\theta}{dX^2} + Le M \beta_R \exp \left[\varepsilon_R \left(\frac{\theta}{1+\theta} \right) \right] A^m B^n = 0 \quad (3.26)$$

and the boundary conditions become:

X=0:

$$A = \exp \left[-\varepsilon_s \left(\frac{\theta}{1+\theta} \right) \right] \quad (3.27)$$

$$\exp \left[\varepsilon_{DB} \left(\frac{\theta}{1+\theta} \right) \right] \frac{dB}{dX} = Bi_M \sqrt{Le} \exp \left[\varepsilon_v \left(\frac{\theta}{1+\theta} \right) \right] \left(B - \frac{B}{1+\omega} \right) \quad (3.28)$$

$$\beta_s \exp \left[\varepsilon_{DA} \left(\frac{\theta}{1+\theta} \right) \right] \frac{dA}{dX} = \frac{d\theta}{dX} - Bi_H (\theta - \theta_G) - \beta_v \exp \left[\varepsilon_{DB} \left(\frac{\theta}{1+\theta} \right) \right] \frac{dB}{dX} \quad (3.29)$$

X=1:

$$B = 1 \quad (3.30)$$

$$-\exp\left[\varepsilon_{DA}\left(\frac{\theta}{1+\theta}\right)\right] \frac{dA}{dX} = M Le (\alpha'-1) \exp\left[\varepsilon_R\left(\frac{\theta}{1+\theta}\right)\right] A^m B^n + \beta' \sqrt{Le} (A - A_0) \quad (3.31)$$

$$-\frac{d\theta}{dX} = M \beta_R Le (\alpha'-1) \exp\left[\varepsilon_R\left(\frac{\theta}{1+\theta}\right)\right] A^m B^n + \gamma' (\theta - \theta_0) \quad (3.32)$$

and the enhancement factor becomes:

$$E_{\text{non}}^* = -Le \exp\left[\varepsilon_{DA}\left(\frac{\theta_i}{1+\theta_i}\right)\right] \left[\frac{dA}{dX}\right]_{X=0} \quad (3.33)$$

where θ_i is the dimensionless interfacial temperature. It should be noted that in the subsequent numerical computations the dimensionless ratio of the heat to mass transfer film thickness has been related to the Lewis number in accordance with the analysis of (Al-Ubaidi et al., 1990):

$$\frac{\delta_H}{\delta_M} = \sqrt{Le} = \sqrt{\frac{\alpha}{D_A}} \quad (3.34)$$

There are three nonisothermal film theory models which can be derived as subcases of the present model. Those models considered fast, second-order, nonisothermal gas-liquid reactions and their analysis was confined within the mass transfer film. Bhattacharya et al. (1988) considered a nonvolatile liquid with constant gas diffusivities, Al-Ubaidi et al. (1990) also considered a nonvolatile liquid and finally, Al-Ubaidi and Selim (1992) considered a volatile liquid. The latter two models introduced a

Table 3.1. Definition of Dimensionless Variables and Groups

<u>Dimensionless Variable/Group</u>	<u>Definition</u>
A	$\frac{C_A}{C_{Aib}}$
A_0	$\frac{C_{A0}}{C_{Aib}}$
B	$\frac{C_{B0}}{C_{Bb}}$
X	$\frac{x}{\delta_H}$
θ	$\frac{T - T_b}{T_b}$
θ_0	$\frac{T_0 - T_b}{T_b}$
θ_G	$\frac{T_G - T_b}{T_b}$
Bi_M	$\frac{k_{GB} H_B \delta_M}{D_{Bb}}$
Bi_H	$\frac{h_G \delta_H}{K_L}$
M	$\frac{k_{(m,n)} D_{Ab} C_{Aib}^m C_{Bb}^{(n-1)}}{k_f^2}$
S	$\frac{\nu D_{Ab} C_{Aib}}{D_{Bb} C_{Bb}}$
α'	$\frac{V_L}{a \delta_{II}}$

Table 3.1. Definition of Dimensionless Variables and Groups (continued)

<u>Dimensionless Variable/Group</u>	<u>Definition</u>
β'	$\frac{F_L \delta_M}{a D_{Ab}}$
γ'	$\frac{F_L \rho_L c_p \delta_H}{a K_L}$
β_R	$\frac{(-\Delta H_R) D_{Ab} C_{Aib}}{K_L T_b}$
β_S	$\frac{(-\Delta H_S) D_{Ab} C_{Aib}}{K_L T_b}$
β_V	$\frac{(\Delta H_V) D_{Bb} C_{Bb}}{K_L T_b}$
ε_{DA}	$\frac{E_{DA}}{R T_b}$
ε_{DB}	$\frac{E_{DB}}{R T_b}$
ε_R	$\frac{E_R}{R T_b}$
ε_S	$\frac{(-\Delta H_S)}{R T_b}$
ε_V	$\frac{(+\Delta H_V)}{R T_b}$
ω	$\frac{F_g \delta_g}{a D_{Bg}}$

zero concentration for the gas reactant at the edge of the mass transfer film as a representation of fast reactions, and further they assumed linear temperature profiles in the region between the mass and heat transfer films. The former used a more convenient representation of fast reactions by adapting a zero gradient for the gas reactant concentration at the edge of the mass transfer film and included convective heat loss to the gas phase. There can be seen some simplifications in those models which upon ignorance can lead to misleading results in estimating the enhancement factor and the rate of gas absorption which is essential for gas-liquid reactor design.

The proposed model is more realistic because it includes mass and energy balances in the region between the mass and heat transfer films. It has to be mentioned that four new parameters are introduced in the current model, namely, ω , α' , β' and γ' . The parameter ω determines the composition of the liquid reactant in the bulk gas phase after evaporation and it can be estimated from the gas side mass transfer coefficient ($k_g = \frac{D_{Bg}}{\delta_g}$), the interfacial area, and the gas flow rate (or gas residence time). If the gas residence time is small then ω becomes high and, consequently, the bulk gas phase composition for the liquid reactant becomes small and vice versa. Parameters α' , β' and γ' are the bulk liquid phase reaction parameters. α' is the ratio of the volume of the bulk liquid phase after the heat transfer film to the volume of the heat transfer film and it accounts for the consumption of the gas reactant in the bulk liquid phase and the accompanying heat generation there. Asymptotically, α' ranges from unity to a very high

number, if α' equals unity, then the contribution of the gas reactant consumption and heat generation (for the exothermic case) in the bulk liquid phase is very small and if it is very high the contribution becomes major. On the other hand, β' accounts for the loss of the gas reactant from the bulk liquid phase by the flowing bulk liquid stream. If the liquid residence time is very small, then β' is very high and its contribution becomes important and vice versa. Finally, γ is also related to the liquid residence time and it account for the energy loss in the bulk liquid phase by the flowing bulk liquid stream. If the liquid residence time is very small, then β' is very high and the energy loss from the bulk liquid phase is very high and vice versa.

3.5 *The Asymptotic Behavior of the New Model*

In the previous literature review chapter it was shown that most of the previous studies considered special cases in modeling local gas-liquid reactions. Those cases can be asymptotically derived as subcases from the present model, including isothermal, fast, first-order reactions, second-order reactions and nonvolatile gas-liquid reactions. The current model considers heat effects, general reaction regime, (m,n)th-order reaction kinetics, and a volatile liquid. All of these generalizations make the model applicable to many practical gas-liquid reaction systems, and failing to account to one of them might lead to errors in the results in estimating the enhancement factor and hence the rate of gas absorption. Also, failing to account for such generalizations might affect the possibility of steady state multiplicity, the regions of multiple steady states and the number of steady

state solutions. Figure 3.3 shows a schematic which shows the asymptotic behavior of the proposed general model.

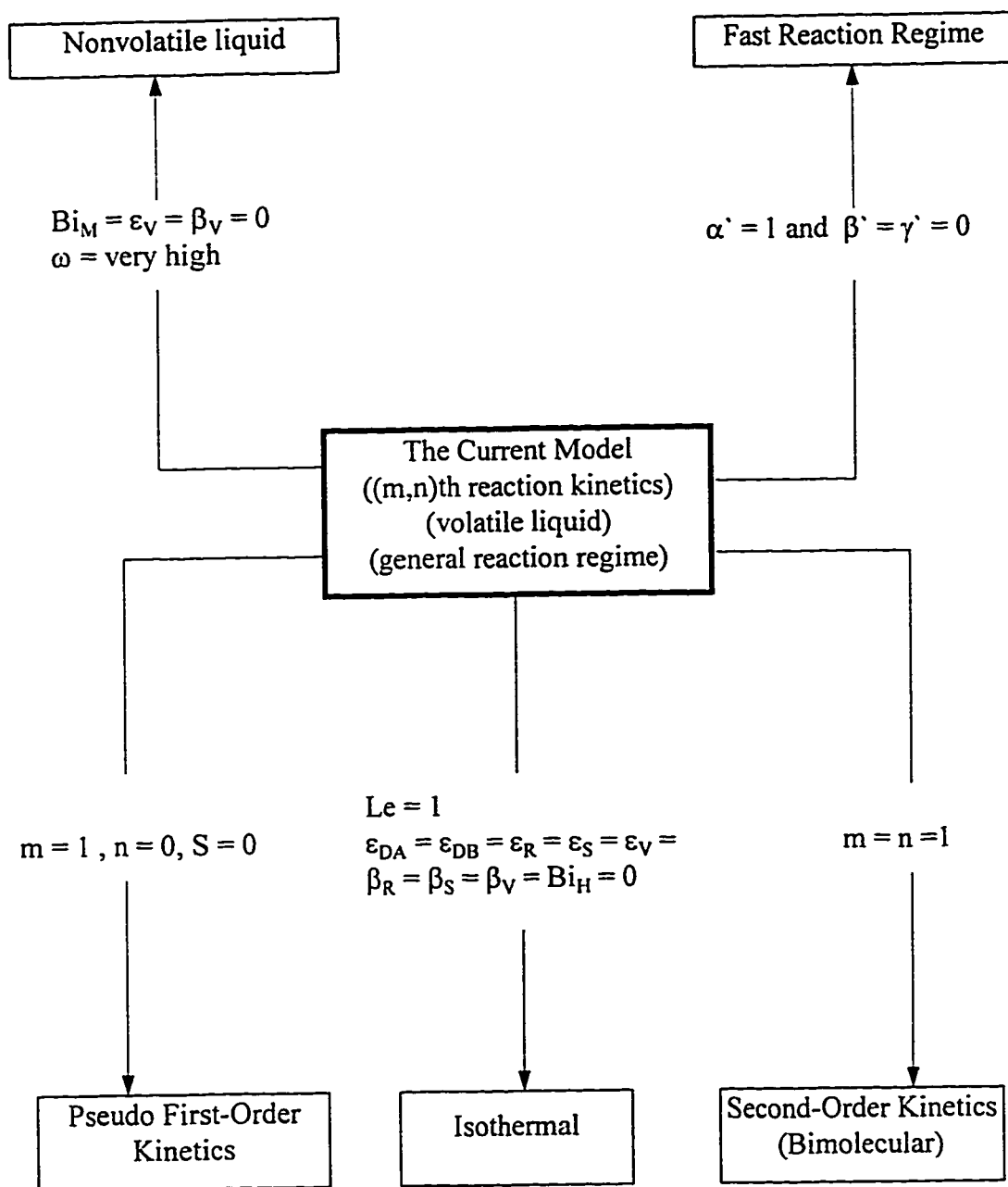


Figure 3.3 The Asymptotic Behavior of the New Model

CHAPTER 4

RESULTS AND DISCUSSION :

SOLUTION AND INVESTIGATION OF THE FILM THEORY MODEL

Having introduced the generalized film theory model in chapter 3, it will be solved in this chapter. The model consists of three coupled second order differential equations, constituting a nonlinear boundary value problem. The model will be solved numerically and the possibility of steady state multiplicity will be investigated. A parametric study will be conducted to study the sensitivity of the model parameters. Also, some of the model parameters will be lumped together and the boundaries for steady state multiplicity for the lumped parameters will be determined. Finally, the model will be applied to some industrial gas-liquid reactions.

4.1 *Solution Method*

The film model equations will be solved using the software packages COLNEW and AUTO, both consisting of collection of subroutines coded in FORTRAN. COLNEW developed by Ascher (1981) is designed for boundary value problems using the method of orthogonal collocations on finite elements. It solves mixed order ODEs and is powerful for stiff systems, however, it fails to find multiple solutions. AUTO developed by Doedel (1981) is designed as a numerical continuation and bifurcation technique. It deals with

nonlinear equations in the form of algebraic systems and ODEs. It uses the method of orthogonal collocations on finite elements for solving ODEs. The Newton-Chord method is used to solve the nonlinear algebraic equations which result from discretization.

COLNEW will be implemented to solve the model equations at a region where a single solution is available. Consequently, the output will be used as an initial guess for AUTO which will continue the solution by changing the bifurcation parameter and searching for multiple solutions for the model equations.

4.2 Model Solution for Some Typical Model Parameters

A typical gas-liquid reaction model parameters combination is shown in Table 4.1. These parameters are applicable to nonisothermal, second-order, and general reactions with a volatile liquid. The results are demonstrated in Figures 4.1 to 4.8. These parameter combinations lead to the existence of multiple steady state solutions for the film theory model. An S-shaped multiplicity pattern is predicted with a maximum of three steady state solutions, two stable branches and one unstable branch. The multiplicity region exists between Hatta number value of 0.652 and 2.569, whereas outside this region only a single solution exists.

Figure 4.1 shows the enhancement factor versus the Hatta number, on which it is shown that the enhancement factor can reach an asymptotic value of 118 at high values of Hatta number. For low values of Hatta number the enhancement factor becomes less than unity which indicates that the chemical gas absorption is less than the maximum rate of physical gas absorption. In Figure 4.2 the dimensionless surface temperature rise versus

Table 4.1 Typical Film Theory Model Parameters Used for Parametric Study

Parameter	Value
m	1
n	1
S	0.01
ϵ_{DA}	3.0
ϵ_{DB}	3.0
ϵ_R	20.0
ϵ_S	4.0
ϵ_V	2.0
β_R	0.005
β_S	0.001
β_V	0.001
Bi_M	0.8
Bi_H	0.6
Le	100.0
α'	20.0
β'	1.0
γ'	1.0
θ_G	0.0
θ_0	0.0
A_0	0.0
ω	0.9013

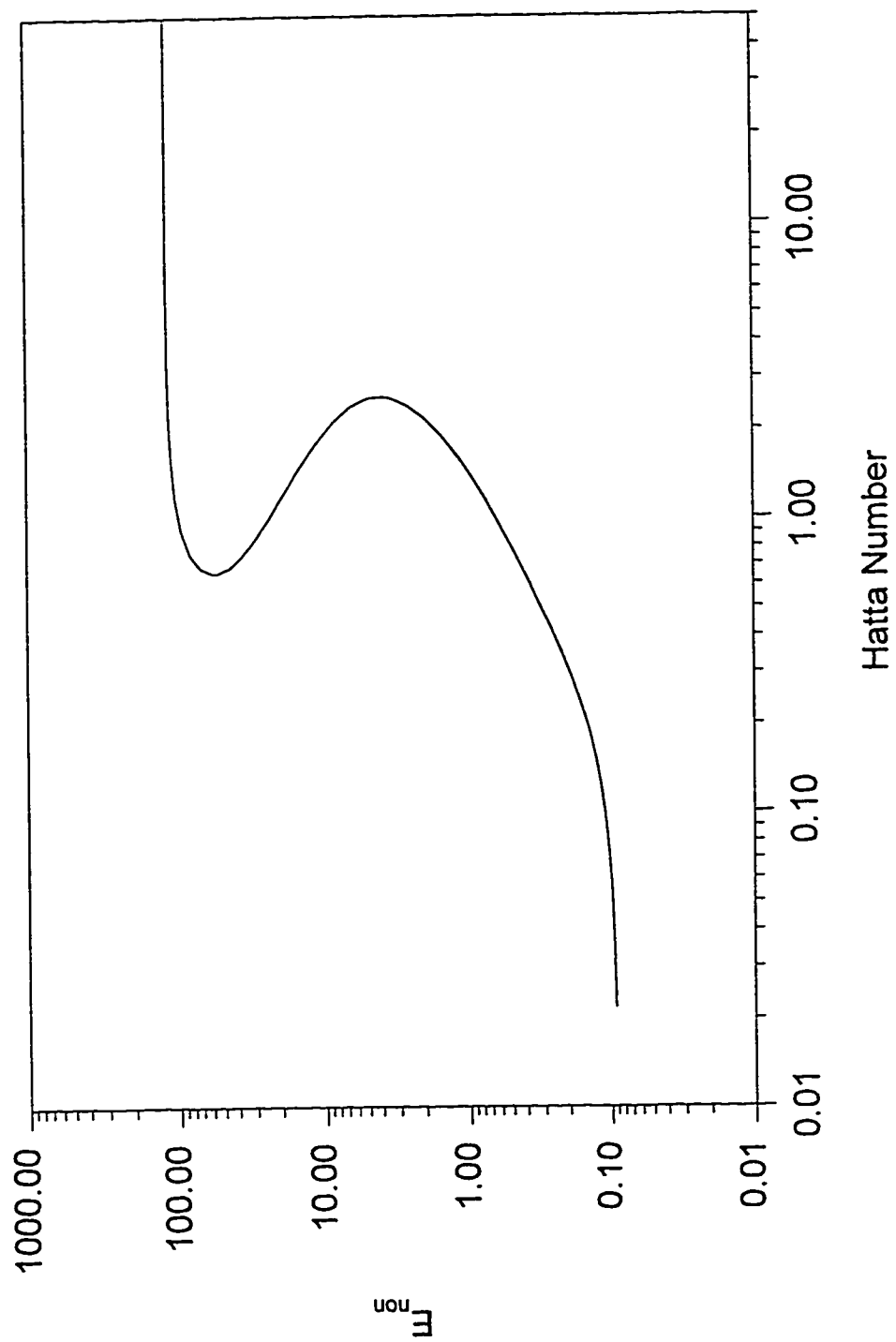


Figure 4.1 The Nonisothermal Enhancement Factor Versus The Hatta Number
for the Basic Model Parameters

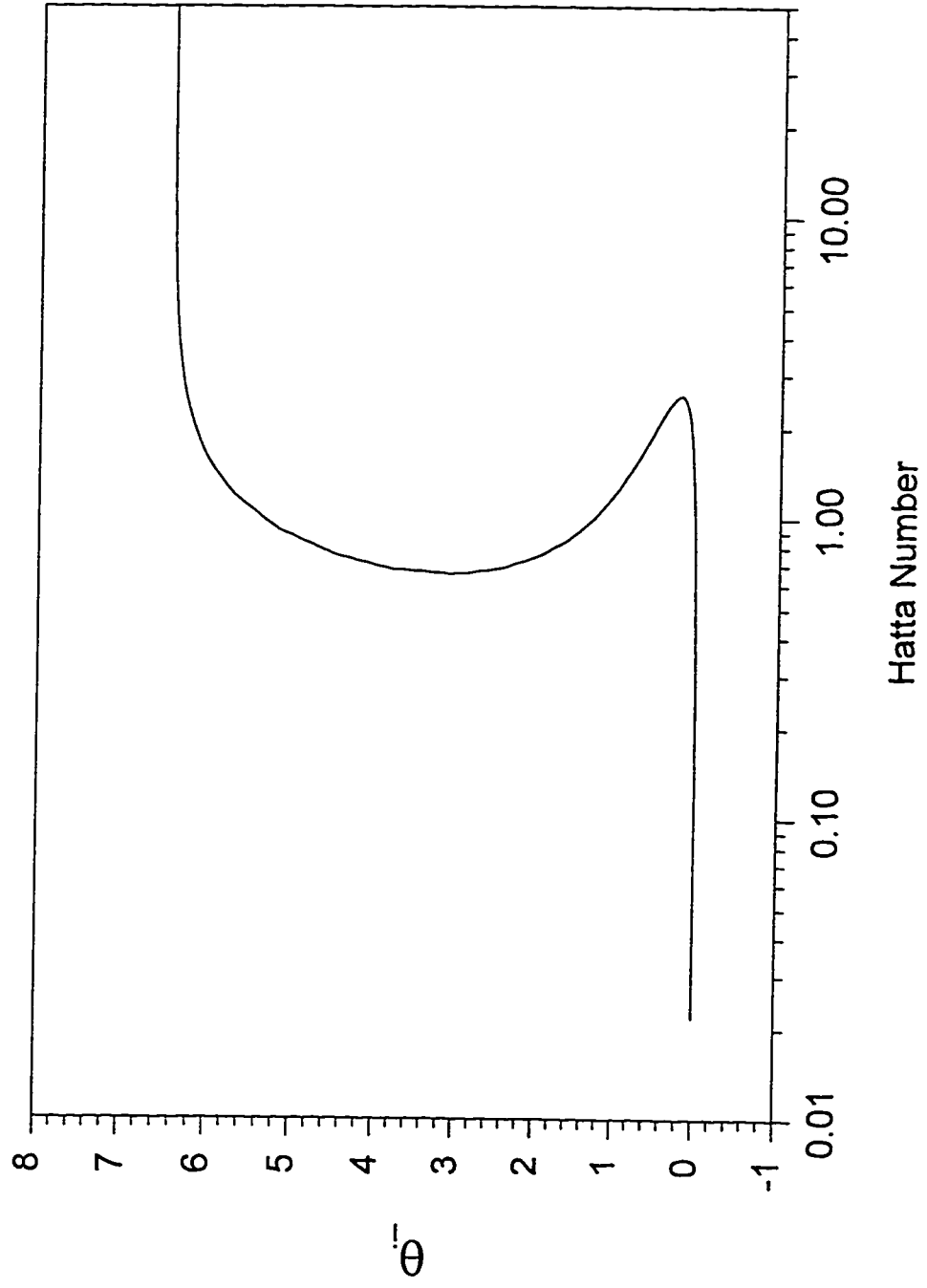


Figure 4.2 The Surface Temperature Rise Versus The Hatta Number for the Basic Model Parameters

the Hatta number is shown. The dimensionless surface temperature rise reaches an asymptotic value of 6.6 at high values of the Hatta number. At low values of the Hatta number the dimensionless surface temperature rise is negligible.

The concentration and temperature profiles across the heat transfer film are shown in Figures 4.3, 4.4, 4.5, 4.6, 4.7 and 4.8 for different values of Hatta number, 0.0, 0.355, 2.569, 0.991, 0.652 and 50.17 respectively. The choice of these Hatta number values is taken such that the first two values are from the first multiplicity branch, and the third value is the first limit point of the bifurcation diagram. The fourth value is taken from the second unstable multiplicity branch, and the fifth value is the second limit point of the bifurcation diagram, and finally, $\sqrt{M} = 50.17$ is taken from the third multiplicity branch.

The dimensionless temperature rise across the heat transfer film averages zero, 0.01, 0.16, 1.03, 2.4 and 5.1 for the Hatta numbers 0.0, 0.355, 2.569, 0.991, 0.652 and 50.17, respectively. It appears that the heat effects are important for the set of parameters selected to conduct this study. For the same Hatta number values, the dimensionless interfacial concentrations for the gas reactant attain the following values 1.0, 0.96, 0.48, 0.04, negligible and zero, respectively. At the edge of the heat transfer film the dimensionless concentrations for the gas reactant become 0.1 and zero for first and second Hatta number values respectively. However, the dimensionless concentration for component A becomes zero at X equals 0.1 and it drops very fast to zero for the third and fourth Hatta numbers, respectively, and it becomes essentially zero for the last two Hatta numbers. The dimensionless interfacial concentration for the liquid reactant is 0.21, 0.21,

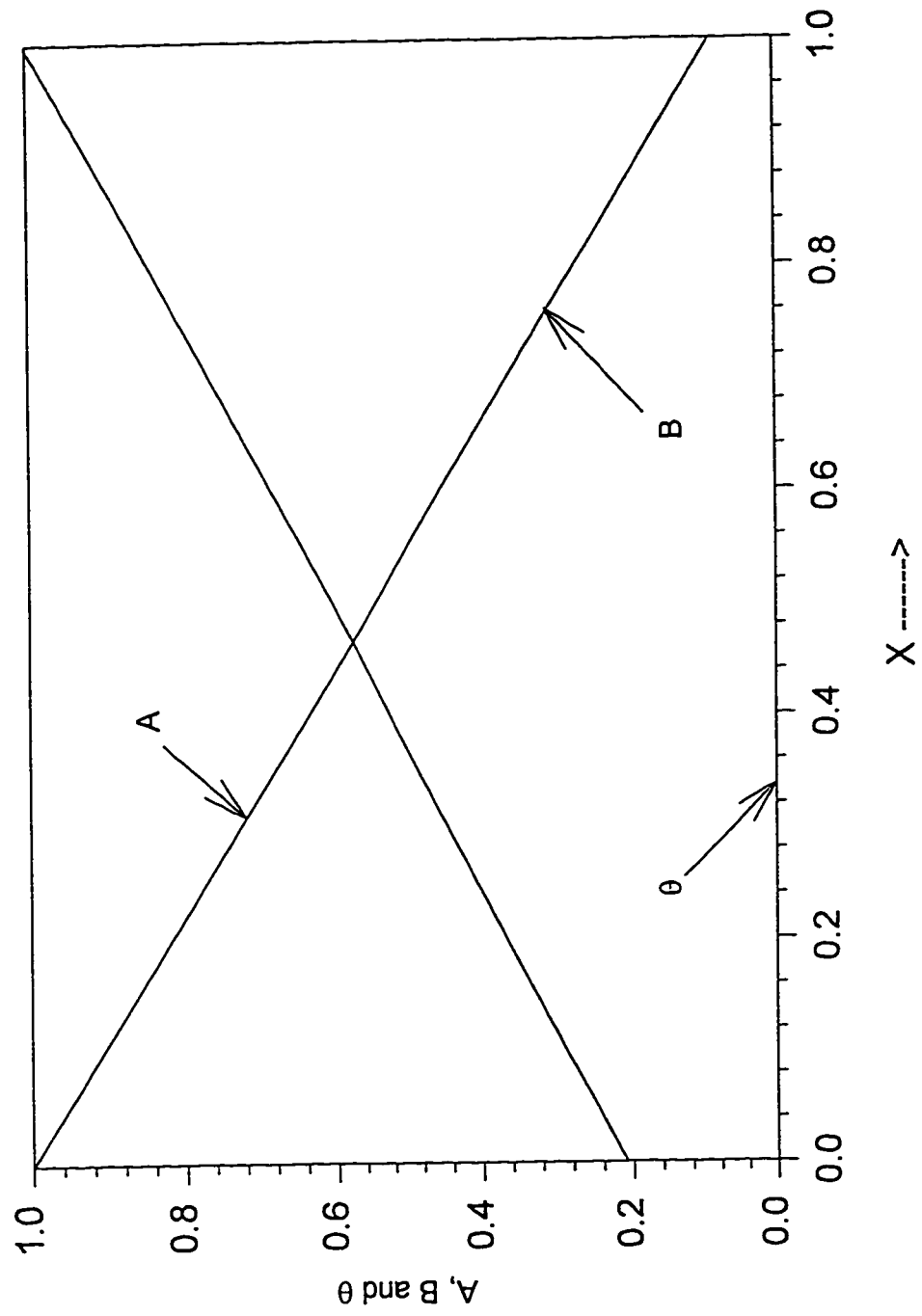


Figure 4.3 Model Prediction for the Concentration and Temperature Profiles for the

Basic Model Parameters, $\sqrt{M} = 0.0$

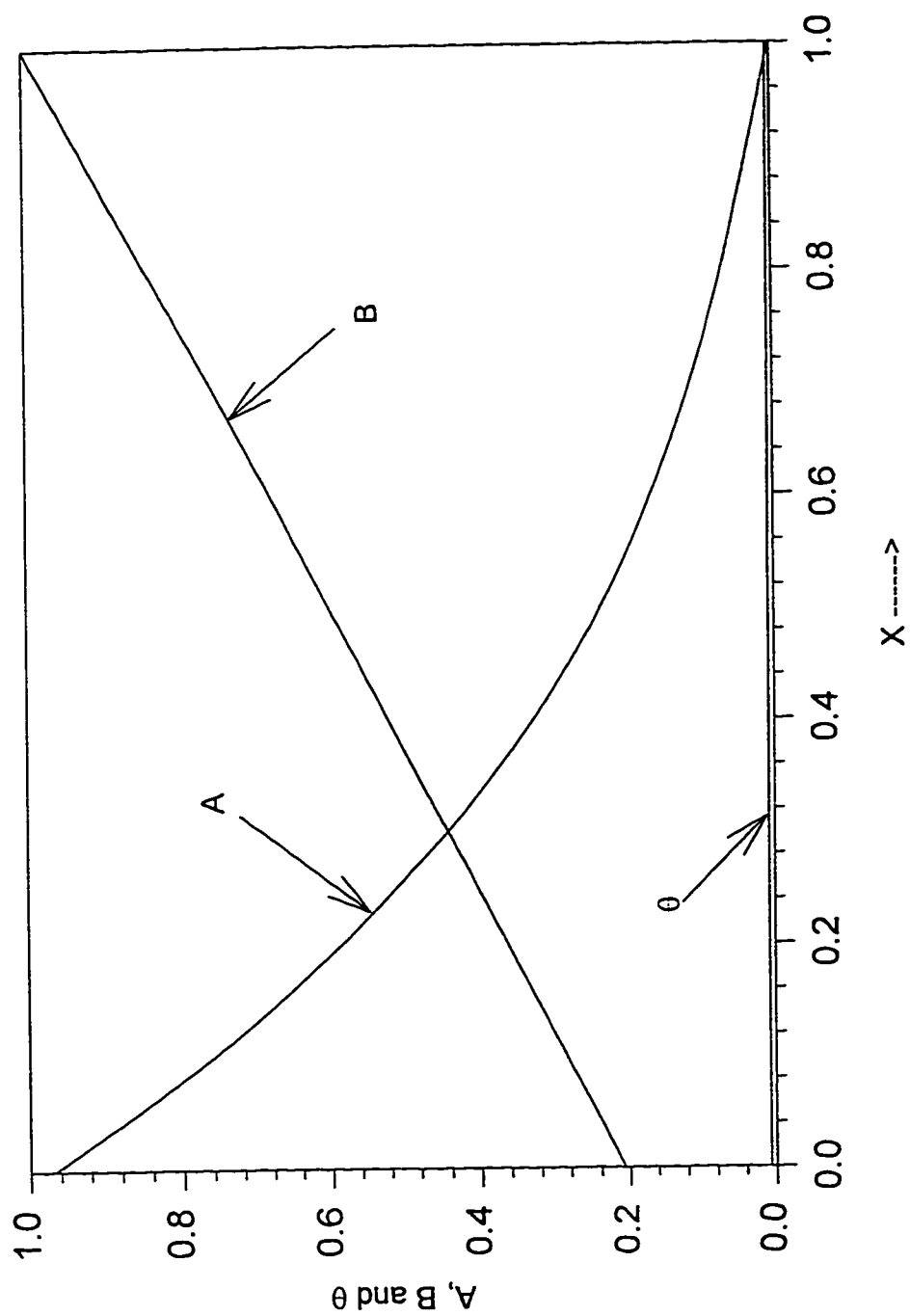


Figure 4.4 Model Prediction for the concentration and Temperature Profiles for the
Basic Model Parameters, $\sqrt{M} = 0.355$

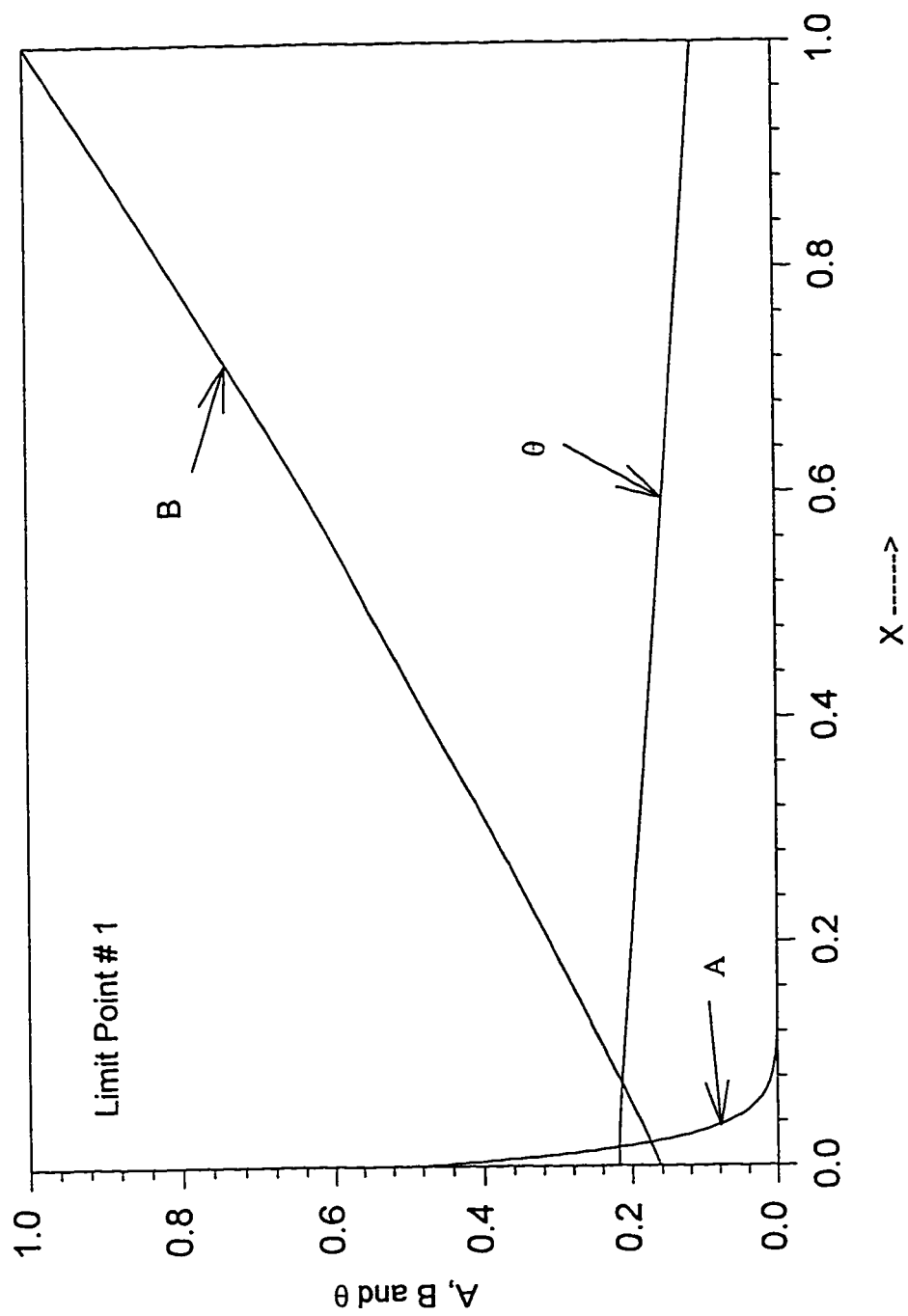


Figure 4.5 Model Prediction for the Concentration and Temperature Profiles for the
Basic Model Parameters, $\sqrt{M} = 2.569$

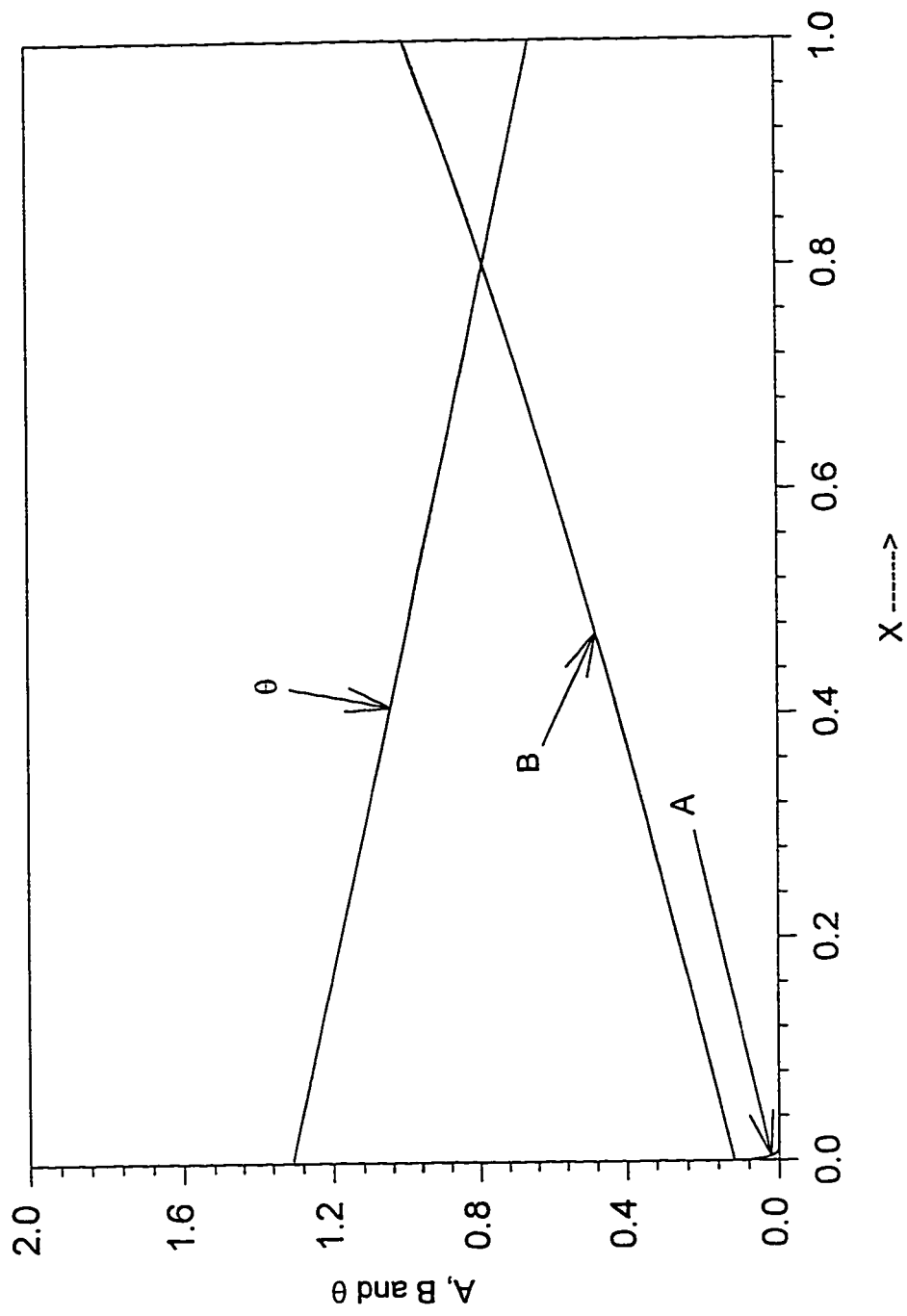


Figure 4.6 Model Prediction for the Concentration and Temperature Profiles for the

Basic Model Parameters, $\sqrt{M} = 0.991$

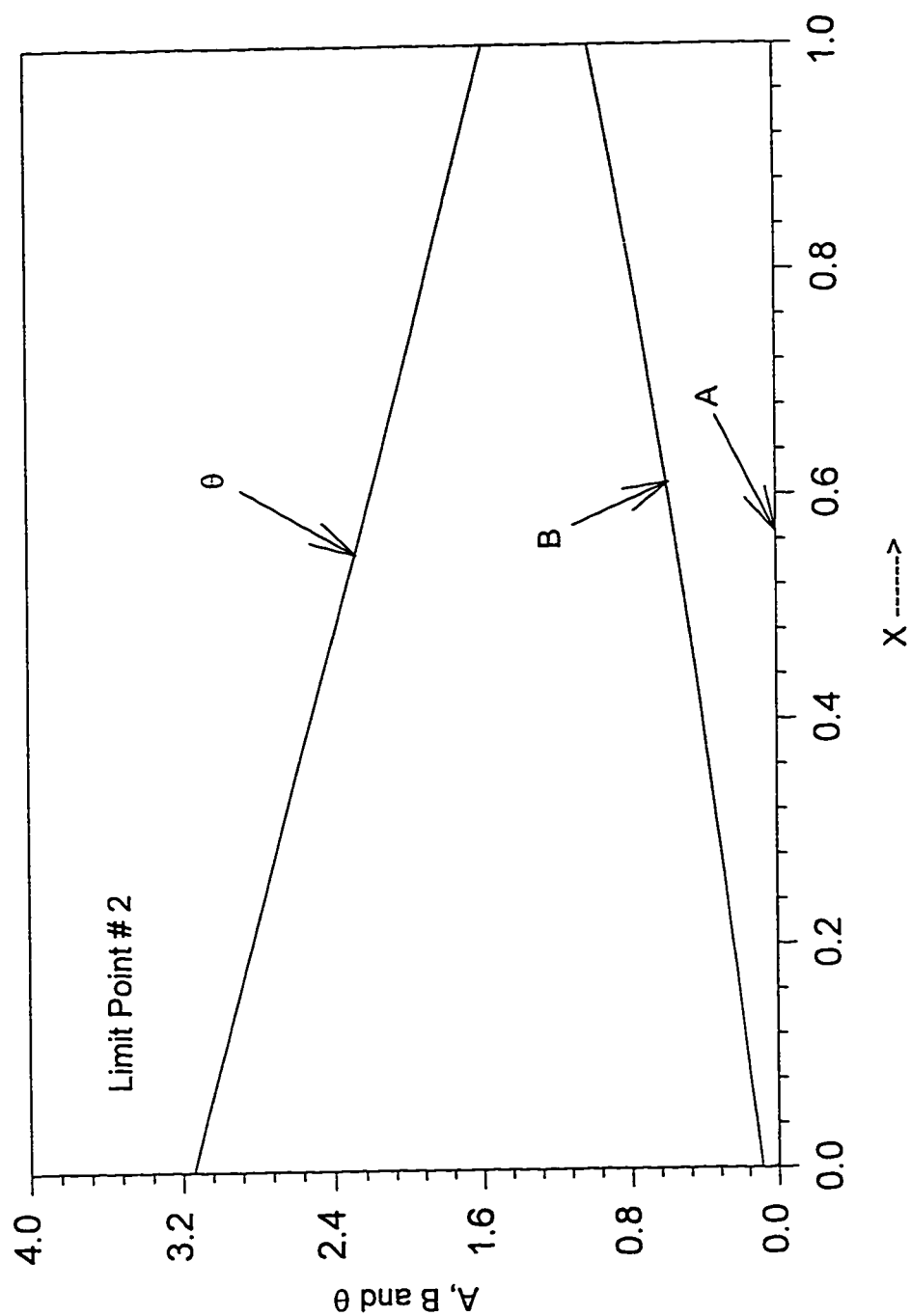


Figure 4.7 Model Prediction for The Concentration and Temperature Profiles for the

Basic Model Parameters, $\sqrt{M} = 0.652$

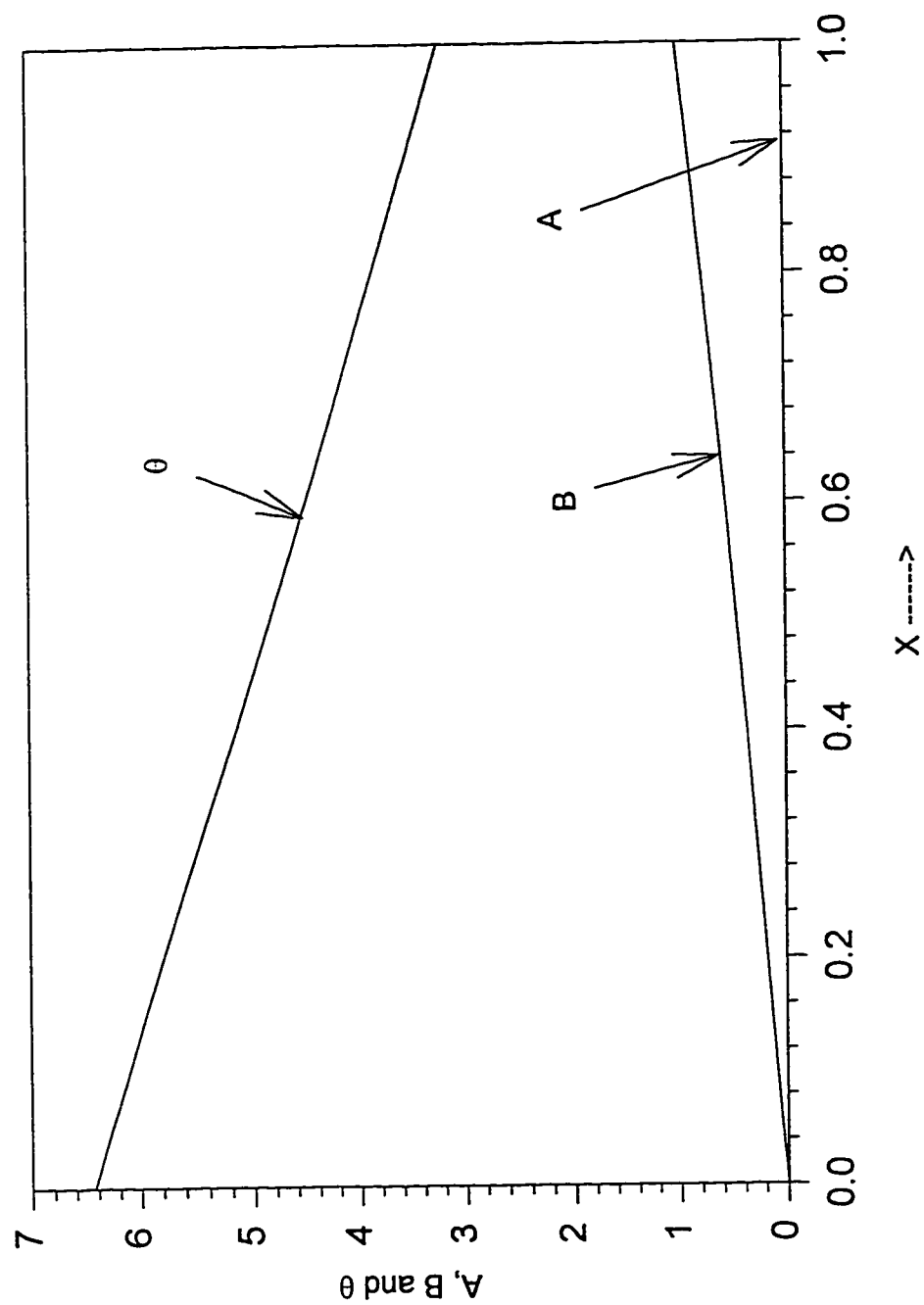


Figure 4.8 Model Prediction for the Concentration and Temperature Profiles for the Basic Model Parameters, $\sqrt{M} = 50.17$

0.16, 0.06, 0.02 and 0.0 for Hatta numbers 0.0, 0.355, 2.569, 0.991, 0.652 and 50.17, respectively.

It appears that the heat effects become more important and the reaction regime changes from slow to fast and to instantaneous as we move to trace the multiplicity branches from the first, second to the third branch.

4.3 Parametric Study

In this section a parametric study is carried out to test the sensitivity of the model to different model parameters. The typical model parameters in Table 4.1 are used to conduct this study, and the Hatta number, \sqrt{M} , will always be used as a free bifurcation parameter. The influence of changing the Hatta number from a small value to high value on the enhancement factor will be demonstrated. Consequently, calculations are repeated by changing a certain parameter while keeping others constant to see the effect of this parameter on the behavior of the enhancement factor versus the Hatta number. The effect of model parameters on the enhancement factor is demonstrated in this parametric study, because the enhancement factor determines the rate of chemical gas absorption and it is very important for reactor design calculations as will be seen in Chapter 5.

4.3.a The Effect of Reaction Orders and the Stoichiometry Parameter

Figure 4.9 shows the effect of changing the reaction orders. When the reaction order for the liquid reactant becomes zero, i.e. a pseudo-first-order reaction ($m = 1$, $n = 0$), the enhancement factor is increased dramatically especially at high values of the Hatta

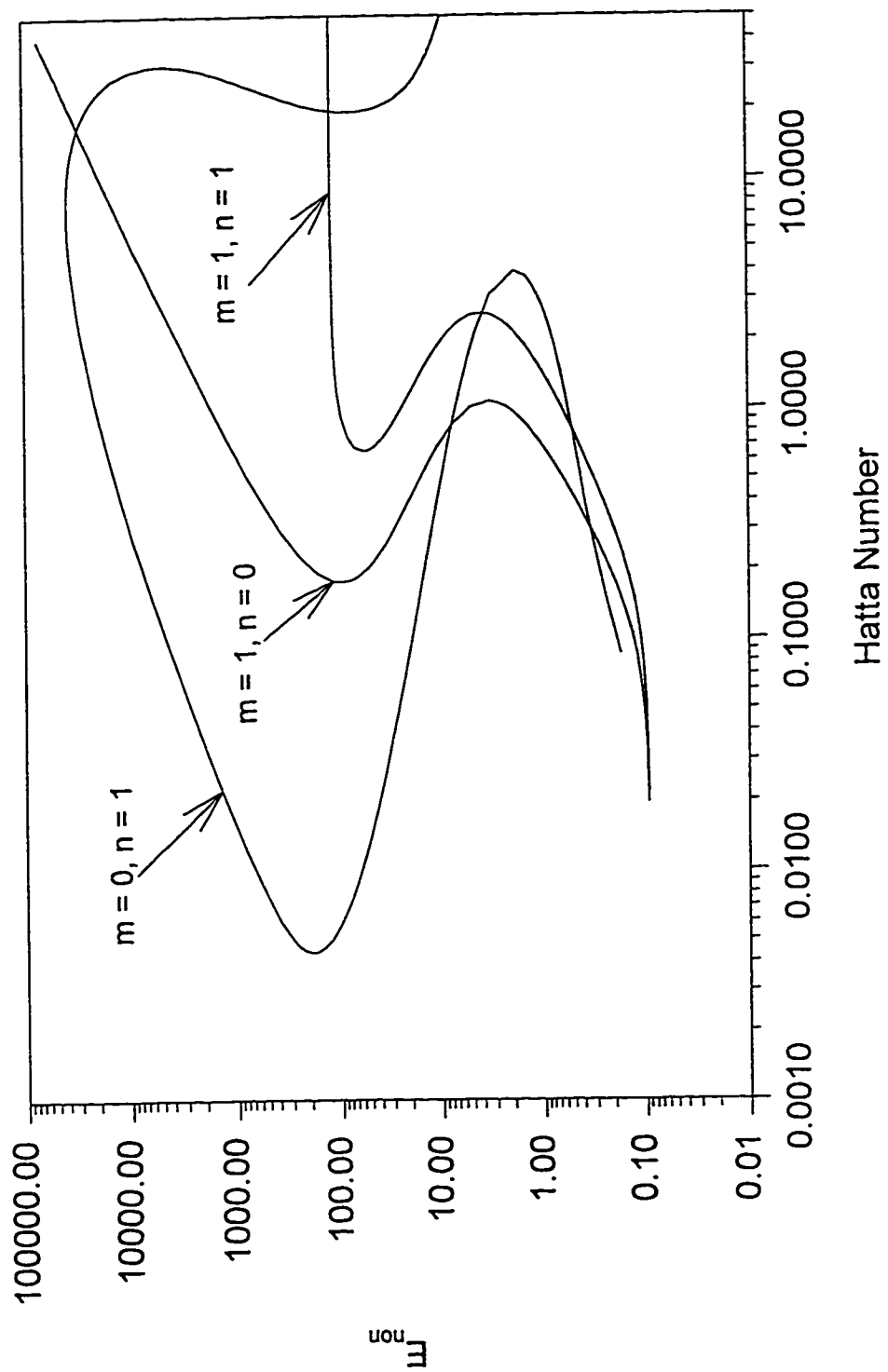


Figure 4.9 The Effect of the Reaction Orders

number. The concentration profile for the liquid reactant becomes constant throughout the heat transfer film and equations 3.25, 3.28 and 3.31 are unnecessary in this case. However, if the gas reactant reaction order is set equal to zero ($m = 0$, $n = 1$), a mushroom type multiplicity is obtained with a very high enhancement factor at the upper branch. This multiplicity behavior is unique and it was not encountered during the study of any other parameter.

The effect of parameter S which is a measure of the reaction stoichiometry and ratio of bulk concentrations of gas and liquid is shown in Figure 4.10. If the value of S is set equal to zero, the enhancement factor is increased dramatically and that asymptotically reaches the pseudo-first-order reaction case. The enhancement factor is reduced when S is increased. It is interesting to note that multiplicity will even be destroyed at relatively high values of S . The effect of S becomes noticeable at relatively high values of the Hatta number.

4.3.b The Effect of Lewis Number

The Lewis number is a measure of the thickness of the heat transfer film to the thickness of the mass transfer film. In Figure 4.11 it is shown that reducing the value of Le will increase the value of the enhancement factor, also, that will shift the multiplicity region to the right of the diagram. The Lewis number is equal to the ratio of the thermal diffusivity to the mass diffusivity, and this ratio has been considered to be constant in the current study since the liquid thermophysical properties and the liquid side mass transfer coefficient are taken to be constant.

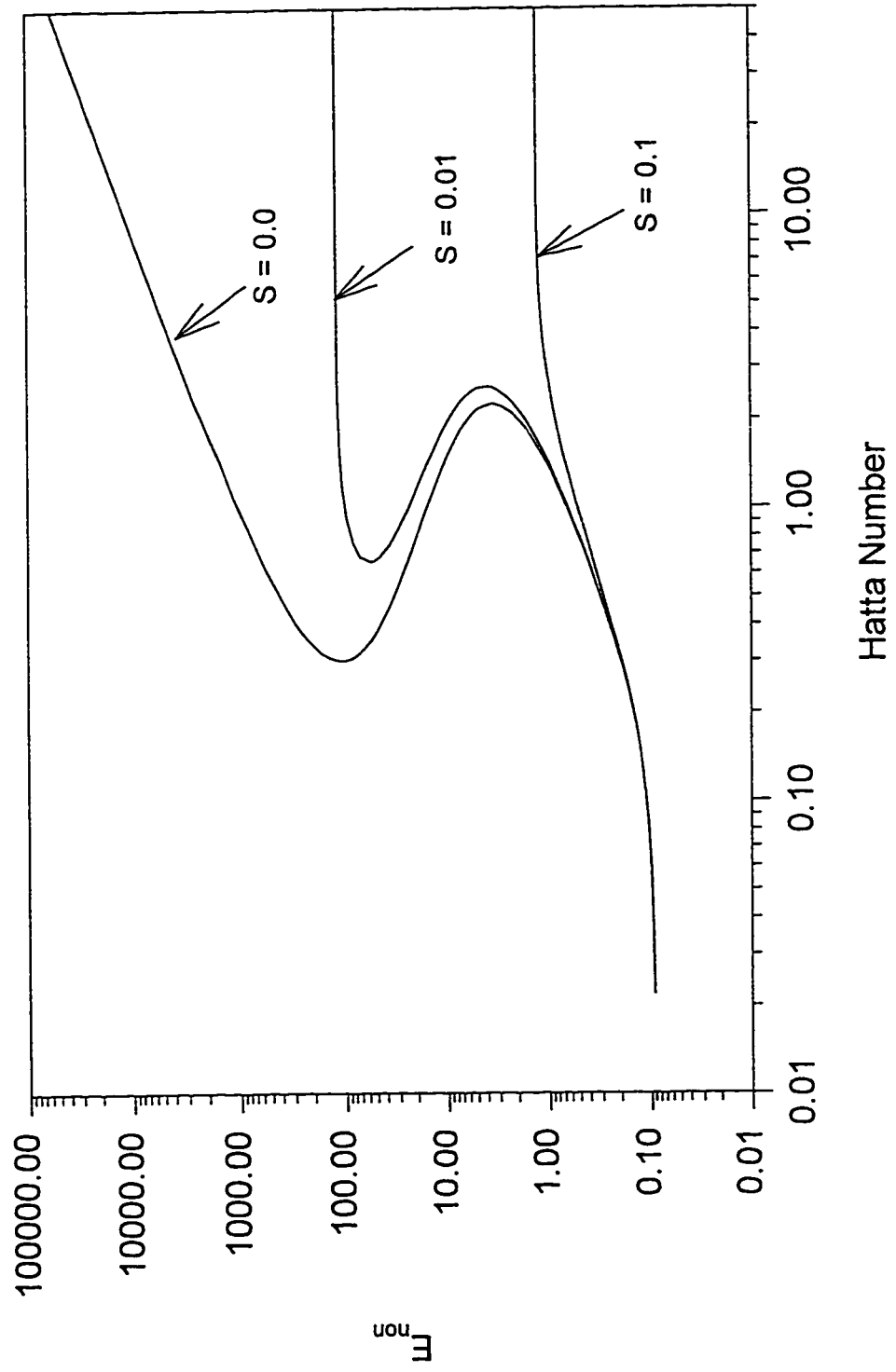


Figure 4.10 The Effect of Parameter S

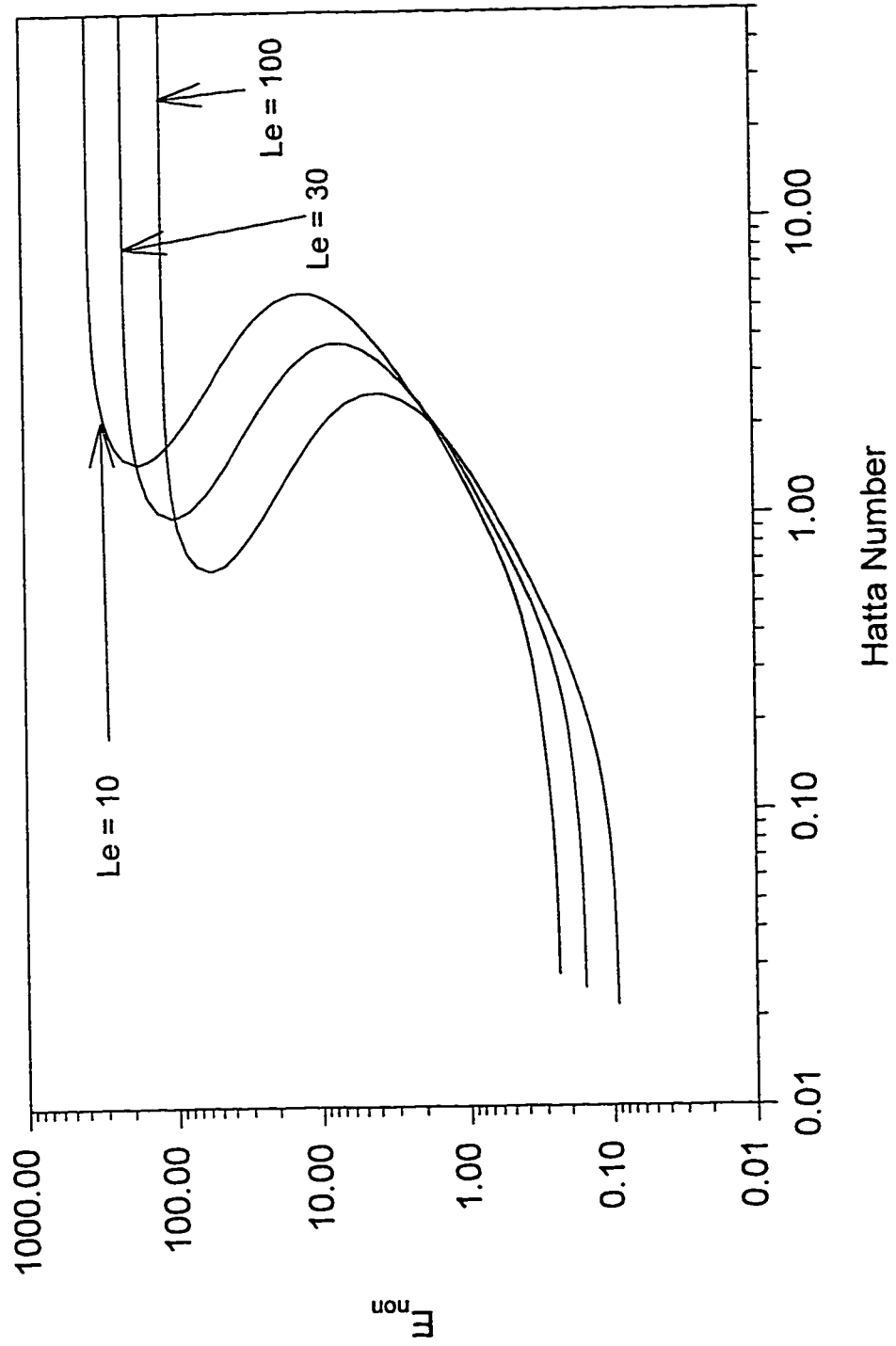


Figure 4.11 The Effect of Parameter Le

4.3.c The Effect of Dimensionless Activation Energies

In the present study, an Arrhenius temperature dependence was considered for the diffusivities, reaction rate constant, solubility and Henry's law constant. The diffusivities and the reaction rate constant are proportionally related to temperature, whereas the gas solubility and the Henry's law constant are inversely related. For nonisothermal gas-liquid reaction systems there will be heat generation due to heats of reaction and solution, and also, heat removal due to convection to the gas phase and conduction to the bulk liquid phase. For the set of parameters in Table 4.1, the heat generation dominates the heat removal which will lead to a net increase in the film temperature as shown in Figures 4.2 to 4.8 . Consequently, it is expected that an increase in the activation energies for diffusion and reaction (ϵ_{DA} , ϵ_{DB} and ϵ_R) will increase the enhancement factor, but an increase in the activation energies of solution and evaporation (ϵ_S and ϵ_V) will lead to a reduction in the enhancement factor.

Figure 4.12 shows the effect of the diffusion activation energies for both reaction components which are considered to be equal ($\epsilon_{DA} = \epsilon_{DB}$), which is the case for many gas-liquid reaction systems. They have a considerable effect on the enhancement factor at high Hatta numbers. If the diffusion activation energies are increased, the enhancement factor will increase dramatically and vice versa. The effect of the reaction activation energy becomes important at moderate values of the Hatta number as shown in Figure 4.13. An increase in the reaction activation energy will increase the enhancement factor. Note also that steady state multiplicity region increases as ϵ_R increases. This observation

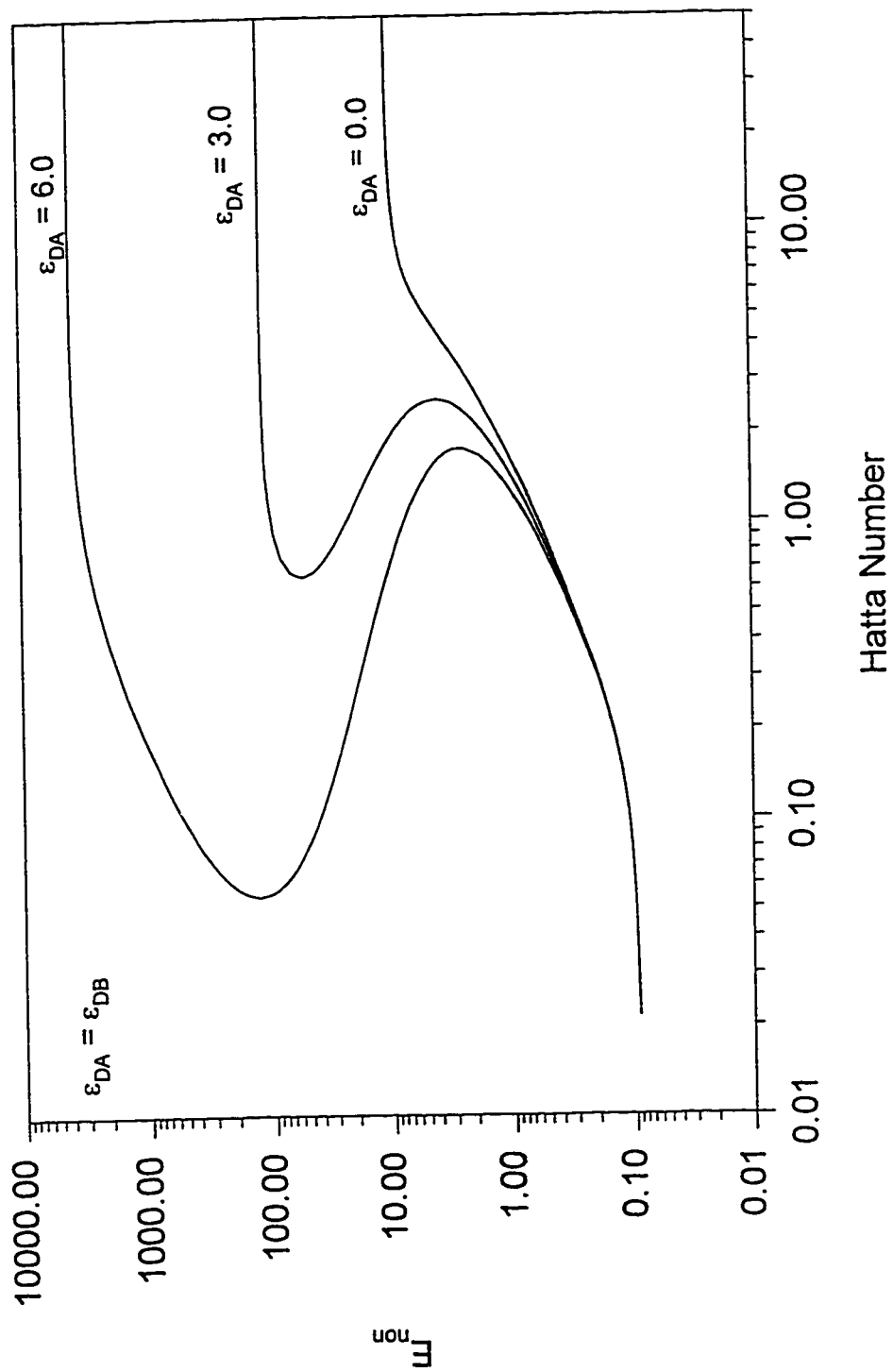


Figure 4.12 The Effect of Parameter ϵ_{DA}

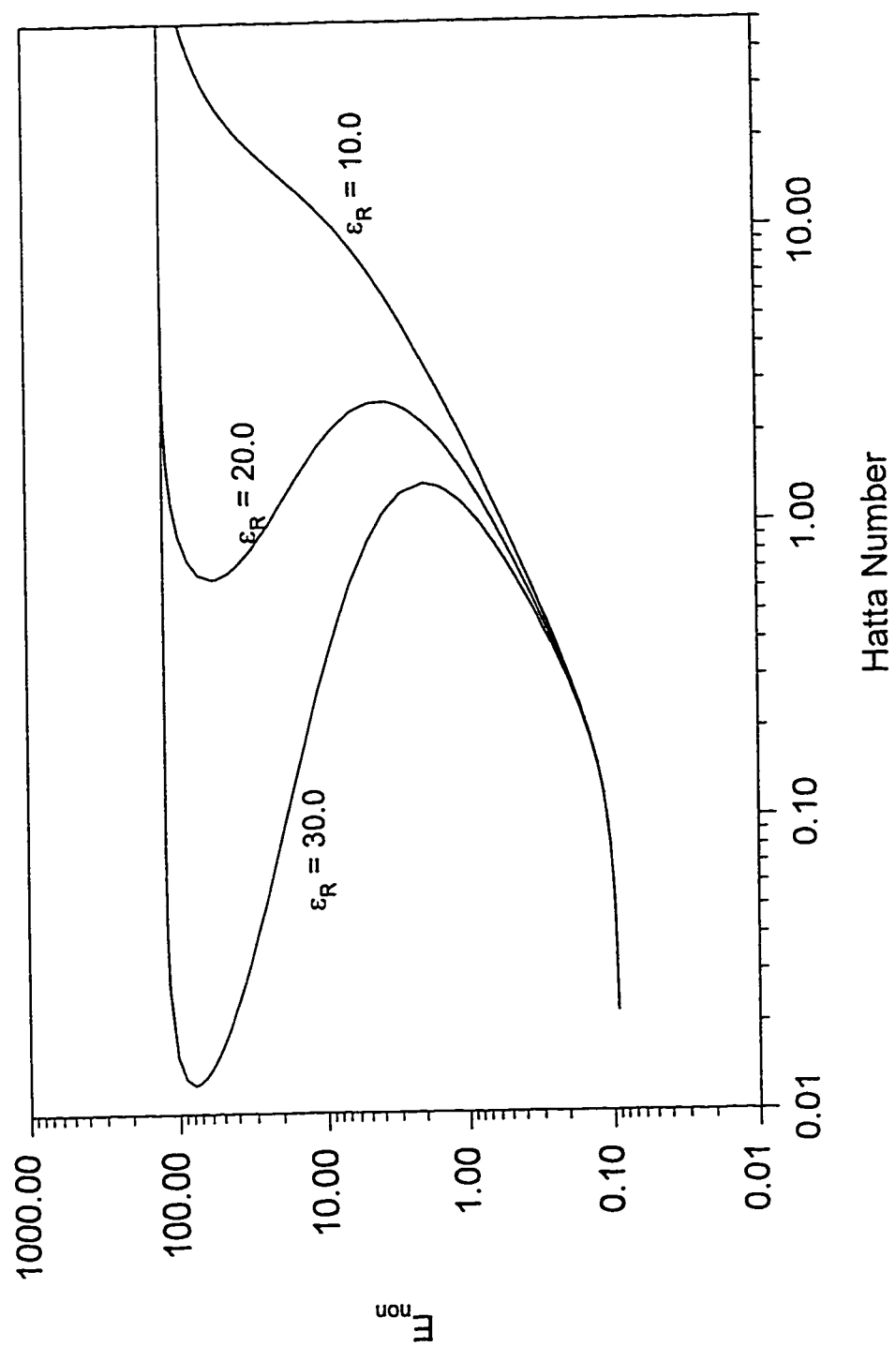


Figure 4.13 The Effect of Parameter ϵ_R

agrees with that of Allan and Mann (1982). The effect of the solubility activation energy, ϵ_S , is shown in Figure 4.14. At moderate values of Hatta number, a reduction of ϵ_S will increase the enhancement factor. We can observe here also that steady state multiplicity will disappear at high ϵ_S values. Also, the same behavior is noticed for ϵ_V , but the effect is less severe as shown in Figure 4.15.

For the set of parameters chosen it appears from the asymptotic behavior of Figures 4.12, 4.13, 4.14 and 4.15 that effect ϵ_{DA} , ϵ_R , ϵ_S and ϵ_V is important for the regions of multiplicity. Multiplicity will be destroyed at low values of ϵ_{DA} and ϵ_R and at high values of ϵ_S and ϵ_V . However, the region of multiplicity becomes bigger at high values of ϵ_{DA} and ϵ_R and at low values of ϵ_S and ϵ_V .

4.3.d The Effect of the Dimensionless Heats of Reaction, Solution and Evaporation

Figures 4.16, 4.17 and 4.18 show the effect of increasing the heats of reaction, solution and evaporation. As β_R and β_S are increased the enhancement factor is increased and the region of multiple steady states becomes bigger. For the set of parameters in Table 4.1, if β_R is set equal to zero a unique solution is obtained, and for this case the major contribution of heat generation due to the heat of reaction is eliminated. However, if the minor contribution of heat generation due to the heat of solution is neglected (i.e. when $\beta_S = 0.0$), we still observe that steady state multiplicity exists. The effect of the dimensionless heat of evaporation β_V is almost negligible as shown in Figure 4.18. It can be deduced therefore that the amount of heat removal due to evaporation to the gas phase has a very little effect at least for the set of parameters chosen to conduct this study.

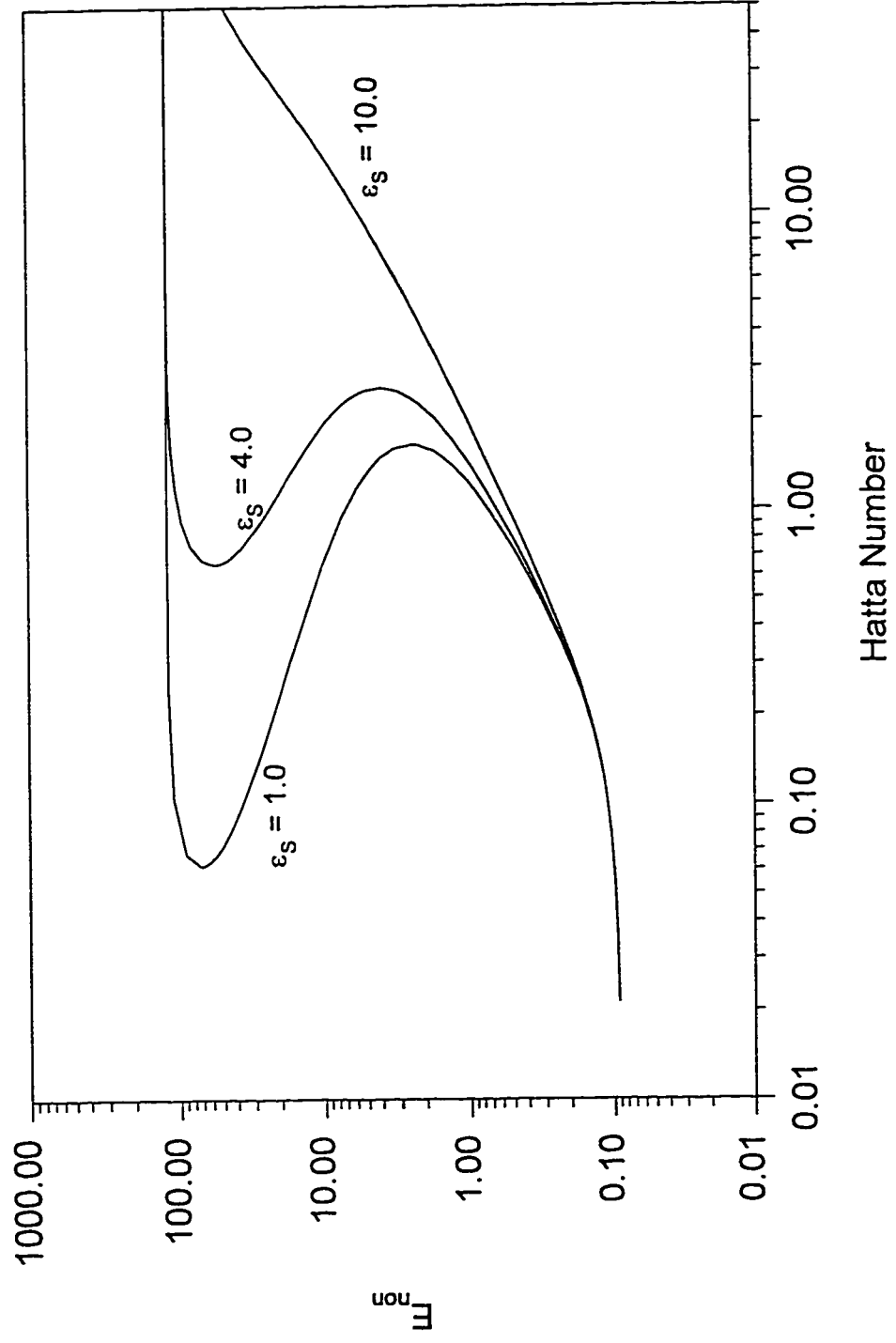


Figure 4.14 The Effect of Parameter ϵ_S

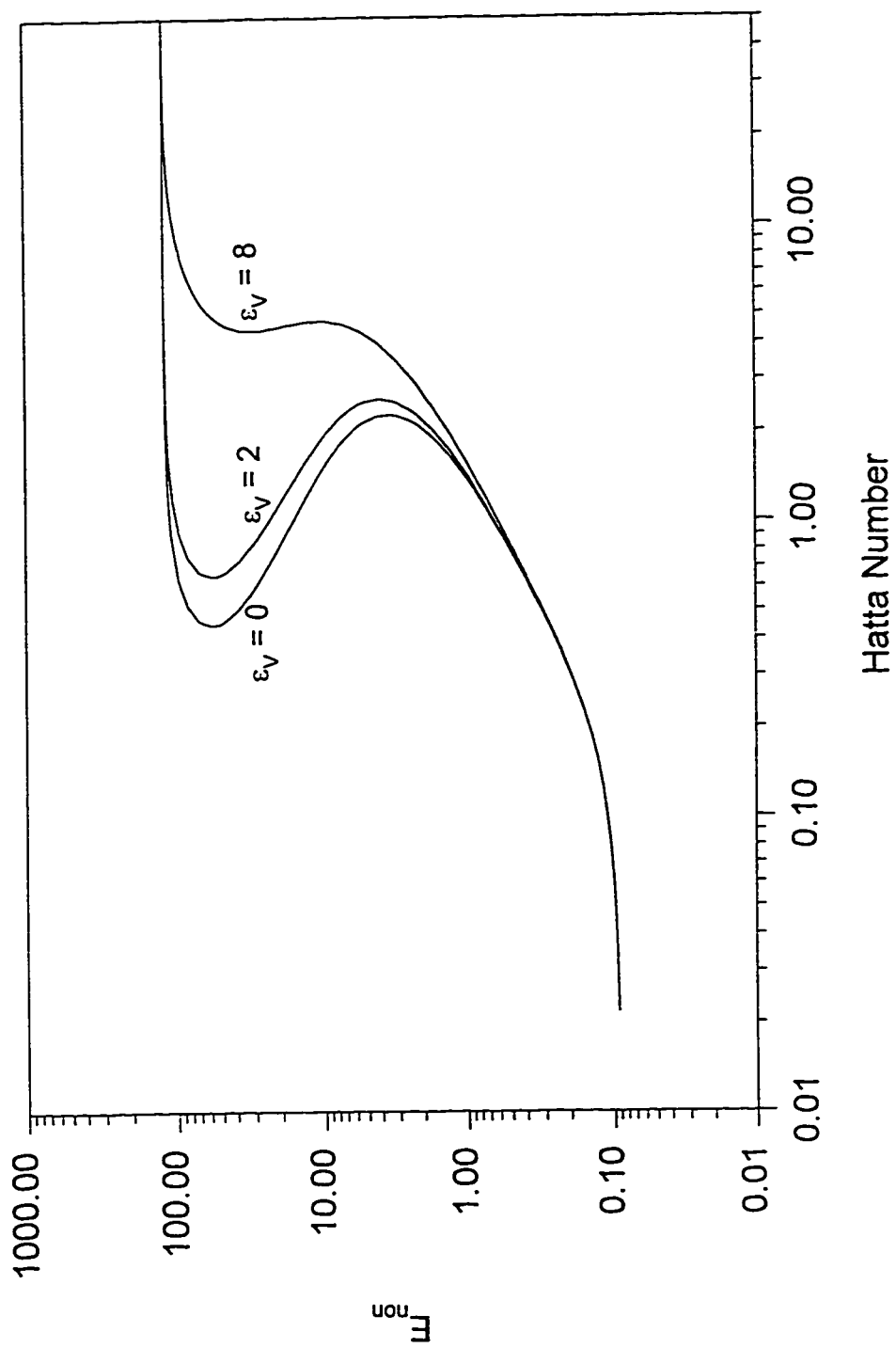


Figure 4.15 The Effect of Parameter ϵ_V

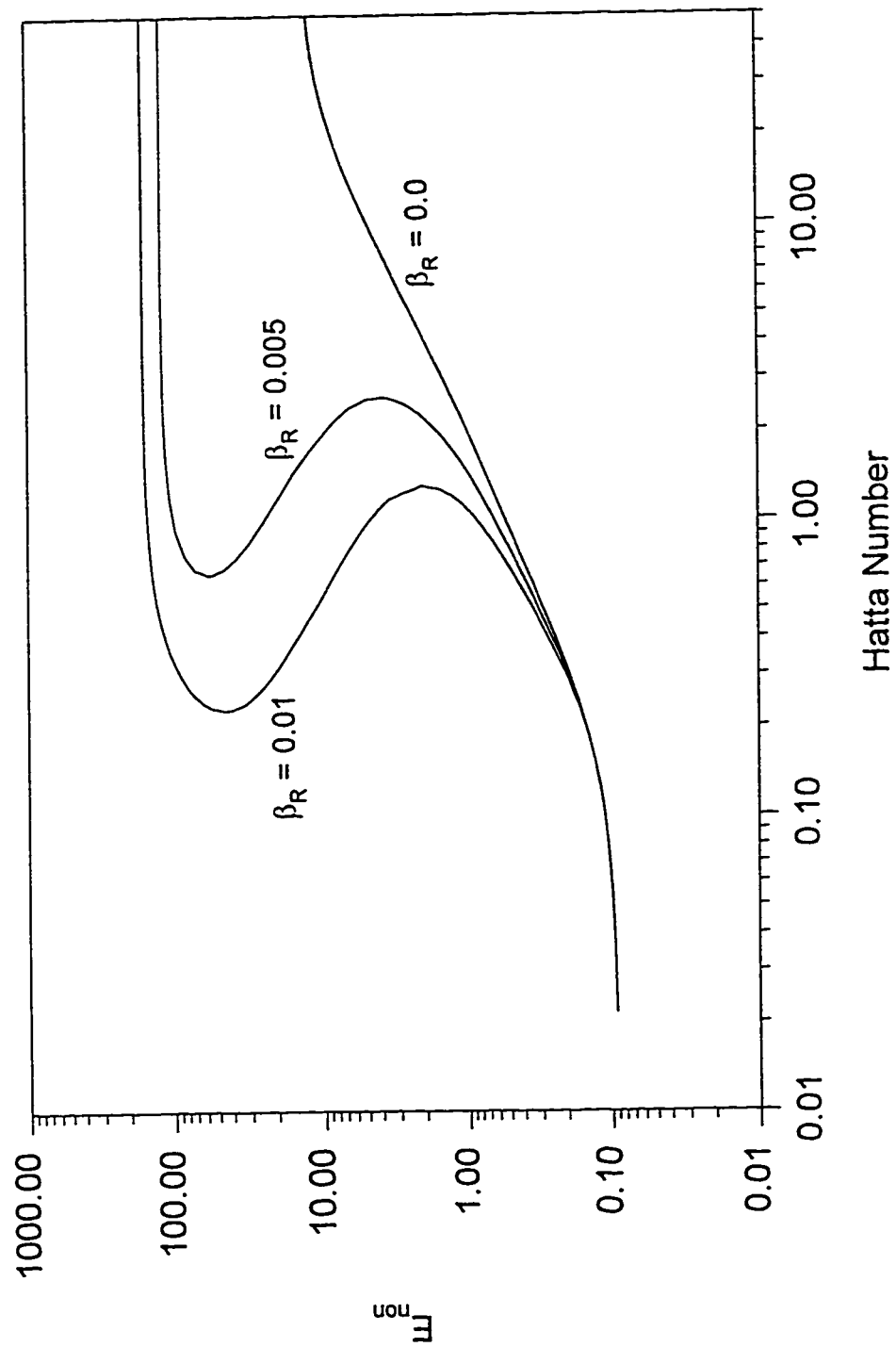


Figure 4.16 The Effect of Parameter β_R

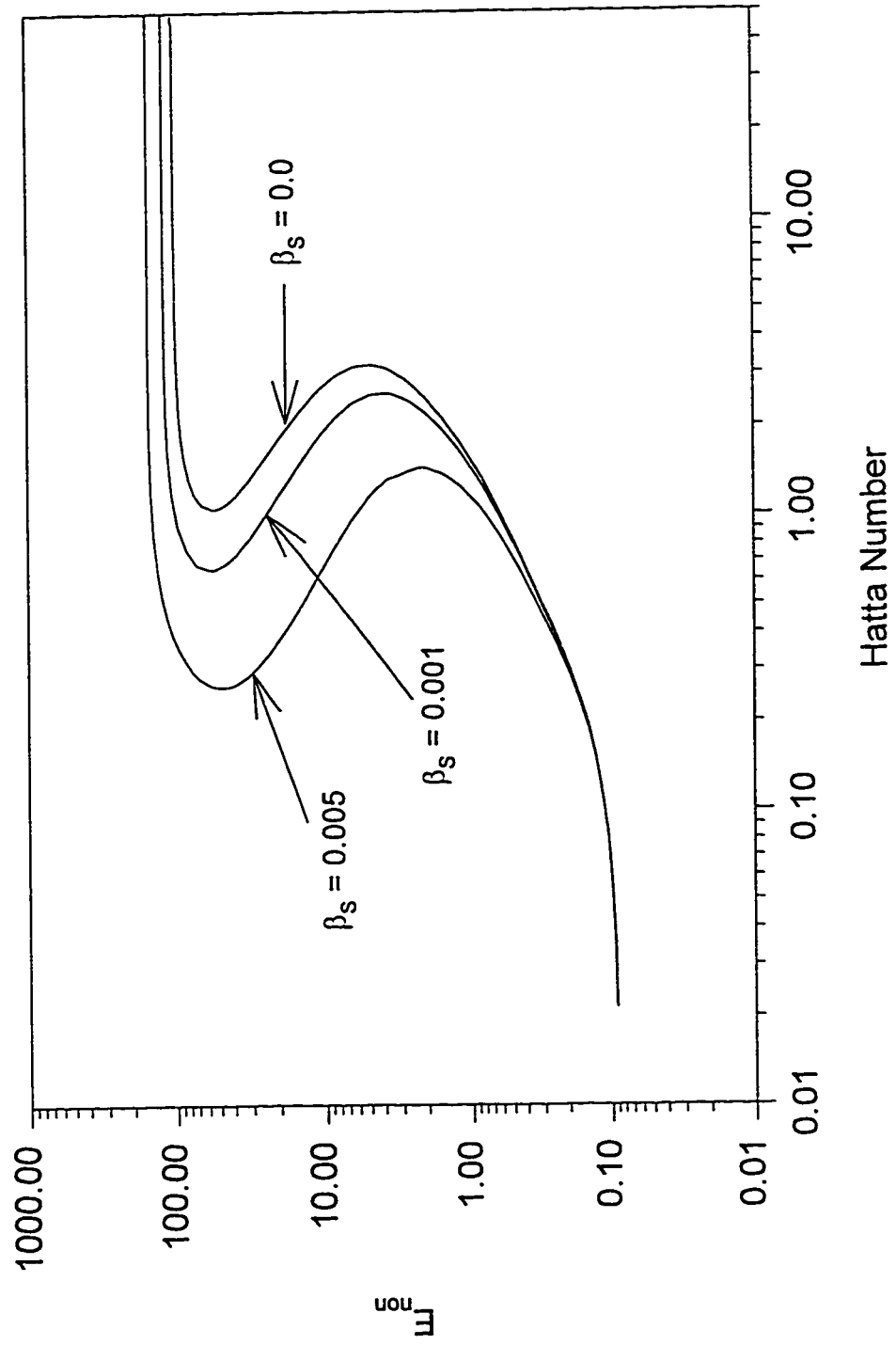


Figure 4.17 The Effect of Parameter β_s

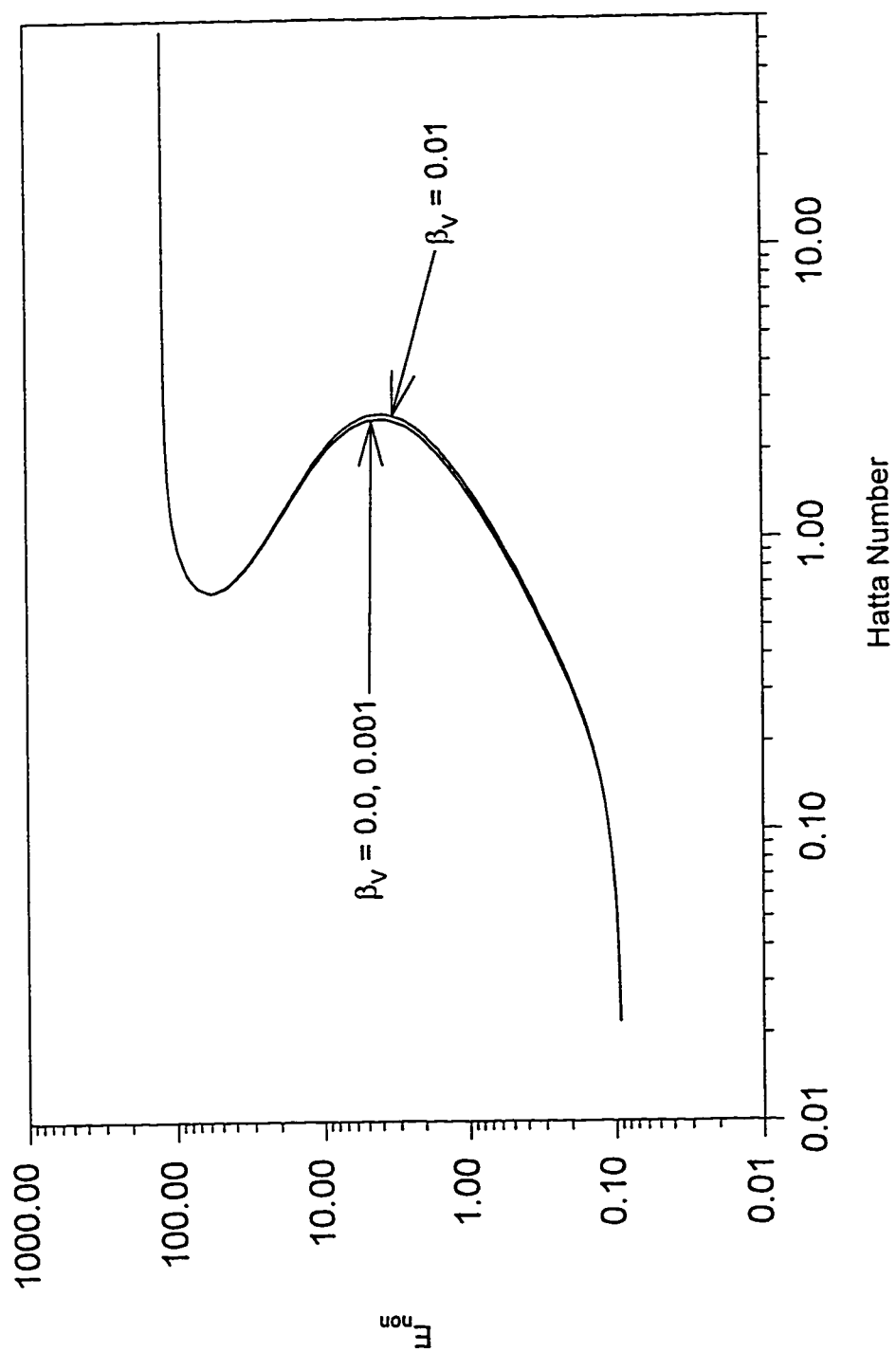


Figure 4.18 The Effect of Parameter β_V

4.3.e The Effect of Biot Numbers and Parameter ω

The effect of Biot Number for heat transfer, Bi_H , is shown in Figure 4.19 . Bi_H is a measure of the convective heat removal to the gas phase, and as this parameter becomes smaller the amount of heat convection becomes less and the enhancement factor is increased. However, the effect of Bi_H at low Hatta numbers is negligible. The effect of Biot number for mass transfer, Bi_M , is shown in Figure 4.20 . Bi_M is a measure of material loss from the liquid film to the gas phase by means of evaporation. The mass which is evaporating to the gas phase carries with it energy, and the lower is the energy loss the more is the enhancement factor. Consequently, the smaller is the Bi_M the greater is the enhancement factor. The effect of parameter ω on the enhancement factor is shown in Figure 4.21.a . The concentration of the liquid reactant, B , in the gas phase after evaporation is determined from parameter ω as shown in equation 3.28

$$\left(B_G = \frac{B(\delta_H = 0)}{1 + \omega} \right).$$

The parameter ω has an asymptotic behavior on B_G , if ω is very

large, then B_G is very small, and if ω is zero then the concentration of the liquid reactant in the gas phase after evaporation equals its concentration in the gas-liquid interface (i.e. $B_G = \text{maximum}$). From Figure 4.21.a, it looks that the parameter ω has a relatively small effect on the enhancement factor and this effect disappears at high Hatta numbers. At moderate values of Hatta number the parameter ω has also small effect on the surface temperature rise as shown in Figure 4.21.b .

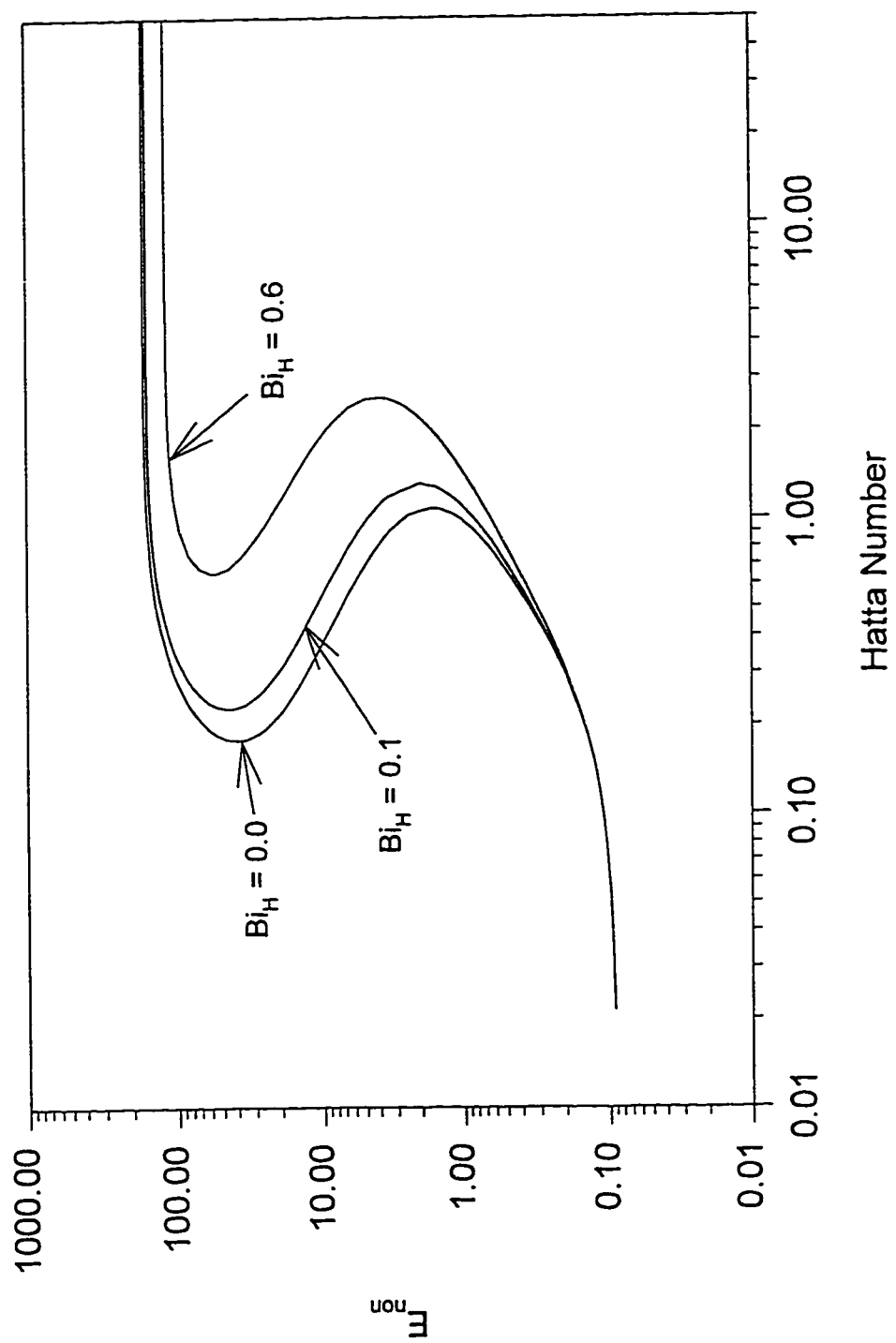


Figure 4.19 The Effect of Parameter Bi_H

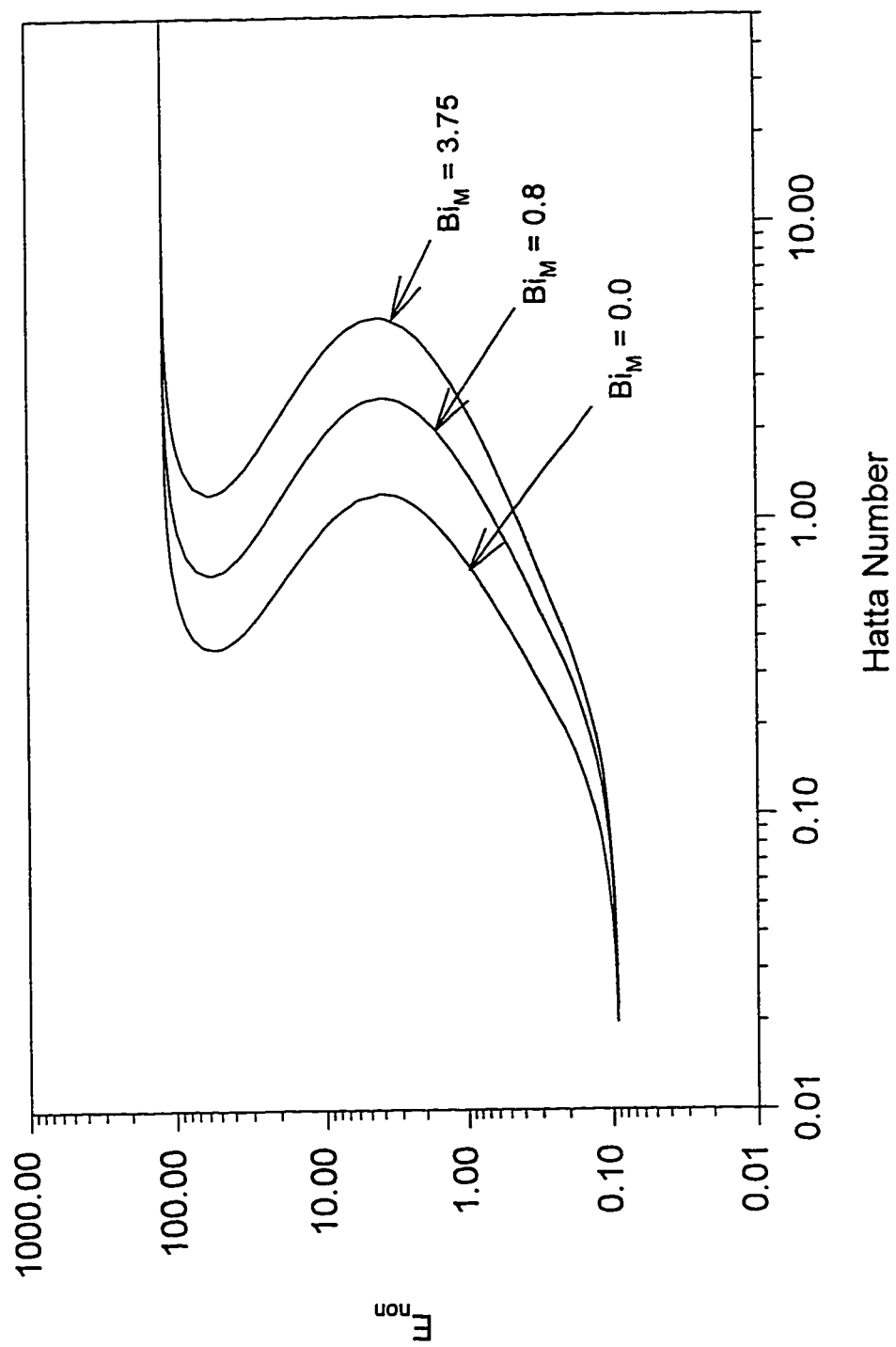


Figure 4.20 The Effect of Parameter Bi_M

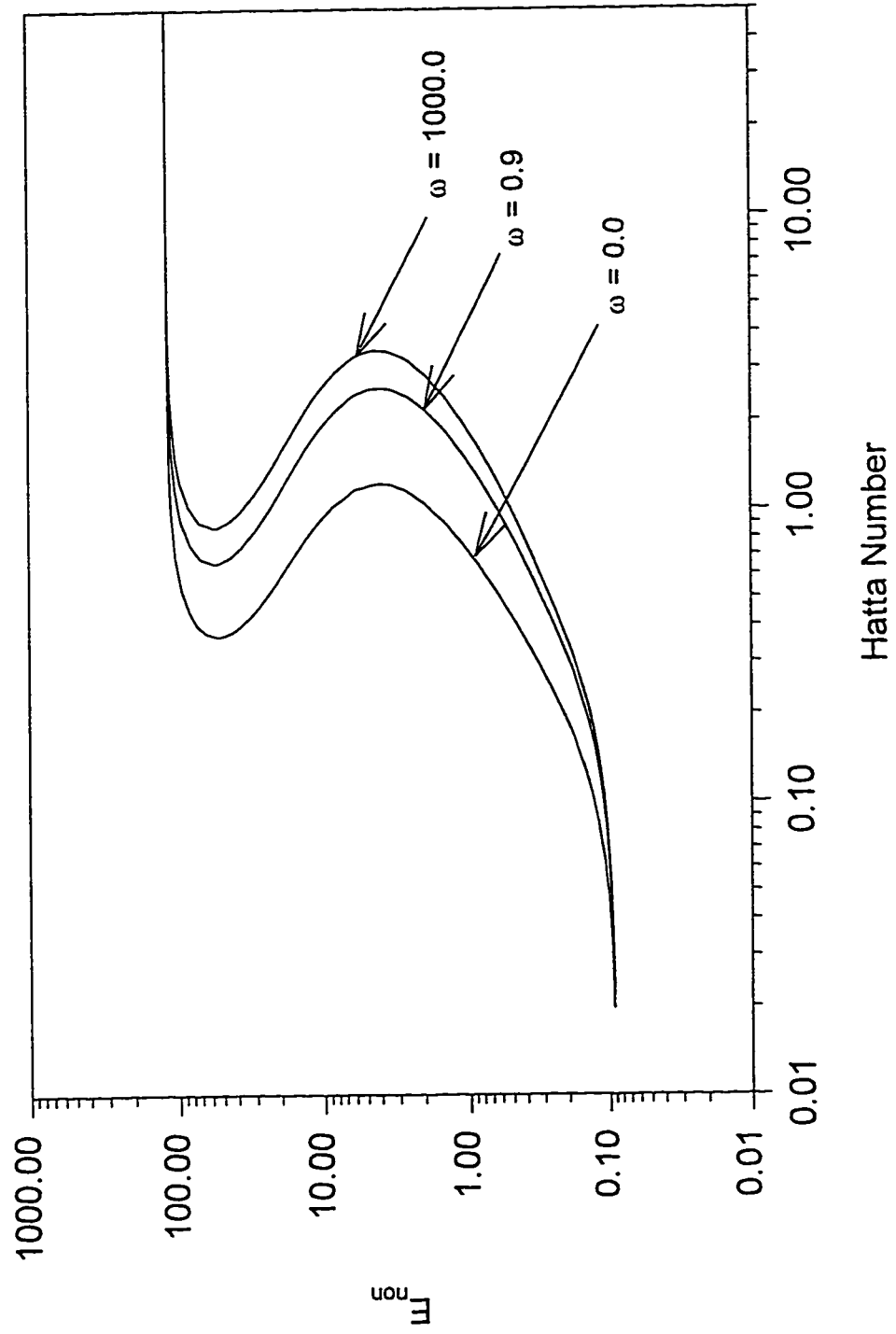


Figure 4.21.a The Effect of Parameter ω on the Enhancement Factor

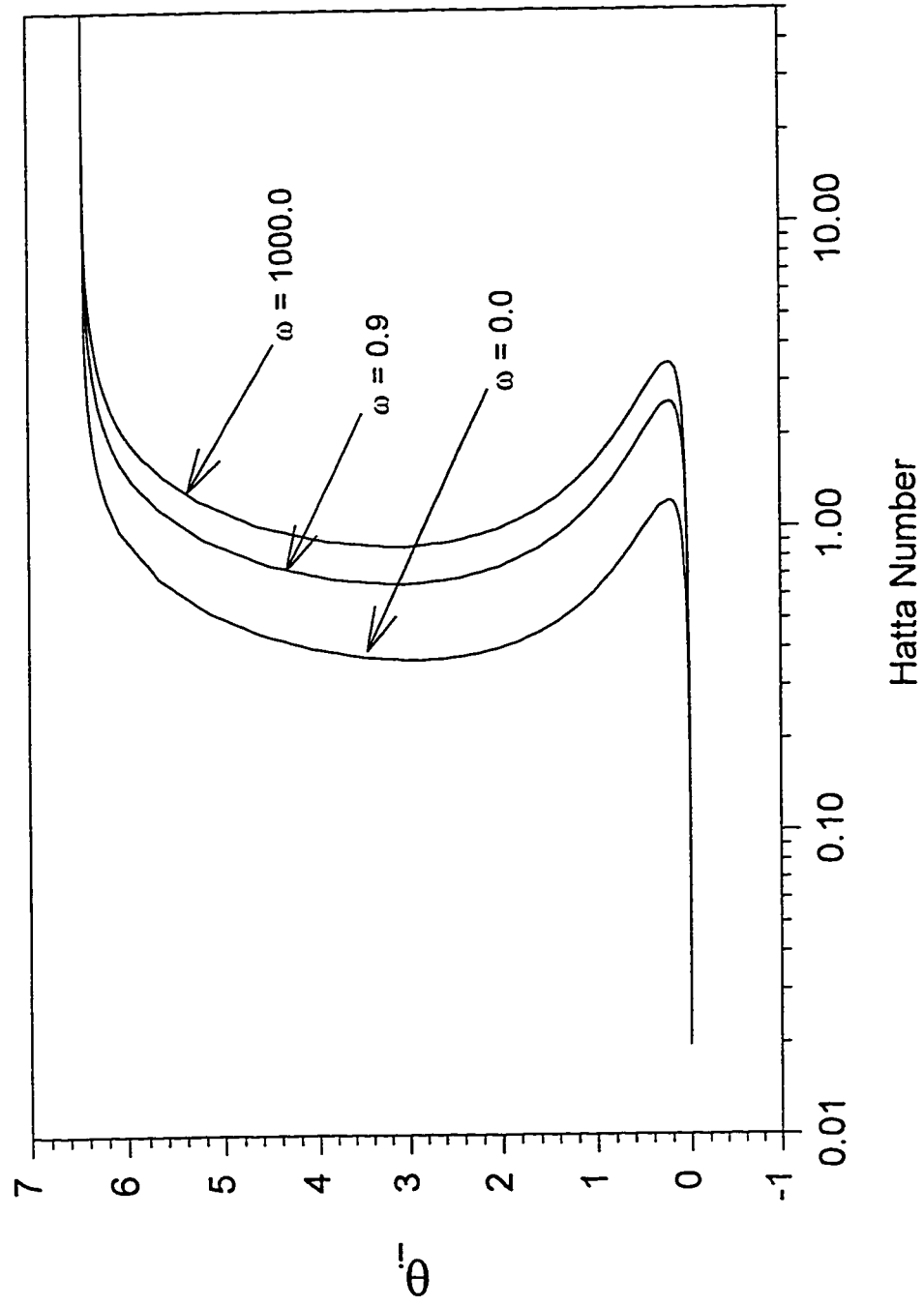


Figure 4.21.b The Effect of Parameter ω on the Surface Temperature Rise

4.3.f The Effect of Bulk Liquid Reaction Parameters

In this study and for the first time in the literature, the consumption of the gas reactant and the generation of heat in the well mixed bulk liquid phase due to chemical reaction and their removal by the flowing liquid was considered. The parameter α' , is the ratio of the volume of the bulk liquid phase beyond the heat transfer film to the volume of the heat transfer film. This parameter ranges asymptotically from unity to a very high number. If α' is unity then the bulk liquid reaction contribution can be small, however, if $\alpha' \gg 1$ then the contribution can be significant. For the set of parameters in Table 4.1, Figure 4.22.a shows that parameter α' has a very little effect on the enhancement factor for very low values of Hatta number, and Figure 4.22.b shows that parameter α' has almost no effect on the surface temperature rise. Parameter β' is related to the liquid residence time and it is a measure of the material carried out by the flowing liquid. Also, this parameter has little effect on the enhancement factor for small values of Hatta number and almost no effect on the surface temperature rise as shown in Figures 4.23.a and 4.23.b for the set of parameters in Table 4.1. Notice that the set of parameters in Table 4.1 makes the bulk liquid concentration of the gas reactant (A at δ_H) equals zero at relatively high values of Hatta number as shown in Figures 4.4-4.8. If the gas-liquid reaction is in the fast reaction regime, then the concentration of the gas reactant in the bulk liquid phase is zero and the contribution of the bulk liquid reaction parameters, α' and β' , will not be observed.

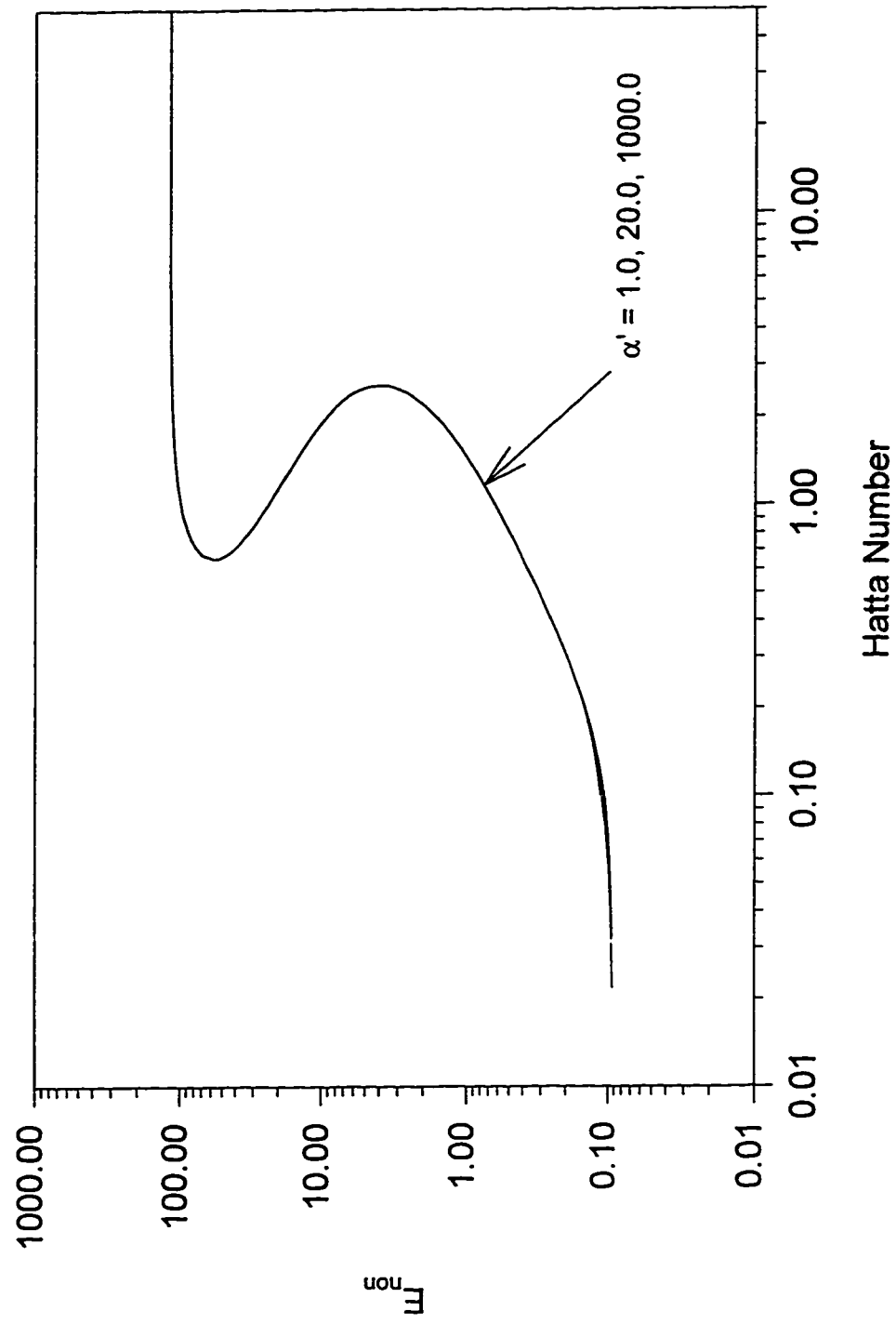


Figure 4.22.a The Effect of Parameter α' on The Enhancement Factor

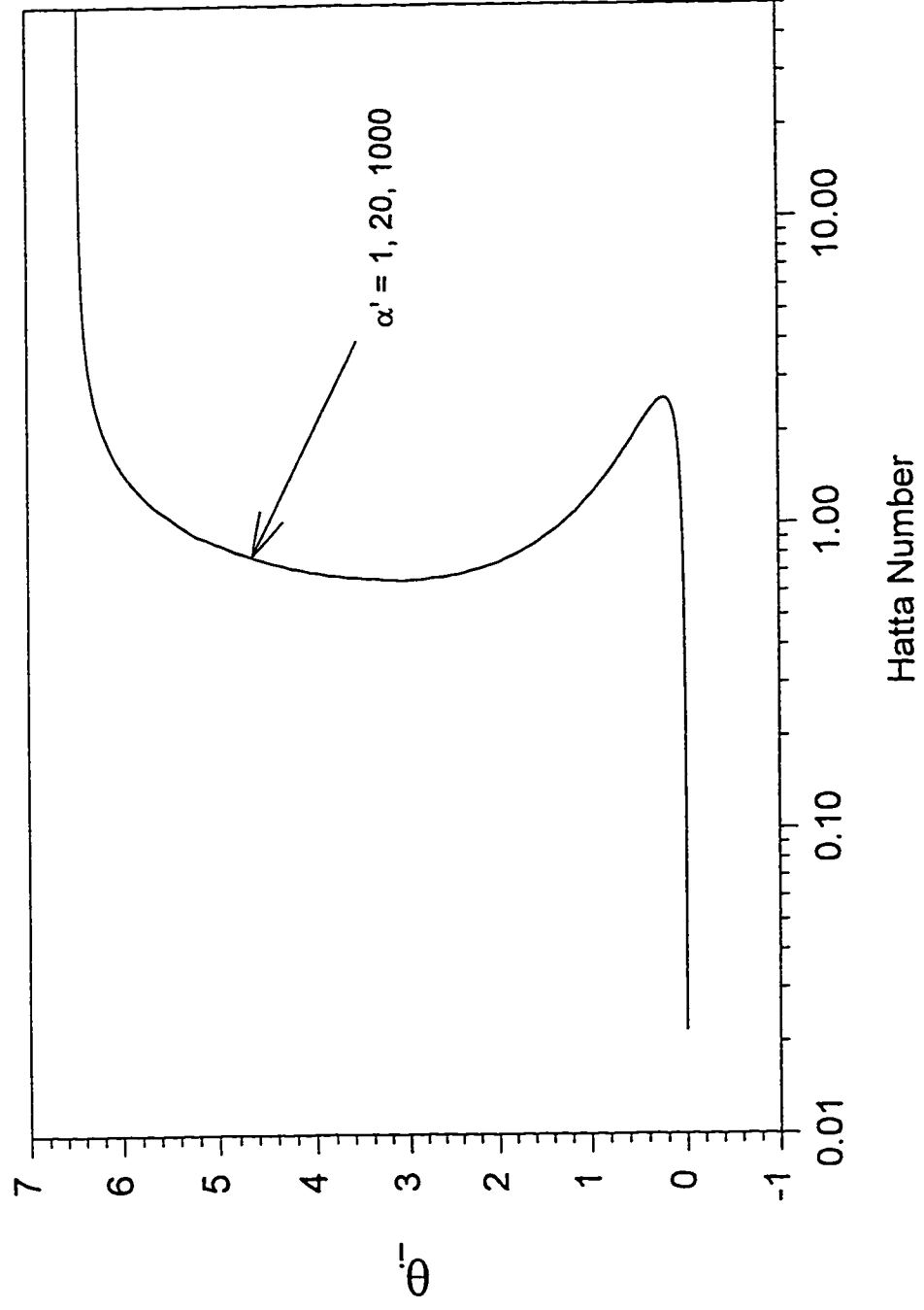


Figure 4.22.b The Effect of Parameter α' on the Surface Temperature Rise

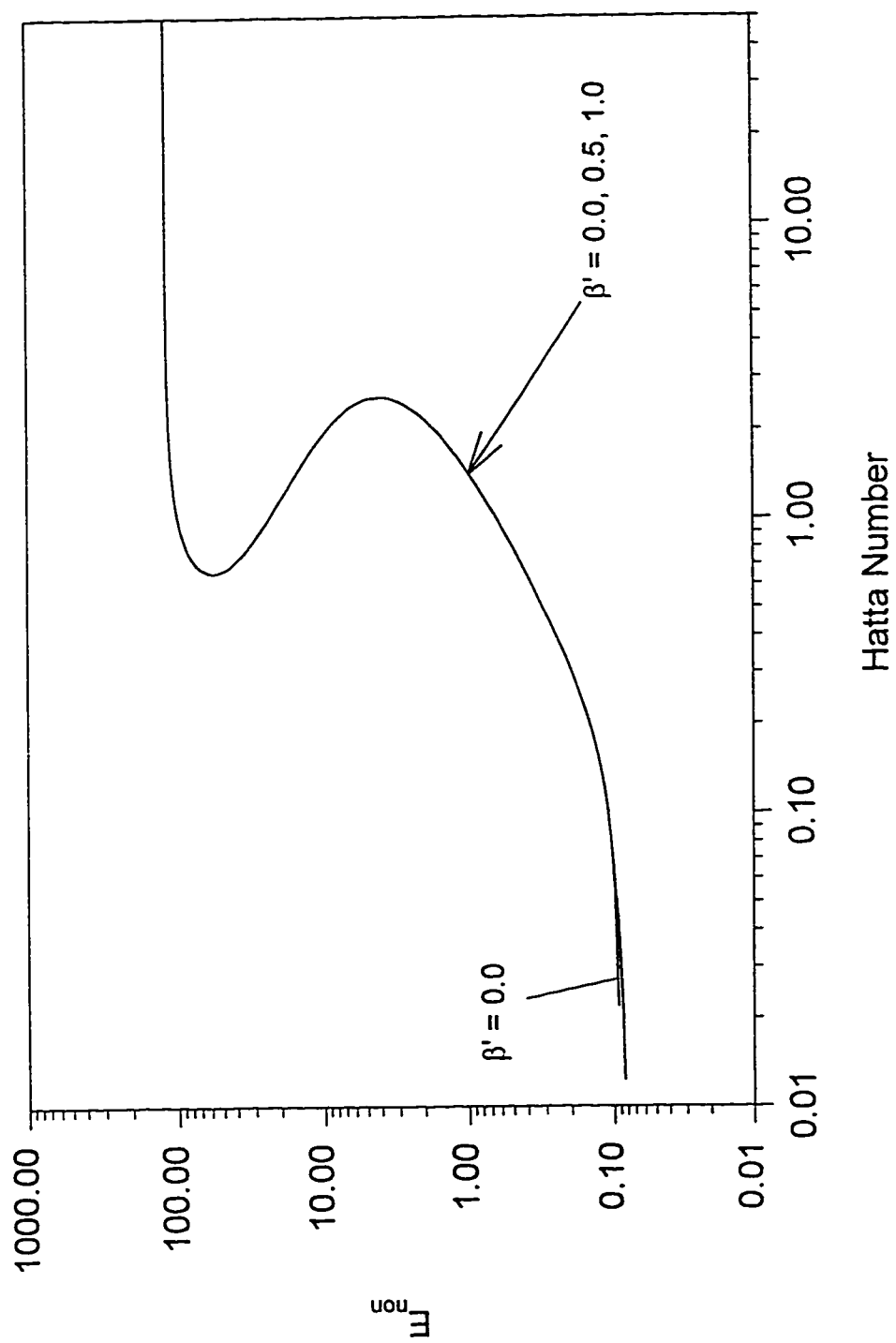


Figure 4.23.a The Effect of Parameter β' on the Enhancement Factor

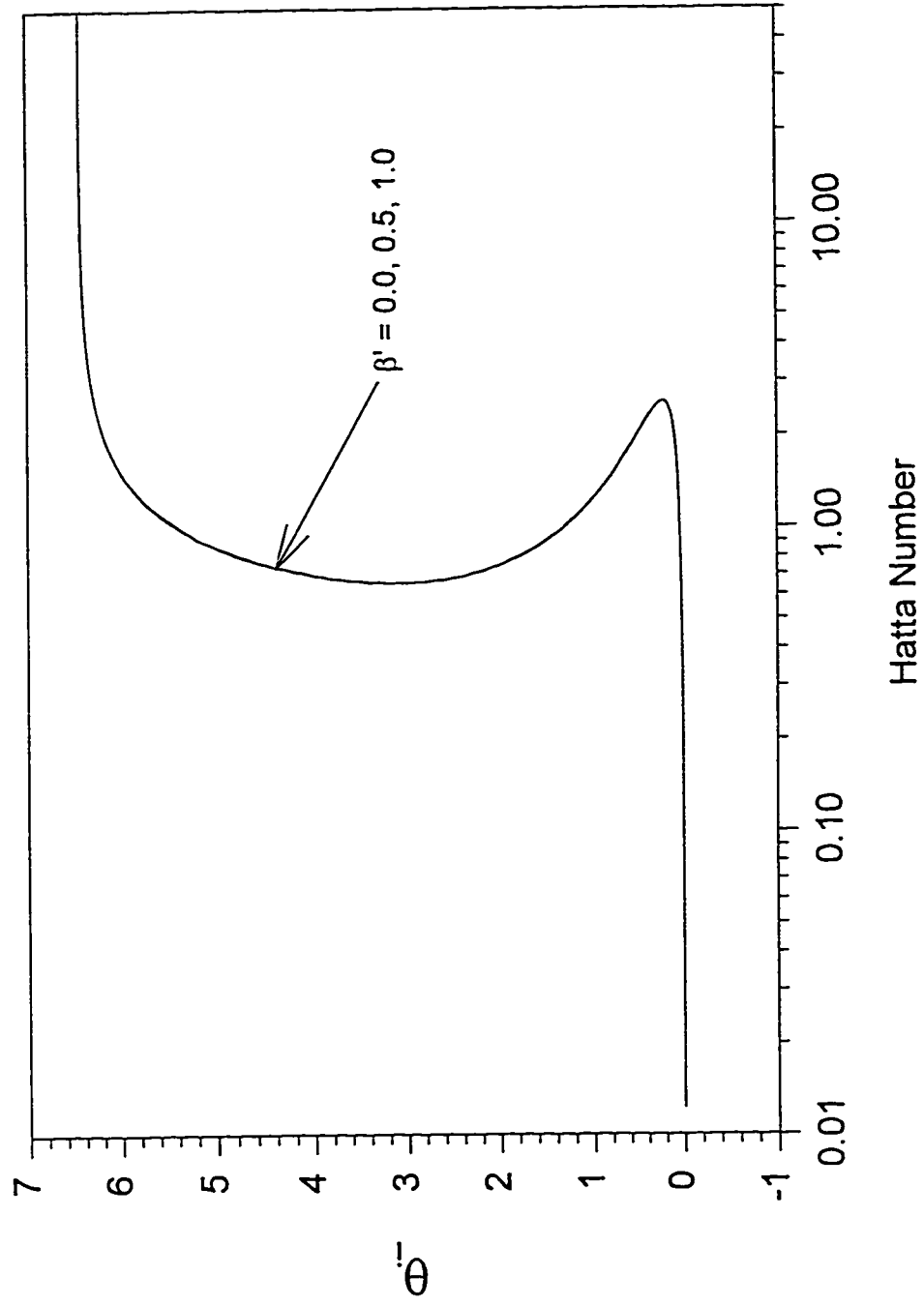


Figure 4.23.b The Effect of Parameter β' on the Surface Temperature Rise

The parameter γ' accounts for the heat removed by the flowing bulk liquid phase. Since the heat effects for the present system are important as shown in Figure 4.2, the parameter γ' has a noticeable effect on the enhancement factor and the surface temperature rise as shown in Figures 4.24.a and 4.24.b, respectively. If γ' is very small the heat removal by the flowing liquid phase is small and the enhancement factor is larger and the surface temperature rise is larger and vice versa.

4.3.g The Effect of Reactor Inlet Temperatures and Inlet Liquid Concentration

The effect of the reactor inlet liquid temperature, θ_0 , is shown in Figure 4.25. If the inlet reactor temperature becomes higher, the enhancement factor becomes higher at moderate values of the Hatta number. The same effect is noticed for the reactor inlet gas temperature, θ_G , as shown in Figure 4.26. If the inlet reactor temperatures are higher than the reactor temperature then there will be a net positive energy addition by the inlet reactor streams. The effect of the gas reactant composition in the inlet liquid stream, A_0 , is shown in Figure 4.27 and it has negligible effect on the enhancement factor.

4.4 Lumping of the Heats of Reaction and Solution Parameters

The present model contains 21 dimensionless parameters. The parametric study presented above indicate that the reaction and stoichiometry parameters, the activation energy parameters, the heats of reaction and solution parameters and the Biot numbers appear to have an effect on the local film theory model behavior. Some of these parameters if combined together in an algebraic manner would simplify the model

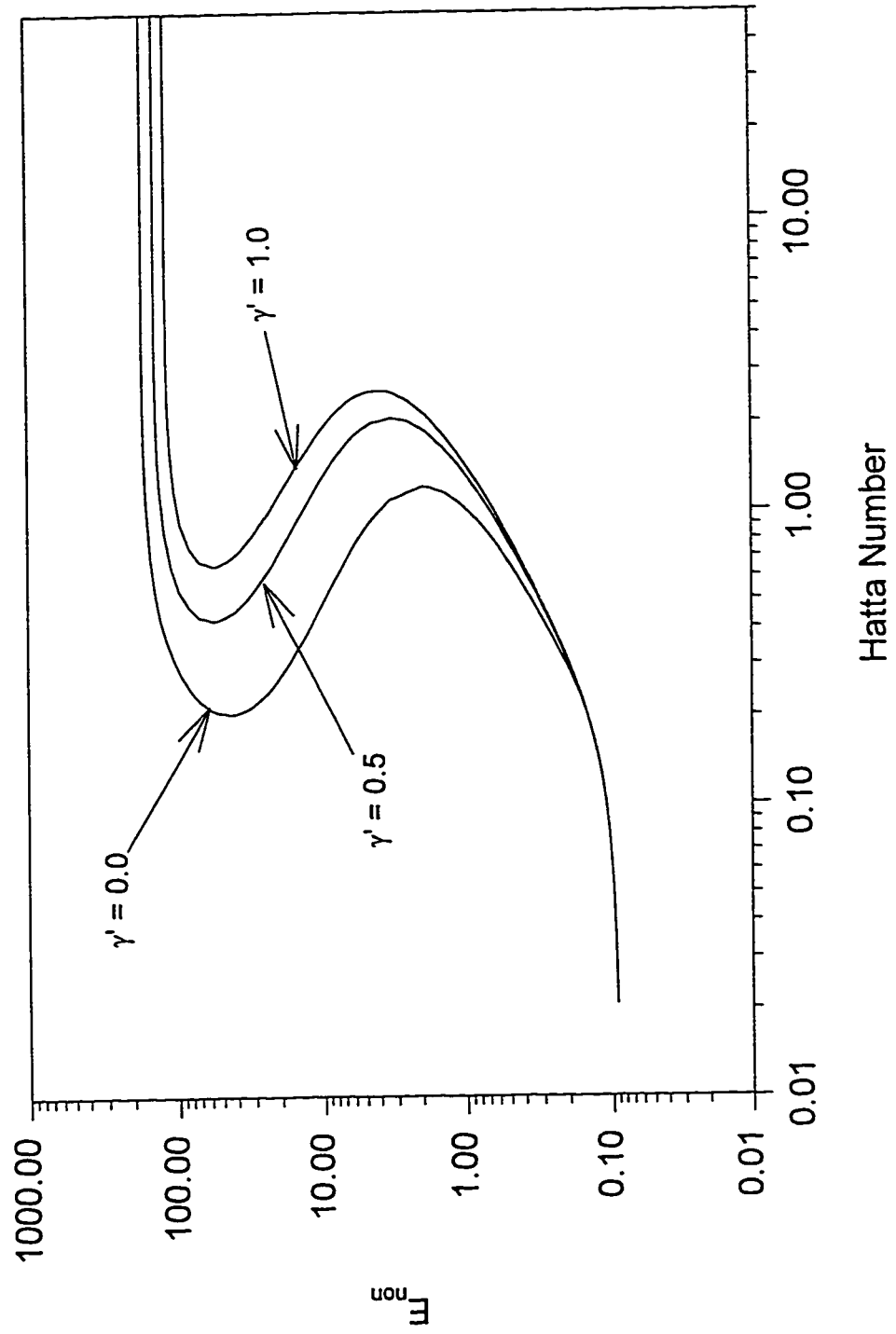


Figure 4.24.a The Effect of Parameter γ' on the Enhancement Factor

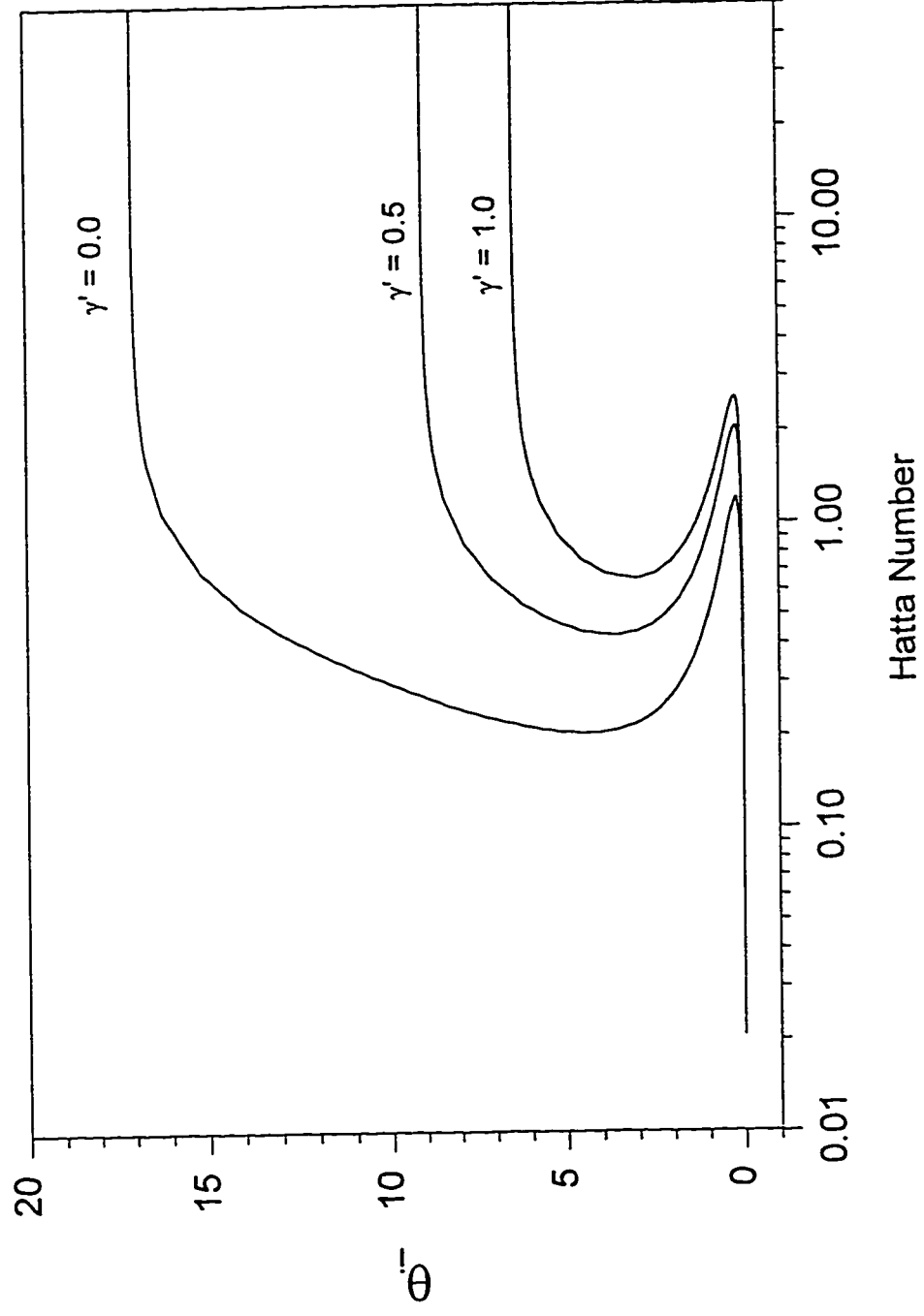


Figure 4.24.b The Effect of Parameter γ' on the Surface Temperature Rise

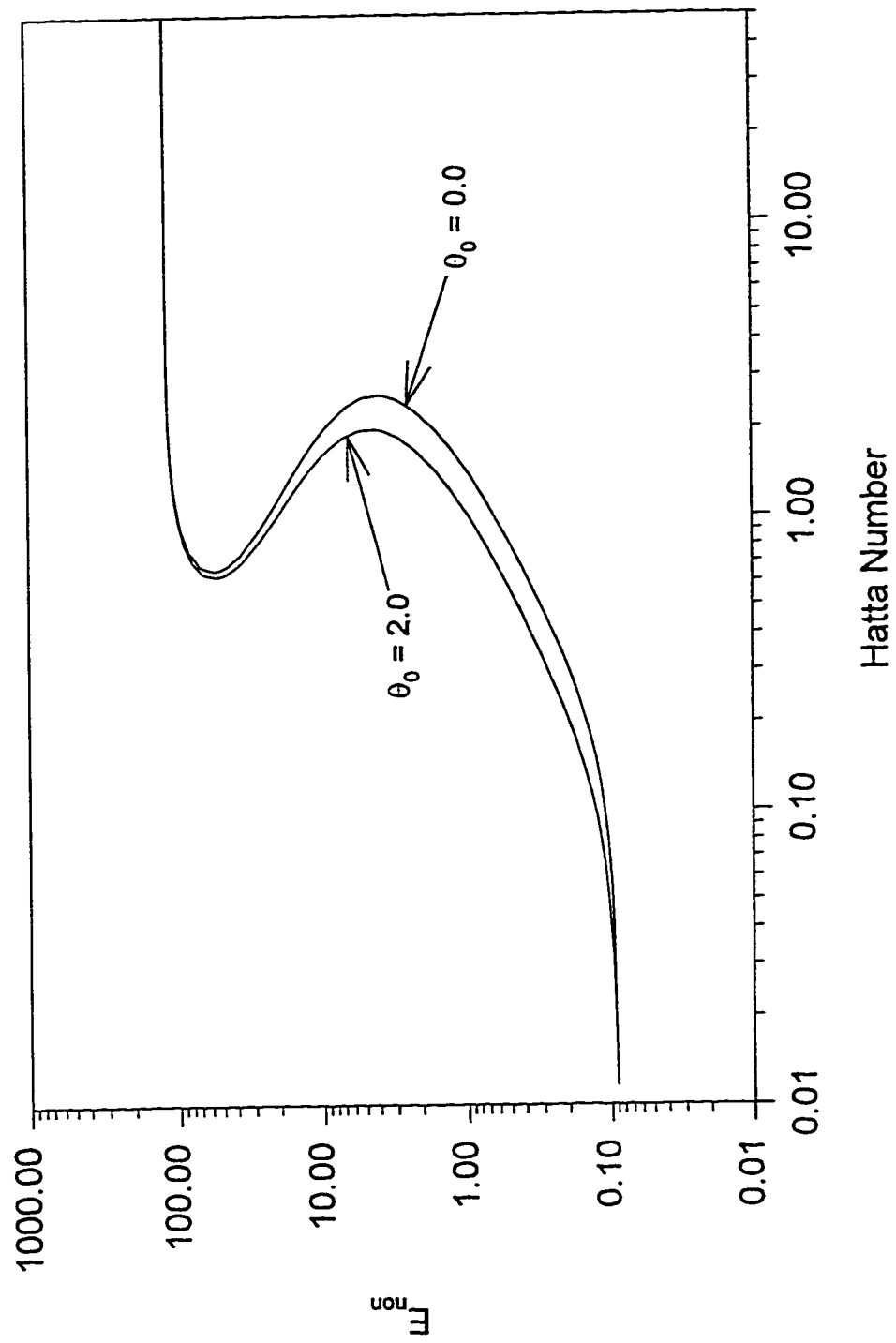


Figure 4.25 The Effect of Parameter θ_0

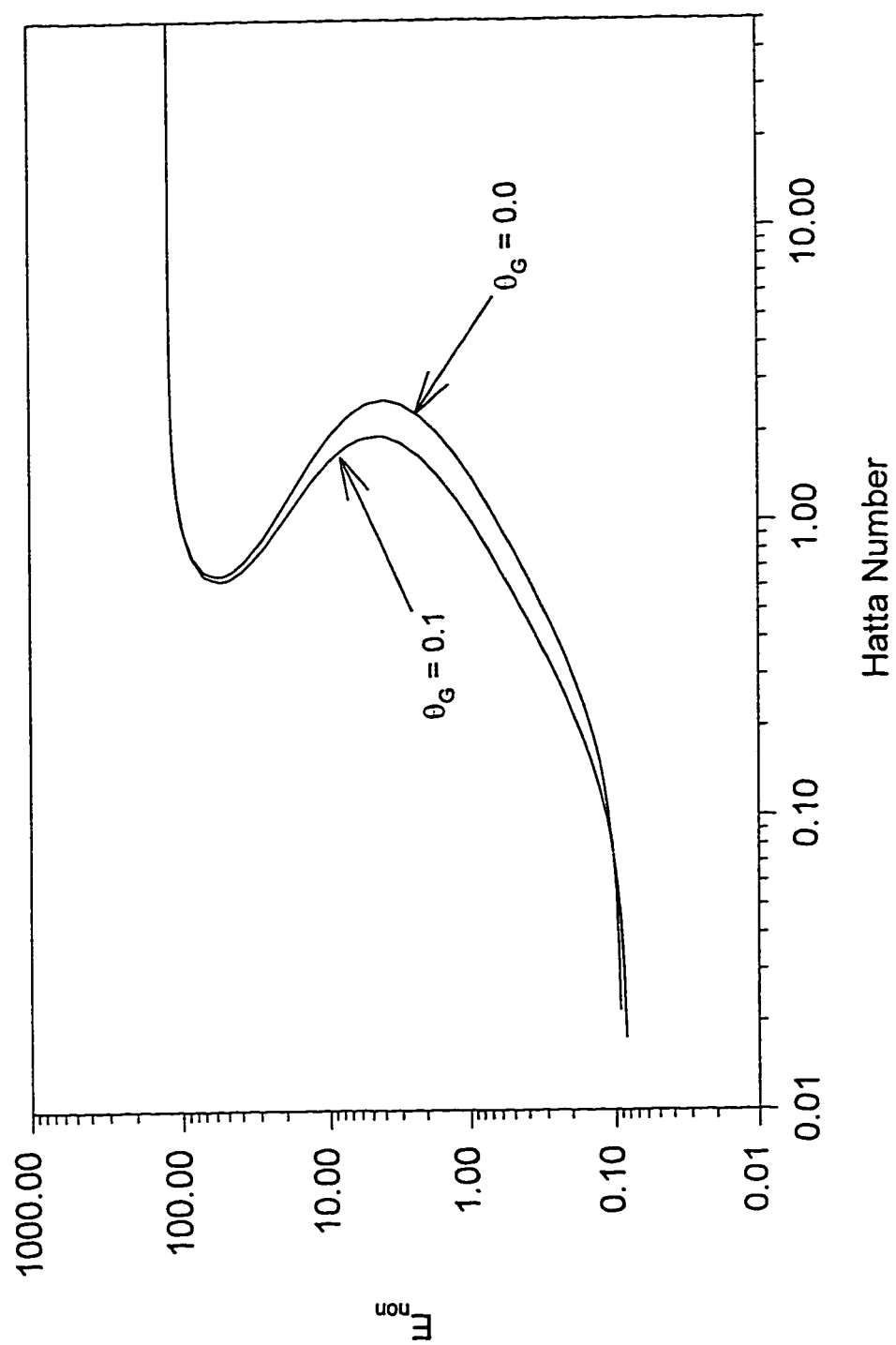


Figure 4.26 The Effect of Parameter θ_G

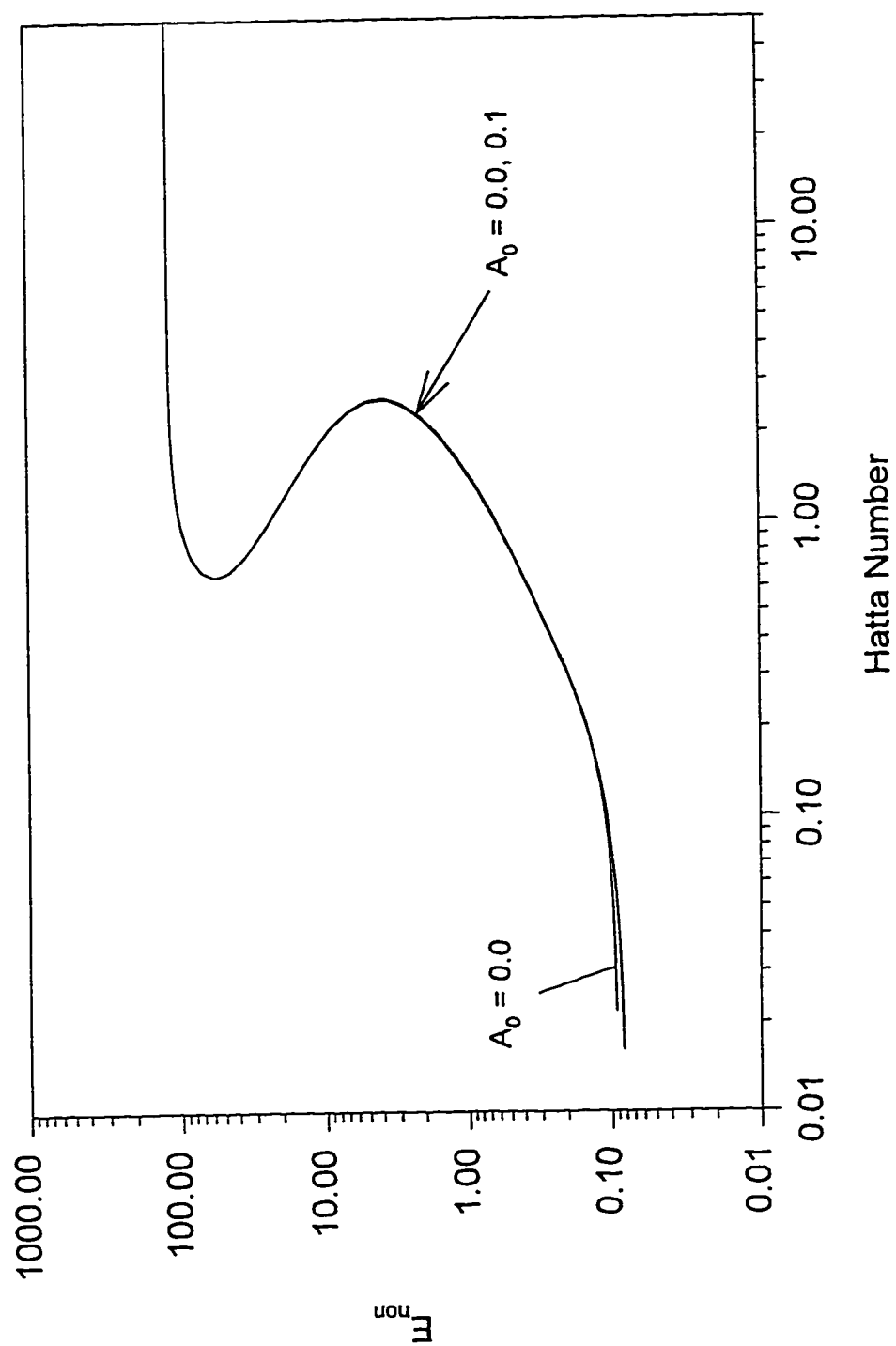


Figure 4.27 The Effect of Parameter A_0

sensitivity analysis as well as the steady state multiplicity analysis. In doing so, some involved mathematical analysis is necessary. Such complications are out of the scope of the present work. However, through the physical understanding of the problem and some observations of the parametric study graphs in section 4.3 as well as some trial and error calculations it was possible to combine some of the model parameters.

The counter effect of temperature on the gas solubility and the chemical reaction rate made it possible to combine the activation energies of reaction and solution. Similarly, the heat generation in the heat transfer film is due to heats of reaction and solution and that would lead us to combine β_R and β_S . The following two combinations were obtained

$$\epsilon_{\text{eff}} = \frac{\epsilon_R}{2} - \epsilon_S \quad (4.1)$$

$$\beta_{\text{eff}} = \beta_R + \beta_S \quad (4.2)$$

The dimensionless group ϵ_{eff} is called the *effective activation energy of reaction and solution* and β_{eff} is called the *effective heat of reaction and solution*. No matter how ϵ_R and ϵ_S are changed the model predictions will be the same as long as ϵ_{eff} is kept constant and the same applies for β_R , β_S and β_{eff} . Different values of ϵ_R , ϵ_S , β_R and β_S were tried while keeping ϵ_{eff} and β_{eff} constant to confirm the validity of equations 4.1 and 4.2. Table 4.2 shows the values of those parameters used for the confirmation.

Figures 4.28 and 4.29 show the model prediction for enhancement factor and the dimensionless surface temperature rise using the different values of ϵ_R and ϵ_S for $\epsilon_{\text{eff}} = 6.0$

Table 4.2 Values of ϵ_R , ϵ_S , β_R and β_S Used to Test Validity of Equations 4.1 and 4.2

ϵ_R	ϵ_S	ϵ_{eff}	β_R	β_S	β_{eff}
20.0	4.0	6.0	0.005	0.001	0.006
25.0	5.5	6.0	0.005	0.001	0.006
30.0	9.0	6.0	0.005	0.001	0.006
16.0	2.0	6.0	0.005	0.001	0.006
13.0	0.5	6.0	0.005	0.001	0.006
20.0	4.0	6.0	0.005	0.001	0.006
20.0	4.0	6.0	0.00055	0.0005	0.006
20.0	4.0	6.0	0.00045	0.00015	0.006
20.0	4.0	6.0	0.0006	0.000	0.006
20.0	4.0	6.0	0.004	0.002	0.006

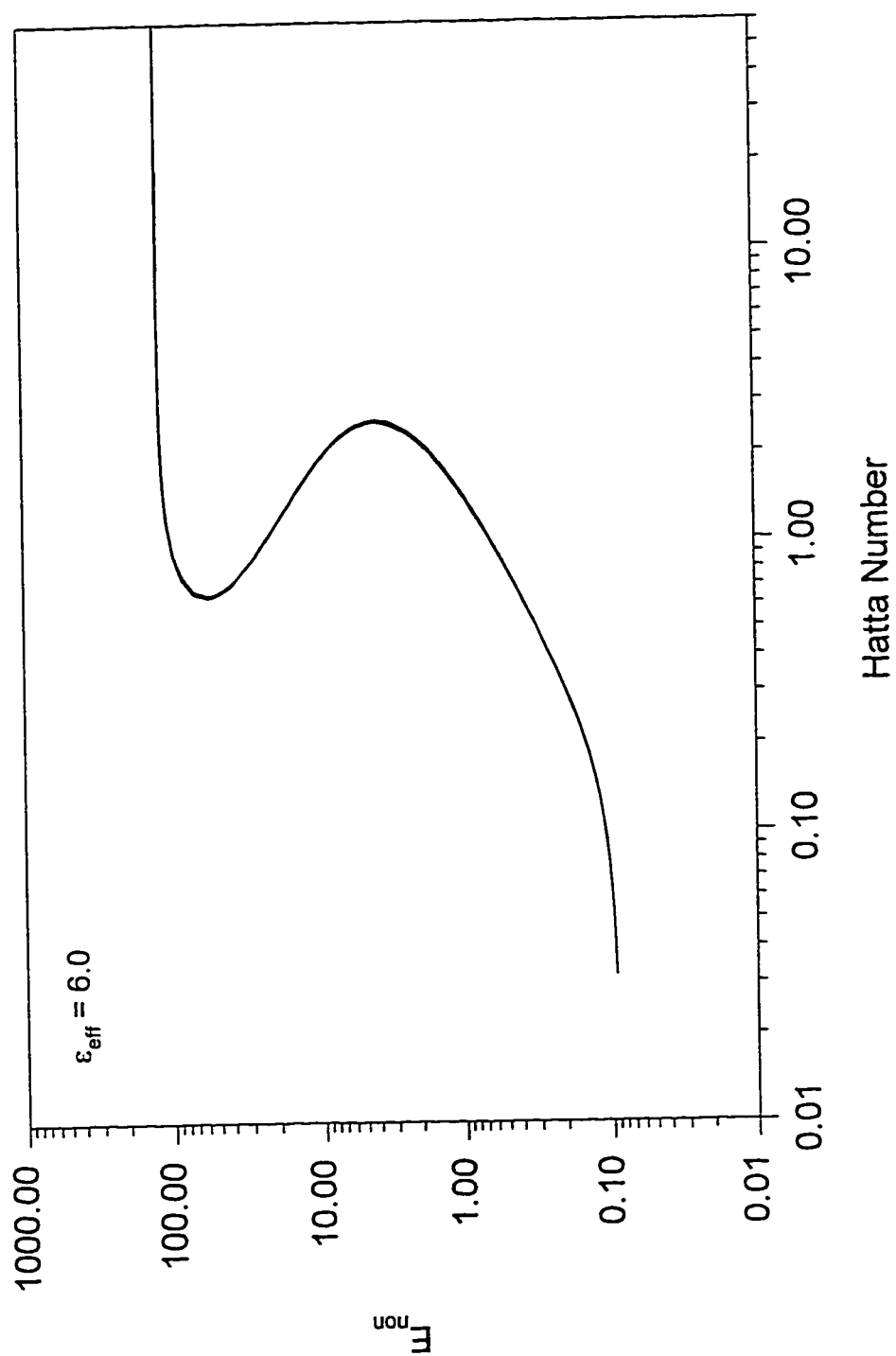


Figure 4.28 The Enhancement Factor for Constant ϵ_{eff} with different Values ϵ_R and ϵ_S as Shown in Table 4.2

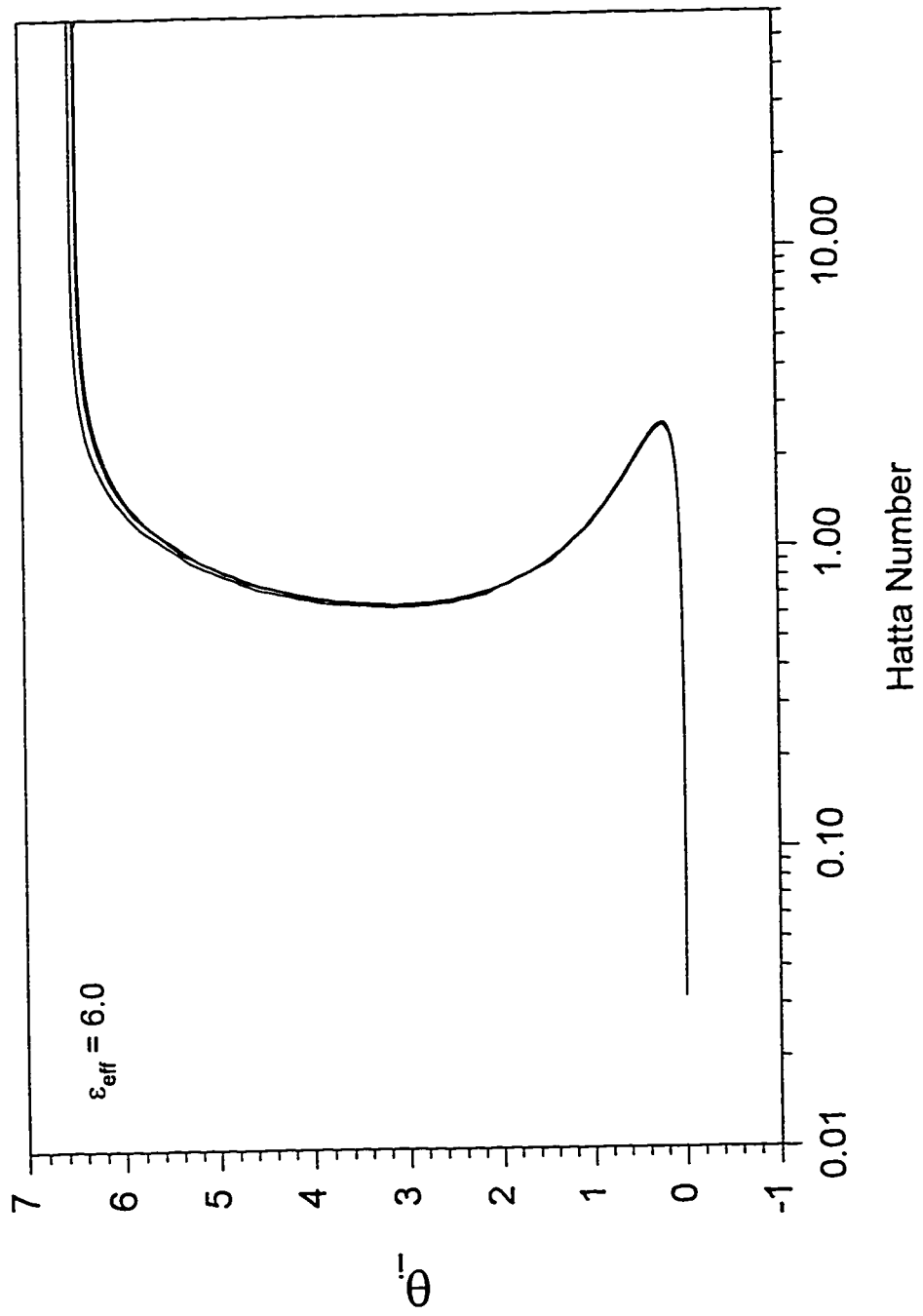


Figure 4.29 The Dimensionless Surface Temperature Rise for Constat ϵ_{eff} and Different Values of ϵ_R and ϵ_S as Shown in Table 4.2

as shown in Table 4.2. Also, the different values of β_R and β_S in the Table for $\beta_{eff} = 0.006$ were used to find the enhancement factor and the dimensionless surface temperature rise in Figures 4.30 and 4.31. The conformance of the combinations in equations 4.1 and 4.2 is excellent as shown in the graphs. However, very little deviation is noticed in Figure 4.29 for the surface temperature rise at high Hatta numbers.

The combined groups ϵ_{eff} and β_{eff} will be used to find criteria for multiple steady states. By fixing all model parameters and one of the two groups, two-parameter continuation analysis (changing both Hatta number and one of the groups) was carried by AUTO. In doing so, AUTO will determine the multiplicity borders for the model. For the set of parameters shown in Table 4.1, Figure 4.32 shows that multiple steady states will occur if the value of ϵ_{eff} is greater than 2.7682. Also, for the same set of parameters in Table 4.1, Figure 4.33 shows that multiplicity will occur if the value of β_{eff} is greater than 0.0031488

4.5 Model Application to Some Industrial Gas-Liquid Reactions

The local film theory model equations will be applied to some real gas-liquid reaction systems of industrial importance. Those systems include the chlorination of n-decane, sulfonation of dodecylbenzene, and chlorination of toluene. All of these gas-liquid reactions are essentially second-order. For these systems, the physiochemical data needed to evaluate the dimensionless model parameters was extracted from the literature as shown in Tables 4.3, 4.4 and 4.5. However, data for the gas side heat transfer coefficient, gas side mass transfer coefficient and Henry's law constant were not available

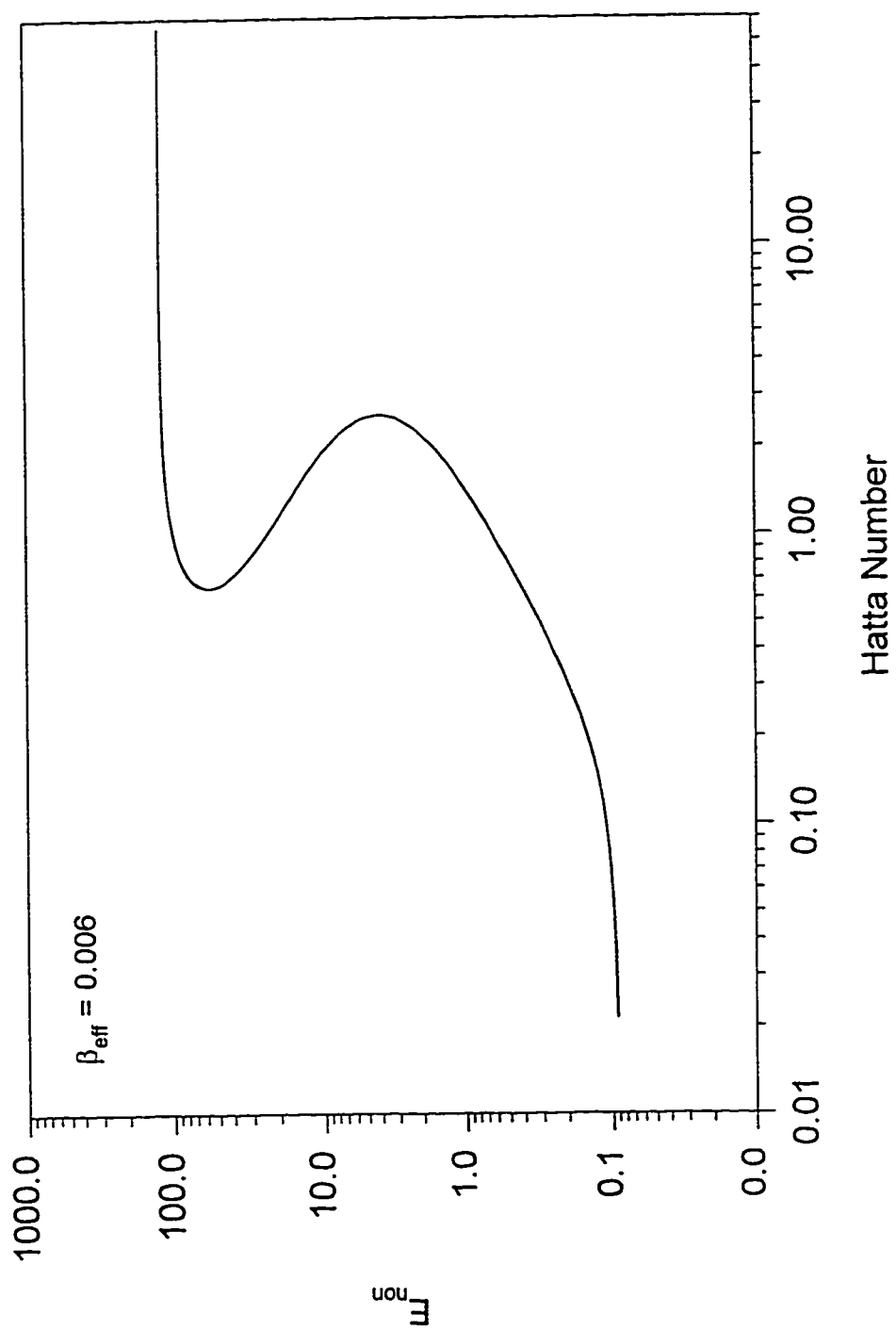


Figure 4.30 The Enhancement Factor for Constant β_{eff} and Different Values of β_R and β_S as Shown in Table 4.2

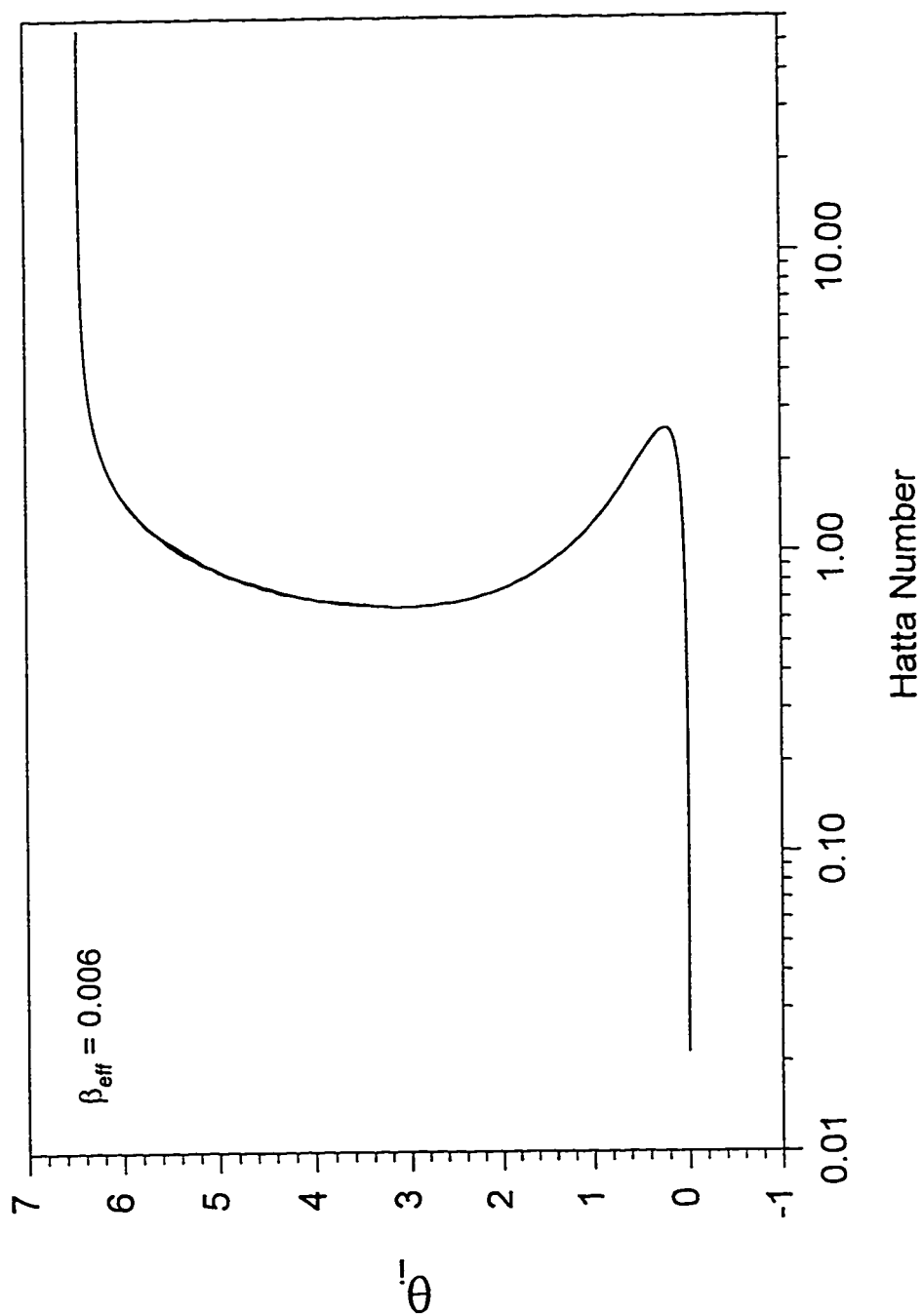


Figure 4.31 The Dimensionless Surface Temperature Rise for Constant β_{eff} and Different Values of b_R and b_S as Shown in Table 4.2

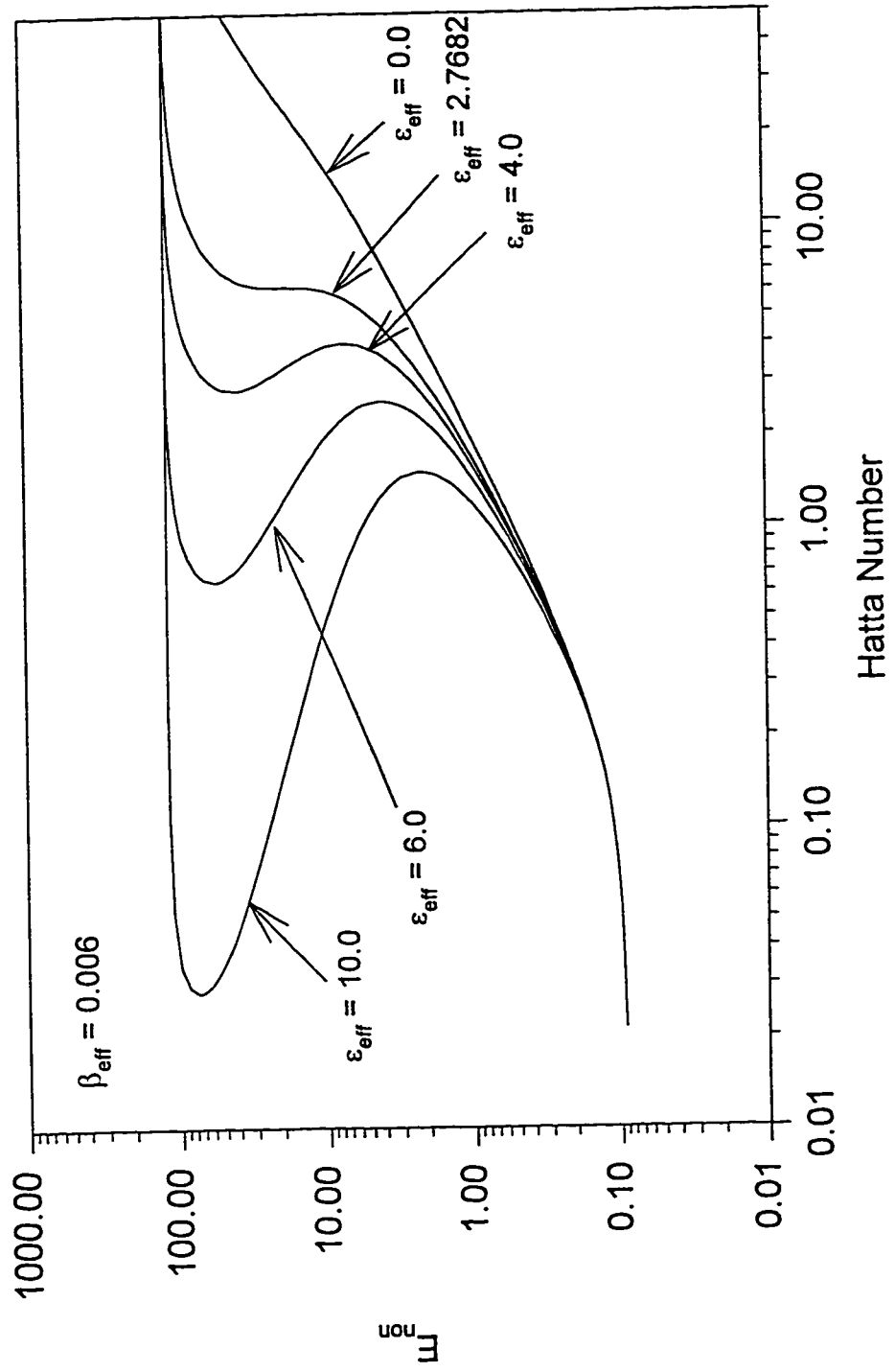


Figure 4.32 Two Parameter Continuation for ϵ_{eff}

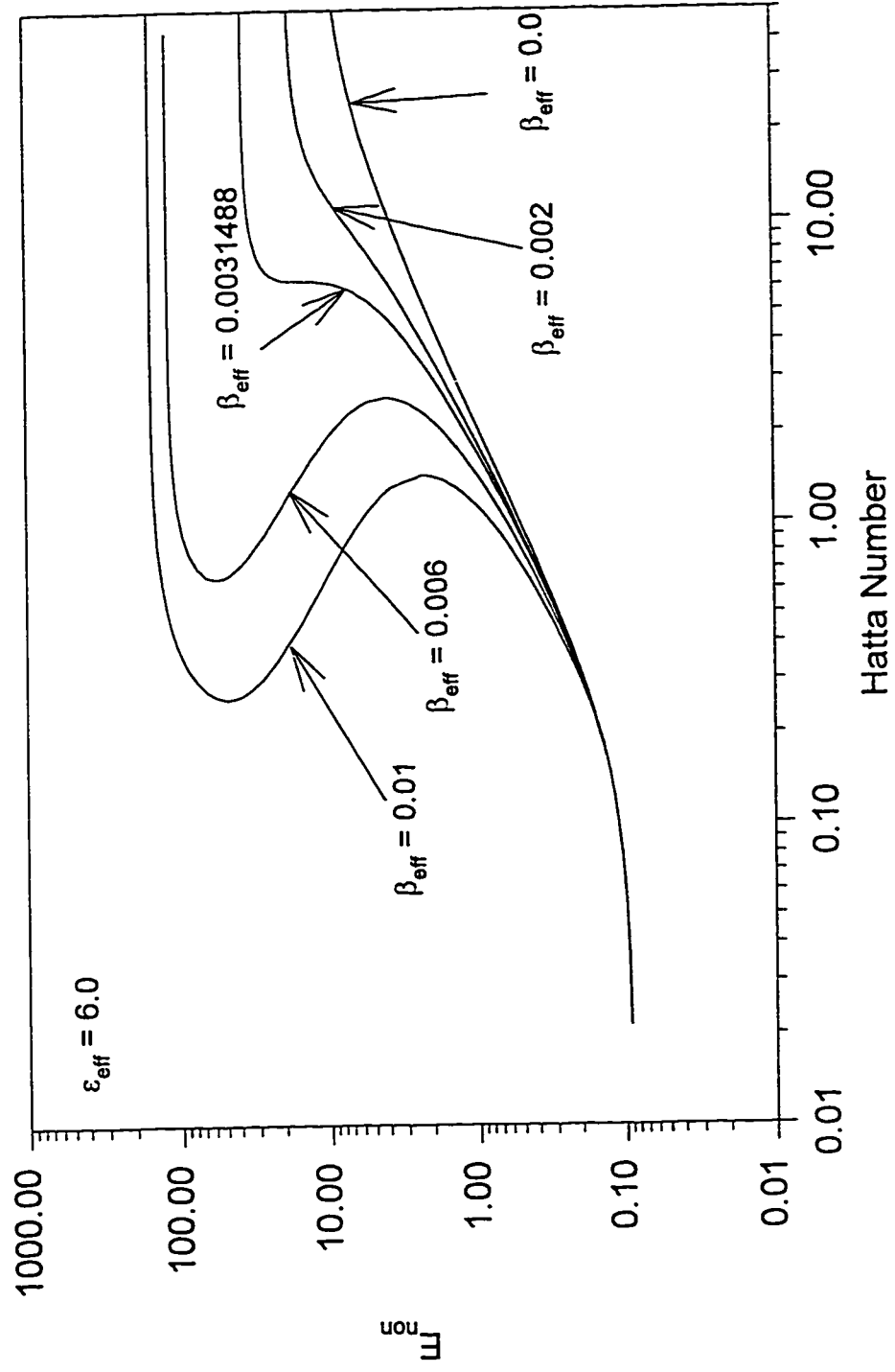


Figure 4.33 Two Parameter Continuation for β_{eff}

to calculate the Biot numbers. Consequently, different values of the Biot numbers will be used to demonstrate the solution of the model.

The enhancement factor and the surface temperature rise for the chlorination of n-decane system are shown in Figures 4.34 to 4.37 for different values of Biot numbers for which a single steady state solution was obtained. Heat effects appear to be minor for this system even at low values of Bi_H that the dimensionless surface temperature rise can reach a maximum value of 0.2 . *Therefore, the isothermal assumption used by previous investigators in modeling gas-liquid CSTRs with this reaction system appears to be justified.* Negative surface temperature rises are noticed at low Hatta numbers when the mass transfer Biot number is greater than zero. The volatility effects for this system are appreciable at moderate values of the Hatta number and when Bi_M is increased the enhancement factor is reduced. The heat and volatility effects are reduced when the value heat transfer Biot number is increased.

The same values of Biot numbers were adopted for the sulfonation of dodecylbenzene as shown in Figures 4.38 to 4.41, for which it is shown that no steady state multiplicity is observed. This system shows a strange behavior for Bi_H value of 0.1, that the heat effects are lower at low values of Bi_H . Also, a decrease in the surface temperature rise is noticed when the Hatta number is increased as shown in Figure 4.39. Moreover, when the mass transfer Biot number is increased the enhancement factor increases. These results are inconsistent with the parametric study in section 4.3 . However, when the value of Bi_H equals 10.0, minor positive surface temperature rises are

Table 4.3 Physiochemical Data for the Chlorination of n-Decane System

DATA	UNITS	CHLORINATION OF N-DECANE	SOURCE
$(-\Delta H_R)$	cal/mole	26,000	Sharma et al. (1976)
$(-\Delta H_S)$	cal/mole	4,500	Sharma et al. (1976)
(ΔH_V)	cal/mole	9,569	Daubert (1987)
E_R	cal/mole	29,000	Sharma et al. (1976)
E_{DA}	cal/mole	3,147	Hoffman et al. (1974)
E_{DB}	cal/mole	3,147	Hoffman (1974)
C_{Aib}	mol/cm ³	4.2×10^{-5}	Bhattacharya et al. (1988)
C_{Bb}	mol/cm ³	3.0×10^{-5}	Bhattacharya et al. (1988)
D_{Ab}	cm ² /sec	2.7×10^{-5}	Huang and Varma (1981)
D_{Bb}	cm ² /sec	1.0×10^{-5}	Huang and Varma (1981)
K_L	cal/(cm sec K)	3.312×10^{-4}	Bhattacharya et al. (1988)
T_b	K	322	Bhattacharya et al. (1988)
α	cm ² /sec	8.12×10^{-4}	Hoffman (1974)

Table 4.4 Physiochemical Data for the Sulfonation of Dodecylbenzene System

DATA	UNITS	SULFONATION OF DDB	SOURCE
$(-\Delta H_R)$	cal/mole	40,750	Moyes (1976)
$(-\Delta H_S)$	cal/mole	10,043	Al-Ubaidi and Selim (1992)
(ΔH_V)	cal/mole	2,009	Al-Ubaidi and Selim (1992)
E_R	cal/mole	17,790	Al-Ubaidi and Selim (1992)
E_{DA}	cal/mole	1,808	Al-Ubaidi and Selim (1992)
E_{DB}	cal/mole	3,778	Al-Ubaidi and Selim (1992)
C_{Aib}	mol/cm ³	$1.273 \cdot 10^{-3}$	Al-Ubaidi and Selim (1992)
C_{Bb}	mol/cm ³	$35.0 \cdot 10^{-3}$	Al-Ubaidi and Selim (1992)
D_{Ab}	cm ² /sec	$1.0 \cdot 10^{-3}$	Al-Ubaidi and Selim (1992)
D_{Bb}	cm ² /sec	$1.0 \cdot 10^{-3}$	Al-Ubaidi and Selim (1992)
K_L	cal/(cm sec K)	$7.7 \cdot 10^{-3}$	Al-Ubaidi and Selim (1992)
T_b	K	298	Al-Ubaidi and Selim (1992)
α	cm ² /sec	$2.0 \cdot 10^{-4}$	Al-Ubaidi and Selim (1992)

Table 4.5 Physiochemical Data for the Chlorination of Toluene System

DATA	UNITS	CHLORINATION OF TOLUENE	SOURCE
$(-\Delta H_R)$	cal/mole	30,000	Moyes (1976)
$(-\Delta H_S)$	cal/mole	5,213	Mann and Clegg (1975)
(ΔH_V)	cal/mole	803	Al-Ubaidi and Selim (1992)
E_R	cal/mole	16,069	Al-Ubaidi and Selim (1992)
E_{DA}	cal/mole	1,808	Al-Ubaidi and Selim (1992)
E_{DB}	cal/mole	2,582	Al-Ubaidi and Selim (1992)
C_{Aib}	mol/cm ³	$2.67 \cdot 10^{-3}$	Mann and Clegg (1975)
C_{Bb}	mol/cm ³	$150.0 \cdot 10^{-3}$	Al-Ubaidi and Selim (1992)
D_{Ab}	cm ² /sec	$3.5 \cdot 10^{-3}$	Al-Ubaidi and Selim (1992)
D_{Bb}	cm ² /sec	$3.5 \cdot 10^{-3}$	Al-Ubaidi and Selim (1992)
K_L	cal/(cm sec K)	$3.56 \cdot 10^{-4}$	Moyes (1976)
T_b	K	298	Al-Ubaidi and Selim (1992)
α	cm ² /sec	$1.05 \cdot 10^{-3}$	Al-Ubaidi and Selim (1992)

noticed and the volatility becomes detrimental for the enhancement factor as shown in Figures 4.40 and 4.41 .

Unlike the last two systems, the chlorination of toluene exhibits steady state multiplicity with very high heat effects and becomes very sensitive to the volatility as shown in Figures 4.42 to 4.45. A strange multiplicity pattern is observed at low values of Bi_H with an extremely high and unrealistic surface temperature rises. Five steady state solutions can be obtained when Bi_M equals zero for a small range of Hatta number values as shown in Figure 4.42 . The heat effects are less severe for large values of heat transfer Biot number and only three steady state solutions are obtained for the nonvolatile liquid case. Still the volatility has a large effect at the high heat Biot number, that the multiplicity can be destroyed when Bi_M is high.

We should re-emphasize that the choice of the Biot numbers was arbitrary for the three systems (as no data was found) and some of the values used might be unrealistic which might give strange results as shown in Figure 4.38, 4.39, 4.42 and 4.43.

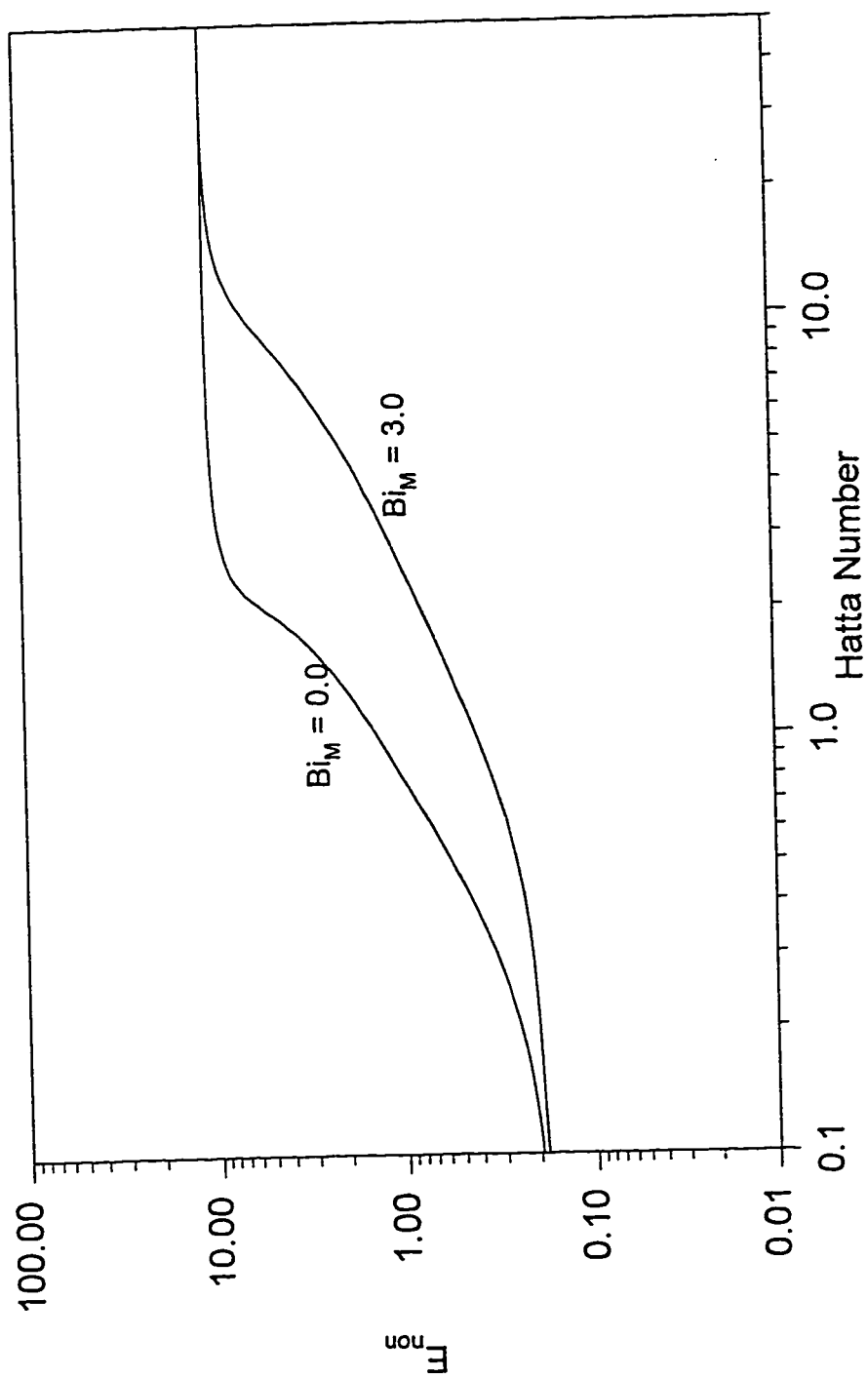


Figure 4.34 The Enhancement Factor for Cl_2 -Decane System ($Bi_H = 0.1$)

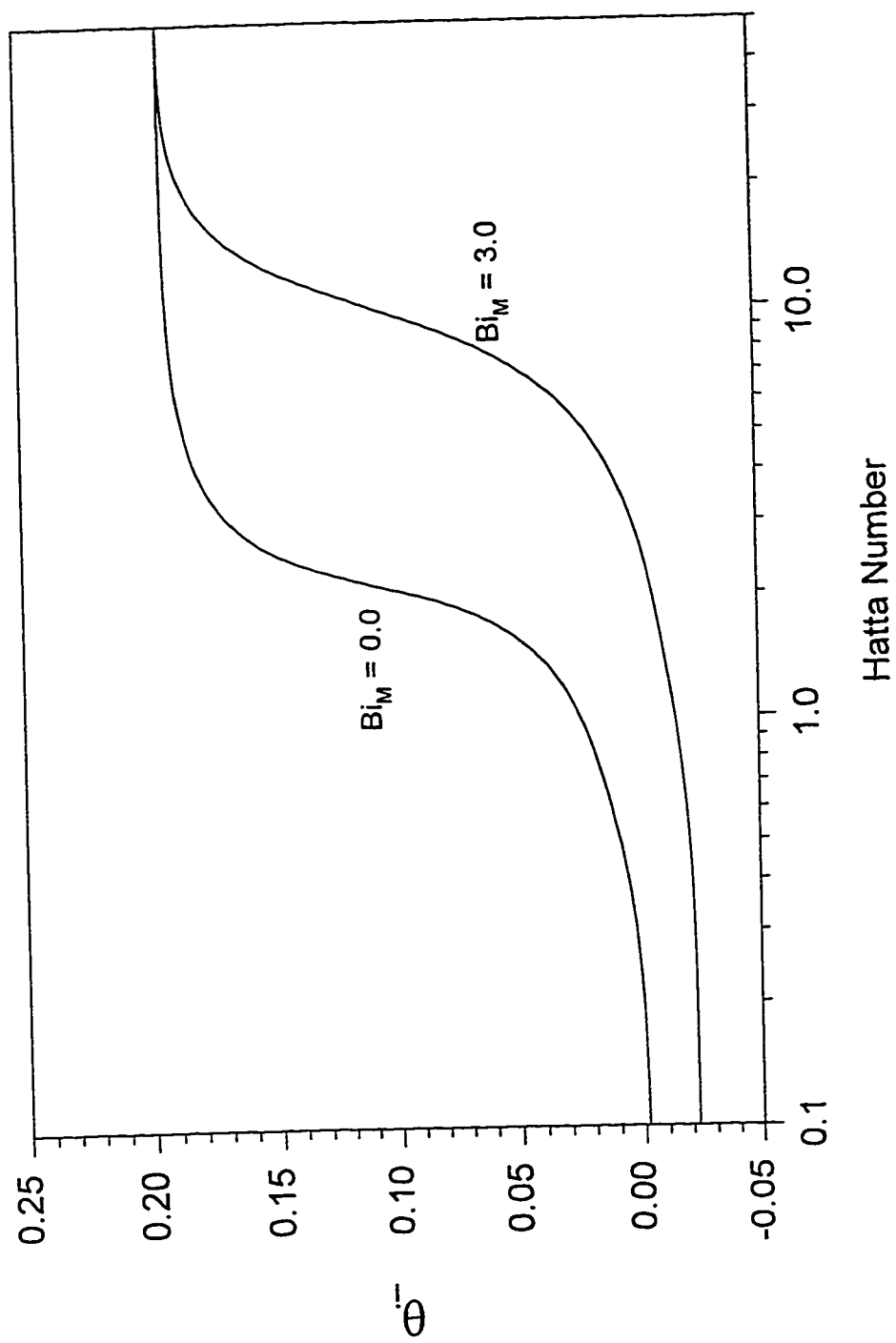


Figure 4.35 The Surface Temperature Rise for Cl_2 -Decane System ($\text{Bi}_H = 0.1$)

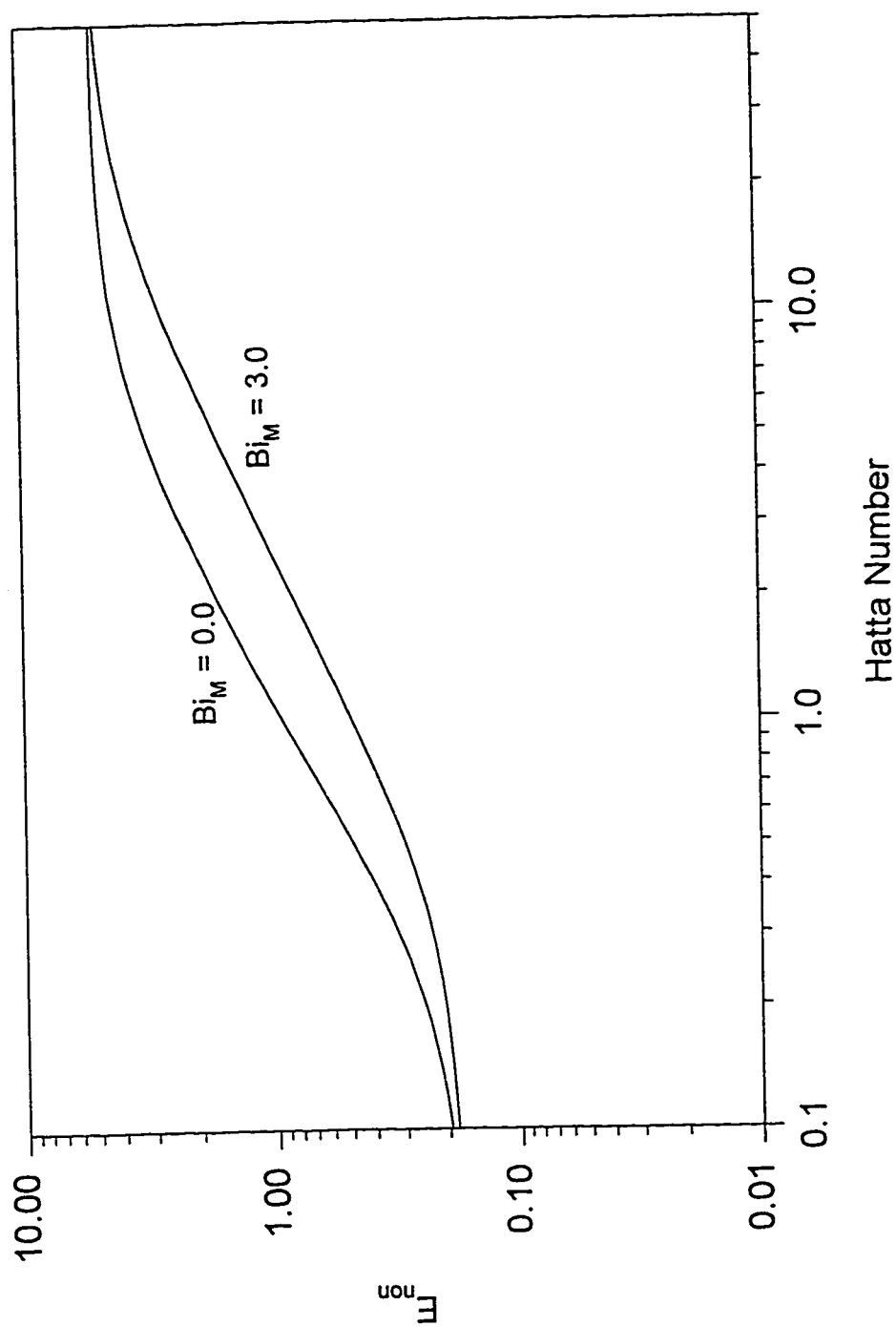


Figure 4.36 The Enhancement Factor for Cl_2 - Decane System ($\text{Bi}_H = 10.0$)

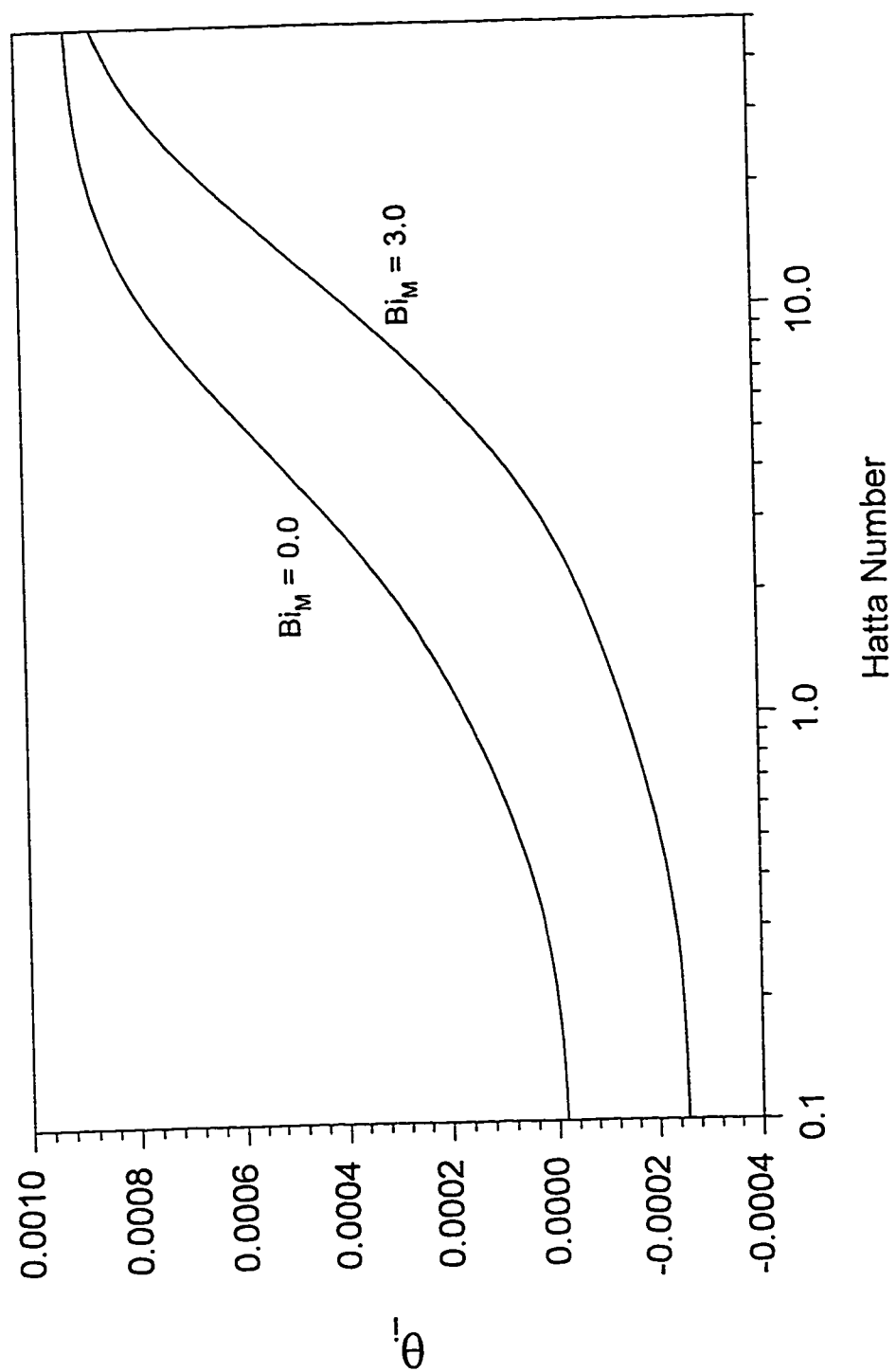


Figure 4.37 The Surface Temperature Rise for The Cl_2 -Decane System ($\text{Bi}_H = 10.0$)

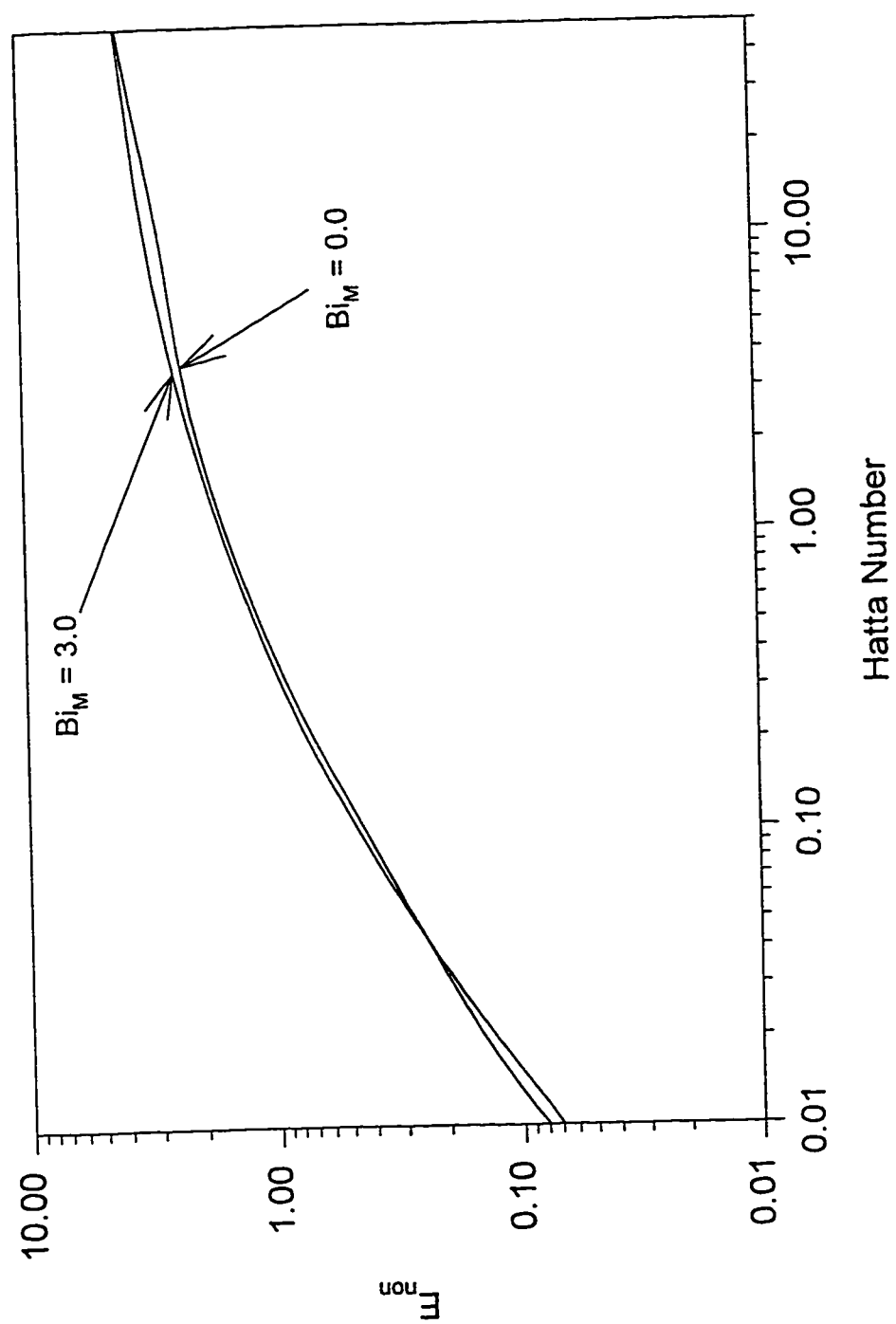


Figure 4.38 The Enhancement Factor for Sulfonation of DDB System ($Bi_H = 0.1$)

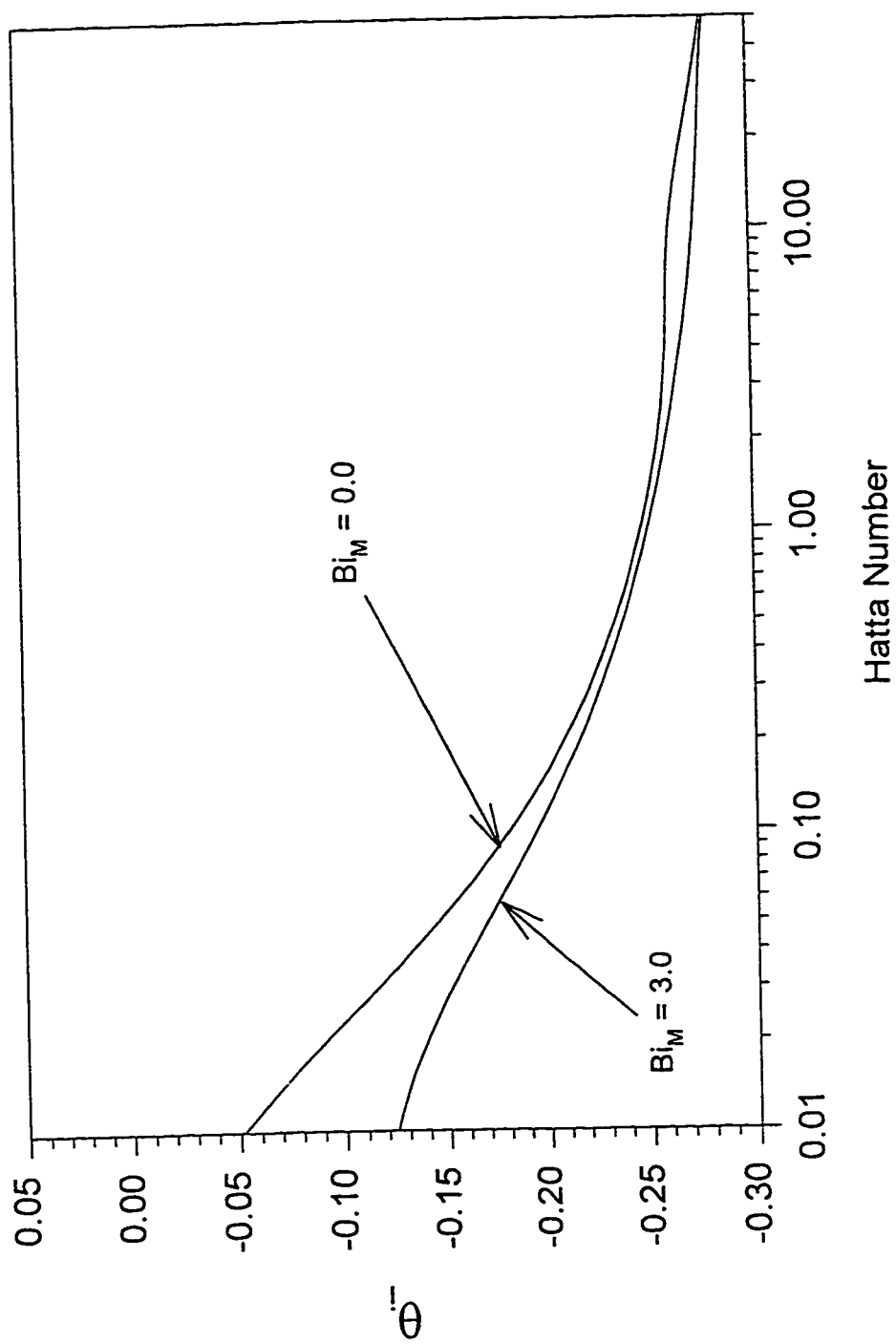


Figure 4.39 The Surface Temperature Rise for Sulfonation of DDB System ($Bi_H=0.1$)

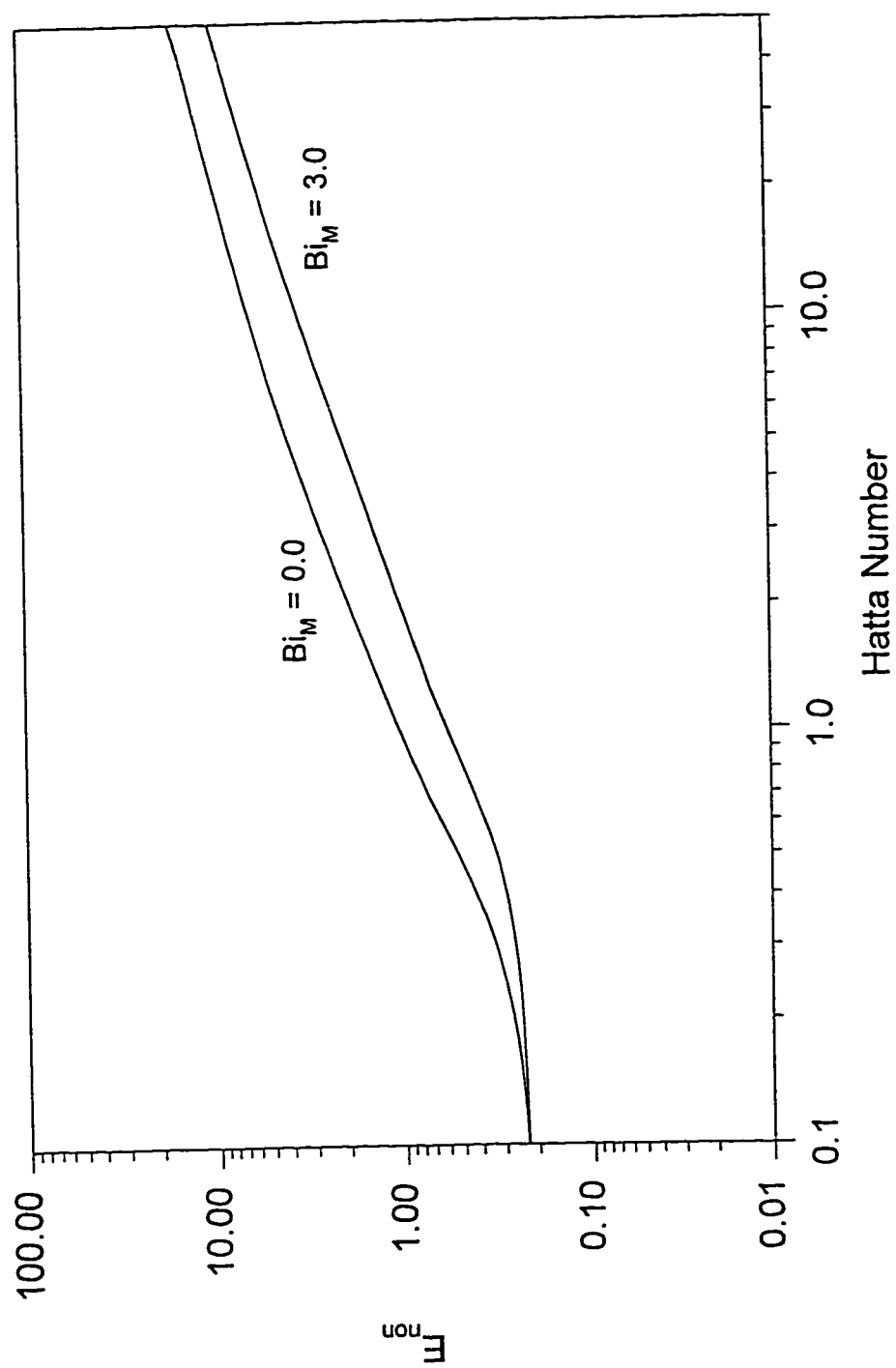


Figure 4.40 The Enhancement Factor for Sulfonation of DDB System ($Bi_H = 10.0$)

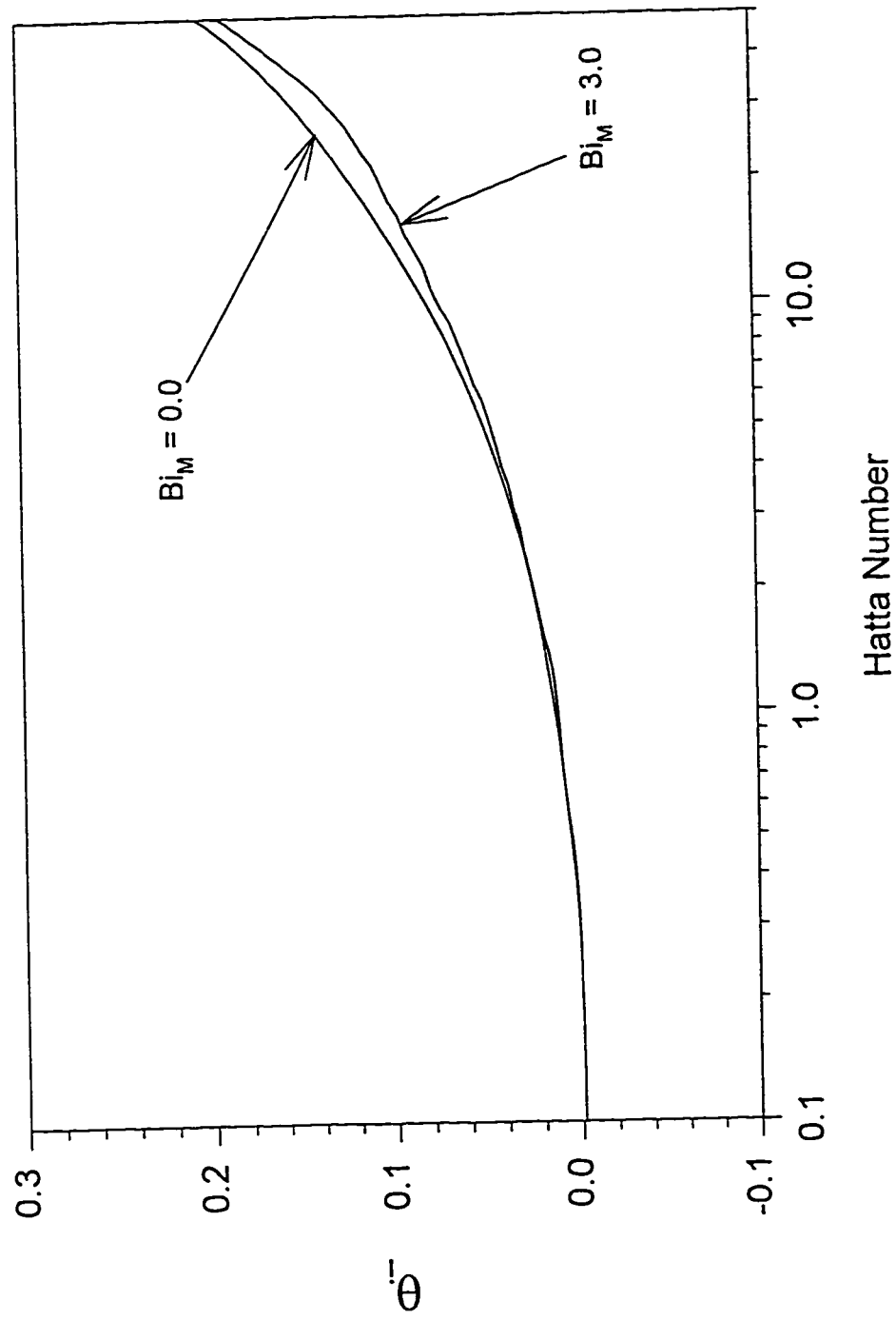


Figure 4.4.1 The Surface Temperature Rise for Sulfonation of DDB System ($Bi_H = 10.0$)

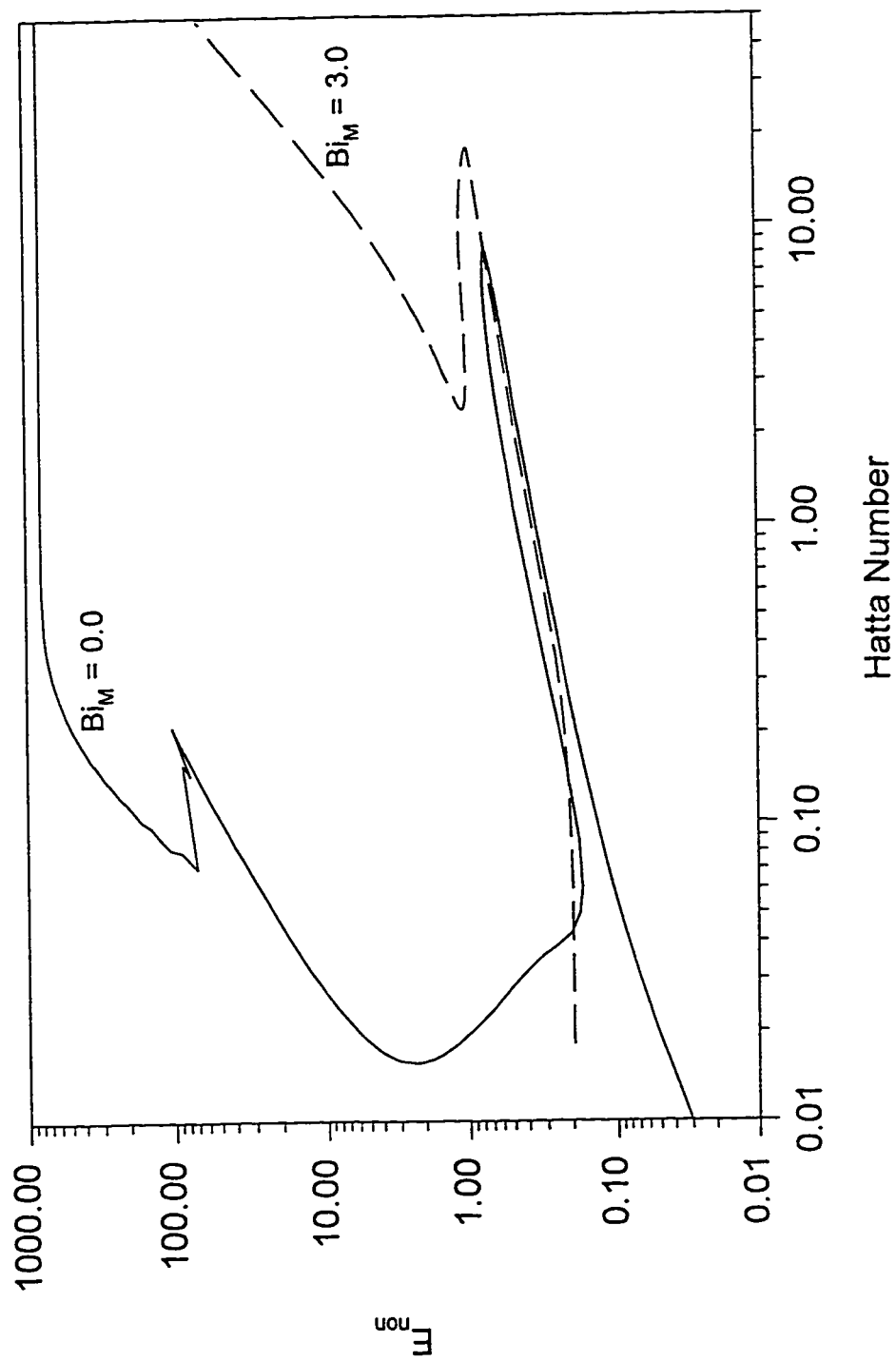


Figure 4.42 The Enhancement Factor for Cl_2 - Toluene System ($\text{Bi}_H = 0.1$)

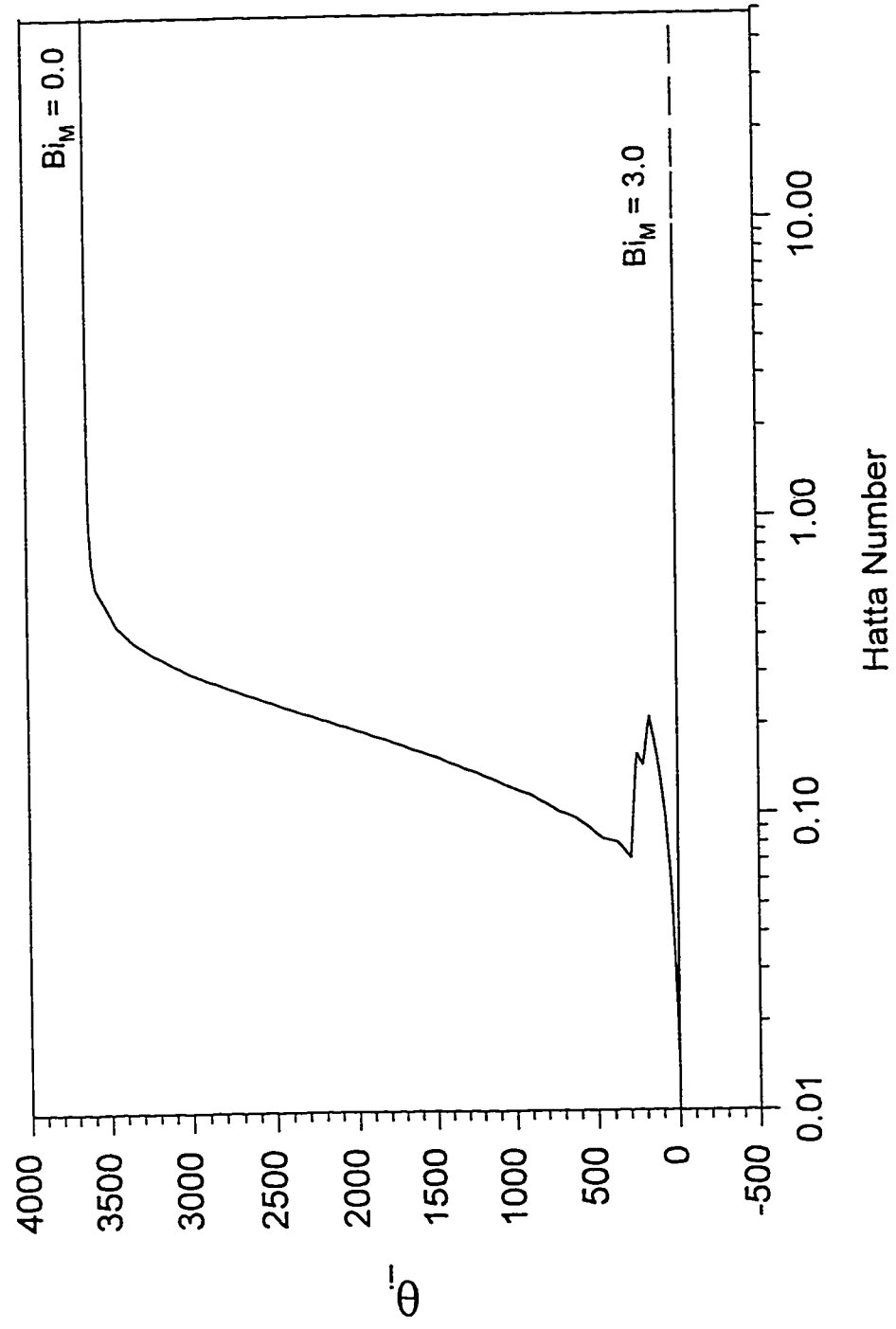


Figure 4.43 The Surface Temperature Rise for Cl_2 -Toluene System ($\text{Bi}_H = 0.1$)

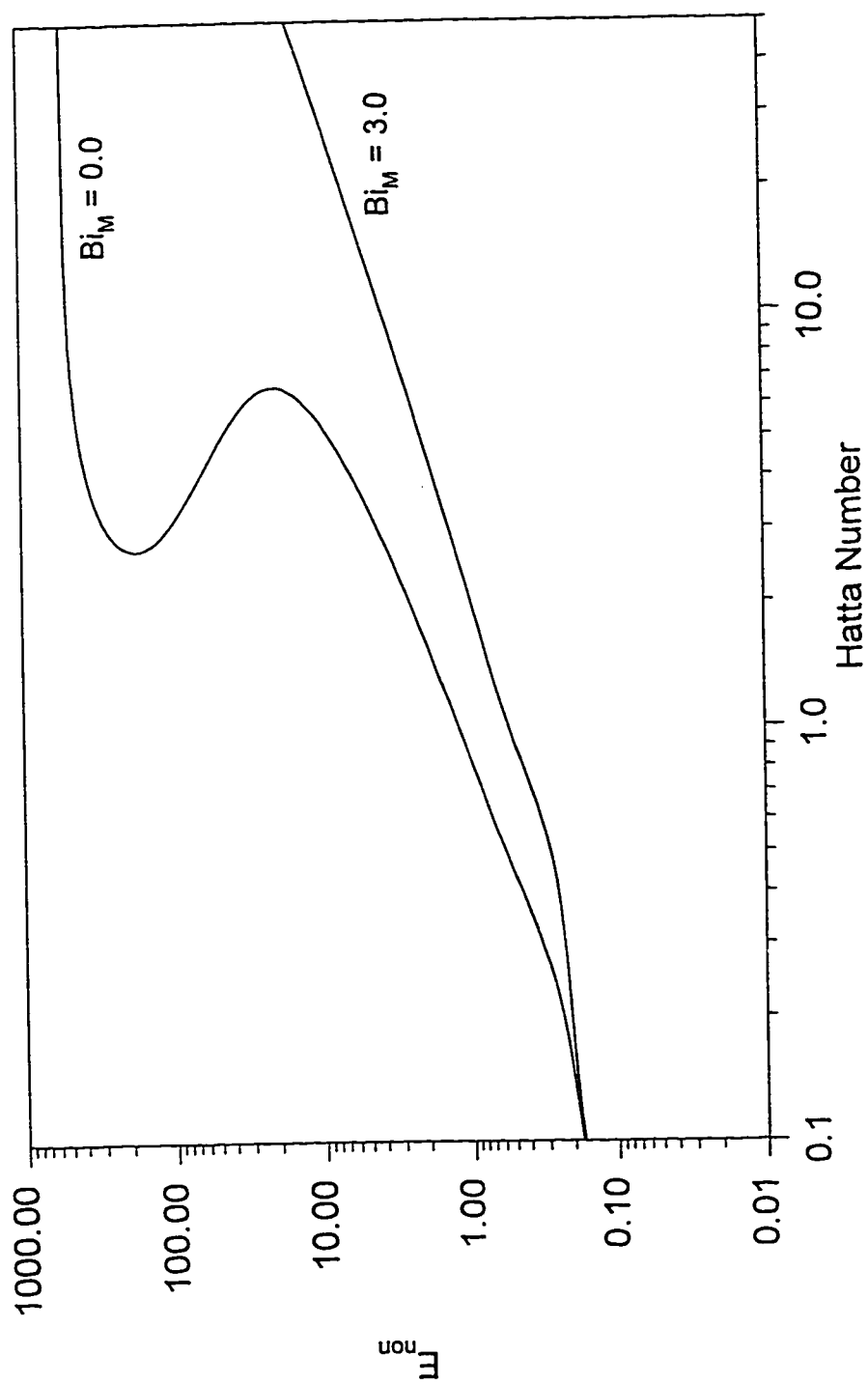


Figure 4.44 The Enhancement Factor for CL_2 - Toluene System ($Bi_H = 10.0$)

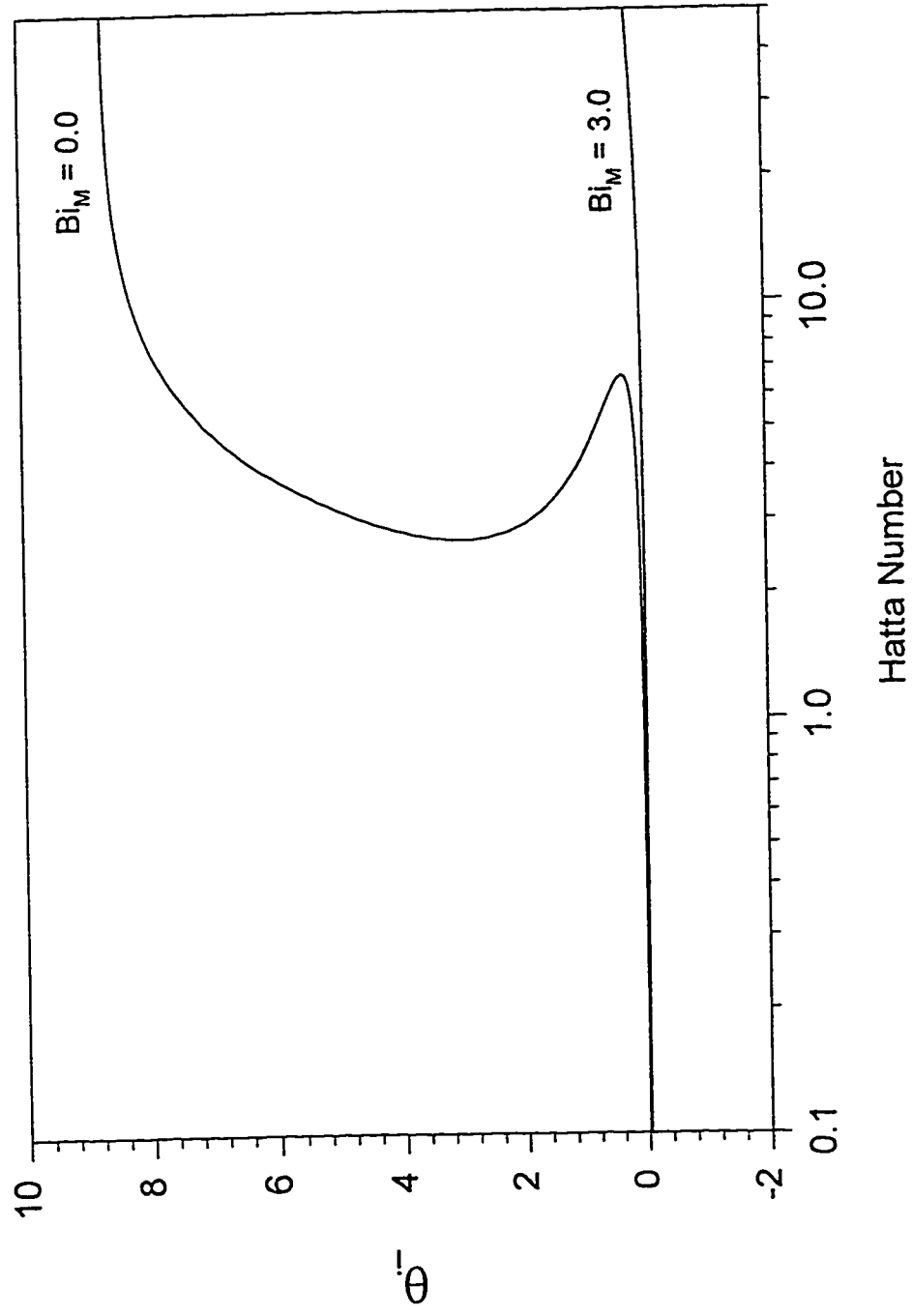


Figure 4.45 The Surface Temperature Rise for Cl_2 -Toluene System ($\text{Bi}_H = 10.0$)

CHAPTER 5

RESULTS AND DISCUSSION : **LOCAL MODEL APPLICATION TO A GLOBAL** **REACTOR DESIGN PROBLEM**

In this chapter the film-theory is used to model the local gas absorption in gas-liquid CSTR simulation. In chapter 2 it was shown that in previous literature, approximate solutions for the local gas absorption problem were used. Here no approximation for the enhancement factor will be adopted. However, the boundary value problem will be solved numerically and will be linked with a global reactor design problem.

5.1 *Global Model Assumptions*

The following assumptions will be used for the gas-liquid reactor modeling which are similar to those mostly implemented in literature :

1. The thermophysical properties of the gas and the liquid, interfacial area, gas holdup, mass transfer coefficient, diffusion coefficients, and volumetric flow rate of the liquid are independent of temperature and conversion.
2. The liquid feed to the reactor does not contain any dissolved gaseous reactant. The gas feed is composed of species A and other inert species.

3. The gas-side resistance to mass transfer is negligible. The liquid products are nonvolatile.
4. The total pressure is independent of temperature and position in the reactor.
5. Phase equilibria of the gaseous reactant follows Henry's law :

$$P_{Ai} = [H_A \exp(\Delta H_s / RT)] A_i \quad (5.1)$$

6. The ideal gas law applies, and the temperature dependence of the reaction rate constant is described by the Arrhenius law.

5.2 Derivation of the Global Model Equations

With the assumptions in the preceding section, the following steady state balances can be written :

mass balance for the gas reactant :

$$N_{gf} y_{Af} - N_g y_A = R_A V_R + F_l A_l \quad (5.2)$$

mass balance for the liquid reactant :

$$F_l (B_{lf} - B_l) = v R_A V_R \quad (5.3)$$

energy balance :

$$F_l \rho_l C_{pl} (T_{lf} - T) + N_{gf} C_{pg} T_{gf} - N_g C_{pg} (1 - y_B) T + (-\Delta H_s - \Delta H_R) R_A V_R + (-\Delta H_s) F_l A_l - (\Delta H_v) N_g y_B - US(T - T_c) = 0 \quad (5.4)$$

The rate of gas absorption can be expressed in terms of the enhancement factor :

$$R_A V_R + F_l A_l = k_l^0 a V_R A_i E_{\text{non}}^* \quad (5.5)$$

A_i is the interfacial concentration of the gas reactant and it has to be determined from the Henry's law equation (5.1):

$$A_i = \frac{P_{Ai}}{H_A} \exp\left(\frac{-\Delta H_s}{RT}\right) \quad (5.6)$$

Since the gas phase resistance is negligible, then :

$$P_{Ai} = P_{Ag} = y_A P \quad (5.7)$$

and applying the ideal gas law :

$$P = \frac{N_g RT}{F_g} \quad (5.8)$$

also,

$$\frac{F_g}{F_{gf}} = \frac{N_g RT / P}{N_{gf} RT_f / P_f} \approx \frac{N_g T}{N_{gf} T_f} \quad (5.9)$$

Further, the following material balance can be written to find y_A :

$$y_A N_g = y_{Af} N_{gf} (1 - x_A) \quad (5.10)$$

where x_A is the conversion of gas reactant. Combining equations (5.6), (5.7), (5.8), (5.9)

and (5.10) yields :

$$A_i = \frac{RT_f}{H_A} \frac{A_{gf} (1 - x_A) N_{gf}}{N_g} \exp\left(\frac{-\Delta H_s}{RT}\right) \quad (5.11)$$

where $A_{gf} = \frac{y_{Af} N_{gf}}{F_{gf}}$, the feed concentration of gas reactant.

Writing inert material balance :

$$N_{gf} (1 - y_{Af}) = N_g (1 - y_A - y_B) \quad (5.12)$$

and defining the conversion of the gas reactant as :

$$x_A = 1 - \frac{y_A N_g}{y_{Af} N_{gf}} \quad (5.13)$$

Combining equations (5.12) and (5.13) yields :

$$\frac{N_{gf}}{N_g} = \frac{1 - y_B}{1 - y_{Af} x_A} \quad (5.14)$$

Substituting (5.14) into (5.11) gives the final equation of the interfacial concentration of the gas reactant :

$$A_i = \frac{RT_f}{H_A} \frac{A_{gf} (1 - y_B) (1 - x_A)}{(1 - y_{Af} x_A)} \exp\left(\frac{-\Delta H_s}{RT}\right) \quad (5.15)$$

Combining equations (5.2), (5.5), (5.13) and (5.15) leads to the following equation for the conversion of gas reactant A :

$$x_A = \frac{k_l^0 a V_R R T_{gf} E_{\text{non}}^* (1 - y_B) (1 - x_A)}{H F_{gf} (1 - y_{Af} x_A)} \exp\left(\frac{(-\Delta H_s)}{RT_{lf}}\right) \quad (5.16)$$

The conversion of the liquid reactant B can be derived by combining equations (5.2) and (5.3) as follows :

$$x_B = 1 - \frac{B_l}{B_{lf}} = v \left(\frac{F_{gf} / F_l}{B_{lf} / A_{gf}} x_A - \frac{A_l}{B_{lf}} \right) \quad (5.17)$$

Combining the energy balance equation (5.4) and (5.5), and by using (5.14) and (5.15) the energy balance equation becomes :

$$\begin{aligned}
& - \left[\frac{F_l}{F_g} + \frac{\rho_{gf} C_{Pg}}{\rho_l C_{Pl}} (1 - y_{Af} x_A) \right] \frac{T - T_{lf}}{T_{lf}} + \frac{(-\Delta H_S - \Delta H_R) A_{gf}}{\rho_l C_{Pl} T_{lf}} \frac{k_l^0 a V_R R T_{gf}}{H_A F_{gf}} \\
& E_{\text{non}}^* \frac{(1 - y_B)(1 - x_A)}{(1 - y_{Af} x_A)} \exp\left(\frac{-\Delta H_S}{RT}\right) + \left(\frac{\rho_{gf} C_{Pg}}{\rho_l C_{Pl}} + \frac{-\Delta H_v \rho_{gf}}{\rho_l C_{Pl} T_{lf}} \frac{y_B}{1 - y_B} \right) y_{Af} x_A \\
& + \frac{\rho_{gf} C_{Pg}}{\rho_l C_{Pl}} \left(\frac{T_{gf}}{T_{lf}} - 1 \right) - \frac{-\Delta H_v \rho_{gf}}{\rho_l C_{Pl} T_{lf}} \frac{y_B}{1 - y_B} - \frac{(-\Delta H_R) F_l A_{gf}}{\rho_l C_{Pl} T_{lf} F_{gf}} \frac{B_{lf}}{A_{gf}} \frac{A_l}{B_{lf}} \\
& - \frac{(-\Delta H_S - \Delta H_R) A_{gf}}{\rho_l C_{Pl} T_{lf}} \left(\frac{T - T_{lf}}{T_{lf}} - \frac{T_c - T_{lf}}{T_{lf}} \right) = 0
\end{aligned} \tag{5.18}$$

5.3 The Global Model Equations in Dimensionless Form

The dimensionless groups in Table 5.1 are convenient for the global problem. Applying those dimensionless groups to equations (5.15) to (5.18) leads to the following dimensionless equations :

$$A_i = \frac{H_0 A_{gf} (1 - y_B)(1 - x_A)}{(1 - y_{Af} x_A)} \exp\left(\frac{\delta}{1 + \theta_b}\right) \tag{5.19}$$

$$x_A = \frac{D_g E_{\text{non}}^* (1 - y_B)(1 - x_A)}{(1 - y_{Af} x_A)} \exp\left(\frac{\delta}{1 + \theta_b}\right) \tag{5.20}$$

$$x_B = v \left(\frac{Q}{q} x_A - a_l \right) \tag{5.21}$$

Table 5.1 Definition of Dimensionless Variables and Groups

Dimensionless Variable/Group	Definition
a_l	$\frac{A_l}{B_{lf}}$
q	$\frac{B_{lf}}{A_{gf}}$
Q	$\frac{F_{gf}}{F_l}$
p	$\frac{(-\Delta H_R)F_l A_{gf}}{\rho_l C_{pl} T_{lf} F_{gf}}$
v	$\frac{(-\Delta H_v) \rho_{gf}}{\rho_l C_{pl} T_{lf}}$
r	$\frac{\rho_{gf} C_{pg}}{\rho_l C_{pl}}$
B	$\frac{[(-\Delta H_s) + (-\Delta H_R)]A_{gf}}{\rho_l C_{pl} T_{lf}}$
D_{gf}	$\frac{ak_l^0 V_R H_0}{F_{gf}}$
H_0	$\frac{RT_{gf}}{H_A}$
θ_b	$\frac{T - T_{lf}}{T_{lf}}$
θ_{bc}	$\frac{T_c - T_{lf}}{T_{lf}}$
θ_{br}	$\frac{T_{gf}}{T_{lf}}$
α	$\frac{1}{Q} + r$
β	$\frac{US}{F_{gf} \rho_l C_{pl}}$
δ	$\frac{(-\Delta H_s)}{RT_{lf}}$

$$\begin{aligned}
& -\left[\frac{1}{Q} + r(1 - y_{Af}x_A)\right]\theta_b + BD_g E_{\text{non}}^* \frac{(1 - y_B)(1 - x_A)}{(1 - y_{Af}x_A)} \exp\left(\frac{\delta}{1 + \theta_b}\right) \\
& + \left(r + v \frac{y_B}{1 - y_B}\right)y_{Af}x_A + r(\theta_{br} - 1) - v \frac{y_B}{1 - y_B} - pqa_1 - B(\theta_b - \theta_{bc}) = 0
\end{aligned} \tag{5.22}$$

Combining equations (5.20) and (5.22) yield to the following equations :

$$x_A = \frac{(\alpha + \beta)\theta_b + pqa_1 + v \frac{y_B}{1 - y_B} - \beta\theta_{bc} - r(\theta_{br} - 1)}{B + \left[v + \frac{y_B}{1 - y_B} + r(1 + \theta_b)\right]y_{Af}} \tag{5.23}$$

$$\theta_b = \frac{\left[B + \left(r + v \frac{y_B}{1 - y_B}\right)y_{Af}\right]x_A + \beta\theta_{bc} + r(\theta_{br} - 1) - v \frac{y_B}{1 - y_B} - pqa_1}{\alpha + \beta - ry_{Af}x_A} \tag{5.24}$$

Note that a single nonlinear equation for the reactor temperature is obtained by substituting equation (5.23) into (5.22). Equation (5.24) can be used to find the a-priori temperature bounds which are useful for numerical calculations. Physical considerations indicate that an upper bound for the reactor temperature is achieved when $x_A = 1$, $a_1 = 0$ and $y_B = 0$. Therefore,

$$\theta_{bUB} = \frac{B + ry_{Af} + \beta\theta_{bc} + r(\theta_{br} - 1)}{\alpha + \beta - ry_{Af}} \tag{5.25}$$

On the other hand, the lower bound for the reactor temperature is achieved when $x_A = a_1 = 0$. Therefore,

$$\theta_{bLB} = \frac{\beta\theta_{bC} + r(\theta_{br} - 1) - v \frac{y_B}{1 - y_B}}{\alpha + \beta} \quad (5.26)$$

Now the steady state reactor temperature is bounded between a lower and an upper values (i.e. $\theta_{bLB} \leq \theta_b \leq \theta_{bUB}$).

5.4 Method of Solution

It was proved in literature that the algebraic model equations for a nonisothermal gas-liquid CSTR could exhibit steady state multiplicity (chapter 2, section 2.f). Also, the possibility of multiple steady states was shown to exist for the local nonisothermal problem in this thesis (chapter 4). The software AUTO does not handle systems of algebraic-differential equations to trace multiple solutions. Therefore, an iterative code needs to be developed to find multiple solutions for the local-global problems.

Upon substituting equation (5.23) into (5.22) we basically have one implicit equation for the reactor steady state temperature. To solve equation (5.22), E_{non}^* and A_1 have to be determined by solving the local model equations. However, solving those equations needs determining the values of C_{Bb} (B_1) and T_b (T) which have to be determined from the global model. The two problems are linked together now as shown in Figure 5.1 and an iterative code needs to be developed to handle such a problem. Different methods were tried to solve equation (5.22) and find its multiple solutions including, the Newton-Raphson method, Secant method and Bisection method. The former two methods failed to find multiple solutions of the equation using a lot of trial

and error procedures for the initial guess. However, the use of the Bisection method was successful in finding the multiple solutions for the equation. A value for the dimensionless reactor temperature is guessed and subsequently the gas conversion, interfacial concentration and liquid concentration are calculated via equations (5.23), (5.19) and (5.21), respectively. The enhancement factor and the bulk liquid concentration for the gas reactant are calculated by solving the boundary value problem equations (3.24) to (3.32) using COLNEW package. Solutions for equation (5.22) are then searched between the upper and the lower bounds for the reactor temperature. During the Bisection, each time when a new reactor temperature is adopted, x_A , A_i , and B_i are calculated and COLNEW is called to find E_{non}^* and A_i . A computer code is developed to perform the above procedure. The algorithm in Figures 5.2 to 5.4 gives a detailed schematic for the program.

5.5 Global Model Simulation Results and Discussion

The objective of this work is to demonstrate how to link the differential equations for the local problem with the algebraic equations for the global problem without using any approximation for the enhancement factor and the bulk liquid concentration for the gas reactant. None of the previous studies attempted to do that, however, approximate expressions for the enhancement factor and bulk liquid concentration for the gas reactant were used. Those expressions constitute systems of algebraic implicit equations for an isothermal local film model and a general reaction regime, and they were derived by Van Krevelen and Hoftijzer (1948) and Teramoto et al. (1969). With those approximate

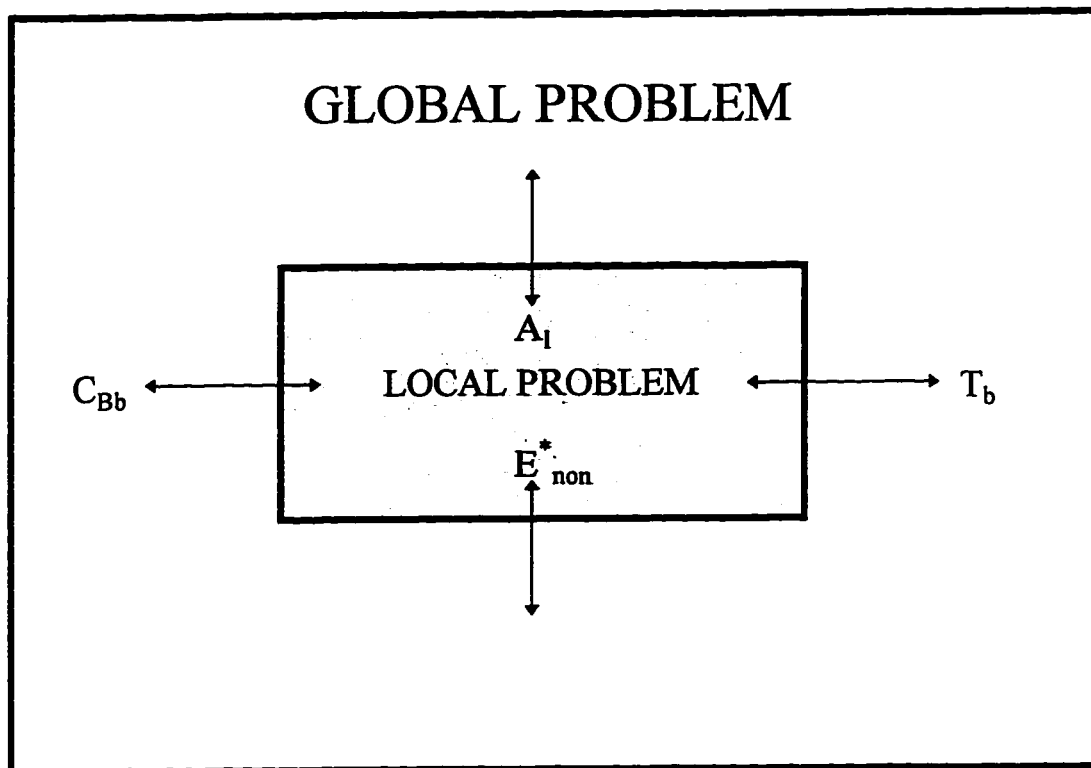


Figure 5.1 Link Between Local and Global Problems

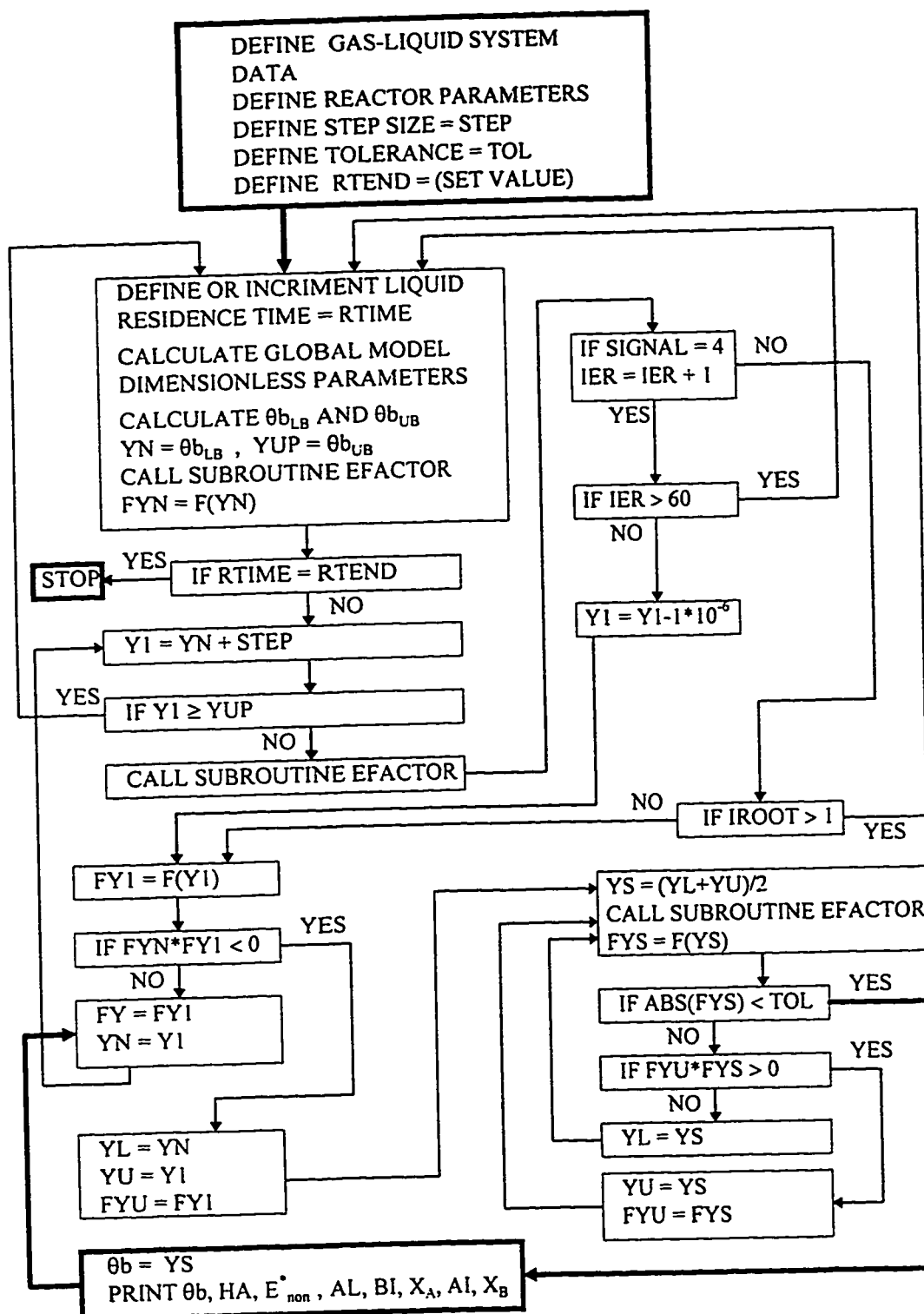


Figure 5.2 Algorithm for Main Program to Find Multiple Solution of Equation (5.22) ($F(\theta_b)$).

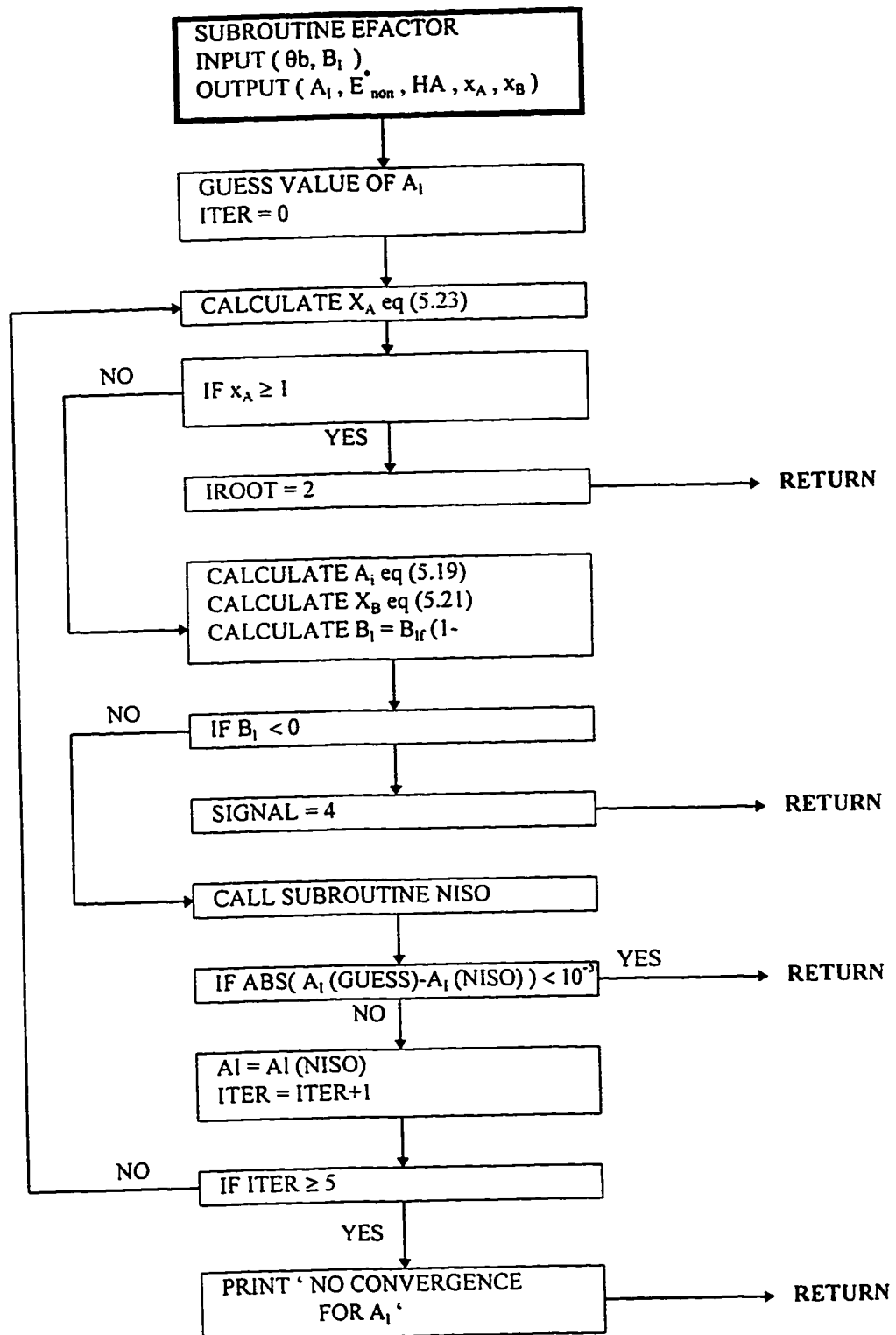


Figure 5.3 Algorithm for Subroutine EFACOR

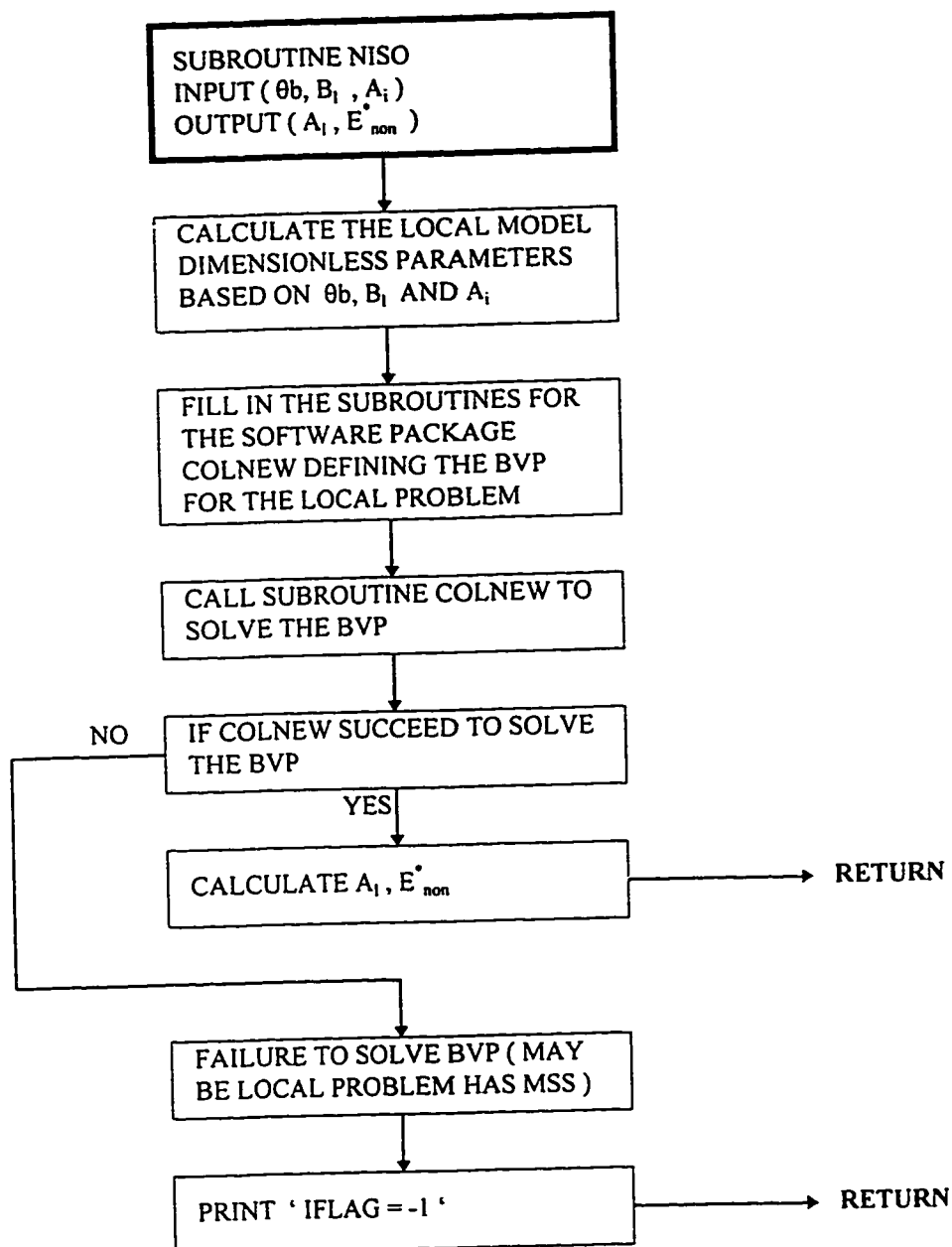


Figure 5.4 Algorithm for Subroutine NISO

solutions, the link between the local and the global models becomes relatively much simpler than that when using differential models for the local problem. The drawback with available approximate solutions that they were confined to isothermal local systems. However, there are some industrial gas-liquid systems which exhibits high heat effects like the chlorination of toluene system as shown in Chapter 4.

Nonadiabatic CSTR simulation was done and a lot of troubles were faced to solve the nonisothermal local model equations since COLNEW cannot find multiple solutions for the BVP. As a first step in the direction and for demonstration purposes, an isothermal and nonvolatile local differential model will be implemented to show how the link between the local and global problems can be achieved. We would rather leave the inclusion of heat effects and the liquid volatility for future work. The chlorination of n-decane system will be implemented for the reactor simulations. The local temperature gradients for this system are minor as shown in the parametric studies in chapter 4. The results will be compared with the experimental predictions of Ding et al. (1974), consequently the physiochemical data and the reactor operational parameters were taken to be like those of Huang and Varma (1981) as they are used as a representative of the experimental results. Data is shown in Table 5.2 . Since the local model is isothermal and nonvolatile, the following parameters are set equal to zero : $\theta_0 = \theta_G = Bi_M = Bi_H = \beta_R = \beta_S = \beta_V = \epsilon_{DA} = \epsilon_{DB} = \epsilon_R = \epsilon_S = \epsilon_V = v = y_B = 0$. With these set of parameters the local model will not exhibit steady state multiplicity and the computations will become much simpler. At this stage we would introduce another assumption that the gas and the liquid are at the same

Table 5.2 Parameters Used for the CSTR Simulation

DATA	VALUE	UNITS
m	1	-
n	1	-
ρ_{lf}	$3.1 \cdot 10^{-3}$	gmol/cm ³
ρ_{gf}	$4.2 \cdot 10^{-3}$	gmol/cm ³
C_{pg}	6.5	ca/(gmol. ^o K)
C_{pl}	75	ca/(gmol. ^o K)
D_A	$6 \cdot 10^{-5}$	cm ² /sec
D_B	$6 \cdot 10^{-5}$	cm ² /sec
k_l	0.04	cm/sec
E_R	29000	cal/gmol
k_2 (50 ^o C)	0.005	cm ³ /(gmol.sec)
$-\Delta H_S$	4500	cal/gmol
$-\Delta H_R$	26000	cal/gmol
H_0	0.0018	-
B_{lf}	$5.1 \cdot 10^{-3}$	gmol/cm ³
T_{lf}	297	^o K
T_{gf}	297	^o K
T_C	298	^o K
F_{gf}	18.5	cm ³ /sec
V_R	400	cm ³
\underline{a}	3	cm ⁻¹
US	0.03	cal/(^o K.sec)
y_{Af}	1	-
ε_L	0.86	-

temperature inside the reactor.

Figures 5.5 to 5.10 shows the nonadiabatic CSTR model predictions for the case of varying liquid residence time and constant gas flow rate. An isola-type multiplicity is predicted over the liquid residence times ranging between 22 to 136 minutes where a maximum of three solutions was obtained. In Figure 5.5, three branches of reactor temperature are shown, a low temperature branch, a middle temperature branch and a high temperature branch. The low branch averages 26°C which is almost equal to the feed temperatures. Consequently, we can see that for this branch the liquid conversion is equal zero as shown in Figure 5.7. The gas conversion starts high, then it will drop as the liquid residence time is increased. The Hatta number is equal to zero and consequently the enhancement factor is also zero as shown in Figures 5.8 and 5.9. Figure 5.10 shows that the gaseous reactant concentration in the bulk liquid phase is high for the low temperature branch. It can be concluded that the absorption process is basically a physical absorption or in other word the reaction regime is very slow for this low branch.

The high temperature branch shows opposite behavior, that the reactor temperature is high averaging 170°C . The gas conversion decreases from 0.6 to 0.26, however, the liquid conversion increases from 0.32 to 0.92. The Hatta number increases from 0.07 to a maximum of 0.36 at liquid residence time equals 70 min then it will drop back to 0.07. The enhancement factor increases very sharply from 0.72 to reach a plateau of 1.1 for a wide range of liquid residence time then it will drop to 0.42. The gas reactant concentration in the bulk liquid is essentially zero indicating a fast reaction regime for this

high temperature branch. Finally, the middle temperature branch is an unstable branch behaving in between the other two branches.

The model prediction is compared with the experimental result of Ding et al. (1974) as shown in Figure 5.5 . It has to be mentioned here that this is almost the only related experimental study available in literature. However, the reaction system in that study is complex unlike the present model which considers a single irreversible reaction. Qualitatively, the model agrees reasonably well with the experimental results for the liquid residence time range from 2 to 82 minutes. The experimental study did not continue the isola because it stopped at residence time equals 82 minutes. Little deviation is observed for the low and the high temperature branches, however, deviation increases for the middle branch as the residence time is increased.

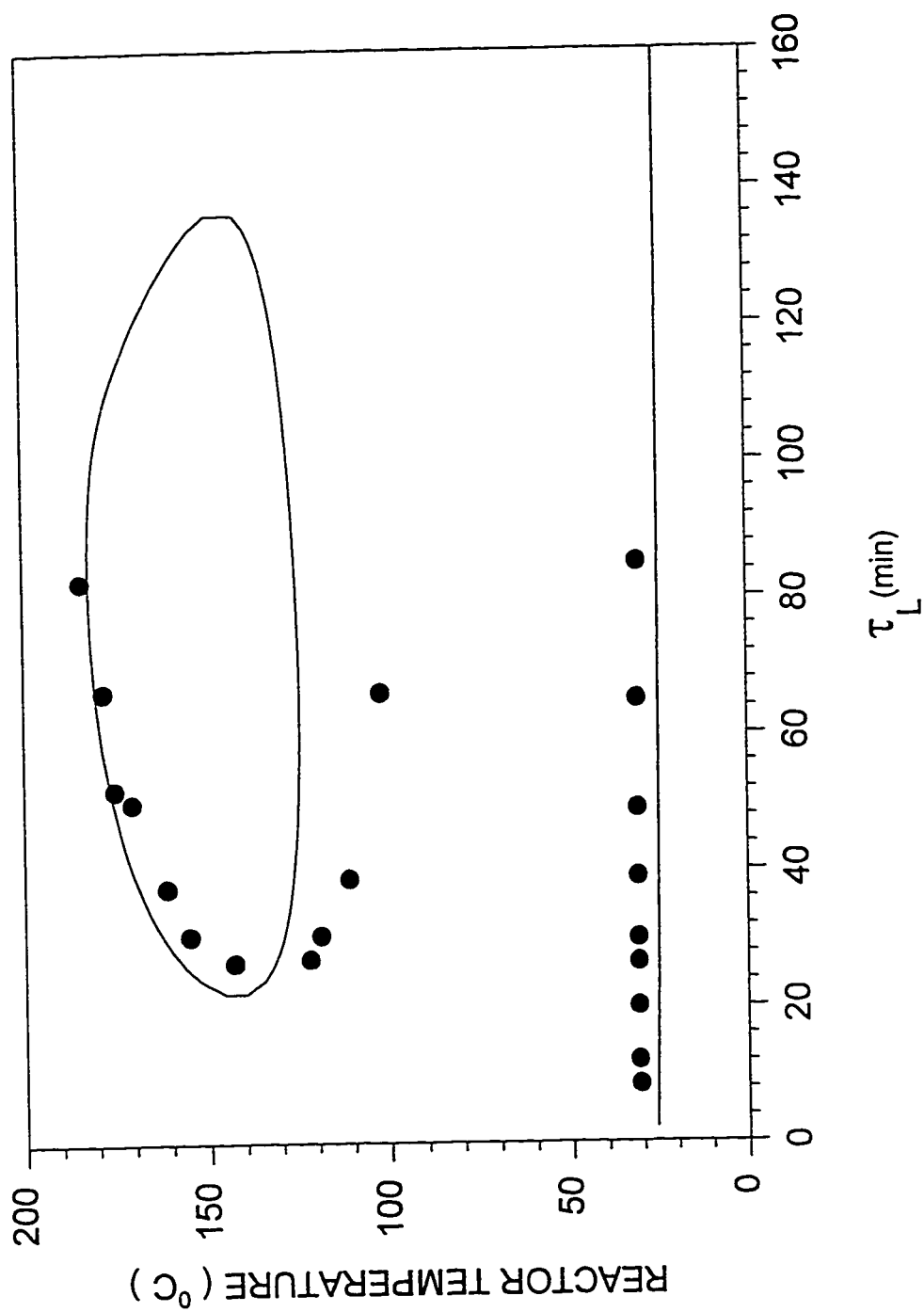


Figure 5.5 Change of Reactor Temperature With the Liquid Residence Time

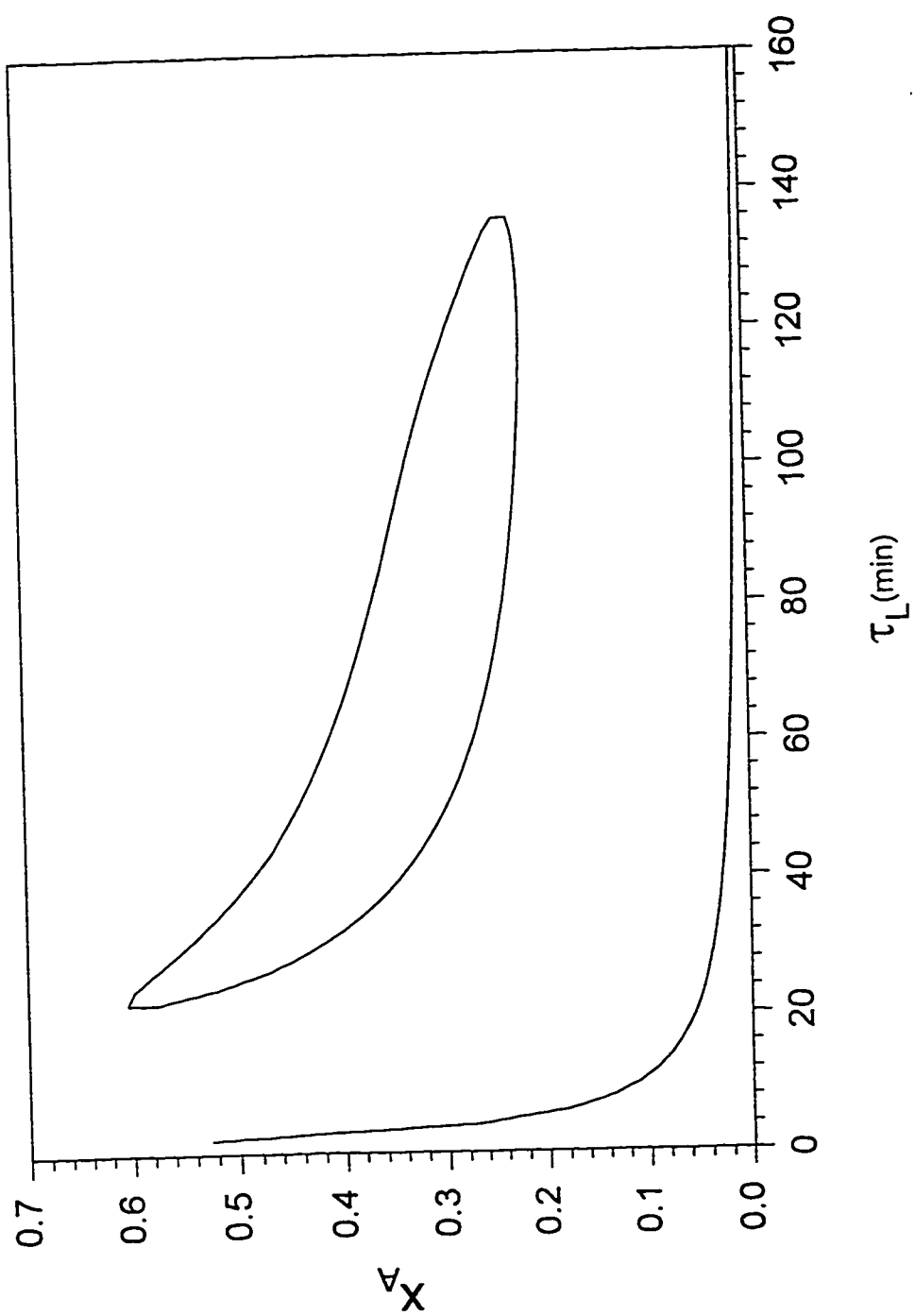


Figure 5.6 Change of the Gas Conversion With The Liquid residence Time

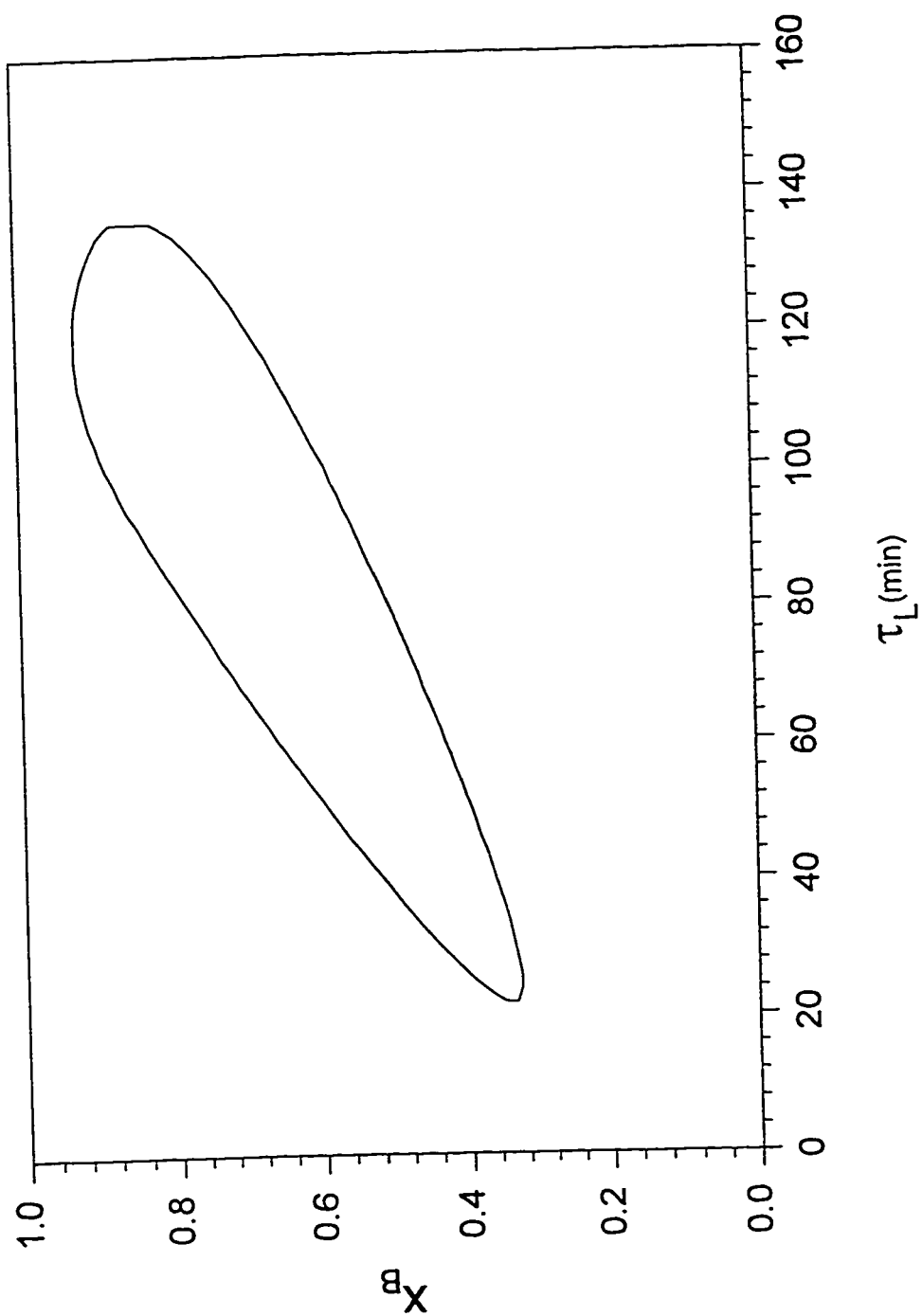


Figure 5.7 Change of the Liquid Conversion With the Liquid Residence Time

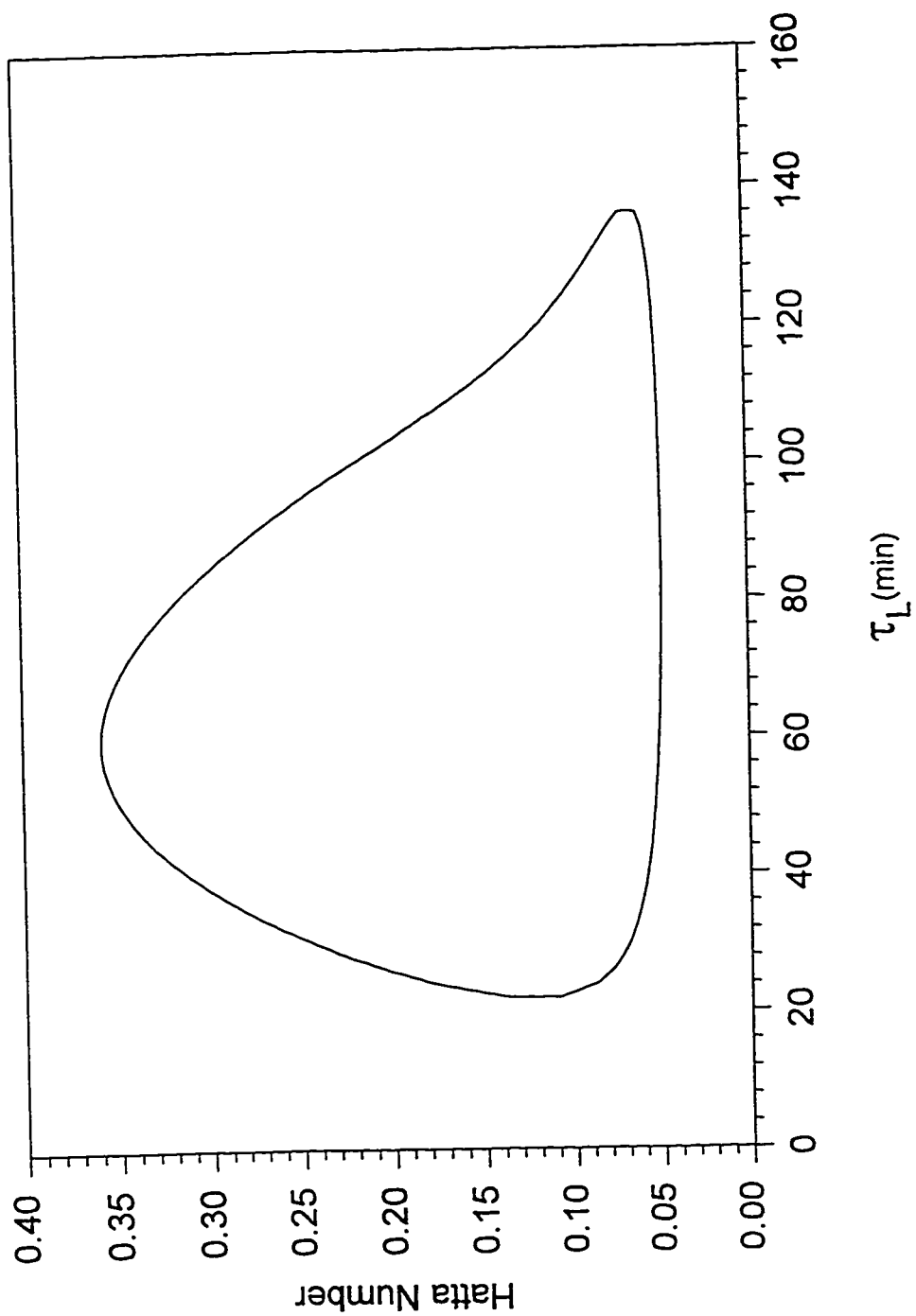


Figure 5.8 Change of the Hatta Number With the Liquid Residence Time

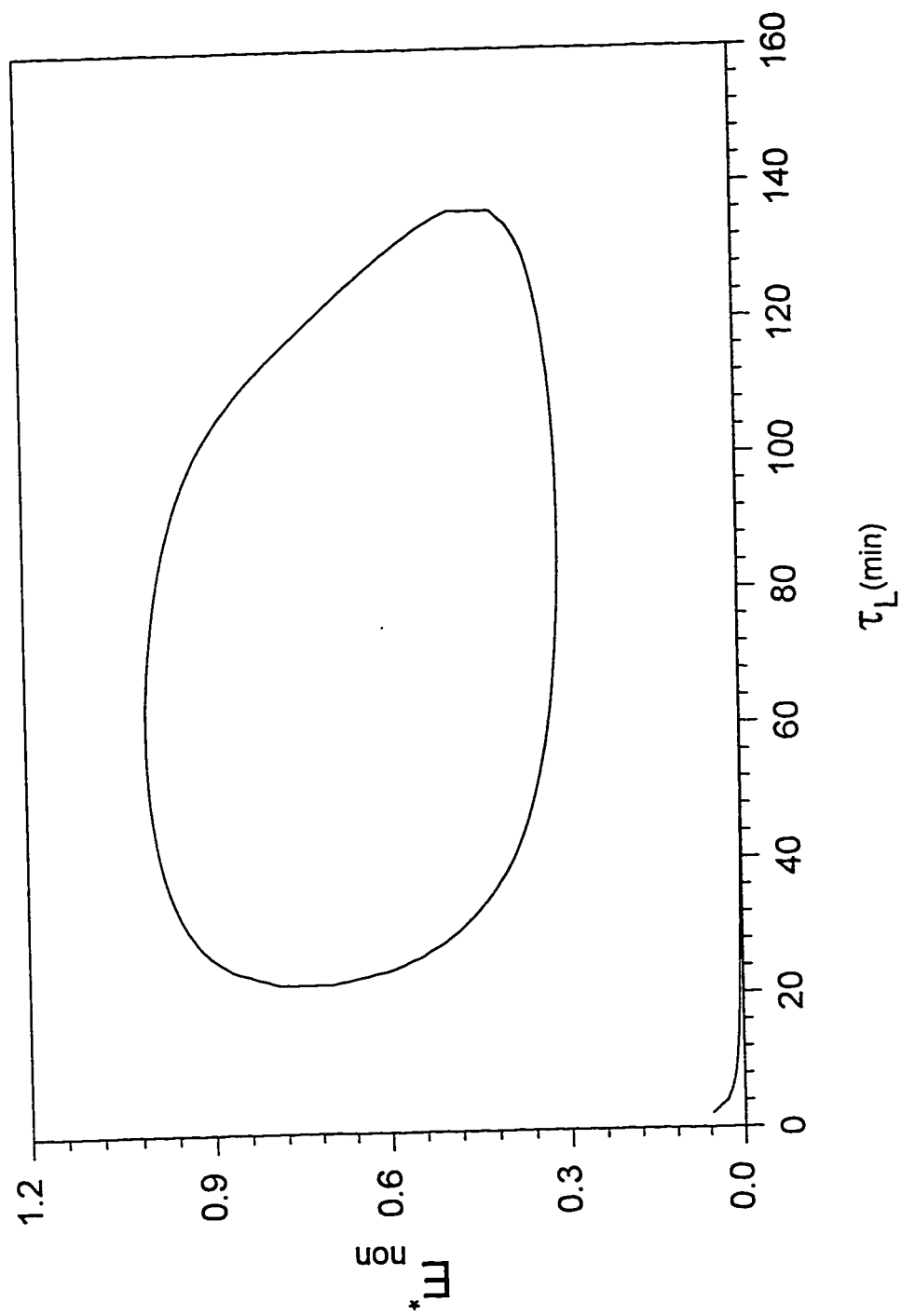


Figure 5.9 The Change of the Enhancement Factor With the Liquid Residence Time

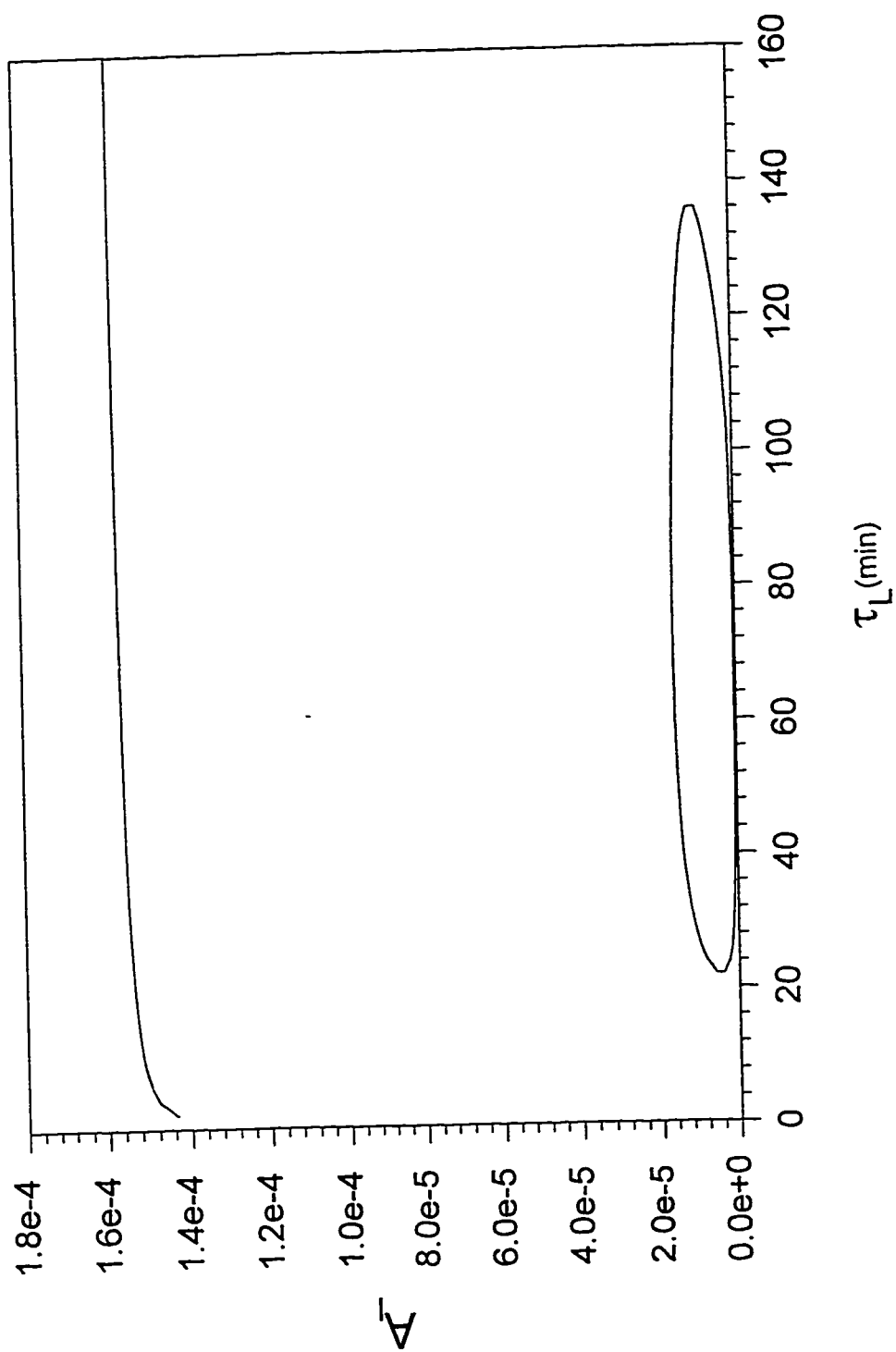


Figure 5.10 Change of the Gaseous Reactant Concentration in the Bulk Liquid With the Liquid Residence Time

CHAPTER 6

CONCLUSIONS AND RECOMMENDATIONS

1. A survey of the available literature indicates that heat effects are very important to be considered when modeling gas-liquid reactions.
2. Film and penetration theories were mostly used to model gas-liquid reaction. The film theory is physically easier to visualize and mathematically simpler to deal with and it has been mostly used to model gas-liquid reactors.
3. A comprehensive film model was developed to consider an m th-, n th-order irreversible reaction kinetics, and the general reaction regime including the slow, fast, and instantaneous reactions. The model accounts for the diffusion of mass and heat to the bulk liquid phase, also the convection of mass and heat to the bulk gas phase.
4. A material balance for the liquid reactant was carried out in the gas film to know its concentration in the gas phase after evaporation.
5. The local model equations were solved using the method of orthogonal collocations on finite elements using the software codes AUTO and COLNEW.
6. The model solution indicates the existence of static bifurcation (multiple steady states) under certain model parameter combinations.

7. A comprehensive parametric study was conducted using a certain model parameter combinations. It appears that the model equations are sensitive to heat effects parameters, reaction orders, stoichiometry parameter and the Biot numbers. Those parameters affects the steady state multiplicity of the model.
8. Through the physical understanding of the model and some trail and error calculations, the heats of solution and reaction parameters were lumped in algebraic manner. Borders of steady state multiplicity were determined for the model equations based on those lumped parameters.
9. The local model equations were applied to three industrial gas-liquid reaction systems, the chlorination of n-decane, the sulfonation of dodecylbenzene and the chlorination of toluene. The chlorination of toluene was found to be more sensitive to heat effects of volatility.
10. The local model equations for an isothermal nonvolatile liquid case were linked with a nonadiabatic CSTR design model in the complex form without any approximation for the enhancement factor and the bulk liquid concentration for the gas reactant.
11. An iterative algorithm was developed to link the local model with the global reactor model. In doing so the bisection method was used to solve the reactor equations and the software COLNEW was used to solve the local model equations.

12. The local-global models were applied for the chlorination of n-decane system, for which the developed algorithm predicted steady state multiplicity for the gas-liquid CSTR problem.
13. It is recommended to carry out an experimental study for a nonisothermal gas-liquid reaction system and collect all necessary physiochemical, kinetic and volatility data. Further, this system will be applied in a reactor experiment to investigate the reactor steady state multiplicity.
14. It is recommended also to link the present local model with the reactor model taking into account the heat effects, the liquid volatility and the reactor hydrodynamic parameters and compare the model predictions with the experiments.

NOMENCLATURE

A	Dimensionless concentration, defined in Table 3.1
A	Concentration of gas reactant
\underline{a}	Interfacial area per unit volume of reactor
a_i	Dimensionless parameter defined in Table 5.1
B	Dimensionless concentration, defined in Table 3.1
B_i	Biot number, defined in Table 3.1
B	Concentration of liquid reactant
\mathbf{B}	Dimensionless parameter defined in Table 5.1
C	Concentration
C_p	Heat capacity
D	Diffusion coefficient
D_{gf}	Dimensionless parameter defined in Table 5.1
E_D	Activation energy of diffusion
E_{non}^*	Nonisothermal enhancement factor
E_R	Activation energy of reaction
F	Volumetric flow rate
H	Henry's law constant
H_0	Dimensionless parameter defined in Table 5.1

h_G	Gas-side heat transfer coefficient
K_L	Liquid Thermal conductivity
$k_{(m,n)}$	Reaction rate constant for the (m,n)th-order reaction
k_G	Gas-side mass transfer coefficient
k_l^0	Liquid-side mass transfer coefficient
Le	Lewis number, defined in Table 3.1
\sqrt{M}	Hatta number, defined in Table 3.1
N	Gas molar flow rate
P	Pressure
p	Dimensionless parameter defined in Table 5.1
Q	Dimensionless parameter defined in Table 5.1
q	Dimensionless parameter defined in Table 5.1
R	Reactor rate of reaction
r	Dimensionless parameter defined in Table 5.1
S	Dimensionless parameter, defined in Table 3.1
T	Absolute temperature
US	Reactor overall heat transfer coefficient
v	Dimensionless parameter defined in Table 5.1
V	Reactor volume
x	Distance from interface into liquid phase
X	Dimensionless distance inside liquid-side film

x	Conversion
y	Mole fraction in gas phase

Greek Symbols

α	Thermal diffusivity of liquid phase
α'	Dimensionless parameter, defined in Table 3.1
α	Dimensionless parameter defined in Table 5.1
β	Dimensionless parameter defined in Table 5.1
β'	Dimensionless parameter, defined in Table 3.1
β_j	Dimensionless parameter, defined in Table 3.1, $j = R, S, V$
γ'	Dimensionless parameter, defined in Table 3.1
θ_b	Dimensionless parameter defined in Table 5.1
θ_{bC}	Dimensionless parameter defined in Table 5.1
θ_{br}	Dimensionless parameter defined in Table 5.1
δ	Dimensionless parameter defined in Table 5.1
δ_H	Liquid film heat-transfer thickness
δ_M	Liquid film mass-transfer thickness
ϵ_j	Dimensionless parameter, defined in Table 3.1, $j = A, B, R, S, V$
ν	Stoichiometric coefficient
ρ	Density

Subscripts

A	Gaseous reactant
B	Liquid reactant
b	Bulk liquid conditions
f	Feed to the reactor
g	Gas
G	Gas
H	Heat
i	Interface
L	Liquid
M	Mass
R	Reactor

REFERENCES

1. Allan, J.C., "Nonisothermal Gas Absorbtion with Chemical Reaction," M.Sc. Thesis, University of Manchester, Manchester, England (1987).
2. Allan, J.C., and R. Mann, "Reactive Exothermic Gas Absorbtion-Improved Analytical Predictions from a Hyperbolic Solubility Approximation," Chem. Eng. Sci., 34, 413-415 (1979).
3. Allan, J.C., and R. Mann, "Heat and Mass Transfer Multiplicity in Exothermic Gas Absorbtion," Can. J. Chem. Eng., 60, 566-568 (1982).
4. Al-Ubaidi, B.H., and M.S. Selim, "Role of Liquid Reactant Volitility in Gas Absorption with an Exothermic Reaction," AIChE J., 38, 363-376 (1992).
5. Al-Ubaidi, B.H., M.S. Selim, and A.A. Shaikh, "Nonisothermal Gas Absorbtion Accompanied by a Second -Order Irreversible Reaction", AIChE J., 36, 141-146 (1990).
6. Asai, S., O.E.Potter, and H. Hikita, "Nonisothermal Gas Absorbtion with Chemical Reaction," AIChE J. 31, 1304-1311 (1985).
7. Ascher, U., J. Christiansen, and R. D. Russell, "Algorithm 569. COLSYS: Collocation Software for Boundary-Value ODEs," ACM Trans. Math. Softw., 7, 223 (1981).
8. Bhattacharya, A., R.V. Gholap, and R.V. Chaudhari, "An Analysis of Gas Absorption Accompanied by an Exothermic Consecutive Reaction," Chem. Eng. Sci., 34, 2890-2893 (1988).
9. Bhattacharya, A., R.V. Gholap, and R.V. Chaudhari, "Gas Absorption with Bimolecular (1,1 Order) Reaction," AIChE J., 33, 1507-1513 (1987).
10. Bhattacharya, A., R.V. Gholap, and R.V. Chaudhari, "Gas Absorption with Exothermic Bimolecular Reaction in a Thin Liquid Film: Fast Reactions," the Can. J. Chem. Eng., 66, 599-604 (1988).
11. Bourne, J.R., U.V. Stockar, and G.C. Coggan, "Gas Absorbtion with Heat Effects," Ind. Eng. Chem. Process. Design Develop., 13, 115-123 (1974).

12. Brauner, N., "Non-Isothermal Vapor Absorption into Falling Film," *Int. J. Heat Mass Transfer*, 34, 767-784 (1991).
13. Carberry J.J., "Influence of Temperature Gradients in Rapid Absorption-Reaction," *Chem. Eng. Sci.*, 21, 951-952 (1966).
14. Chiang, S.H., and H.L. Toor, "Interfacial Resistance in the Absorption of Oxygen by Water," *AIChE J.*, 5, 165-168 (1959).
15. Chang, Y. C., and D.C. Hwang, "Interfacial Resistance in Exothermic Gas Absorption with Chemical Reaction," *Chem. Eng. J.*, 38, 187-193 (1988).
16. Changluo, Z., Z. Rongxian, J. Gengming, and W. Qingzi. "A Mathematical Model and Simulation for non Isothermal Gas Absorption With Chemical Reaction," *J. Chem. Ind. and Eng.*, 2, 115-129 (1987).
17. Chatterjee, S.G., and E.R. Altwick, "Film and Penetration Theories for a first-Order Reaction in Exothermic Gas Absorption," *Can. J. Chem. Eng.*, 65, 454-461 (1987).
18. Chiang, S.H., and H.L. Toor, "Gas Absorption Accompanied by a Large Heat Effect and Volume Change of the Liquid Phase," *AIChE J.*, 10, 398-402 (1964).
19. Clegg, G.T, and R. Mann, "A Penetration Model for Gas Absorption with First-Order Chemical Reaction Accompanied by Large Heat Effects," *Chem. Eng. Sci.*, 24, 321-329 (1969).
20. Clegg, G.T, and R.B.F. Kilgannon, "Gas Absorption Accompanied by Large Heat Effect and Volume Change in the Liquid Phase: The System Hydrogen Chloride/Ethylene Glycol," *Chem. Eng. Sci.*, 26, 669-674 (1971).
21. Cook, A.E., and E Moore, "Gas Absorption with a First Order Chemical Reaction and Large Heat Effect," *Chem. Eng. Sci.*, 27, 605-613 (1972).
22. Danckwerts P.V., "Absorption by Simoltaneous Diffusion and Chemical Reaction," *Trans. Fraday Soc.*, 300-304 (1950).
23. Danckwerts P.V., "Temperature Effects Accompaniying The Absorption of Gases in Liquids," *App. Sci. Res.*, A3, 385-390 (1953).

24. Danckwerts P.V., "Gas-Absorption Accompanied by First-Order Reaction: Concentration of Product, Temperature-Rise and Depletion of Reactant," *Chem. Eng. Sci.*, 22, 472-473 (1967).
25. Danckwerts P.V., "Gas-Liquid Reactions," McGraw-Hill, New York(1970).
26. Danckwerts P.V., and A.M. Kennedy, "Kinetics of Liquid-Film Process in Gas Absorption. Part I: Models of the Absorption Process," *Trans. Instn. Chem. Engrs*, 32, S49-S52 (1954).
27. Datta, R., and R.G. Rinker, "Penetration Theory Solution for Gas Absorption and Chemical Reaction in Cocurrent and Countercurrent Flow Wetted-Wall Columns," *Can. J. Chem. Eng.*, 62, 78-84 (1984).
28. De Coursey, W.J., "Absorption With Chemical Reaction," *Chem. Eng. Sci.*, 29, 1867 (1974)
29. Ding, Y.J.S., S. Sharma, and D. Luss, "Steady-State Multiplicity and control of the Chlorination of Liquid n-Decane in an Adiabatic Continuously Stirred Tank Reactor," *Ind. Eng. Chem. Fundam.*, 13, 76-82 (1974).
30. Doedel, E. J., "AUTO : A program for the automatic bifurcation analysis of autonomous systems," *Cong. Num.* 30, 265-284 (1981).
31. Doraiswamy, L.K., and M.M. Sharma, "Heterogeneous Reactions: Analysis, Examples, and Reactor Design," Vol 2, John Wiley & Sons, New York (1984).
32. Evans, J.D., and M.S. Selim, "Penetration Theory Analysis For Nonisothermal Gas Absorption Accompanied by a Second-Order Chemical Reaction," *Chem. Eng. Comm.*, 90, 103-124 (1990).
33. Frank. M.J.W., J.A.M. Kuipers, G.F. Versteeg, and P.M. Van Swaaij, "Modelling of Simultaneous Mass and Heat Transfer With Chemical Reaction Using the Maxwell-Stefan Theory-I. Model Development and Isothermal Study," *Chem. Eng. Sci.*, 50, 1645-1659 (1995a).
34. Frank. M.J.W., J.A.M. Kuipers, R. Krishna, and P.M. Van Swaaij, "Modelling of Simultaneous Mass and Heat Transfer With Chemical Reaction Using the Maxwell-Stefan Theory-II. Non-Isothermal Study," *Chem. Eng. Sci.*, 50, 1661-1671 (1995b).
35. Green, S.J., and S.H. Chiang, "An Experimental Study of Interfacial Temperature and Movement in Gas Absorption," *Chem. Eng. Prog. Symp. Ser.*, 67, 64-70 (1971).

36. Hajji A., and W.M. Worek, "Transient Heat and Mass Transfer in Film Absorption of Finite Depth With Nonhomogeneous Boundary Conditions," *Int. J. Heat Mass Transfer*, 35, 2101-2108 (1992).
37. Hancock M.D. and C.N. Kenney, "The Stability and Dynamics of a Gas-Liquid Reactor," *Chem. Eng. Sci.*, 32, 629-639 (1977).
38. Higbie, R., *Trans. AIChE*, 31, 365-389 (1935).
39. Hikita H., and S. Asai, "Gas Absorption With (m,n)-th Order Irreversible Chemical Reaction," *Int. Chem. Eng.*, 4, 332-340 (1964).
40. Hiraoka, M., and K. Tanaka, "Analysis of Simoltananeous Heat and Mass Transfer with Chemical Reaction," *J. Chem. Eng. Japan*, 2, 37-45 (1969).
41. Hoffman L.A., "Theoretical Study of Steady State Multiplicity and Stability in Gas-Liquid Continuous Stirred Tank Reactors," M.S. Thesis, University of Houston, Texas (1974).
42. Hoffman A.L., S. Sharma, and D. Luss, "Steady State Multiplicity of Adiabatic Gas-Liquid Reactors," *AIChE J.*, 21, 318-326 (1975).
43. Huang, J.D.T., and A. Varma, "Steady-State Uniqueness and Multiplicity of Nonadiabatic Gas-Liquid CSTRs," *AIChE J.* 27, 481-489 (1981a).
44. Huang, J.D.T., and A. Varma, "Steady State Uniqueness and Multiplicity of Nonadiabatic Gas-Liquid CSTRs; Part II: Discrimination Among Rival Reaction Models," *AIChE J.*, 27, 489-495 (1981b).
45. Huang, J.D.T., and A. Varma, "Steady-State and Dynamic Behavior of Fast Gas-Liquid Reactions in Non-adiabatic Continuous Stirred Tank Reactors," *Chem. Eng. J.*, 21, 47-57 (1981c).
46. Ikemizu, K., S. Morooka, Y. Kato, and H. Shinohara, "Measurements of Gas-Liquid Interfacial Temperature in Gas Absorption With Heat Generation ," *Kagaku Ronbunshu*, 4, 496-501 (1978).
47. Ikemizu, K., S. Morooka, Y. Kato, and H. Shinohara, "Heat Evolotion in Gas Absorption Accompaying an Exothermic Instantaneous Irreversible Reaction," *Int. Chem. Eng.*, 19, 611-616 (1979).
48. Keller, H. B., "Numerical solution of bifurcation and nonlinear eigenvalue problems," Academic Press, 359-384 (1977).

49. Landau J., "Absorption Accompanied by a Zero-Order Reaction," *Can. J. Chem. Eng.*, **68**, 599-607 (1990).
50. Mann, R., and G.T. Clegg, "Gas Absorption with an Unusual Chemical Reaction: The Chlorination of Toluene," *Chem. Eng. Sci.*, **30**, 97-101 (1975).
51. Mann, R., and H. Moyes, "Exothermic Gas Absorption with Chemical Reaction," *AIChE J.*, **23**, 17-23 (1977).
52. Mann, R., P. Knysh, and J.C. Allan; "Exothermic Gas Absorption with Complex Reaction: Sulfonation and discoloration in the Absorption of Sulfur Trioxide in Dedecylbenzene," *Am. Chem. Soc. Symp. Ser.*, **196**, 441-456 (1982).
53. Moyes H., "Exothermic Gas Absorption with Chemical Reaction: the Film Theory Model," M.S. Thesis, University of Manchester, Manchester (1976).
54. Mustafa I., "Multiplicity Behavior in Nonisothermal Gas Absorption Accompanied With Second Order Irreversible Exothermic Reaction", M.S. Thesis, Colorado School of Mines, Golden, Colorado (1993).
55. Ponter, A.B., S. Vijayan, and K. Craine, "Nonisothermal Absorption with Chemical Reaction," *J. Chem. Eng. Japan*, **7**, 225-229 (1974).
56. Raghuram, S., and Y.T. Shah, "Criteria for Unique and Multiple Steady States for a Gas-Liquid Reaction in an Adiabatic CSTR," *Chem. Eng. J.*, **13**, 81-92 (1977).
57. Raghuram, S., Y.T. Shah, and J.W. Tierney, "Multiple Steady States in a Gas-Liquid Reactor," *Chem. Eng. J.*, **17**, 63-75 (1979).
58. Shah, Y.T., "Gas-Liquid Interface Temperature rise in the Case of Temperature Dependent Physical, Transport, and Reaction Properties," *Chem. Eng. Sci.*, **27**, 1469-1474 (1972).
59. Shaikh, A.A., "Effect of Gas-Side Resistance on Steady State Multiplicity in Gas-Liquid CSTRs," *Chem. Eng. Comm.*, **52**, 331-337 (1987).
60. Shaikh, A.A., A. Jamal, and S.M. Zarook, "Boundary-Value Problems in Reactive Gas Absorption," *Chem. Eng. J.*, **57**, 27-38 (1995).

61. Shaikh, A.A., and A. Varma, "Modeling of Gas-Liquid Continuous-Stirred Tank Reactors (CSTRs)," *Am. Chem. Soc. Symp. Ser.*, 237, 95-106 (1984b).
62. Shaikh, A.A., and A. Varma, "On The Steady State Uniqueness and Multiplicity in Gas-Liquid Continuous Stirred Tank Reactors With Fast Reactions," *Chem. Eng. J.*, 29, 59-65 (1984a).
63. Shaikh, A.A., S.H. Batran, and S.M. Zarook, "Effect of Liquid Reactant Volatility on the Behavior of Gas-Liquid CSTRs," *Proc. Third Saudi Engineering Conference, Riyadh*, 1, 372-378 (1991).
64. Shaikh, A.A., and S.M. Zarook, "A Modelling Analysis of Non-Isothermal Bubble Column Reactors," *Chem. Eng. Sci.*, 51, 3065-3070 (1996).
65. Sharma, S., L.A. Hoffman, and D. Luss, "Steady State Multiplicity of Adiabatic Gas-Liquid Reactors," *AIChE J.*, 22, 324-331 (1976).
66. Sherwood, T.K., R.L. Pigford, , and C.R. Wilke, "Mass Transfer, McGraw-Hill, New York (1975).
67. Saul'yev, V.K., "Integration of Equations of the Parabolic Type With the Method of Nets," Macmillan, New York (1964)
68. Singh, C.P., and Y.T. Shah, "The Effect of Gas Feed Temperature on The Steady State Multiplicity of an Adiabatic CSTR With a Fast Pseudo-First-Order Reaction," *Chem. Eng. J.*, 23, 101-104 (1982).
69. Starzak, M., and S. Ledakowicz, "On Boundary Conditions to the Film Model of Mass Transfer in Chemical Absorption," *Can. J. Chem. Eng.*, 66, 1008-1012 (1988).
70. Suresh, A.K., S. Asai, and O.E. Potter, "Temperature-Dependent Physical Properties in Physical Gas Absorption," *Chem. Eng. Sci.*, 38, 127-133 (1983).
71. Tripathi, G., K.N. Shukla, and R.N. Pandey, "Absorption of Gas by Liquid with Large Heat Effect," *Can. J. Chem. Eng.*, 52, 691-693 (1974).
72. van Krevelen, D. W., and P.J. Hoftijzer, "Kinetics of Gas-Liquid Reactions," Part 1, *Rec. Trav. Chim.*, 563-586 (1948).
73. Verma, S.L., and G.B. Delancey, "Thermal Effects in Gas Absorption," *AIChE J.*, 21, 96-102 (1975).

74. White, D., Jr., and L.E. Johns, "Temperature Rise Multiplicity in the Absorption of Chemically Reactive Gases," *Chem. Eng. Sci.*, 40, 1598-1601 (1985).
75. White, D., Jr., and L.E. Johns, "The Diffusional Limitation on the Temperature Rise in the Absorption of Chemically Reactive Gases," *Chem. Eng. Comm.*, 48, 177-190 (1986a).
76. White, D., Jr., and L.E. Johns, "Gas-Liquid Reaction Systems: A Heuristic Model and Its Steady State Solution," *AIChE J.*, 32, 981-990 (1986b).
77. Whitman, W.G., "The Two-Film Theory of Gas Absorption," *Chem. Met. Eng.*, 29, 147-149 (1923).

APPENDIX A

DERIVATION OF GAS FILM MODEL EQUATIONS

In chapter 3 the liquid film model was written across the heat transfer film and the variable C_{BG} has appeared. To obtain this variable the following material and energy balances have to be written from $x_g = -\delta_g$ to $x_g = 0$:

material balance for component A :

$$\frac{d}{dx_g} \left(D_{Ag} \frac{dC_A}{dx_g} \right) - (-r_A) = 0 \quad (A.1)$$

material balance for component B :

$$\frac{d}{dx_g} \left(D_{Bg} \frac{dC_B}{dx_g} \right) - v(-r_A) = 0 \quad (A.2)$$

energy balance :

$$K_g \frac{d^2 T}{dx_g^2} + (-\Delta H_R)(-r_A) = 0 \quad (A.3)$$

The following boundary conditions can be used for the above differential equations:

at $x_g = -\delta_g$:

$$C_A = C_{A_{gb}} \quad (A.4)$$

$$a D_{Bg} \frac{dC_{Bg}}{dx_g} = F_g (C_{Bg} - C_{Bg0}) \quad (A.5)$$

$$a K_g \frac{dT}{dx_g} = F_g \rho_g C_{Pg} (T - T_{g0}) \quad (A.6)$$

at $x_g = 0$

$$C_A = C_{A_{gi}} \quad (A.7)$$

$$C_B = C_{B_{gi}} \quad (A.8)$$

$$T = T_i \quad (A.9)$$

Assuming Henry's law and the ideal gas law are applicable equations (A.7) and (A.8) can be written as follows :

$$C_{Agi} = \frac{H_{Ab}}{RT} \exp \left[\frac{\Delta H_v}{R} \left(\frac{1}{T} - \frac{1}{T_b} \right) \right] C_{Ai} \quad (A.10)$$

$$C_{Bgi} = \frac{H_{Bb}}{RT} \exp \left[\frac{\Delta H_v}{R} \left(\frac{1}{T} - \frac{1}{T_b} \right) \right] C_{Bi} \quad (A.11)$$

Now the gas film equations are linked with the liquid film equations, as a result an iterative procedure need to be followed in order to solve them. the following procedure is suggested :

1. Guess C_{BG} in equation (3.11) .
2. Solve numerically the liquid film equations and obtain C_{Ai} , C_{Bi} and T_i .
3. Solve the gas film equations using C_{Ai} , C_{Bi} and T_i obtained from step 2 .
4. From gas film equations solution get C_{BG} .
5. Check if C_{BG} (step 4) equals C_{BG} (guess). If almost equal go to step 6 else change the guess and go to step 2.

6. Stop.

The above procedure is lengthy and it will not be implemented in the present work.

Therefore, simplifying assumptions in 5, 6 and 7 in chapter 3 will be applied and the gas film equations will be simplified to :

$$\frac{d^2 C_{Bg}}{dx_g^2} = 0 \quad (A.12)$$

at $x_g = -\delta_g$:

$$aD_{Bg} \frac{dC_{Bg}}{dx_g} = F_g (C_{Bg} - C_{Bg0}) \quad (A.13)$$

and at $x_g = 0$

$$C_{Bg} = C_{Bgi} \quad (A.14)$$

Equations (A.12), (A.13) and (A.14) make a linear boundary value problem which can be solved analytically. Integration of equation (A.12) yields :

$$C_{Bg}(x_g) = C_1 x_g + C_2 \quad (A.15)$$

where C_1 and C_2 are constants of integration. Substituting boundary condition (A.14) in (A.15) yields :

$$C_2 = C_{Bgi} \quad (A.16)$$

Substituting boundary condition (A.13) with the result (A.16) in (A.15) yields :

$$C_1 = \frac{F_g (C_{Bgi} - C_{Bg0})}{aD_{Bg} + F_g \delta_g} \quad (A.17)$$

Now the concentration profile for the liquid reactant in the gas film can be written as follows :

$$C_{Bg}(x_g) = \frac{F_g (C_{Bgi} - C_{Bg0})}{aD_{Bg} + F_g \delta_g} x_g + C_{Bgi} \quad (A.18)$$

The composition of the liquid reactant in the bulk gas phase (C_{Bg}) can be obtained by replacing x_g with $-\delta_g$ in equation (A.18):

$$C_{Bg} = \frac{C_{Bgi} + \frac{F_g \delta_g}{aD_{Bg}} C_{Bg0}}{1 + \frac{F_g \delta_g}{aD_{Bg}}} \quad (A.19)$$

APPENDIX B1

SAMPLE OF INPUT SUBROUTINE TO AUTO

```
SUBROUTINE OPEN_UNITS
OPEN(UNIT=3,FILE='C:\AUTOCOL\AUTOGABS\STUDY\DI\AUTOUT\FOR003.DAT',
1 STATUS='UNKNOWN')
OPEN(UNIT=6,FILE='C:\AUTOCOL\AUTOGABS\STUDY\DI\AUTOUT\FOR006.DAT',
1 STATUS='UNKNOWN')
OPEN(UNIT=7,FILE='C:\AUTOCOL\AUTOGABS\STUDY\DI\AUTOUT\FOR007.DAT',
1 STATUS='UNKNOWN')
OPEN(UNIT=8,FILE='C:\AUTOCOL\AUTOGABS\STUDY\DI\AUTOUT\FOR008.DAT',
1 STATUS='UNKNOWN')
OPEN(UNIT=9,FILE='C:\AUTOCOL\AUTOGABS\STUDY\DI\AUTOUT\FOR009.DAT',
1 STATUS='UNKNOWN')
OPEN(UNIT=10,FILE='C:\AUTOCOL\AUTOGABS\STUDY\DI\AUTOUT\NISO.OUT',
1 STATUS='UNKNOWN')
OPEN(UNIT=1,FILE='C:\AUTOCOL\AUTOGABS\PACKAGES\AUTO.FOR',
1 STATUS='UNKNOWN')
OPEN(UNIT=11,FILE='C:\AUTOCOL\AUTOGABS\STUDY\DI\STPNT.FOR',
1 STATUS='UNKNOWN')
OPEN(UNIT=12,FILE='C:\AUTOCOL\AUTOGABS\STUDY\DI\AUTOUT\FIT.OUT',
1 STATUS='UNKNOWN')
OPEN(UNIT=19,FILE='C:\AUTOCOL\AUTOGABS\STUDY\DI\AUTOUT\GRAPH.DAT',
1 STATUS='UNKNOWN')
OPEN(UNIT=20,FILE='C:\AUTOCOL\AUTOGABS\STUDY\DI\AUTOUT\ENON.DAT',
1 STATUS='UNKNOWN')
RETURN
END

C
SUBROUTINE INPUT_DATA (EPSLDA,EPSLDB,EPSLS,EPSLR,EPSLV,BETAS,
1BETAR,BETAV,LE,DELHM,DHM,S,BIH,BIM,M,N,GAMMA,BETA,ALPHA,THETAG,
1THETA0,OMEGA,A0,VAL_RM,EPSLEFF,BETAFF)
IMPLICIT DOUBLE PRECISION (A-H,O-Z)
REAL*8 LE
COMMON /START/ START_RM

C
C DIMENSIONLESS MODEL PARAMETERS
C
M      =      0
N      =      1
VAL_RM = 0.0
S      = 0.01
```



```

EPSLDA = 3.0
EPSLDB = 3.0
EPSLR = 20.0
EPSLS = 4.0
EPSLV = 2.0
BETAR = 0.005
BETAS = 0.001
BETAV = 0.001
BIM = 0.8
BIH = 0.6
DELHM = 10.0
LE = 100.0
ALPHA = 20.0
BETA = 1.0
GAMMA = 1.0
THETAG = 0.0
THETA0 = 0.0
A0 = 0.0
OMEGA = 0.90130
DHM = 100.0
EPSLEFF = epslr/2.0-epsls
BETAEFF = betar+betas
START_RM = VAL_RM
C
RETURN
END
C
SUBROUTINE INIT
C
IMPLICIT DOUBLE PRECISION (A-H,O-Z)
REAL*8 LE
COMMON /BLBCN/ NDIM,IPS,IRS,ILP,ICP(20),PAR(20)
COMMON /BLCDE/ NTST,NCOL,IAD,ISP,ISW,IPLT,NBC,NINT
COMMON /BLDLS/ DS,DSMIN,DSMAX,IADS
COMMON /BLLIM/ NMX,NUZR,RL0,RL1,A0,A1
COMMON /BLMAX/ NPR,MXBF,IID,ITMX,ITNW,NWTN,JAC
COMMON /BLRCN/ HALF,ZERO,ONE,TWO,HMACH,RSMALL,RLARGE
COMMON /BLTHT/ THETAL(20),THETAU
COMMON /OUTPT/ NDIMOUT,IOUT
CALL INPUT_DATA (EPSLDA,EPSLDB,EPSLS,EPSLR,EPSLV,BETAS,
1 BETAR,BETAV,LE,DELHM,DHM,S,BIH,BIM,M,N,GAMMA,BETA,ALPHA,
2 THETAG,THETA0,OMEGA,A0,VAL_RM,EPSLEFF,BETAEFF)
C
NTST = 10
NCOL = 7
DS = 0.01
DSMIN = 0.001
DSMAX = 100.0
IRS = 235
ISW = 1
ICP(2) = 2

```

```

      RLO  = VAL_RM                !<--- STARTING VALUE OF PAR(1)
      RL1  = 100000.0
      ITMX  = 50
      A0    = 0.0
      A1    = 1000000.0
      IADS  = 1
      NDIM  = 6
      NDIMOUT = 2
      NBC   = 6
      NINT  = 0
      NPR   = 1
      NMX   = 9999
      NUZR  = 0
      ILP   = 1
      IAD   = 3
      IPS   = 4
      ICP(1) = 1
      JAC   = 0
C
      RETURN
      END
C
C*****
C
C      SUBROUTINE FUNC(NDIM,U,ICP,PAR,IJAC,F,DFDU,DFDP)
C      IMPLICIT DOUBLE PRECISION (A-H,O-Z)
C      REAL*8 LE
C      DIMENSION U(NDIM),PAR(20),F(NDIM),DFDU(NDIM,NDIM),DFDP(NDIM,20)
C
C      DATA INPUT
C
C      CALL INPUT_DATA (EPSLDA,EPSLDB,EPSLS,EPSLR,EPSLV,BETAS,
C      1 BETAR,BETAV,LE,DELHM,DHM,S,BIH,BIM,M,N,GAMMA,BETA,ALPHA,
C      2 THETAG,THETA0,OMEGA,A0,VAL_RM,EPSLEFF,BETAEFF)
C
C      EEA  = DEXP(EPSLDA*U(5)/(1.0+U(5)))
C      EEB  = DEXP(EPSLDB*U(5)/(1.0+U(5)))
C      EER  = DEXP(EPSLR *U(5)/(1.0+U(5)))
C
C      DE's
C
C      F(1) = U(2)
C      F(2) = -EPSLDA*U(2)*U(6)/(1.0+U(5))**2+DHM*PAR(1)*
C      1 EER*U(1)**M*U(3)**N/EEA
C      F(3) = U(4)
C      F(4) = -EPSLDB*U(4)*U(6)/(1.0+U(5))**2+DHM*PAR(1)*
C      1 S*EER*U(1)**M*U(3)**N/EEB
C      F(5) = U(6)
C      F(6) = -BETAR*PAR(1)*DHM*EER*U(1)**M*U(3)**N
C
C      RETURN

```

```

END
C
C*****
C
C      SUBROUTINE BCND(NDIM,PAR,ICP,NBC,U0,U1,FB,IJAC,DBC)
C      IMPLICIT DOUBLE PRECISION (A-H,O-Z)
C      DIMENSION PAR(20),ICP(20),U0(NDIM),U1(NDIM),FB(NBC),DBC(NBC,20)
C      REAL*8 LE
C
C      CALL INPUT_DATA (EPSLDA,EPSLDB,EPSLS,EPSLR,EPSLV,BETAS,
C      1 BETAR,BETAV,LE,DELHM,DHM,S,BIH,BIM,M,N,GAMMA,BETA,ALPHA,
C      2 THETAG,THETA0,OMEGA,A0,VAL_RM,EPSLEFF,BETAEFF)
C
C      EEA0 = DEXP( EPSLDA*U0(5)/(1.0+U0(5)))
C      EEB0 = DEXP( EPSLDB*U0(5)/(1.0+U0(5)))
C      EER0 = DEXP( EPSLR *U0(5)/(1.0+U0(5)))
C      EES0 = DEXP(-EPSLS *U0(5)/(1.0+U0(5)))
C      EEV0 = DEXP( EPSLV *U0(5)/(1.0+U0(5)))
C
C      EEA1 = DEXP( EPSLDA*U1(5)/(1.0+U1(5)))
C      EEB1 = DEXP( EPSLDB*U1(5)/(1.0+U1(5)))
C      EER1 = DEXP( EPSLR *U1(5)/(1.0+U1(5)))
C      EES1 = DEXP(-EPSLS *U1(5)/(1.0+U1(5)))
C      EEV1 = DEXP( EPSLV *U1(5)/(1.0+U1(5)))
C
C      BC'S
C
C      FB(1) = U0(1)-EES0
C      FB(2) = EEB0*U0(4)-BIM*DELHM*EEV0*(U0(3)-U0(3))/(1.0+OMEGA))
C      FB(3) = BETAS*EEA0*U0(2)-U0(6)+BIH*(U0(5)-THETAG)+
C      1 BETAV*EEB0*U0(4)
C      FB(4) =-EEA1*U1(2)-PAR(1)*DHM*(ALPHA-1.0)*EER1*U1(1)**M*
C      1 U1(3)**N-BETA*DELHM*(U1(1)-A0)
C      FB(5) = U1(3)-1.0
C      FB(6) = U1(6)+BETAR*PAR(1)*DHM*(ALPHA-1.0)*U1(1)**M*
C      1 U1(3)**N*EER1+GAMMA*(U1(5)-THETA0)
C
C      RETURN
C      END
C
C*****
C
C      SUBROUTINE X0(MIU,T,UP,IBR,NTOT,ATYPE,LAB)
C      IMPLICIT DOUBLE PRECISION (A-H,O-Z)
C      REAL*8 LE
C      COMMON /BLBCN/ NDIM,IPS,IRS,ILP,ICP(20),PAR(20)
C      COMMON /START/ START_RM
C      DIMENSION UP(MIU,NDIM)
C      CHARACTER*2 ATYPE
C      CALL INPUT_DATA (EPSLDA,EPSLDB,EPSLS,EPSLR,EPSLV,BETAS,
C      1 BETAR,BETAV,LE,DELHM,DHM,S,BIH,BIM,M,N,GAMMA,BETA,ALPHA,

```

```

2 THETAG,THETA0,OMEGA,A0,VAL_RM,EPSLEFF,BETAEFF)
  IF (PAR(ICP(1)).EQ.START_RM) THEN
    CALL WRITE_DATA (EPSLDA,EPSLDB,EPSLS,EPSLR,EPSLV,BETAS,
1 BETAR,BETAV,LE,DELHM,DHM,S,BIH,BIM,M,N,GAMMA,BETA,ALPHA,
2 THETAG,THETA0,OMEGA,A0,EPSLEFF,BETAEFF)
    WRITE (20,1)
    WRITE (*,102) ICP(1),ICP(2)
    GO TO 10
  ELSE
  ENDIF
  IF (IRS .GT. 0 .AND. NTOT .EQ. 2) THEN
    WRITE (*,102) ICP(1),ICP(2)
    WRITE (19,*) '      RESTART COMBUTATION'
    WRITE (20,*) '      RESTART COMBUTATION'
  ELSE
  ENDIF
10 ENON =DEXP(EPSLDA*UP(1,5)/(1.0+UP(1,5)))*UP(1,2)/DELHM
  HA = DSQRT(PAR(ICP(1)))
  WRITE (20,2) HA,ENON,UP(1,5)
  WRITE (19,3) HA,ENON,UP(1,5)
1  FORMAT(28X,'HATTA',11X,'ENON',11X,'THETAi')
2  FORMAT(20X,3E16.6)
3  FORMAT(20X,3E16.6)
  WRITE(*,101)IBR,NTOT,ATYPE,LAB,PAR(1),PAR(ICP(2))
  1,ENON,UP(1,5)
101 FORMAT(14,1X,15,1X,A2,I4,E14.6,2X,E14.6,2X,E14.6,F12.6)
102 FORMAT(' BR PT TY LAB',4X,'PAR(',I2,')',10X,'PAR(',I2,')',
  110X,'ENON',9X,'THETAi')
C
  RETURN
  END
C
C*****
C
C  SUBROUTINE X1(MIU,T,UP,IBR,NTOT,ATYPE,LAB)
C  IMPLICIT DOUBLE PRECISION (A-H,O-Z)
C  COMMON /BLBCN/ NDIM,IPS,IRS,ILP,ICP(20),PAR(20)
C  DIMENSION UP(MIU,NDIM)
C
  RETURN
  END
C
C*****
C
C  SUBROUTINE OUTPUT(U,Y,NDIMOUT)
C
C  IMPLICIT DOUBLE PRECISION (A-H,O-Z)
C  COMMON /BLBCN/ NDIM,IPS,IRS,ILP,ICP(20),PAR(20)
C  DIMENSION U(*),Y(*)
C
  Y(1) = U(1)

```

```

Y(2) = U(2)
Y(3) = U(3)
Y(4) = U(4)
Y(5) = U(5)
Y(6) = U(6)
C
  RETURN
  END
C
C*****
C
C  SUBROUTINE ICND(NDIM,PAR,ICP,NINT,U,UOLD,UDOT,UPOLD,FI,
  I      IJAC,DINT)
  IMPLICIT DOUBLE PRECISION (A-H,O-Z)
C
C (This problem has no integral constraints.)
C
  RETURN
  END
C
C*****
C
C  FUNCTION USZR(I,NUZR,PAR)
  IMPLICIT DOUBLE PRECISION (A-H,O-Z)
  DIMENSION PAR(20)
C
  GOTO(1,2)I
C
  1  USZR=PAR(1)-1.0000000D0
  RETURN
  2  USZR=PAR(1)-4.0000000D0
  RETURN
  END
C
C*****
C
C  SUBROUTINE FOPT
  RETURN
  END
C
C*****
C
C  SUBROUTINE WRITE_DATA (EPSLDA,EPSLDB,EPSLS,EPSLR,EPSLV,BETAS,
  1 BETAR,BETAV,LE,DELHM,DHM,S,BIH,BIM,M,N,GAMMA,BETA,ALPHA,THETAG,
  2 THETA0,OMEGA,A0,EPSLEFF,BETAEFF)
  IMPLICIT DOUBLE PRECISION (A-H,O-Z)
  REAL*8 LE
  WRITE(20,1)
  1'EPSLEF= ',EPSLEFF ,
  1'BETAEF= ',BETAEFF ,
  1'EPSLDA= ',EPSLDA,

```

```

I'EPSLDB='EPSLDB,
I'EPSLS ='EPSLS ,
I'EPSLR ='EPSLR ,
I'EPSLV ='EPSLV ,
I'BETAS ='BETAS ,
I'BETAR ='BETAR ,
I'BETAV ='BETAV ,
I'LE  ='LE  ,
I'DELHM ='DELHM ,
I'DHM  ='DHM  ,
I'S   ='S   ,
I'BIH  ='BIH  ,
I'BIM  ='BIM  ,
I'M    ='M    ,
I'N    ='N    ,
I'GAMMA ='GAMMA ,
I'BETA  ='BETA  ,
I'ALPHA ='ALPHA ,
I'THETAG='THETAG,
I'THETA0='THETA0,
I'OMEGA ='OMEGA ,
I'A0   ='A0
I  FORMAT(11(A,E12.6/),5(A,E12.6/),2(A,I11/),7(A,E12.6/))
C
  RETURN
  END

```

APPENDIX B2

SAMPLE OF MAINE PROGRAM AND INPUT SUBROUTINES TO COLNEW

```

IMPLICIT REAL*8 (A-H,O-Z)
DIMENSION FSPACE(1000000),ISPACE(100000),
1      IPAR(11),LTOL(6),M(3),TOL(6),Z(6),ZETA(6)
REAL*8  EPSLDA,EPSLDB,EPSLR,EPSLS,EPSLV,BETAR,BETAS,BETAV,
1      A0,OMEGA,THETA0,THETAG,BIM,BIH,ALPHA,BETA,GAMMA,
2      LE,S,VAL_RM,DELHM
COMMON  EPSLDA,EPSLDB,EPSLR,EPSLS,EPSLV,BETAR,BETAS,BETAV
COMMON  A0,OMEGA,THETA0,THETAG,BIM,BIH,ALPHA,BETA,GAMMA
COMMON  S,VAL_RM,DELHM,SM,SN
INTEGER SM,SN
EXTERNAL FSUB,DFSUB,GSUB,DGSUB,GUESS
C
C  READ MODEL PARAMETERS
C
C  CALL OPEN_UNITS
C  CALL INPUT_DATA (EPSLDA,EPSLDB,EPSLS,EPSLR,EPSLV,BETAS,
1BETAR,BETAV,LE,DELHM,DHM,S,BIH,BIM,SM,SN,GAMMA,BETA,ALPHA,
2THETAG,THETA0,OMEGA,A0,VAL_RM,EPSLEFF,BETAEFF)
C
C  DETERMINE NO. OF DIFFERENTIAL EQUATIONS
C
C  NCOMP=3
C
C  ORDER OF DIFFERENTIAL EQUATIONS
C
C  M(1)=2
C  M(2)=2
C  M(3)=2
C
C  SET INTERVAL ENDS
C
C  ALEFT=0.d0
C  ARIGHT=1.d0
C
C  GIVE LOCATION OF THE SIDE CONDITIONS
C
C  ZETA(1)=0.d0
C  ZETA(2)=0.d0

```

```

ZETA(3)=0.d0
ZETA(4)=1.d0
ZETA(5)=1.d0
ZETA(6)=1.d0
C
C  IPAR VALUES
C  PROBLEM IS NON-LINEAR
C
  IPAR(1)=1
C
C  4 COLLOCATION POINTS PER SUB-INTERVAL
C
  IPAR(2)=4
C
C  INITIAL MESH OF SUB-INTERVAL
C
  IPAR(3)=0
C
C  SIX TOLERANCES ON Z AND ITS DERIVATIVES
C
  IPAR(4)=6
  DO 1 I=1,6
    LTOL(I)=I
    TOL(I)=0.00001
1  CONTINUE
C
C  DIMENSION OF WORK ARRAY FSPACE AND WORK ARRAY ISPACE C
C
  IPAR(5)=1000000
  IPAR(6)=100000
C
C  NO SELECTED PRINTOUT
C
  IPAR(7)= 0
C
C  GENERATE A UNIFORM INITIAL MESH
C
  IPAR(8)=0
C
C  INITIAL SOLUTION IS PROVIDED BY THE USER
C
  IPAR(9)=1
C
C  THE PROBLEM IS REGULAR
C
  IPAR(10)=1
C
C  NO FIXED POINT IN THE MESH OTHER THAN LEFT AND RIGHT
C
  IPAR(11)=0
C

```



```

IITER = 0
DO 10 II=1,1
  IITER = IITER + 1
  IF(IITER.NE.1) THEN
    IPAR(9)=3
    IPAR(3)=ISPACE(1)
  ENDIF
  HA=DSQRT(VAL_RM)
C
C  CALL SUBROUTINE COLNEW
C
  CALL COLNEW (NCOMP, M, ALEFT, ARIGHT, ZETA, IPAR, LTOL,
1  TOL, FIXPNT, ISPACE, FSPACE, IFLAG, FSUB, DFSUB, GSUB, DGSUB, GUESS)
C  IF(IFLAG.EQ.-1) THEN
    PRINT *, ' IFLAG =', IFLAG
    NP1=21
    X=0.d0
C
C  OUTPUT RESULTS
C
    WRITE(10,101) VAL_RM
    DO 2 III=1,NP1
      CALL APPSLN(X,Z,FSPACE,ISPACE)
      WRITE(10,102) X,Z(1),Z(2),Z(3),Z(4),Z(5),Z(6)
      IF (X.EQ.0.D0)THEN
        ENON=-DEXP(-EPSLDA*Z(5)/(1.D0+Z(5)))/DELHM*Z(2)
        THETA1=Z(5)
      ELSE
        ENON=0
      ENDIF
      X=X+0.05d0
2  CONTINUE
C  WRITE(8,104) IITER,HA,THETA1,ENON
10  CONTINUE
C
C  FORMAT STATEMENTS
C
101  FORMAT(2X,E14.6)
102  FORMAT(7E14.6)
  STOP
  END
C*****
C
C  SUBROUTINE GUESS
C
C  OBJECTIVE :
C
C  EVALUATE THE INITIAL APPROXIMATION FOR Z(U(X))
C
C  USAGE : COLNEW
C*****
SUBROUTINE GUESS (X,Z,DMVAL)

```

```

      IMPLICIT REAL*8 (A-H,O-Z)
      DIMENSION Z(6),DMVAL(3)
      COMMON  EPSLDA,EPSLDB,EPSLR,EPSLS,EPSLV,BETAR,BETAS,BETAV
      COMMON  A0,OMEGA,THETA0,THETAG,BIM,BIH,ALPHA,BETA,GAMMA
      COMMON  S,VAL_RM,DELHM,SN,SM
      INTEGER  SM,SN
      Z(1)= 1.0
      Z(2)=-1.0
      Z(3)= 1.0
      Z(4)= 0.0
      Z(5)= 0.0
      Z(6)= 0.0
      DMVAL(1)=0.0
      DMVAL(2)=0.0
      DMVAL(3)=0.0
      RETURN
      END
C*****
C
C   OBJECTIVE : EVALUATE F(X,Z(U(X)) AT A POINT X
C
C   USAGE : COLNEW
C
C*****
      SUBROUTINE FSUB (X,Z,F)
      IMPLICIT REAL*8 (A-H,O-Z)
      DIMENSION F(3),Z(6)
      COMMON  EPSLDA,EPSLDB,EPSLR,EPSLS,EPSLV,BETAR,BETAS,BETAV
      COMMON  A0,OMEGA,THETA0,THETAG,BIM,BIH,ALPHA,BETA,GAMMA
      COMMON  S,VAL_RM,DELHM,SN,SM
      INTEGER  SM,SN
C
      EEA = DEXP( EPSLDA*Z(5)/(1.0+Z(5)))
      EEB = DEXP( EPSLDB*Z(5)/(1.0+Z(5)))
      EER = DEXP( EPSLR *Z(5)/(1.0+Z(5)))
      EES = DEXP(-EPSLS *Z(5)/(1.0+Z(5)))
      EEV = DEXP( EPSLV *Z(5)/(1.0+Z(5)))
C
      F(1) = DELHM**2*VAL_RM*EER/EEA*Z(1)**SM*Z(3)**SN-
1      EPSLDA/(1.0D0+Z(5))**2*Z(6)*Z(2)
      F(2) = DELHM**2*S*VAL_RM*EER/EEB*Z(1)**SM*Z(3)**SN-
1      EPSLDB/(1.0D0+Z(5))**2*Z(6)*Z(4)
      F(3) =-DELHM**2*BETAR*VAL_RM*EER*Z(1)**SM*Z(3)**SN
      RETURN
      END
C*****
C
C   SUBROUTINE DFSUB
C
C   OBJECTIVE : EVALUATE THE JACOBIAN OF F(X,Z)
C

```

```

C  USAGE : COLNEW
C
C*****
SUBROUTINE DFSUB (X,Z,DF)
IMPLICIT REAL*8 (A-H,O-Z)
DIMENSION DF(6,6),Z(6)
COMMON  EPSLDA,EPSLDB,EPSLR,EPSLS,EPSLV,BETAR,BETAS,BETAV
COMMON  A0,OMEGA,THETA0,THETAG,BIM,BIH,ALPHA,BETA,GAMMA
COMMON  S,VAL_RM,DELHM,SN,SM
INTEGER SM,SN
EEA = DEXP( EPSLDA *Z(5)/(1.0+Z(5)))
EEB = DEXP( EPSLDB *Z(5)/(1.0+Z(5)))
EER = DEXP( EPSLR *Z(5)/(1.0+Z(5)))
EES = DEXP(-EPSLS *Z(5)/(1.0+Z(5)))
EEV = DEXP( EPSLV *Z(5)/(1.0+Z(5)))
DO 10 I = 1, 6
DO 20 J = 1, 6
  DF(I,J) = 0.D0
20 CONTINUE
10 CONTINUE
C
DF(1,1)= SM*DELHM**2*VAL_RM*EER/EEA*Z(1)**(SM-1)*Z(3)**SN
DF(1,2)=-EPSLDA/(1.0D0+Z(5))**2*Z(6)
DF(1,3)= SN*DELHM**2*VAL_RM*EER/EEA*Z(1)**SM*Z(3)**(SN-1)
DF(1,5)= DELHM**2*VAL_RM*EER/EEA*(EPSLR-EPSLDA)/(1.0D0+Z(5))**2
1  *Z(1)**SM*Z(3)**SN+2.0D0*EPSLDA/(1.0+Z(5))**3*Z(6)*Z(2)
DF(1,6)=-EPSLDA/(1.0D0+Z(5))**2*Z(2)
C
DF(2,1)= SM*DELHM**2*S*VAL_RM*EER/EEB*Z(1)**(SM-1)*Z(3)**SN
DF(2,3)= SN*DELHM**2*S*VAL_RM*EER/EEB*Z(1)**SM*Z(3)**(SN-1)
DF(2,4)=-EPSLDB/(1.0D0+Z(5))**2*Z(6)
DF(2,5)= DELHM**2*S*VAL_RM*EER/EEB*(EPSLR-EPSLDB)/(1.0D0+Z(5))**2
1  *Z(1)**SM*Z(3)**SN+2.0D0*EPSLDB/(1.0D0+Z(5))**3*Z(6)*Z(4)
DF(2,6)=-EPSLDB/(1.0D0+Z(5))**2*Z(4)
C
DF(3,1)=-SM*DELHM**2*BETAR*VAL_RM*EER*Z(1)**(SM-1)*Z(3)**SN
DF(3,3)=-SN*DELHM**2*BETAR*VAL_RM*EER*Z(1)**SM*Z(3)**(SN-1)
DF(3,5)=-DELHM**2*BETAR*VAL_RM*EER*Z(1)**SM*Z(3)**SN*
1  EPSLR/(1.0D0+Z(5))**2
RETURN
END
C*****
C
C  SUBROUTINE GSUB
C
C  OBJECTIVE : EVALUATE THE I-TH COMPONENT OF G (X,Z)
C
C  USAGE : COLNEW
C
C*****
SUBROUTINE GSUB(I,Z,G)

```

```

      IMPLICIT REAL*8 (A-H,O-Z)
      DIMENSION Z(6)
      COMMON  EPSLDA,EPSLDB,EPSLR,EPSLS,EPSLV,BETAR,BETAS,BETAV
      COMMON  A0,OMEGA,THETA0,THETAG,BIM,BIH,ALPHA,BETA,GAMMA
      COMMON  S,VAL_RM,DELHM,SN,SM
      INTEGER SM,SN
      EEA = DEXP( EPSLDA*Z(5)/(1.0+Z(5)))
      EEB = DEXP( EPSLDB*Z(5)/(1.0+Z(5)))
      EER = DEXP( EPSLR *Z(5)/(1.0+Z(5)))
      EES = DEXP(-EPSLS *Z(5)/(1.0+Z(5)))
      EEV = DEXP( EPSLV *Z(5)/(1.0+Z(5)))
      GO TO (10,20,30,40,50,60),I
10    G = Z(1)-EES
      RETURN
20    G = EEB*Z(4)-BIM*DELHM*EEV*(Z(3)-Z(3))/(1.0+OMEGA))
      RETURN
30    G = BETAS*EEA*Z(2)-Z(6)+BIH*(Z(5)-THETAG)+BETAV*EEB*Z(4)
      RETURN
40    G =-EEA*Z(2)-VAL_RM*DELHM**2*(ALPHA-1.D0)*EER*Z(1)**SM*Z(3)**SN
      I  -BETA*DELHM*(Z(1)-A0)
      RETURN
50    G = Z(3)-1.D0
      RETURN
60    G = Z(6)+VAL_RM*BETAR*DELHM**2*(ALPHA-1.D0)*EER*Z(1)**SM*Z(3)**SN
      I  +GAMMA*(Z(5)-THETA0)
      RETURN
      END
C*****
C
C   SUBROUTINE : DGSUB
C
C   OBJECTIVE :  EVALUATE THE I-TH ROW OF THE JACOBIAN OF G(X,U(X))
C
C   USAGE : COLNEW
C
C*****
C   SUBROUTINE DGSUB(I,Z,DG)
      IMPLICIT REAL*8 (A-H,O-Z)
      DIMENSION DG(6),Z(6)
      COMMON  EPSLDA,EPSLDB,EPSLR,EPSLS,EPSLV,BETAR,BETAS,BETAV
      COMMON  A0,OMEGA,THETA0,THETAG,BIM,BIH,ALPHA,BETA,GAMMA
      COMMON  S,VAL_RM,DELHM,SN,SM
      INTEGER SM,SN
      EEA = DEXP( EPSLDA*Z(5)/(1.0+Z(5)))
      EEB = DEXP( EPSLDB*Z(5)/(1.0+Z(5)))
      EER = DEXP( EPSLR *Z(5)/(1.0+Z(5)))
      EES = DEXP(-EPSLS *Z(5)/(1.0+Z(5)))
      EEV = DEXP( EPSLV *Z(5)/(1.0+Z(5)))
      GO TO (10,20,30,40,50,60),I
10    DG(1)=1.0D0
      DG(2)=0.D0

```

```

DG(3)=0.D0
DG(4)=0.D0
DG(5)=EES*EPSLS/(1.0D0+Z(5))**2
DG(6)=0.D0
RETURN
20  DG(1)=0.D0
    DG(2)=0.D0
    DG(3)=-BIM*DELHM*EEV*(1.0-1.0/(1.0+OMEGA))
    DG(4)=EEB
    DG(5)=EEB*Z(4)*EPSLDB/(1.0D0+Z(5))**2-BIM*DELHM*EEV*(Z(3)-Z(3)/
1    (1.0+OMEGA))*EPSLV/(1.0D0+Z(5))**2
    DG(6)=0.D0
    RETURN
30  DG(1)=0.D0
    DG(2)=BETAS*EEA
    DG(3)=0.D0
    DG(4)=BETAV*EEB
    DG(5)=BETAS*EEA*Z(2)*EPSLDA/(1.0D0+Z(5))**2+BIH+BETAV*EEB*
1    Z(4)*EPSLDB/(1.0D0+Z(5))**2
    DG(6)=-1.0D0
    RETURN
40  DG(1)=-SM*VAL_RM*DELHM**2*(ALPHA-1.D0)*EER*Z(1)**(SM-1)*Z(3)**SN
1    -BETA*DELHM
    DG(2)=-EEA
    DG(3)=-SN*VAL_RM*DELHM**2*(ALPHA-1.D0)*EER*Z(1)**SM*Z(3)**(SN-1)
    DG(4)=0.D0
    DG(5)=-EEA*Z(2)*EPSLDA/(1.0D0+Z(5))**2-VAL_RM*DELHM**2*
1    (ALPHA-1.D0)*EER*EPSLR/(1.0+Z(5))**2*Z(1)**SM*Z(3)**SN
    DG(6)=0.D0
    RETURN
50  DG(1)=0.D0
    DG(2)=0.D0
    DG(3)=1.d0
    DG(4)=0.D0
    DG(5)=0.D0
    DG(6)=0.D0
    RETURN
60  DG(1)=SM*VAL_RM*BETAR*DELHM**2*(ALPHA-1.D0)*EER*Z(1)**(SM-1)*
1    Z(3)**SN
    DG(2)=0.D0
    DG(3)=SN*VAL_RM*BETAR*DELHM**2*(ALPHA-1.D0)*EER*Z(1)**SM*Z(3)
1    *(SN-1)
    DG(4)=0.D0
    DG(5)=VAL_RM*BETAR*DELHM**2*(ALPHA-1.D0)*EER*Z(1)**SM*Z(3)**SN*
1    EPSLR/(1.0D0+Z(5))**2+GAMMA
    DG(6)=1.0D0
    RETURN
END

```

APPENDIX B3

PROGRAM XPOLCOE TO FIT OUTPUT OF COLNEW AND USE IT AS A GUESS FOR AUTO

```

PROGRAM xpolcoe
C  driver for routine polcoe
C  ( EXTRACTED AND MODIFIED FROM THE NUMERICAL RECEPIES )
C
INTEGER NP
REAL*8 PI
REAL*8 VAL_RM,EPSLR,EPSLS,EPSLV,BETAR,BETAS,BETAV,BIM,BIH,DELHM
PARAMETER(NP=4,NDATA=21)
INTEGER i,j,nfunc
REAL*8 f,sum,x,xa(ndata),coeff(NP),ya1(ndata),ya2(ndata)
1  ,ya3(ndata),ya4(ndata),ya5(ndata),ya6(ndata)
CALL OPEN_UNITS
READ(10,*) VAL_RM
WRITE(11,*) ' SUBROUTINE STPNT(NDIM,U,PAR,T)'
WRITE(11,*) ' IMPLICIT DOUBLE PRECISION (A-H,O-Z)'
WRITE(11,*) ' DIMENSION U(NDIM),PAR(20)'
WRITE(11,101) 'PAR(1) =',VAL_RM
101 FORMAT(6X,A,E16.6)
do 12 i=1,NDATA
  READ(10,*) xa(i),ya1(i),ya2(i),ya3(i),ya4(i)
1  ,ya5(i),ya6(i)
12  continue
C
C
C
call polcoe(xa,ya1,NP,coeff)
WRITE(12,*) ' coefficients for data set # 1'
WRITE(12,'(1x,6f12.6)') (coeff(i),i=1,NP)
WRITE(12,'(1x,t10,a1,t20,a4,t29,a10)')
*  'x','f(x)','polynomial'
do 141 i=1,ndata
  x=xa(i)
  f=ya1(i)
  sum=coeff(NP)
  do 131 j=NP-1,1,-1
    sum=coeff(j)+sum*x
131  continue
  WRITE(12,'(1x,3f12.6)') x,f,sum
141  continue
WRITE(12,*) '*****'

```

```

WRITE(11,100) 'U(1) =',COEFF(1),'+',COEFF(2,')*T+',
1      COEFF(3,')*T**2+',COEFF(4,')*T**3'
C
C
C
call polcoe(xa,ya2,NP,coeff)
WRITE(12,*) ' coefficients for data set # 2'
WRITE(12,'(1x,6f12.6)') (coeff(i),i=1,NP)
WRITE(12,'(1x,t10,a1,t20,a4,t29,a10)')
*   'x','f(x)','polynomial'
do 142 i=1,ndata
  x=xa(i)
  f=ya2(i)
  sum=coeff(NP)
  do 132 j=NP-1,1,-1
    sum=coeff(j)+sum*x
132  continue
    WRITE(12,'(1x,3f12.6)') x,f,sum
142  continue
WRITE(12,*) '*****'
WRITE(11,100) 'U(2) =',COEFF(1),'+',COEFF(2,')*T+',
1      COEFF(3,')*T**2+',COEFF(4,')*T**3'
C
C
C
call polcoe(xa,ya3,NP,coeff)
WRITE(12,*) ' coefficients for data set # 3'
WRITE(12,'(1x,6f12.6)') (coeff(i),i=1,NP)
WRITE(12,'(1x,t10,a1,t20,a4,t29,a10)')
*   'x','f(x)','polynomial'
do 143 i=1,ndata
  x=xa(i)
  f=ya3(i)
  sum=coeff(NP)
  do 133 j=NP-1,1,-1
    sum=coeff(j)+sum*x
133  continue
    WRITE(12,'(1x,3f12.6)') x,f,sum
143  continue
WRITE(12,*) '*****'
WRITE(11,100) 'U(3) =',COEFF(1),'+',COEFF(2,')*T+',
1      COEFF(3,')*T**2+',COEFF(4,')*T**3'
C
C
C
call polcoe(xa,ya4,NP,coeff)
WRITE(12,*) ' coefficients for data set # 4'
WRITE(12,'(1x,6f12.6)') (coeff(i),i=1,NP)
WRITE(12,'(1x,t10,a1,t20,a4,t29,a10)')
*   'x','f(x)','polynomial'
do 144 i=1,ndata

```

```

        x=xa(i)
        f=ya4(i)
        sum=coeff(NP)
        do 134 j=NP-1,1,-1
            sum=coeff(j)+sum*x
134      continue
        WRITE(12,'(1x,3f12.6)') x,f,sum
144      continue
        WRITE(12,*) '*****'
        WRITE(11,100) 'U(4) =',COEFF(1),'+(',COEFF(2),')*T+(',
1          COEFF(3),')*T**2+',('COEFF(4),')*T**3'
C
C
C
        call polcoe(xa,ya5,NP,coeff)
        WRITE(12,*) ' coefficients for data set # 5'
        WRITE(12,'(1x,6f12.6)') (coeff(i),i=1,NP)
        WRITE(12,'(1x,t10,a1,t20,a4,t29,a10)')
        * 'x','f(x)', 'polynomial'
        do 145 i=1,ndata
            x=xa(i)
            f=ya5(i)
            sum=coeff(NP)
            do 135 j=NP-1,1,-1
                sum=coeff(j)+sum*x
135          continue
            WRITE(12,'(1x,3f12.6)') x,f,sum
145          continue
            WRITE(12,*) '*****'
            WRITE(11,100) 'U(5) =',COEFF(1),'+(',COEFF(2),')*T+(',
1          COEFF(3),')*T**2+',('COEFF(4),')*T**3'
C
C
C
        call polcoe(xa,ya6,NP,coeff)
        WRITE(12,*) ' coefficients for data set # 6'
        WRITE(12,'(1x,6f12.6)') (coeff(i),i=1,NP)
        WRITE(12,'(1x,t10,a1,t20,a4,t29,a10)')
        * 'x','f(x)', 'polynomial'
        do 146 i=1,ndata
            x=xa(i)
            f=ya6(i)
            sum=coeff(NP)
            do 136 j=NP-1,1,-1
                sum=coeff(j)+sum*x
136          continue
            WRITE(12,'(1x,3f12.6)') x,f,sum
146          continue
            WRITE(12,*) '*****'
            WRITE(11,100) 'U(6) =',COEFF(1),'+(',COEFF(2),')*T+(',
1          COEFF(3),')*T**2+',('COEFF(4),')*T**3'

```



```

C
C
C
  WRITE(11,*)'  RETURN'
  WRITE(11,*)'  END'
100 FORMAT(6X,A,1X,'(',E13.6,')',A,2(E13.6,A),/,5X,'1',7X,A,E13.6,A)
  END
C/* (C) Copr. 1986-92 Numerical Recipes Software +%{.. */
  SUBROUTINE polcoe(x,y,n,cof)
  IMPLICIT REAL*8 (A-H,O-Z)
  INTEGER n,NMAX
  REAL*8 cof(n),x(n),y(n)
  PARAMETER (NMAX=15)
  INTEGER i,j,k
  REAL*8 b,ff,phi,s(NMAX)
  do 11 i=1,n
    s(i)=0.
    cof(i)=0.
11  continue
    s(n)=x(1)
    do 13 i=2,n
      do 12 j=n+1-i,n-1
        s(j)=s(j)-x(i)*s(j+1)
12  continue
      s(n)=s(n)-x(i)
13  continue
      do 16 j=1,n
        phi=n
        do 14 k=n-1,1,-1
          phi=k*s(k+1)+x(j)*phi
14  continue
          ff=y(j)/phi
          b=1.
          do 15 k=n,1,-1
            cof(k)=cof(k)+b*ff
            b=s(k)+x(j)*b
15  continue
16  continue
      return
  END
C (C) Copr. 1986-92 Numerical Recipes Software +%{..

```

APPENDIX B4

SAMPLE OF PROGRAM AND SUBROUTINES USED TO SOLVE THE REACTOR PROBLEM

```

PROGRAM CSTR
IMPLICIT DOUBLE PRECISION (A-H,O-Z)
REAL*8 KL,KGA,K0,K,KCI,KSTAR
COMMON /DUMMY/ K0,H0,DELTA,VALPHA,VBETA,B,P,AGF,BLF,BIGQ,Q,DA,
!      KL,ALPHAP,BL,BI,SMALLR,V,FGF,ASUB,TLF,VR,YAF,ER,
!      THETAR,THETAC,KCI,PCI,XB,SIGNAL,IROOT,AI
C
OPEN(6,FILE='CSTR.DAT')
OPEN(7,FILE='TEMP.DAT')
CALL DATA(RHOLF,RHOL,H0,RHOGF,DELHR,DELHS,BLF,VR,ASUB,EPSLL,
!KL,US,CPL,CPG,TLF,TGF,TC,FGF,KGA,R,YAF,ER,K0,AGF,DA,DB,HA,Q,
!SMALLR,B,DGF,THETAC,THETAR,VBETA,DELTA,ALPHAP,PCI)
STEP = 0.01
TOL = 0.000001
DO 1000 RSTIME = 37.5,37,-0.1
WRITE(*, '(/,A)') ' .....
! .....
WRITE(6, '(/,A)') ' .....
! .....
C
TAUL = RSTIME*60.0
KCI = EPSLL/KL/ASUB/TAUL
FL = EPSLL*VR/TAUL
P = DELHR*FL*AGF/(RHOL*CPL*TLF*FGF)
BIGQ = FGF/FL
VALPHA = 1.0/BIGQ+SMALLR
THTLB = (VBETA*THETAC+SMALLR*(THETAR-1.0))/(VALPHA+VBETA)
THTUB = (B+SMALLR*YAF+VBETA*THETAC+SMALLR*(THETAR-1.0))/
! (VALPHA+VBETA-SMALLR*YAF)
C
WRITE(*, '(5X,A,F16.6,A)') 'TAUL(MIN) =',RSTIME,' <-----'
WRITE(*, '(5X,A,F16.6)') 'LOWER BOUND =',(THTLB*297.+297.-273.15)
WRITE(*, '(5X,A,F16.6,/)') 'UPPER BOUND =',(THTUB*297.+297.-273.15)
WRITE(*, '(4X,A,7(8X,A))') 'T','CM','EA','AL','BI','XA','AI','BL'
WRITE(6, '(5X,A,F16.6,A)') 'TAUL(MIN) =',RSTIME,' <-----'
WRITE(6, '(5X,A,F16.6)') 'LOWER BOUND =',THTLB
WRITE(6, '(5X,A,F16.6,/)') 'UPPER BOUND =',THTUB
WRITE(6, '(4X,A,7(8X,A))') 'T','CM','EA','AL','BI','XA','AI','BL'
YN = THTLB

```

```

YUP = THTUB
IER = 0
YIER = 1.0D-4
IROOT = 0
NCTL = 0
SIGNAL = 0.0
CALL EFACOR(TAUL,EA,AL,YN,CM,XA)
IF(SIGNAL .GT. 1.0) GO TO 100
FY = -(1.0/BIGQ+SMALLR*(1.-YAF*XA))*YN+B*DGF*EA*(1.-XA)/
! (1.-YAF*XA)*DEXP(DELTA/(1.+YN))+SMALLR*YAF*XA+
! SMALLR*(THETAR-1.)-P*Q*AL/BLF-B*(YN-THETAC)
30 Y1 = YN+STEP
IF(Y1 .GE. YUP) GO TO 90
35 CALL EFACOR(TAUL,EA,AL,Y1,CM,XA)
IF(SIGNAL .EQ. 4.0) GO TO 100
IF(SIGNAL .EQ. 2.0) GO TO 1000
IF(IROOT .GT. 1) GO TO 1000
FY1 = -(1.0/BIGQ+SMALLR*(1.-YAF*XA))*Y1+B*DGF*EA*(1.-XA)/
! (1.-YAF*XA)*DEXP(DELTA/(1.+Y1))+SMALLR*YAF*XA+
! SMALLR*(THETAR-1.)-P*Q*AL/BLF-B*(Y1-THETAC)
FYFY1 = FY*FY1
IF(FYFY1 .LT. 0.0) GO TO 50
40 FY = FY1
YN = Y1
GO TO 30
50 YL = YN
YU = Y1
FYU = FY1
60 YS = (YL+YU)/2.0
CALL EFACOR(TAUL,EA,AL,YS,CM,XA)
IF(DABS(YU-YL) .LT. TOL) GO TO 80
FYS = -(1.0/BIGQ+SMALLR*(1.-YAF*XA))*YS+B*DGF*EA*(1.-XA)/
! (1.-YAF*XA)*DEXP(DELTA/(1.+YS))+SMALLR*YAF*XA+
! SMALLR*(THETAR-1.)-P*Q*AL/BLF-B*(YS-THETAC)
FYUFYS = FYU*FYS
IF(FYUFYS .GT. 0.0) GO TO 70
YL = YS
GO TO 60
70 YU = YS
FYU = FYS
GO TO 60
80 THETA = YS
T = THETA*TLF+TLF-273.15
WRITE(*,('F8.2,7F10.5')) T,CM,EA,AL,BI,XA,AI,BL
WRITE(6,('F8.2,7F10.5')) T,CM,EA,AL,BI,XA,AI,BL
WRITE(7,('2F8.2,7F16.10')) rstime,T,CM,EA,AL,BI,XA,AI,BL
c WRITE(7,('2F16.6')) RSTIME,T
GO TO 40
90 NCTL = NCTL+1
IF(NCTL .GT. 1) GO TO 1000
Y1 = YUP

```

```

      GO TO 35
100  IER=IER+1
      IF(IER.GT.60) GO TO 19
      IF(IER.GT.20) YIER=1.D-5
      IF(IER.GT.40) YIER=1.D-6
      IF(IER.GT.50) YIER=1.D-7
      YI=YI-YIER
      GO TO 35
19   WRITE(*,*) 'IER =',IER
1000 CONTINUE
      END
C-----
      SUBROUTINE EFACTOR(TAUL,EA,AL,Y,CM,XA)
C-----
      IMPLICIT DOUBLE PRECISION (A-H,O-Z)
      REAL*8 KL,KGA,K0,K,KCI,KSTAR
      LOGICAL check
      COMMON /DUMMY/ K0,H0,DELTA,VALPHA,VBETA,B,P,AGF,BLF,BIGQ,Q,DA,
!           KL,ALPHA,BL,BI,SMALLR,V,FGF,ASUB,TLF,VR,YAF,ER,
!           THETAR,THETAC,KCI,PCI,XB,SIGNAL,IROOT,AI
C
      TB  = Y*TLF+TLF
      AL  = 0.00001
      ITER = 0
10  XA  = ((VALPHA+VBETA)*Y+P*Q*AL/BLF-VBETA*THETAC)/
!      (B+SMALLR*YAF*(1.0+Y))
      IF(XA .GE. 1.0) GO TO 62
      AI  = H0*AGF*(1.0-XA)/(1.0-YAF*XA)*DEXP(DELTA/(1.0+Y))
      XB  = BIGQ/Q*XA-AL/BLF
      BL  = BLF*(1.0-XB)
      IF (BL .LT. 0.0) GO TO 60
C
      TGF = TLF
      CALL NISO(TAUL,TB,BL,AI,TGF,TLF,CM,EA,ALNUM,BI)
C
      IF (ALNUM .LT. 0.0) ALNUM = 0.0
      IF (DABS(AL - ALNUM) .LT. 1.d-7) GO TO 22
      AL  = ALNUM
      ITER = ITER+1
      IF(ITER .GE. 5) GO TO 40
      GO TO 10
22  RETURN
40  PRINT*, ' NO CONVERGENCE FOR AL '
      RETURN
60  SIGNAL = 4.0
      RETURN
62  IROOT=2
      WRITE(6,*) 'Y =',(Y*297.+297.-273.15),'XG =',XA
      WRITE(*, '(/2(A,F16.6,4X))') 'Y =',(Y*297.+297.-273.15),'XG =',XA
      RETURN
      END

```



```

1      IPAR(11),LTOL(6),M(3),TOL(6),Z(6),ZETA(6)
REAL*8  KKL,KL,K0,MUE,LE,KG,K2,K2B
REAL*8  EPSLDA,EPSLDB,EPSLR,EPSLS,EPSLV,BETAR,BETAS,BETAV,
1      A0,OMEGA,THETA0,THETAG,BIM,BIH,ALPHA,BETA,GAMMA,
2      LE,S,VAL_RM,DELHM
COMMON  EPSLDA,EPSLDB,EPSLR,EPSLS,EPSLV,BETAR,BETAS,BETAV
COMMON  A0,OMEGA,THETA0,THETAG,BIM,BIH,ALPHA,BETA,GAMMA
COMMON  S,VAL_RM,DELHM,SM,SN
INTEGER SM,SN
EXTERNAL FSUB,DFSUB,GSUB,DGSUB,GUESS
C
C  PHYSIOCHEMICAL PARAMETERS FOR THE
C  CHLORINATION OF N-DECANE
C
DELHS  =-4500.0
DELHR  =-26000.0
DELHV  = 9569.0
EDA    = 3147.0
EDB    = 3147.0
LE     = 1.0
ER     = 29000.0
DAB    = 6.0D-5
DBB    = DAB
KKL    = 3.312D-4
R      = 1.987
MUE    = 1
VL     = 0.86*400.0
A      = 3.0*400.0
KL     = 0.04
DELTAM = DAB/KL
DELTAH = LE**0.5*DELTAM
FL     = VL/TAUL
RHOL   = 5.1E-3
RHOG   = 4.2D-5
CPL    = 80.0
KG     = KL
K2     = 0.005
TSTAR  = 50.0+273.15
K2B    = K2/DEXP(-ER/R*(1/TSTAR-1/TB))
C
C  DIMENSIONLESS MODEL PARAMETERS
C
C  SM    = 1
C  SN    = 1
C  VAL_RM = K2B*DAB*CAIB**(SM-1)*CBB**(SN)/KL**2
C  S     = MUE*DAB*CAIB/DBB/CBB
C  EPSLDA = EDA/R/TB
C  EPSLDB = EDB/R/TB
C  EPSLR  = ER/R/TB
C  EPSLS  =-DELHS/R/TB
C  EPSLV  = DELHV/R/TB

```

```

C  BETAR  =-DELHR*DAB*CAIB/KKL/TB
C  BETAS  =-DELHS*DAB*CAIB/KKL/TB
C  BETAV  = DELHV*DBB*CBB/KKL/TB
C  BIH    = 0.01
C  DELHM  = LE**0.5
C  DHM    = DELHM**2.0
C  BIM    = 0.0
C  GAMMA  = FL*RHOL*CPL*DELTAH/A/KKL
C  BETA   = FL*DELTAM/A/DAB
C  ALPHA  = VL/A/DELTAH
C  OMEGA  = 1000.0
C  THETAG = (TGF-TB)/TB
C  THETA0 = (TLF-TB)/TB
C  A0     = 0.0
SM      = 1
SN      = 1
VAL_RM  = K2B*DAB*CAIB**(SM-1)*CBB**(SN)/KL**2
S       = MUE*DAB*CAIB/DBB/CBB
EPSLDA  = 0.0
EPSLDB  = 0.0
EPSLR   = 0.0
EPSLS   = 0.0
EPSLV   = 0.0
BETAR   = 0.0
BETAS   = 0.0
BETAV   = 0.0
BIH     = 0.0
BIM     = 0.0
GAMMA   = FL*RHOL*CPL*DELTAH/A/KKL
BETA    = FL*DELTAM/A/DAB
ALPHA   = VL/A/DELTAH
OMEGA   = 1000.0
THETAG  = 0.0
THETA0  = 0.0
A0      = 0.0
DELHM   = 1.0
DHM     = DELHM**2.0
C
C  DETERMINE NO. OF DIFFERENTIAL EQUATIONS
C
C  NCOMP=3
C
C  ORDER OF DIFFERENTIAL EQUATIONS
C
C  M(1)=2
C  M(2)=2
C  M(3)=2
C
C  SET INTERVAL ENDS
C
C  ALEFT=0.d0

```

```

    ARIGHT=1.d0
C
C   GIVE LOCATION OF THE SIDE CONDITIONS
C
    ZETA(1)=0.d0
    ZETA(2)=0.d0
    ZETA(3)=0.d0
    ZETA(4)=1.d0
    ZETA(5)=1.d0
    ZETA(6)=1.d0
C
C   IPAR VALUES
C   PROBLEM IS NON-LINEAR
C
    IPAR(1)=1
C
C   7 COLLOCATION POINTS PER SUB-INTERVAL
C
    IPAR(2)=7
C
C   INITIAL MESH OF SUB-INTERVAL
C
    IPAR(3)=0
C
C   SIX TOLERANCES ON Z AND ITS DERIVATIVES
C
    IPAR(4)=6
    DO 1 I=1,6
    LTOL(I)=I
    TOL(I)=0.00001
1   CONTINUE
C
C   DIMENSION OF WORK ARRAY FSPACE AND WORK ARRAY ISPACE C
C
    IPAR(5)=1000000
    IPAR(6)=40000
C
C   NO SELECTED PRINTOUT
C
    IPAR(7)= 1
C
C   GENERATE A UNIFORM INITIAL MESH
C
    IPAR(8)=0
C
C   INITIAL SOLUTION IS PROVIDED BY THE USER
C
    IPAR(9)=1
C
C   THE PROBLEM IS REGULAR
C

```



```

      IPAR(10)=1
C
C   NO FIXED POINT IN THE MESH OTHER THAN LEFT AND RIGHT
C
      IPAR(11)=0
C
      IITER = 0
      DO 10 II=1,1
1000  IITER = IITER + 1
      IF(IITER.NE.1) THEN
        IPAR(9)=3
        IPAR(3)=ISPACE(1)
      ENDIF
      HA=DSQRT(VAL_RM)
C
C   CALL SUBROUTINE COLNEW
C
      CALL COLNEW (NCOMP, M, ALEFT, ARIGHT, ZETA, IPAR, LTOL,
1  TOL, FIXPNT, ISPACE, FSPACE, IFLAG, FSUB, DFSUB, GSUB, DGSUB, GUESS)
      IF(IFLAG.NE.1) THEN
        IF(IITER .EQ. 1) GO TO 1000
        PRINT *,
        PRINT *,
        PRINT *,
        PRINT *, ' IFLAG =', IFLAG, ' ??????????????????????'
      WRITE(*,103)
      I'TB   =',TB ,
      I'CBB  =',CBB ,
      I'VAL_RM =',VAL_RM,
      I'S    =',S ,
      I'EPSLDA =',EPSLDA,
      I'EPSLDB =',EPSLDB,
      I'EPSLR  =',EPSLR,
      I'EPSLS  =',EPSLS,
      I'EPSLV  =',EPSLV,
      I'BETAR  =',BETAR,
      I'BETAS  =',BETAS,
      I'BETAV  =',BETAV,
      I'BIM    =',BIM ,
      I'BIH    =',BIH ,
      I'DELHM  =',DELHM,
      I'LE     =',LE ,
      I'ALPHA  =',ALPHA,
      I'BETA   =',BETA ,
      I'GAMMA  =',GAMMA,
      I'THETAG =',THETAG,
      I'THETA0 =',THETA0
103  FORMAT(21(6X,A,F11.5))
      ELSE
      ENDIF
      NP1=11

```

```

      X=0.d0
C
C  OUTPUT RESULTS
C
      DO 2 III=1,NP1
      CALL APPSLN(X,Z,FSPACE,ISPACE)
C      WRITE(7,102) X,Z(1),Z(2),Z(3),Z(4),Z(5),Z(6)
      IF (X.EQ.0.D0)THEN
      ENON=-DEXP(-EPSLDA*Z(5)/(1.D0+Z(5)))/DELHM*Z(2)
      AI=Z(1)
      BI=Z(3)
      ELSE
      ENDIF
      X=X+0.1d0
2  CONTINUE
      DM = 1.0
      CALL APPSLN(DM,Z,FSPACE,ISPACE)
      AL = Z(1)*CAIB
10  CONTINUE
C
C  FORMAT STATMENTS
C
101  FORMAT(2X,E14.6)
102  FORMAT(7E14.6)
      RETURN
      END
C*****
C
C      SUBROUTINE GUESS
C
C      OBJECTIVE :
C
C      EVALUATE THE INITIAL APPROXIMATION FOR Z(U(X))
C
C      USAGE : COLNEW
C*****
      SUBROUTINE GUESS (X,Z,DMVAL)
      IMPLICIT REAL*8 (A-H,O-Z)
      DIMENSION Z(6),DMVAL(3)
      COMMON  EPSLDA,EPSLDB,EPSLR,EPSLS,EPSLV,BETAR,BETAS,BETAV
      COMMON  A0,OMEGA,THETA0,THETAG,BIM,BIH,ALPHA,BETA,GAMMA
      COMMON  S,VAL_RM,DELHM,SN,SM
      INTEGER  SM,SN
      Z(1)= 1.0
      Z(2)= -1.0
      Z(3)= 1.0
      Z(4)= 0.0
      Z(5)= 0.0
      Z(6)= 0.0
      DMVAL(1)=0.0
      DMVAL(2)=0.0

```

```

DMVAL(3)=0.0
RETURN
END
C*****
C
C   OBJECTIVE : EVALUATE F(X,Z(U(X)) AT A POINT X
C
C   USAGE : COLNEW
C
C*****
C   SUBROUTINE FSUB (X,Z,F)
C   IMPLICIT REAL*8 (A-H,O-Z)
C   DIMENSION F(3),Z(6)
C   COMMON  EPSLDA,EPSLDB,EPSLR,EPSLS,EPSLV,BETAR,BETAS,BETAV
C   COMMON  A0,OMEGA,THETA0,THETAG,BIM,BIH,ALPHA,BETA,GAMMA
C   COMMON  S,VAL_RM,DELHM,SN,SM
C   INTEGER  SM,SN
C
C   EEA = DEXP( EPSLDA*Z(5)/(1.0+Z(5)))
C   EEB = DEXP( EPSLDB*Z(5)/(1.0+Z(5)))
C   EER = DEXP( EPSLR *Z(5)/(1.0+Z(5)))
C   EES = DEXP(-EPSLS *Z(5)/(1.0+Z(5)))
C   EEV = DEXP( EPSLV *Z(5)/(1.0+Z(5)))
C
C   F(1) = DELHM**2*VAL_RM*EER/EEA*Z(1)**SM*Z(3)**SN-
C   1 EPSLDA/(1.0D0+Z(5))**2*Z(6)*Z(2)
C   F(2) = DELHM**2*S*VAL_RM*EER/EEB*Z(1)**SM*Z(3)**SN-
C   1 EPSLDB/(1.0D0+Z(5))**2*Z(6)*Z(4)
C   F(3) =-DELHM**2*BETAR*VAL_RM*EER*Z(1)**SM*Z(3)**SN
C   RETURN
C   END
C*****
C
C   SUBROUTINE DFSUB
C
C   OBJECTIVE : EVALUATE THE JACOBIAN OF F(X,Z)
C
C   USAGE : COLNEW
C
C*****
C   SUBROUTINE DFSUB (X,Z,DF)
C   IMPLICIT REAL*8 (A-H,O-Z)
C   DIMENSION DF(6,6),Z(6)
C   COMMON  EPSLDA,EPSLDB,EPSLR,EPSLS,EPSLV,BETAR,BETAS,BETAV
C   COMMON  A0,OMEGA,THETA0,THETAG,BIM,BIH,ALPHA,BETA,GAMMA
C   COMMON  S,VAL_RM,DELHM,SN,SM
C   INTEGER  SM,SN
C   EEA = DEXP( EPSLDA*Z(5)/(1.0+Z(5)))
C   EEB = DEXP( EPSLDB*Z(5)/(1.0+Z(5)))
C   EER = DEXP( EPSLR *Z(5)/(1.0+Z(5)))
C   EES = DEXP(-EPSLS *Z(5)/(1.0+Z(5)))

```

```

      EEV = DEXP( EPSLV *Z(5)/(1.0+Z(5)))
      DO 10 I = 1, 6
      DO 20 J = 1, 6
        DF(I,J) = 0.D0
20    CONTINUE
10    CONTINUE
C
      DF(1,1)= SM*DELHM**2*VAL_RM*EER/EEA*Z(1)**(SM-1)*Z(3)**SN
      DF(1,2)=-EPSLDA/(1.0D0+Z(5))**2*Z(6)
      DF(1,3)= SN*DELHM**2*VAL_RM*EER/EEA*Z(1)**SM*Z(3)**(SN-1)
      DF(1,5)= DELHM**2*VAL_RM*EER/EEA*(EPSLR-EPSLDA)/(1.0D0+Z(5))**2
1      *Z(1)**SM*Z(3)**SN+2.0D0*EPSLDA/(1.0+Z(5))**3*Z(6)*Z(2)
      DF(1,6)=-EPSLDA/(1.0D0+Z(5))**2*Z(2)
C
      DF(2,1)= SM*DELHM**2*S*VAL_RM*EER/EEB*Z(1)**(SM-1)*Z(3)**SN
      DF(2,3)= SN*DELHM**2*S*VAL_RM*EER/EEB*Z(1)**SM*Z(3)**(SN-1)
      DF(2,4)=-EPSLDB/(1.0D0+Z(5))**2*Z(6)
      DF(2,5)= DELHM**2*S*VAL_RM*EER/EEB*(EPSLR-EPSLDB)/(1.0D0+Z(5))**2
1      *Z(1)**SM*Z(3)**SN+2.0D0*EPSLDB/(1.0D0+Z(5))**3*Z(6)*Z(4)
      DF(2,6)=-EPSLDB/(1.0D0+Z(5))**2*Z(4)
C
      DF(3,1)=-SM*DELHM**2*BETAR*VAL_RM*EER*Z(1)**(SM-1)*Z(3)**SN
      DF(3,3)=-SN*DELHM**2*BETAR*VAL_RM*EER*Z(1)**SM*Z(3)**(SN-1)
      DF(3,5)=-DELHM**2*BETAR*VAL_RM*EER*Z(1)**SM*Z(3)**SN
1      EPSLR/(1.0D0+Z(5))**2
      RETURN
      END
C*****
C
C   SUBROUTINE GSUB
C
C   OBJECTIVE : EVALUATE THE I-TH COMPONENT OF G (X,Z)
C
C   USAGE : COLNEW
C
C*****
C   SUBROUTINE GSUB(I,Z,G)
C   IMPLICIT REAL*8 (A-H,O-Z)
C   DIMENSION Z(6)
C   COMMON  EPSLDA,EPSLDB,EPSLR,EPSLS,EPSLV,BETAR,BETAS,BETAV
C   COMMON  A0,OMEGA,THETA0,THETAG,BIM,BIH,ALPHA,BETA,GAMMA
C   COMMON  S,VAL_RM,DELHM,SN,SM
C   INTEGER SM,SN
C   EEA = DEXP( EPSLDA*Z(5)/(1.0+Z(5)))
C   EEB = DEXP( EPSLDB*Z(5)/(1.0+Z(5)))
C   EER = DEXP( EPSLR *Z(5)/(1.0+Z(5)))
C   EES = DEXP(-EPSLS *Z(5)/(1.0+Z(5)))
C   EEV = DEXP( EPSLV *Z(5)/(1.0+Z(5)))
C   GO TO (10,20,30,40,50,60),I
10  G = Z(1)-EES
      RETURN

```

```

20  G = EEB*Z(4)-BIM*DELHM*EEV*(Z(3)-Z(3)/(1.0+OMEGA))
    RETURN
30  G = BETAS*EEA*Z(2)-Z(6)+BIH*(Z(5)-THETAG)+BETAV*EEB*Z(4)
    RETURN
40  G = -EEA*Z(2)-VAL_RM*DELHM**2*(ALPHA-1.D0)*EER*Z(1)**SM*Z(3)**SN
    I  -BETA*DELHM*(Z(1)-A0)
    RETURN
50  G = Z(3)-1.D0
    RETURN
60  G = Z(6)+VAL_RM*BETAR*DELHM**2*(ALPHA-1.D0)*EER*Z(1)**SM*Z(3)**SN
    I  +GAMMA*(Z(5)-THETA0)
    RETURN
    END
C*****
C
C   SUBROUTINE : DGSUB
C
C   OBJECTIVE : EVALUATE THE I-TH ROW OF THE JACOBIAN OF G(X,U(X))
C
C   USAGE : COLNEW
C
C*****
C   SUBROUTINE DGSUB(I,Z,DG)
C   IMPLICIT REAL*8 (A-H,O-Z)
C   DIMENSION DG(6),Z(6)
C   COMMON  EPSLDA,EPSLDB,EPSLR,EPSLS,EPSLV,BETAR,BETAS,BETAV
C   COMMON  A0,OMEGA,THETA0,THETAG,BIM,BIH,ALPHA,BETA,GAMMA
C   COMMON  S,VAL_RM,DELHM,SN,SM
C   INTEGER SM,SN
C   EEA = DEXP( EPSLDA*Z(5)/(1.0+Z(5)))
C   EEB = DEXP( EPSLDB*Z(5)/(1.0+Z(5)))
C   EER = DEXP( EPSLR *Z(5)/(1.0+Z(5)))
C   EES = DEXP(-EPSLS *Z(5)/(1.0+Z(5)))
C   EEV = DEXP( EPSLV *Z(5)/(1.0+Z(5)))
C   GO TO (10,20,30,40,50,60),I
10  DG(1)=1.0D0
    DG(2)=0.D0
    DG(3)=0.D0
    DG(4)=0.D0
    DG(5)=EES*EPSLS/(1.0D0+Z(5))**2
    DG(6)=0.D0
    RETURN
20  DG(1)=0.D0
    DG(2)=0.D0
    DG(3)=-BIM*DELHM*EEV*(1.0-1.0/(1.0+OMEGA))
    DG(4)=EEB
    DG(5)=EEB*Z(4)*EPSLDB/(1.D0+Z(5))**2-BIM*DELHM*EEV*(Z(3)-Z(3)/
    I  (1.0+OMEGA))*EPSLV/(1.D0+Z(5))**2
    DG(6)=0.D0
    RETURN
30  DG(1)=0.D0

```

```

DG(2)=BETAS*EEA
DG(3)=0.D0
DG(4)=BETAV*EEB
DG(5)=BETAS*EEA*Z(2)*EPSLDA/(1.0D0+Z(5))**2+BIH+BETAV*EEB*
1  Z(4)*EPSLDB/(1.0D0+Z(5))**2
DG(6)=-1.0D0
RETURN
40  DG(1)=-SM*VAL_RM*DELHM**2*(ALPHA-1.D0)*EER*Z(3)**SN
1  -BETA*DELHM
DG(2)=-EEA
DG(3)=-SN*VAL_RM*DELHM**2*(ALPHA-1.D0)*EER*Z(1)**SM*Z(3)**(SN-1)
DG(4)=0.D0
DG(5)=-EEA*Z(2)*EPSLDA/(1.0D0+Z(5))**2-VAL_RM*DELHM**2*
1  (ALPHA-1.D0)*EER*EPSLR/(1.0+Z(5))**2*Z(1)**SM*Z(3)**SN
DG(6)=0.D0
RETURN
50  DG(1)=0.D0
DG(2)=0.D0
DG(3)=1.d0
DG(4)=0.D0
DG(5)=0.D0
DG(6)=0.D0
RETURN
60  DG(1)=SM*VAL_RM*BETAR*DELHM**2*(ALPHA-1.D0)*EER*
1  Z(3)**SN
DG(2)=0.D0
DG(3)=SN*VAL_RM*BETAR*DELHM**2*(ALPHA-1.D0)*EER*Z(1)**SM*Z(3)
1  **(SN-1)
DG(4)=0.D0
DG(5)=VAL_RM*BETAR*DELHM**2*(ALPHA-1.D0)*EER*Z(1)**SM*Z(3)**SN*
1  EPSLR/(1.0D0+Z(5))**2+GAMMA
DG(6)=1.0D0
RETURN
END

```